HOMOGENEOUS VS. HETEROGENEOUS COBALT-CATALYZED HYDROGENATIONS: AN EVALUATION OF COBALTATES AND COBALT NANOPARTICLES AS CATALYSTS

Dissertation zur Erlangung des

Doktorgrades der Naturwissenschaften

DR. RER. NAT.

am Institut für Anorganische Chemie

der Fakultät für Chemie und Pharmazie

der Universität Regensburg

vorgelegt von

PHILIPP BÜSCHELBERGER

aus Fladungen

Regensburg 2019

Der Experimentelle Teil der vorliegenden Arbeit wurde in der Zeit zwischen November 2014 und Oktober 2018 unter Anleitung von Prof. Dr. Robert Wolf am Institut für Anorganische Chemie der Universität Regensburg angefertigt.

PROLOGUE

This thesis reports on the synthesis and characterization of low oxidation state cobalt compounds, which are used as (pre-)catalysts for hydrogenation reactions. Chapter 1 reviews recent developments in cobalt-catalyzed hydrogenation reactions and describes the problems in distinguishing between homogeneous and heterogeneous catalysis. In Chapter 2, the catalytic properties and mechanistic characteristics of a series of cobaltate complexes is studied. Chapter 3 presents the preparation and characterization of a potent nanoparticulate cobalt catalyst. The nanoparticles feature a high catalytic activity for the hydrogenation of challenging alkene, imine, and quinoline substrates, facile catalyst separation and can be recycled >10 times. The search for chiral alkene cobaltate complexes as potential catalysts for enantioselective hydrogenation reactions is described in Chapter 4. Chapter 5 describes attempts to synthesize new cobaltate complexes with 2,9-diaryl-1,10-phenanthroline ligands, and the catalytic activity of the resulting compounds is evaluated. Chapter 6 summarizes the results of this thesis.

PROLOG

Diese Dissertation berichtet über die Synthese und Charakterisierung von Verbindungen mit Cobalt in niedrigen Oxidationsstufen, die als (Prä)katalysatoren für Hydrierungsreaktionen Verwendung finden. Kapitel 1 gibt einen Überblick über die jüngeren Entwicklungen im Bereich cobaltkatalysierter Hydrierungsreaktionen und beschreibt die Probleme bei der Unterscheidung zwischen homogener und heterogener Katalyse. In Kapitel 2 werden die katalytischen und mechanistischen Eigenschaften einer Serie von Cobaltatkomplexen untersucht. Kapitel 3 legt die Darstellung und Charakterisierung eines leistungsfähigen, nanopartikulären Kobaltkatalysators dar. Die Nanopartikel zeichnen sich durch eine hohe Aktivität bei der Hydrierung von anspruchsvollen Alkenen, Iminen und Chinolinen und durch einfache Abtrennbarkeit aus und können mehr als zehnmal wiederverwendet werden. Die Suche nach chiralen Alkencobaltatkomplexen als potenzielle Katalysatoren für enantioselektive Hydrierungen wird in Kapitel 4 beschrieben. Kapitel 5 beschreibt den Versuch, neue Cobaltatkomplexe mit 2,9-Diaryl-1,10-phenanthrolinliganden zu synthetisieren, und die katalytische Aktivität der resultierenden Verbindungen wird untersucht. Kapitel 6 fasst die Ergebnisse dieser Dissertation zusammen.

1 COBALT IN HOMOGENEOUS AND HETEROGENEOUS HYDROGENATION CATALYSIS

1.1 Cobalt in Hydrogenation Catalysis

Our world would not be the same without transition metal catalysis. Countless and often irreplaceable industrial processes (e.g. Haber-Bosch, Fischer-Tropsch, Ostwald, Monsanto) utilize transition metals or transition metal compounds as catalysts to produce commodity chemicals. Starting from these bulk chemicals, the synthesis of fine chemicals and pharmaceuticals often also requires transition-metal-catalyzed reaction steps.[1]

Already in the late 1890s, Paul Sabatier developed the first method for the catalytic hydrogenation of unsaturated organic compounds using finely divided metal catalysts what was honored with the Nobel prize in chemistry 1912 (Figure 1.1).[2, 3] Since then, catalytic hydrogenations have developed into one of the most important research areas for organic and inorganic chemists. The Fischer-Tropsch process, for example, was especially used in the first half of the 20th century to convert carbon monoxide and molecular hydrogen to synthetic fuels, utilizing cobalt catalysts, among others.[4]

From the mid-20th century, numerous important developments in the field of transition metal catalysis have made use of platinum group elements. Significant work was done by pioneers like Herbert Lindlar, Geoffrey Wilkinson, and Robert H. Crabtree who developed a series of highly efficient noble metal hydrogenation catalysts, which are still in use in industry and laboratories today.[5] The evolution and the increasing number of different catalyst systems culminated in another Nobel prize in 2001, which was awarded to William S. Knowles and Ryoji Noyori for their work on chirally catalyzed hydrogenation reactions (Figure 1.1).[6, 7] This prize emphasizes the status of catalytic hydrogenation as one of the most important technical processes in chemical synthesis.[1]

Due to financial, economic and environmental concerns, research interest has increasingly moved toward base-metal catalysis over the last decade.[8] In contrast to rare precious metals,
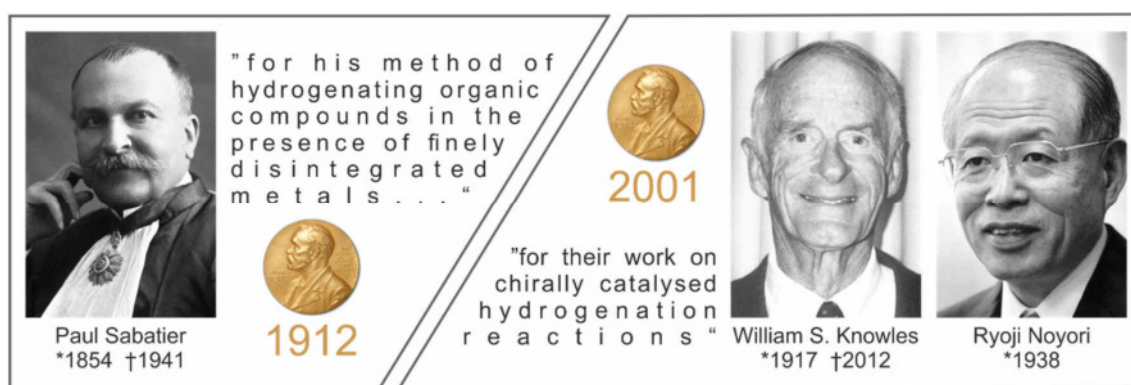
Figure 1.1   1912 (Sabatier, left) and 2001 (Knowles & Noyori, right) Nobel prices in chemistry honoring the important work on catalytic hydrogenation reactions.[3][7]

3d elements benefit from their higher abundance, their consequently lower price, and their often lower toxicity compared to their higher homologues.[9] The amount of cobalt in the Earth's crust, for example, is over 1000 times larger than the overall reserve of platinum-group metals.[10] This chapter gives a short overview over recent innovations concerning cobalt-catalyzed hydrogenation reactions.

1.1.1   Homogeneous Cobalt Catalysts for Hydrogenation Reactions

Primary findings in homogeneous cobalt-catalyzed hydrogenations were already reported more than 50 years ago by Dutton and co-workers, who applied dicobalt octacarbonyl $Co_2(CO)_8$ (**1**) (Figure 1.2) for the hydrogenation of unsaturated fatty acids at relatively harsh conditions (75-180 °C, 17-207 bar H_2) in cyclohexane solutions.[11] Feder et al. investigated the mechanism of the homogeneous hydrogenation of aromatic hydrocarbons with the same precatalyst, suggesting that the cobalt tetracarbonyl radical is a reaction intermediate.[12] The hydrogenation of aromatic hydrocarbons by a discrete cobalt complex was first described by Muetterties and co-workers, who used the η^3-allylcobalt phosphite complex **2** (Figure 1.2).[13] Their catalyst demonstrates a remarkable selectivity toward arenes over olefins.[14] In the early 1970s, Ferrari and Misono reported that phosphine cobalt hydride (carbonyl) complexes catalyze the hydrogenation of alkenes, alkynes and aldehydes.[15] Misono and co-workers showed that $CoH_3(PPh_3)_3$ and $CoH(CO)(PPh_3)$ are active catalysts for the hydrogenation of cyclohexene.[15a] Ferrari and co-workers described the synthesis of complexes with the composition $CoH(CO)_{4-n}(P^nBu_3)_n$ and their application in the hydrogenation of alkynes and aldehydes.[15b] They also considered the kinetics of this homogeneous catalytic reaction and discussed a possible reaction mechanism.[15c]

It took more than 30 years until Budzelaar and co-workers reached the next milestone in cobalt-catalyzed hydrogenation reactions. In 2005, it was discovered that the square planar bis(imino)pyridine (= BIP) Co(I) pincer complex **3** (Figure 1.2) is an active catalyst for the hydrogenation of mono- and disubstituted olefins.[16] A $L^{dip}CoH$ species is likely involved in the catalytic cycle. Budzelaar and co-workers concluded that with the right ligand environment, cobalt is able to show a "rhodium-like" catalysis behavior.

The first CO_2 hydrogenation reactions catalyzed by a series of non-platinum group metals, including cobalt, was reported by Jessop and co-workers.[17] They developed a high-pressure combinatorial screening method for catalysts and found that among other salts, $Co(OAc)_2$ or $CoCl_2$ in combination with different diphosphines are able to catalyze the transformation of CO_2 to formic acid. In 2011, Beller and co-workers introduced a well-defined cobalt dihydrogen complex as a catalyst for the hydrogenation of CO_2 in high yield.[18] Starting from $Co(acac)_2$ and

the tetraphos ligand (PP$_3$ = P(CH$_2$CH$_2$PPh$_2$)$_3$), the [Co(H$_2$)PP$_3$]$^+$ cation **4** (Figure 1.2) was isolated in combination with different stabilizing anions such as [BPh$_4$]$^-$, [BF$_4$]$^-$ and [PF$_6$]$^-$. At this time, **4** featured the best TONs for non-precious metal-catalyzed CO$_2$ and bicarbonate hydrogenation. The same group reported on the (transfer) hydrogenation of N-heterocycles with formic acid or molecular hydrogen under mild conditions, and on the selective hydrogenation of nitriles to primary amines, utilizing catalysts synthesized by the combination of cobalt salts and related tetraphos ligands.[19] In recent years, many more systems for the cobalt-catalyzed hydrogenation of CO$_2$ were reported.[20] The first catalytic system based on a first-row transition metal able to hydrogenate carboxylic acids with molecular dihydrogen as the reductant was found by de Bruin and Elsevier, who used a cationic tris(phosphane) (= triphos) cobalt complex **5** (Figure 1.2).[21]

Chirik and co-workers developed *C$_1$*-symmetric bis(imino)pyridine cobalt precatalysts for the enantioselective hydrogenation of geminal-disubstituted alkenes.[22] Previously, such BIP cobalt complexes were used by Bianchini and co-workers as catalysts for the oligomerization of ethylene.[23] In extended studies, Chirik and others addressed the origin of stereoselectivity and applied their system to the synthesis of biologically important molecule substructures.[24] The same group reported the (asymmetric) hydrogenation of alkenes and enamides with bis(phosphine) cobalt dialkyl complexes **6** (Figure 1.2).[25]

As reported by Stryker and co-workers, a soluble tetrametallic Co(I) cluster **7** (Figure 1.2) catalyzes the hydrogenation of allylbenzene and diphenylacetylene under very mild conditions.[26] This catalyst is structurally unique and can be described as a "molecular square" of four linear coordinated metal centers bridged by the nitrogen atoms of sterically bulky trialkylphosporanimide ligands.
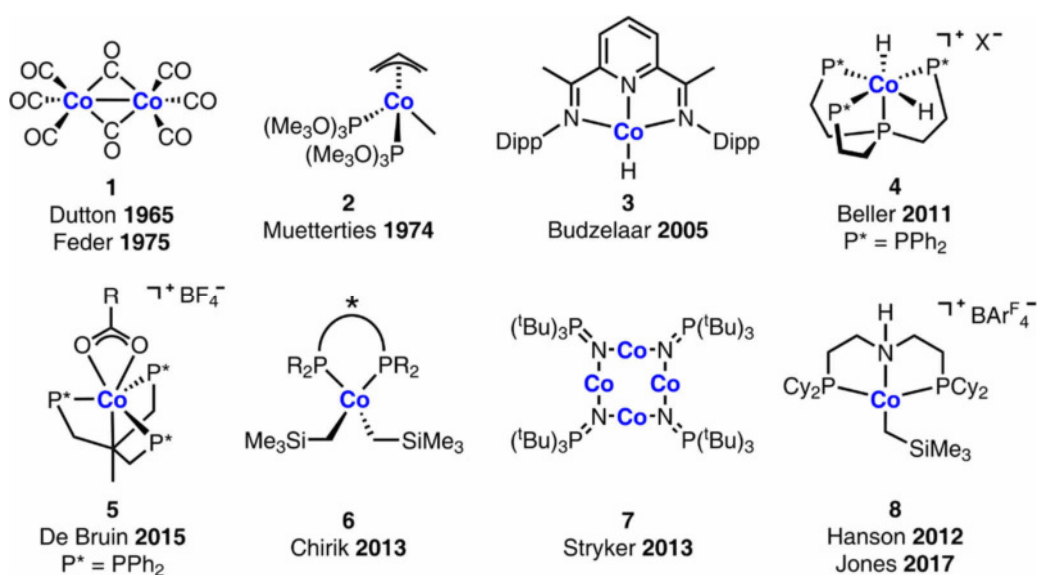
Figure 1.2   Selected ligand and catalyst design concepts for cobalt-catalyzed hydrogenation reactions.

Hanson and co-workers achieved the catalytic (transfer) hydrogenation of alkenes, ketones, aldehydes, and imines under mild conditions utilizing a cobalt(II) alkyl complex **8** (Figure 1.2) which was stabilized by a tridentate PNP pincer ligand.[27] The same catalyst was applied to reversible (de)hydrogenations of N-heterocycles and to the additive-free hydrogenation of esters to alcohols by Jones and co-workers.[28] Kempe and co-workers used a triazine-based ligand design for their PNP pincer cobalt catalyst **9** (Figure 1.3), impressively allowing the selective hydrogenation of carbonyl functions in the presence of C=C bonds.[29] Bernskoetter and co-workers developed the remarkable PNP pincer cobalt catalyst **10**, which features up to 30,000 turnovers in the catalytic hydrogenation of CO_2 under dihydrogen pressure.[20c]

The first cobalt-catalyzed hydrogenation of esters to alcohols was described by Milstein and co-workers in 2015, using an *in situ* reduced PNN pincer cobalt dichlorido complex **11** (Figure 1.3).[30] Peters and co-workers introduced PBP pincer cobalt complexes such as **12** (Figure 1.3), where a boryl-group enables H_2 activation at the transition metal center of the catalyst.[31] With 2 mol% of the complex, styrene and 1-octene were hydrogenated quantitatively within 3 minutes under mild conditions. Dehydrogenation of amine-borane and transfer hydrogenation to styrene were demonstrated as well. A similar reactivity was reported by Waterman and co-workers for cobalt half sandwich complexes.[32]

Fout and co-workers prepared a Co^I–(H_2) catalyst **13** (Figure 1.3) with a monoanionic bis(carbene) pincer ligand under hydrogen pressure from a Co^I–(N_2) precursor.[33] This catalyst proved to be active in the hydrogenation of a series of olefins tolerating functional groups like hydroxyl groups, ketones, anhydrides or aldehydes but it also allows the *E*-selective semi-hydrogenation of alkynes. A variety of this cobalt CCC pincer system showed a good
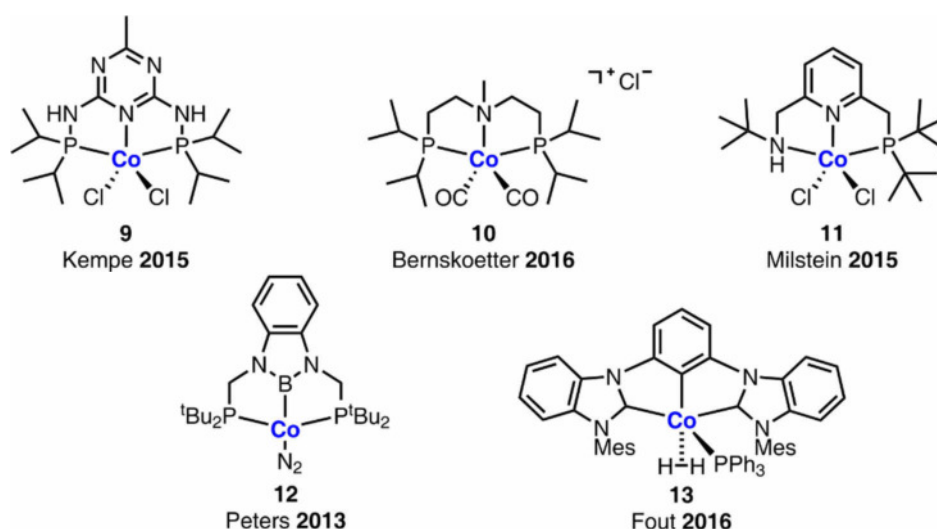
Figure 1.3   Selected cobalt hydrogenation catalysts with different types of pincer ligands featuring boron, carbon, nitrogen, or phosphorus as coordinating atoms.
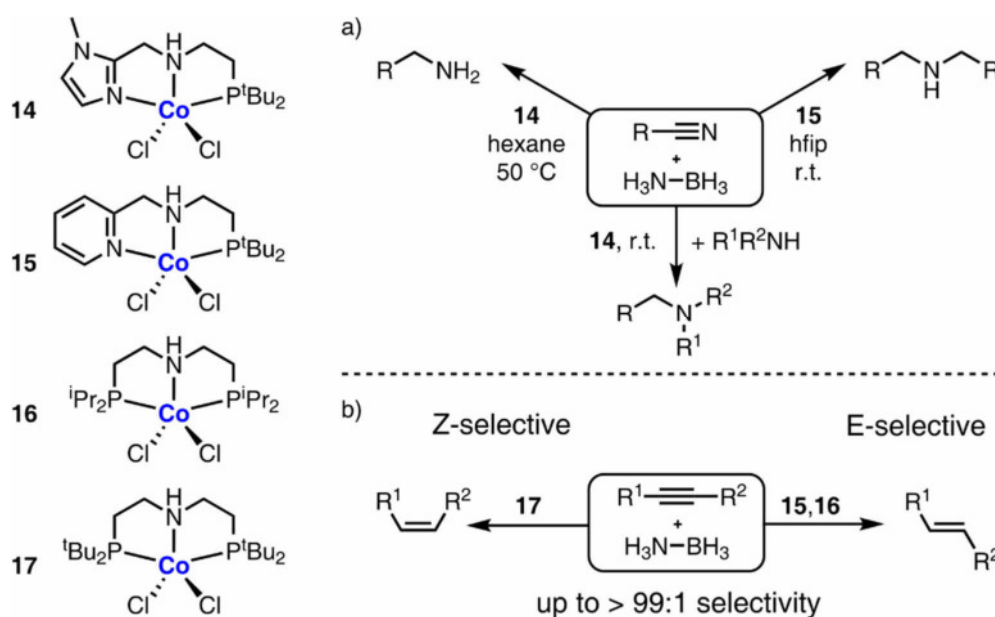
Figure 1.4   Cobalt-based hydrogenation catalysts **14**-**17** by Liu (left) and reactions pathways for a) amine synthesis by reduction of nitriles, and b) *Z*- or *E*-selective transfer-semi-hydrogenation of alkynes.

selectivity toward the hydrogenation of nitriles to primary amines.[34] Notably, in the presence of a ketone functionality, only reduction of the nitrile was observed.

There are many more examples for PNP, PNN, NNN or other cobalt pincer complexes in hydrogenation catalysis.[35] Many of them are already on a highly applicable level as shown by Liu and co-workers who described the catalysts **14** and **15** (Figure 1.4) for a facile synthesis of primary, secondary, or tertiary amines by transfer hydrogenation of different nitriles with ammonia borane coupled with reductive amination (Figure 1.4a).[36] With this method, pharmaceutical molecules can be functionalized in the presence of other reducible functional groups. The same group also reported on the cobalt-catalyzed *Z*- or *E*-selective transfer-semi-hydrogenation of alkynes controlled by rational ligand design with complexes **15**-**17** (Figure 1.4b), which feature PNN or PNP pincer ligands.[37]

Walter and co-workers synthesized a dialkyl cobalt NHC (= N-heterocyclic carbene) complex that serves as a precatalyst for olefin hydrogenation.[38] The formation of cobalt particles after complete substrate consumption was noted and, the question if the active catalyst possesses a heterogeneous or homogeneous nature was addressed. After carefully considering the results of catalyst poisoning experiments and the fact that the particles did not show catalytic activity, the authors suggested a homogeneous mechanism.

The price of a homogeneous transition metal catalyst corresponds to the sum of the metal price and the price of the utilized ligands.[9b] The major drawback of all the previously mentioned examples utilize extravagant ligands, with multi-step syntheses in many cases, rendering the

catalysts and their synthesis expensive even if a cheap and abundant metal is incorporated. Recently, our group found that the bis(anthracene) cobaltate **18** (Scheme 1.1) and its iron counterpart, initially reported by Ellis and co-workers,[39] are potent precatalysts for the hydrogenation of alkenes, alkynes, ketones, and imines.[40] These results showed for the first time that homoleptic arene complexes, which are conceptionally completely different to all established cobalt hydrogenation catalysts (*vide supra*), can be applied in hydrogenation science. No sophisticated ligands or further additives (such as Brookhart's acid in case of Hanson's PNP pincer compounds) are required to create an active catalyst. The metalates only bear cheap and commercially available polyarene ligands that can easily be replaced by π-accepting substrates[39] to form the catalytically active species.

Preliminary studies by ^{1}H-NMR reaction monitoring, reaction progress analyses, and catalyst poisoning experiments supported the postulated mechanism (Scheme 1.1),[40] which was also studied by DFT methods by Chung and co-workers, recently.[41] After addition of dihydrogen, the alkene ligands of the active catalyst are hydrogenated and replaced by new substrate molecules. The DFT calculations propose an unprecedented mechanism, incorporating the three different oxidation states Co(-I)/Co(0)/Co(I), and involving spin crossing between singlet and triplet states. This catalytic cycle differs dramatically from the classical singlet state M(I)/M(III) or M(III)/M(V) catalysis, as it is known for transition metals like rhodium and iridium. In addition, the authors pointed out the importance of the π-acidic anthracene ligands, which promote the single reaction steps with their flexible coordination behavior.

Nonetheless, these results could not completely rule out concerns that the very reactive precatalyst decomposes under reaction conditions and thus, a nanoparticulate, heterogeneous catalyst is operational. For hydrogenation reactions, numerous heterogeneous cobalt catalysts have been reported and pertinent examples are discussed below.
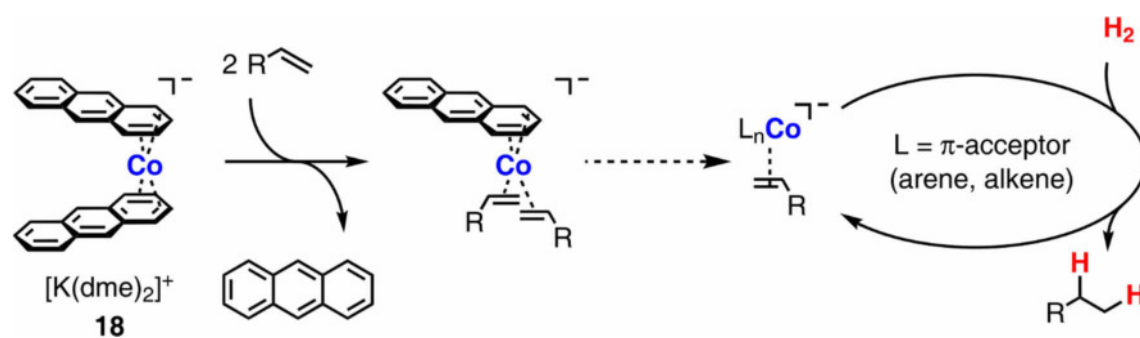
Scheme 1.1 Catalytic concept of the precatalyst activation and hydrogenation reaction with potassium bis(anthracene) cobaltate **18** including π-ligand exchange with an olefinic substrate and subsequent hydrogenation after addition of dihydrogen.

1.1.2   Heterogeneous Cobalt Catalysts for Hydrogenation Reactions

As mentioned above, the most common catalysts for the Fischer-Tropsch process are based on cobalt.[4] Besides, several other cobalt (containing) catalysts were applied to the hydrogenation of carbon monoxide or nitriles already decades ago.[42] Nevertheless, the development of heterogeneous cobalt-based hydrogenation catalysts progressed relatively slowly. In 1955, Pruett patented storable nickel and cobalt hydrogenation catalysts produced under reductive conditions from the corresponding metallocenes. In contrast to the previously known Raney nickel or cobalt catalysts, these finely divided metal catalysts were not pyrophoric and more stable.[43] However, detailed information about the behavior in hydrogenation reactions were only given for nickel, probably because this species was significantly more active. Different levels of activity of Raney cobalt and nickel catalysts for the same reaction type were also reported by other groups.[44] In 1970, Tanaka and co-workers reported on the hydrogenation of ethylene over cobalt oxides including mechanistic studies and a discussion of probable reaction mechanisms.[45] Finke and co-workers investigated the formation and structure of Ziegler-type cobalt and nickel nanoclusters made from Co(neodecanoate)$_2$ or Ni(2-ethylhexanoate)$_2$ and triethylaluminum and applied them to cyclohexene hydrogenation.[46] In many of these cases, the structure and exact composition of the catalyst was unknown or ill-defined.

One of the first examples for a well-defined heterogeneous cobalt hydrogenation catalyst was introduced by Chung and co-workers in 2002.[47] To combine the benefits of nanoparticulate catalysts with the ones of conventional heterogeneous catalysts, cobalt nanoparticles were immobilized on charcoal. The resulting bifunctional catalyst was used to combine hydrogenation and the Pauson-Khand reaction in a one-pot synthesis. The catalyst can easily be recovered and reused several times and is storable in the air for several months without any loss of activity.

The idea of immobilization of catalytically active compounds on support materials was adapted by Beller and co-workers, who developed the first non-noble catalyst for nitroarene reduction in 2013.[48] By adsorption of a molecular cobalt phenanthroline complex onto a carbon support and subsequent pyrolysis, they synthesized a cobalt oxide catalyst (Scheme 1.2, *vide infra*) that is reusable for several times while it is tolerating numerous of other functional groups. Following a similar procedure the same group synthesized *N*-graphene-modified cobalt nanoparticles on alumina for the selective catalytic hydrogenation of heteroarenes.[49]

A range of catalytic systems for the hydrogenation of different functional groups could be obtained until now using the concept of pyrolysis of cobalt precursors in the presence of a support material. Li and co-workers introduced a novel catalyst system for transfer
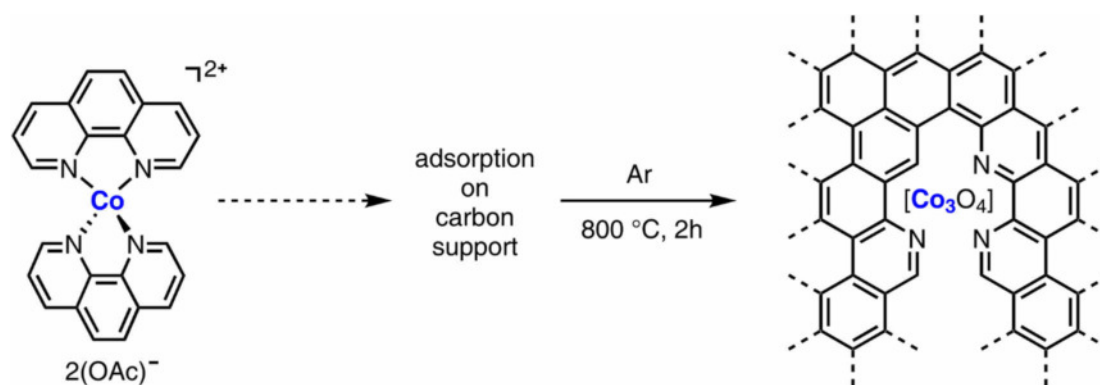
Scheme 1.2   Synthesis of the first non-noble catalyst for nitroarene reduction by Beller and schematic representation of the active cobalt oxide N/C catalyst.[48]

hydrogenation reactions of unsaturated bonds, including aldehydes, ketones, nitro-compounds, imines, and alkenes in 2015.[50] A Co-containing metal-organic framework (= MOF) was used as a sacrificial template in the synthesis of a catalyst for transfer hydrogenations. With isopropanol as a hydrogen donating solvent, the resulting cobalt nano-composite catalyst proved to be highly active and selective. Moreover, no base additives are required and the catalyst is magnetically separable and reusable.

One year later, Wang and co-workers encapsulated cobalt nanoparticles in *N*-doped graphene layers by pyrolysis of cobalt acetate in the presence of melamine and *D*-glucosamine hydrochloride (= GAH).[51] The arising heterogeneous catalyst demonstrated an excellent catalytic activity for the chemoselective hydrogenation of N-heteroarenes and a high stability of the incorporated nanoparticles. Thermal decomposition of $Co(NO_3)_2 \cdot 6\,H_2O$ under similar conditions results in an *in situ* formation of Co^0/Co_3O_4@*N*-doped carbon nanotube (CoO_x@NCNT) hybrids which feature excellent catalytic performance for the hydrogenation of substituted nitroarenes.[52] A perfect chemoselectivity for nitro groups was achieved remaining nitrile, aldehyde, keto, amide, and alkene groups unaffected. These remarkable results made this catalyst superior over most noble metal catalysts, which often must be modified to improve chemoselectivity, mostly at the cost of activity.

Catalysts with a similar selectivity for substituted nitroarenes were also reported by Yuan and Kempe.[53] While Yuan used Co/CoO nanoparticles coated with graphene for the catalytic hydrogenation, Kempe used silicon carbon nitride as support material. Both catalyst systems are highly selective for nitroarene reduction with an extraordinary tolerance towards hydrogenation-sensitive functional groups. In addition, Kempe reported the direct synthesis of imines (Scheme 1.3a) and benzimidazoles (Scheme 1.3b) by reaction of the hydrogenation products with aldehydes or ketones with a base-metal catalyst.
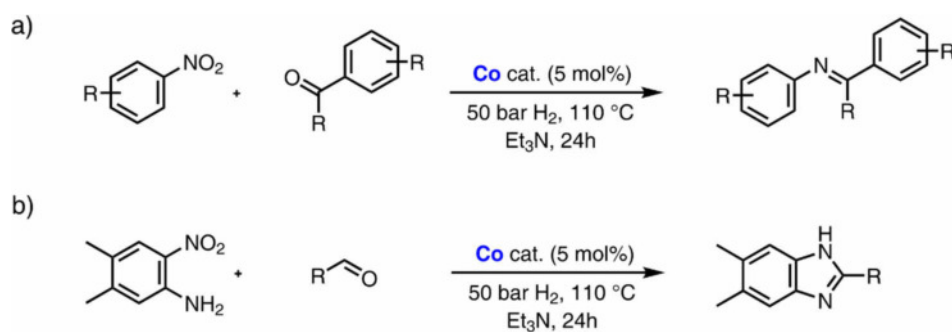
Scheme 1.3 First base-metal-catalyzed direct synthesis of a) imines and b) benzimidazoles from nitroarenes and aldehydes (a and b) or ketones (a) according to Kempe and co-workers.

Beller introduced another cobalt catalyst (supported on α-Al$_2$O$_3$) that shows impressive selectivity toward the hydrogenation of nitriles, aldehydes, and ketones, even in the presence of C=C bonds and features a wide functional group tolerance.[54] There are some more reports by Beller and his co-workers about heterogeneous cobalt-catalyzed (transfer) hydrogenation reactions, all of them including similar catalyst systems synthesized by pyrolysis of a cobalt precursor mostly in the presence of a support material.[55] Recently, they also reported on a general direct synthesis (more than 140 examples) of primary, secondary, and tertiary amines by coupling of carbonyl compounds with ammonia, amines, or nitro compounds in the presence of molecular hydrogen (Scheme 1.4a and b). The scalable reaction is catalyzed by graphitic-shell encapsulated cobalt nanoparticles and was performed in up to 50-gram scale for amphetamine (Scheme 1.4c) and related compounds. Besides, a series of known pharmaceutical products were synthesized to demonstrate the industrial applicability of this system.[56]
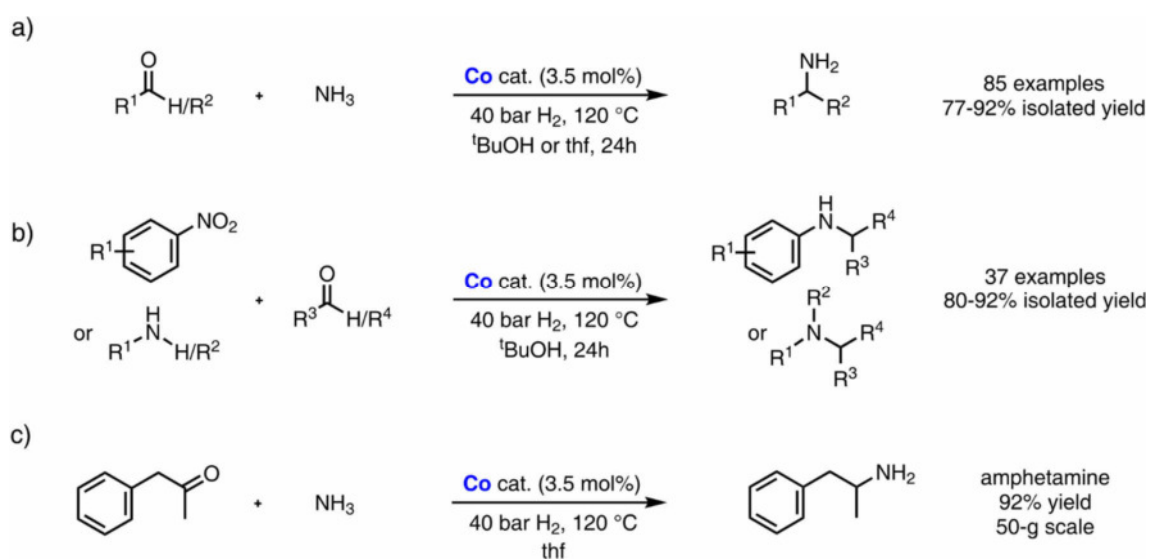
Scheme 1.4 Direct synthesis of a) primary amines from aldehydes and ketones by reductive amination, b) secondary and tertiary amines by reductive alkylation of nitroarenes or amines with carbonyl compounds, and c) amphetamine in a 50-g scale reaction.
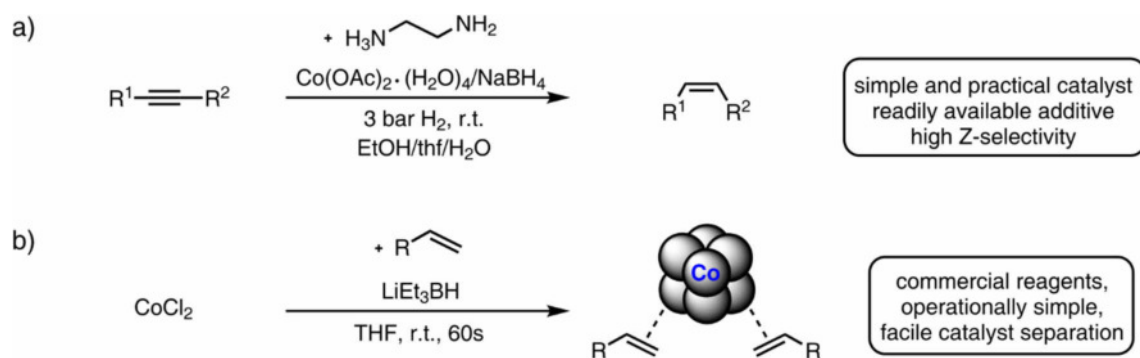
Scheme 1.5   a) *Z*-selective semi-hydrogenation of alkynes with an *in situ* formed cobalt catalyst by Liu, and b) the simple synthetic protocol for a heterogeneous olefin stabilized cobalt catalyst for the hydrogenation of alkenes, carbonyls, imines, and heteroarenes.

Although the majority of recent publications about heterogeneous cobalt-catalyzed hydrogenations deals with polar substrates there are also some reports about the hydrogenation of C=C bonds.[57, 58] The selective semi-hydrogenation of internal and terminal alkynes was achieved with a Co@N-doped graphite catalyst again by Beller and co-workers. The catalyst is synthesized by pyrolysis of cobalt acetate in the presence of 1,10-phenanthroline and a silica support.[59] Up to 93% selectivity for the *Z*-isomer was reached in the case of internal alkynes. Even a higher selectivity for the same isomer of a variety of substrates were reported by Zhang and co-workers, who used an ill-defined heterogeneous catalyst formed *in situ* upon the reduction of cobalt acetate with $NaBH_4$ in the presence of the readily available ethylenediamine as an additive (Scheme 1.5a).[60] Jacobi von Wangelin and co-workers developed a simple protocol for the hydrogenation of alkenes and polar unsaturated bonds under mild conditions. The nanoparticulate catalyst is generated *in situ* from $CoBr_2$ by reduction with $LiEt_3BH$ in the presence of an olefin, i.e. the substrate itself in most cases, or anthracene (Scheme 1.5b). These π-hydrocarbons prevent aggregation of the particles.[61] The hydrogenation of more than 50 terminal and internal alkenes in water with a biowaste-derived catalyst was reported by Beller and co-workers, very recently.[55h] The recyclable and reusable catalyst is easily prepared from $Co(OAc)_2 \cdot 4H_2O$ and chitosan by pyrolysis, and – besides its stability toward air and moisture for months – features a broad functional group tolerance.

1.2   Distinction between Homogeneous and Heterogeneous Catalysis

All these examples show that there has been great success so far in the quest for new active and practical cobalt-based hydrogenation catalysts especially in the last two decades. For further progress in catalyst synthesis, a detailed understanding of the operational mechanism is necessary. While a homogeneous catalyst is characterized by a single active site and mostly is in
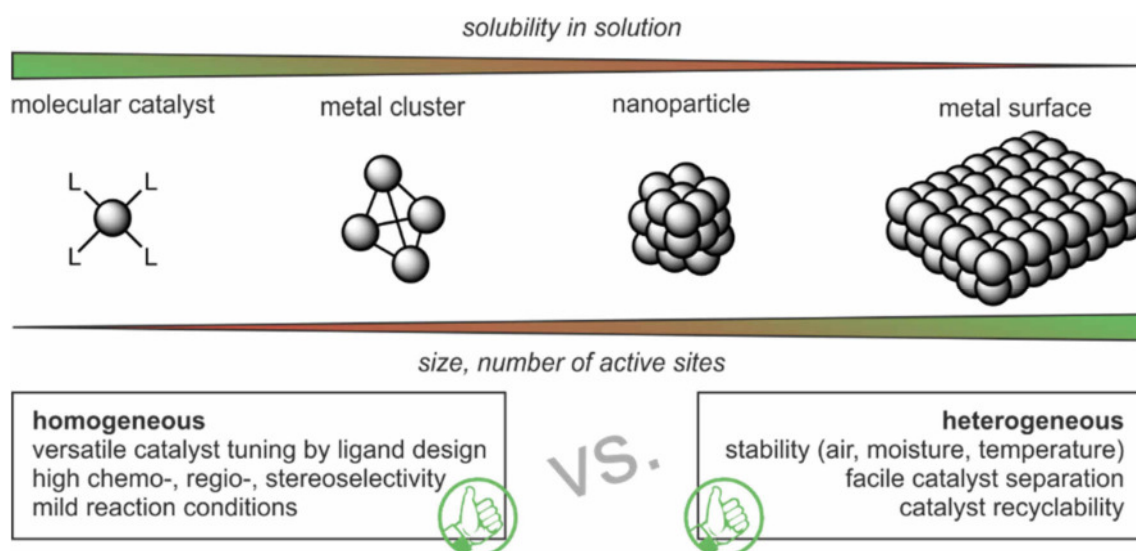
Figure 1.5   Correlation between catalyst solubility and number of active sites (top) and main advantages of homo-and heterogeneous catalysts (bottom).

the same phase as the substrate (e.g. molecular catalyst in solution), its heterogeneous counterpart has multiple active sites and, normally, it is not in the same phase as the substrate (Figure 1.5 top).[62] In general, both types of catalysts have their advantages. Molecular catalysts often operate under mild reaction conditions and offer higher regio-, chemo- and enantioselectivity as well as facile catalyst tuning by rational ligand design. By contrast, the main advantages of classical heterogeneous catalysts are their stability, recyclability, and a facile catalyst separation (Figure 1.5 bottom).[63] Hence, most industrial refinery processes use heterogeneous catalysts, while homogeneous catalysis is mainly applied for the synthesis of fine chemicals and pharmaceuticals. However, mechanistic analyses are often more conveniently performed and more insightful with molecular catalysts than with heterogeneous catalyst materials.[64] Notably, metal clusters and nanoparticles (Figure 1.5, top) are in between the two fields and combine their respective advantages.[65]

Since the differentiation between homo- and heterogeneous is often complicated and in many cases not unambiguous, various methods and techniques may be useful to distinguish between homogeneous and heterogeneous reaction pathways.[66, 67] Mostly, several of these tests must be applied independently to get reliable results. The most important approaches are summarized below.

1.2.1   Spectroscopic Methods

Spectroscopy can be used to detect and identify metal particles. Transmission electron microscopy (= TEM) and dynamic light scattering (DLS) can prove particle formation from solutions of a molecular precatalyst.[66, 67] While TEM can only be applied *post operando* to the

evaporated residues of the reaction mixture, DLS can be used *in situ* to test for particle formation from catalyst solutions and to determine their mean radius. However, both methods must be used in combination with other techniques because of three reasons: 1) a negative result does not conclusively rule out the presence of (undetected) particles, 2) the detection of particles does not necessarily confirm that they are catalytically active, and 3) there is also the possibility of false positive findings in the case of DLS, resulting from the presence of other particles in solution (such as dust particles), and in the case of TEM resulting from particle formation/decomposition upon evaporation of the sample.

X-ray spectroscopic methods such as small angle X-ray scattering (SAXS) or extended X-ray absorption fine structure (EXAFS) were also applied to detect particles or to investigate the presence of metal-ligand and/or metal-metal bonds (the latter are present in metal particles).[67] Moreover, single-crystal X-ray studies are helpful to characterize isolated molecular reaction intermediates.

Nuclear magnetic resonance spectroscopy (NMR) is a powerful *in operando* tool for mechanistic investigations.[68] This technique enables *in situ* monitoring of incidents like substrate consumption, product formation, substrate coordination or ligand dissociation.[68, 69, 70] Furthermore, as it can be used to characterize reaction intermediates it is extensively used in homogeneous catalysis. The biggest handicap of this method is that catalytically active species can be NMR silent or paramagnetic.

1.2.2 Reaction Progress Analysis

The observation of a sigmoidal shaped curve of the reaction profile of a catalytic reaction (Figure 1.6, red) is strong evidence for a heterogeneous mechanism.[66-70] The induction period
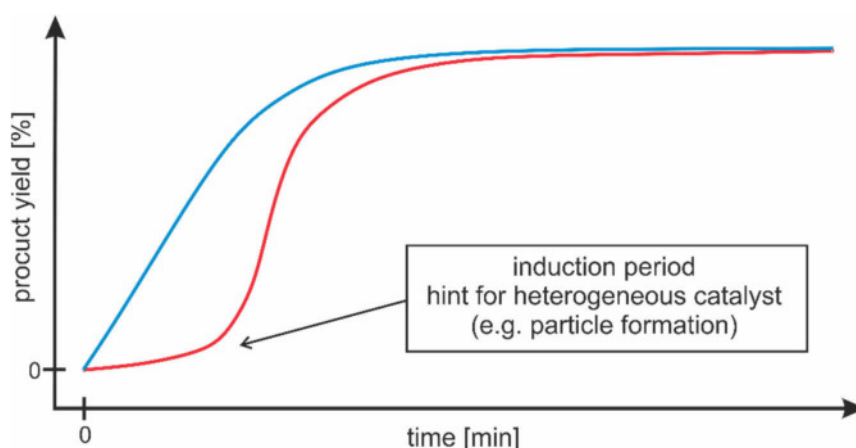

Figure 1.6   Reaction profiles with a sigmoidal curve hinting at heterogeneous catalyst (red) and a constant initial rate suggesting a homogeneous mechanism (blue).

of this curve can be explained by the conversion of a precatalyst to another, catalytically active species under reaction conditions. A homogeneous catalyst should in general initiate a linear product formation or substrate consumption, respectively, right at the beginning of the time scale (Figure 1.6, blue). However, the absence of a sigmoidal curve is not a strict proof for a homogeneous nature of the operating catalyst.[66, 70] If a heterogeneous catalyst is already completely preformed before the addition of substrate, an induction period is not expected.

1.2.3 Catalyst Poisoning

Poisoning tests are another *in operando* technique and allow an immediate monitoring how the activity of a catalyst is affected.[66, 67] Mercury poisoning is a very common test for heterogeneity for about 100 years.[68] Addition of a large excess of mercury to the reaction mixture leads to amalgamation or chemical adsorption on the metal catalyst and, thus, to a suppression of the activity.[69] This method is well explored for the platinum group metals, but not universally applicable for 3d metals. There are reports about effective nickel and cobalt catalyst poisoning,[71] but also about nanoparticulate iron catalysts, which (completely) tolerate the poisoning.[72] In general, the solubility of most of the 3d metals in mercury is very poor.[73] In addition, in some cases an interaction of a molecular species with mercury can also lead to catalyst decomposition. Hence, this test should only be used with caution and in combination with other poisoning tests.

(Sub)-stoichiometric poisoning tests can be carried out with a whole range of coordinating reagents like phosphines, thiols, amines, or alcohols; very common agents are CO, CS_2, 1,10-phenanthroline, PPh_3, and thiophene (Figure 1.7).[66-68] The principle of this method is that the poison strongly binds to a metal center, no matter if it is a molecular one or not. Once coordinated, the poisoning reagent blocks the active site and inhibits further reactions of the catalyst. For heterogeneous catalysts a complete inhibition can be achieved with sub-stoichiometric amounts of poison with respect to the number of metal atoms (Figure 1.7, red), because only a small amount of them is located on the surface of the catalyst and serves as active sites. With this method, one can also estimate the number of metal atoms on the surface by calculating the amount of poison that is needed to gain complete inhibition. For homogeneous catalysts, usually at least one equivalent of the poisoning agent is needed to reach complete inhibition because every metal atom is an active site and, depending on the catalyst, at least one equivalent of poisoning reagent is needed to block all coordination sites.

A special poisoning reagent is [*a,e*]-dibenzocyclooctatetraene (dct, Figure 1.7). This molecule was introduced by Crabtree and co-workers as a selective poison for homogeneous catalysts.[66][74] The dct molecule strongly binds to molecular catalysts, but not to metal
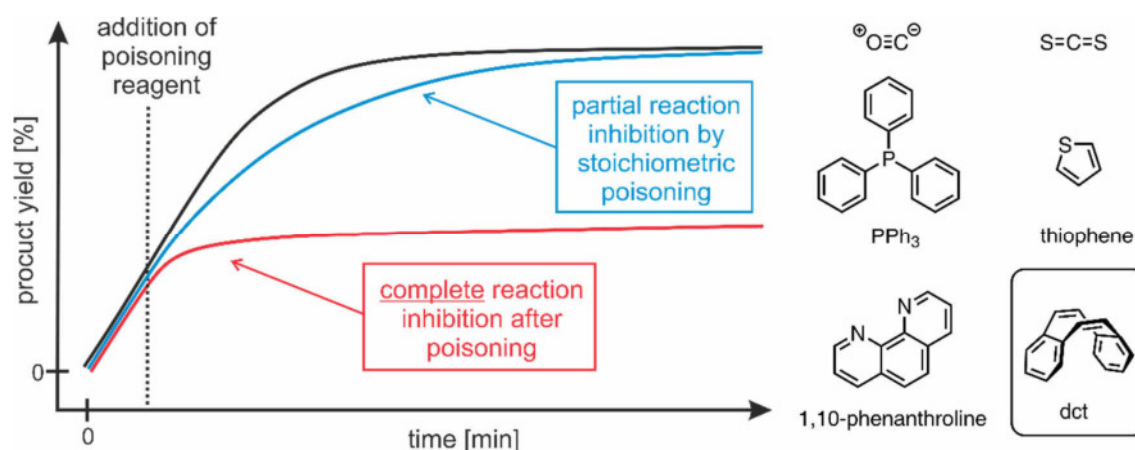
Figure 1.7   Left: Reaction profile of a catalytic reaction: i) without poisoning (black), ii) with ineffective poisoning (blue), and iii) completely inhibited after addition of the poisoning reagent. Right: selected catalyst poisoning reagents.

surfaces. Therefore, an inhibition of a hydrogenation reaction by dct is strong evidence for a homogeneous mechanism and complements the mercury test. It should be noted that dct was mainly tested for group VIII metals so far. Furthermore, the demanding, multi-step synthesis route is a drawback of this reagent.[75]

1.2.4   Stoichiometric Reactions

For a better understanding of a homogeneous, molecular catalyst, it is important to characterize reactive intermediates.[68] If such a species was detected by NMR or other techniques, its isolation for further investigations should be focused. Such a fully characterized intermediate, which has incorporated a substrate instead of its former ligand for example, can be an important building block for a postulated mechanism. Furthermore, the synthesis of compounds formed by stoichiometric reaction of a molecular catalyst with a catalyst poison like PPh$_3$ or dct might be revealing for additional examinations. If the isolation and characterization of such a reaction product succeeds, its behavior under reaction conditions can be further investigated. In activity studies, for example, a designated intermediate of the catalytic cycle should also show some catalytic activity. In contrast, the isolated product of the reaction of a molecular catalyst with a catalyst poison is not expected to show any reactivity. Especially with regard to application or tuning of catalytic properties such knowledge is essential.

1.2.5   Filtration Experiments

A comparison of the activity of a filtered reaction solution and an untreated one can give further insight. A bulk metal catalyst is adsorbed on a high-surface filter aid like Celite or powdered graphite. Afterwards the remaining catalytic activity of the filtrate and of the solid residue can be compared. If both media feature catalytic activity, this indicates that both a homogeneous

besides a heterogeneous catalyst is operational. Ideally, this method allows a determination of a relative contribution of the two mechanistic pathways. If a homogeneous catalyst is assumed, filtration through a small-pore membrane filter can be implemented for the separation. There are some drawbacks of this test, for example, control experiments with authentic homogeneous and heterogeneous catalyst systems are necessary. Moreover, a formation of catalytically active heterogeneous species from a molecular catalyst after contact with the filter aid is possible.[66]

1.2.6 Summary

A detailed understanding of mechanistic processes is necessary for the development of effective homogeneous and heterogeneous catalysts. Since many modern catalysts (e.g. metal clusters or nanoparticles) are blurring the borders between homogeneous and heterogeneous catalysis, the differentiation is often a challenging task. Therefore, several methods were established to discriminate the two general catalytic pathways. Figure 1.8 gives a brief overview of the various methods that can be used. It is most important to note that none of these methods is reliable and definitive by itself, yet it is essential to combine as many of these techniques as possible. As stated by J. Widegreen and R. Finke: *"the identity of the true catalyst must be consistent with all the data"*.[66]
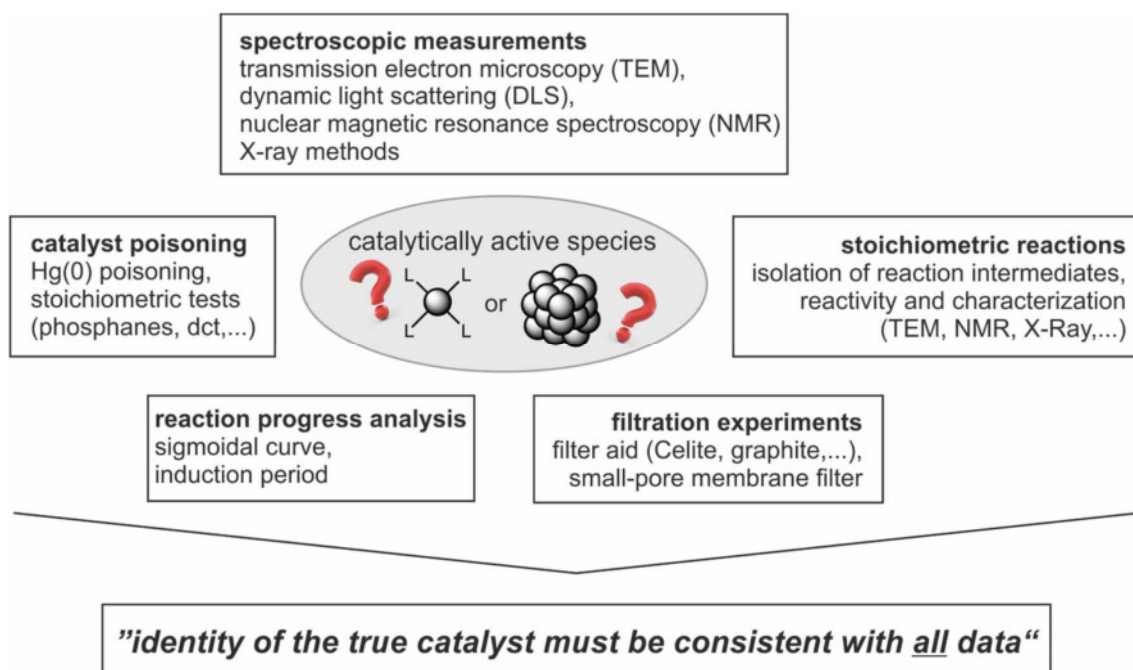

Figure 1.8   Overview about some different methods and techniques for the determination between homogeneous and heterogeneous transition metal catalysis.

1.3   References

[1]   a) *Catalytic Hydrogenation* (Ed.: L. Cerveny), Elsevier, Amsterdam, **1986**; b) *The Handbook of Homogeneous Hydrogenation* (Eds.: J. G. de Vries, C. J. Elsevier), Wiley-VCH, Weinheim, **2007**.

[2]   a) P. Sabatier, J. B. Senderens, *C. R. Hebd. Séances Acad. Sci.* **1897**, *124*, 616-618; b) P. Sabatier, J. B. Senderens, *C. R. Hebd. Séances Acad. Sci.* **1897**, *124*, 1358-1361.

[3]   „The Nobel Prize in Chemistry 1912" Nobelprize.org. Nobel Media AB 2019. Fri. 12 Apr 2019. http://www.nobelprize.org/prizes/chemistry/1912/summary/

[4]   a) F. Fischer, H. Tropsch, Ber. Dtsch. Chem. Ges. B **1926**, 59, 830–831; b) F. Franz, T. Hans, "Process for the Production of Paraffin-Hydrocarbons with More than One Carbon Atom", **1930**, Patent US1746464A.

[5]   a) H. Lindlar, *Helv. Chim. Acta* **1952**, *35*, 446–450; b) J. A. Osborn, F. H. Jardine, J. F. Young, G. Wilkinson, *J. Chem. Soc. A* **1966**, *0*, 1711-1732; c) R. Crabtree, *Acc. Chem. Res.* **1979**, *12*, 331–337.

[6]   a) W. S. Knowles, M. J. Sabacky, B. D. Vineyard, D. J. Weinkauff, *J. Am. Chem. Soc.* **1975**, *97*, 2567–2568; b) H. Doucet, T. Ohkuma, K. Murata, T. Yokozawa, M. Kozawa, E. Katayama, A. F. England, T. Ikariya, R. Noyori, *Angew. Chem. Int. Ed.* **1998**, *37*, 1703–1707.

[7]   "The Nobel Prize in Chemistry 2001" Nobelprize.org. Nobel Media AB 2019. Thu. 11 Apr 2019. http://www.nobelprize.org/prizes/chemistry/2001/summary/

[8]   a) S. Enthaler, K. Junge, M. Beller, *Angew. Chem. Int. Ed.* **2008**, *47*, 3317–3321; b) P. J. Chirik, *Acc. Chem. Res.* **2015**, *48*, 1687–1695.

[9]   a) W. Hess, J. Treutwein, G. Hilt, *Synthesis* **2008**, *2008*, 3537–3562; b) M. S. Holzwarth, B. Plietker, *ChemCatChem* **2013**, *5*, 1650–1679.

[10] W. Ai, R. Zhong, X. Liu, Q. Liu, *Chem. Rev.* **2019**, *119*, 2876–2953.

[11] E. N. Frankel, E. P. Jones, V. L. Davison, E. Emken, H. J. Dutton, *J. Am. Oil Chem. Soc.* **1965**, *42*, 130–134.

[12] H. M. Feder, J. Halpern, *J. Am. Chem. Soc.* **1975**, *97*, 7186–7188.

[13] E. L. Muetterties, F. J. Hirsekorn, *J. Am. Chem. Soc.* **1974**, *96*, 4063–4064.

[14] F. J. Hirsekorn, M. C. Rakowski, E. L. Muetterties, *J. Am. Chem. Soc.* **1975**, *97*, 237–238.

[15] a) M. Hidai, T. Kuse, T. Hikita, Y. Uchida, A. Misono, *Tetrahedron Lett.* **1970**, *11*, 1715–1716; b) G. F. Pregaglia, A. Andreetta, G. F. Ferrari, R. Ugo, *J. Organomet. Chem.* **1971**, *30*, 387–405; c) G. F. Ferrari, A. Andreetta, G. F. Pregaglia, R. Ugo, *J. Organomet. Chem.* **1972**, *43*, 209–212.

[16] Q. Knijnenburg, A. D. Horton, H. van der Heijden, T. M. Kooistra, D. G. H. Hetterscheid, J. M. M. Smits, B. de Bruin, P. H. M. Budzelaar, A. W. Gal, *J. Mol. Catal. A: Chem.* **2005**, *232*, 151–159.

[17] C.-C. Tai, T. Chang, B. Roller, P. G. Jessop, *Inorg. Chem.* **2003**, *42*, 7340–7341.

[18] C. Federsel, C. Ziebart, R. Jackstell, W. Baumann, M. Beller, *Chem. Eur. J.* **2012**, *18*, 72–75.

[19] a) J. R. Cabrero-Antonino, R. Adam, K. Junge, R. Jackstell, M. Beller, *Catal. Sci. Technol.* **2017**, *7*, 1981–1985; b) R. Adam, J. R. Cabrero-Antonino, A. Spannenberg, K. Junge, R. Jackstell, M. Beller, *Angew.*

Chem. Int. Ed. **2017**, *56*, 3216–3220; c) R. Adam, C. B. Bheeter, J. R. Cabrero-Antonino, K. Junge, R. Jackstell, M. Beller, *ChemSusChem* **2017**, *10*, 842–846.

[20] Selected examples: a) M. S. Jeletic, M. T. Mock, A. M. Appel, J. C. Linehan, *J. Am. Chem. Soc.* **2013**, *135*, 11533–11536; b) M. S. Jeletic, M. L. Helm, E. B. Hulley, M. T. Mock, A. M. Appel, J. C. Linehan, *ACS Catal.* **2014**, *4*, 3755–3762; c) A. Z. Spentzos, C. L. Barnes, W. H. Bernskoetter, *Inorg. Chem.* **2016**, *55*, 8225–8233; d) S. A. Burgess, K. Grubel, A. M. Appel, E. S. Wiedner, J. C. Linehan, *Inorg. Chem.* **2017**, *56*, 8580–8589; e) J. Schneidewind, R. Adam, W. Baumann, R. Jackstell, M. Beller, *Angew. Chem. Int. Ed.* **2017**, *56*, 1890–1893; f) L. Wang, L. Wang, J. Zhang, X. Liu, H. Wang, W. Zhang, Q. Yang, J. Ma, X. Dong, S. J. Yoo, J.-G. Kim, X. Meng, F.-S. Xiao, *Angew. Chem. Int. Ed.* **2018**, *57*, 6104–6108.

[21] T. J. Korstanje, J. I. van der Vlugt, C. J. Elsevier, B. de Bruin, *Science* **2015**, *350*, 298–302.

[22] S. Monfette, Z. R. Turner, S. P. Semproni, P. J. Chirik, *J. Am. Chem. Soc.* **2012**, *134*, 4561–4564.

[23] C. Bianchini, G. Mantovani, A. Meli, F. Migliacci, F. Zanobini, F. Laschi, A. Sommazzi, *Eur. J. Inorg. Chem.* **2003**, *2003*, 1620–1631.

[24] a) K. H. Hopmann, *Organometallics* **2013**, *32*, 6388–6399; b) M. R. Friedfeld, M. Shevlin, G. W. Margulieux, L.-C. Campeau, P. J. Chirik, *J. Am. Chem. Soc.* **2016**, *138*, 3314–3324.

[25] a) M. R. Friedfeld, M. Shevlin, J. M. Hoyt, S. W. Krska, M. T. Tudge, P. J. Chirik, *Science* **2013**, *342*, 1076–1080; b) M. R. Friedfeld, G. W. Margulieux, B. A. Schaefer, P. J. Chirik, *J. Am. Chem. Soc.* **2014**, *136*, 13178–13181; c) M. R. Friedfeld, H. Zhong, R. T. Ruck, M. Shevlin, P. J. Chirik, *Science* **2018**, *360*, 888–893; d) G. R. Morello, H. Zhong, P. J. Chirik, K. H. Hopmann, *Chem. Sci.* **2018**, *9*, 4977–4982.

[26] J. Camacho-Bunquin, M. J. Ferguson, J. M. Stryker, *J. Am. Chem. Soc.* **2013**, *135*, 5537–5540.

[27] a) G. Zhang, B. L. Scott, S. K. Hanson, *Angew. Chem. Int. Ed.* **2012**, *51*, 12102–12106; b) G. Zhang, K. V. Vasudevan, B. L. Scott, S. K. Hanson, *J. Am. Chem. Soc.* **2013**, *135*, 8668–8681; c) G. Zhang, S. K. Hanson, *Chem. Commun.* **2013**, *49*, 10151–10153; d) G. Zhang, Z. Yin, J. Tan, *RSC Adv.* **2016**, *6*, 22419–22423.

[28] a) R. Xu, S. Chakraborty, H. Yuan, W. D. Jones, *ACS Catal.* **2015**, *5*, 6350–6354; b) J. Yuwen, S. Chakraborty, W. W. Brennessel, W. D. Jones, *ACS Catal.* **2017**, *7*, 3735–3740.

[29] S. Rösler, J. Obenauf, R. Kempe, *J. Am. Chem. Soc.* **2015**, *137*, 7998–8001.

[30] D. Srimani, A. Mukherjee, A. F. G. Goldberg, G. Leitus, Y. Diskin-Posner, L. J. W. Shimon, Y. Ben David, D. Milstein, *Angew. Chem. Int. Ed.* **2015**, *54*, 12357–12360.

[31] a) T.-P. Lin, J. C. Peters, *J. Am. Chem. Soc.* **2013**, *135*, 15310–15313; b) T.-P. Lin, J. C. Peters, *J. Am. Chem. Soc.* **2014**, *136*, 13672–13683.

[32] J. K. Pagano, J. P. W. Stelmach, R. Waterman, *Dalton Trans.* **2015**, *44*, 12074–12077.

[33] a) K. Tokmic, C. R. Markus, L. Zhu, A. R. Fout, *J. Am. Chem. Soc.* **2016**, *138*, 11907–11913; b) K. Tokmic, A. R. Fout, *J. Am. Chem. Soc.* **2016**, *138*, 13700–13705.

[34] K. Tokmic, B. J. Jackson, A. Salazar, T. J. Woods, A. R. Fout, *J. Am. Chem. Soc.* **2017**, *139*, 13554–13561.

[35] Selected examples: a) R. P. Yu, J. M. Darmon, C. Milsmann, G. W. Margulieux, S. C. E. Stieber, S. DeBeer, P. J. Chirik, *J. Am. Chem. Soc.* **2013**, *135*, 13168–13184; b) A. Mukherjee, D. Srimani, S. Chakraborty, Y. Ben-David, D. Milstein, *J. Am. Chem. Soc.* **2015**, *137*, 8888–8891; c) J. Chen, C. Chen,

C. Ji, Z. Lu, *Org. Lett.* **2016**, *18*, 1594–1597; d) V. G. Landge, J. Pitchaimani, S. P. Midya, M. Subaramanian, V. Madhu, E. Balaraman, *Catal. Sci. Technol.* **2018**, *8*, 428–433; e) K. Junge, B. Wendt, A. Cingolani, A. Spannenberg, Z. Wei, H. Jiao, M. Beller, *Chem. Eur. J.* **2018**, *24*, 1046–1052; f) M. R. Mills, C. L. Barnes, W. H. Bernskoetter, *Inorg. Chem.* **2018**, *57*, 1590–1597; g) P. Puylaert, A. Dell'Acqua, F. E. Ouahabi, A. Spannenberg, T. Roisnel, L. Lefort, S. Hinze, S. Tin, J. G. de Vries, *Catal. Sci. Technol.* **2019**, *9*, 61–64.

[36]   Z. Shao, S. Fu, M. Wei, S. Zhou, Q. Liu, *Angew. Chem. Int. Ed.* **2016**, *55*, 14653–14657.

[37]   S. Fu, N.-Y. Chen, X. Liu, Z. Shao, S.-P. Luo, Q. Liu, *J. Am. Chem. Soc.* **2016**, *138*, 8588–8594.

[38]   A. Enachi, D. Baabe, M.-K. Zaretzke, P. Schweyen, M. Freytag, J. Raeder, M. D. Walter, *Chem. Commun.* **2018**, *54*, 13798–13801.

[39]   a) W. W. Brennessel, V. G. Young Jr., J. E. Ellis, *Angew. Chem. Int. Ed* **2002**, *41*, 1211–1215; b) W. W. Brennessel, R. E. Jilek, J. E. Ellis, *Angew. Chem. Int. Ed.* **2007**, *46*, 6132–6136.

[40]   D. Gärtner, A. Welther, B. R. Rad, R. Wolf, A. Jacobi von Wangelin, *Angew. Chem. Int. Ed.* **2014**, *53*, 3722–3726.

[41]   S.-B. Wu, T. Zhang, L. W. Chung, Y.-D. Wu, *Org. Lett.* **2019**, *21*, 360–364.

[42]   Selected examples: a) C. A. Drake, "Catalytic Hydrogenation of Unsaturated Dinitriles", **1975**, Patent US3880929A; b) R. C. Reuel, C. H. Bartholomew, *J. Catal.* **1984**, *85*, 78–88; c) L. Fu, C. H. Bartholomew, *J. Catal.* **1985**, *92*, 376–387; d) M. J. Harper, "Raney Cobalt Catalyst and a Process for Hydrogenating Organic Compounds Using Said Catalyst", **2000**, Patent US6156694A.

[43]   R. L. Pruett, "Process for Producing Nickel and Cobalt Hydrogenation Catalysts",Patent **1961**, Patent US2999075A.

[44]   a) W. Reeve, J. Christian, *J. Am. Chem. Soc.* **1956**, 78, 860-861; b) B. V. Aller, *J. App. Chem.* **1958**, *8*, 492–495.

[45]   K. Tanaka, H. Nihira, A. Ozaki, *J. Phys. Chem.* **1970**, *74*, 4510–4517.

[46]   W. M. Alley, I. K. Hamdemir, Q. Wang, A. I. Frenkel, L. Li, J. C. Yang, L. D. Menard, R. G. Nuzzo, S. Özkar, K.-H. Yih, K. A. Johnson, R. G. Finke, *Langmuir* **2011**, *27*, 6279–6294.

[47]   S. U. Son, K. H. Park, Y. K. Chung, *Org. Lett.* **2002**, *4*, 3983–3986.

[48]   F. A. Westerhaus, R. V. Jagadeesh, G. Wienhöfer, M.-M. Pohl, J. Radnik, A.-E. Surkus, J. Rabeah, K. Junge, H. Junge, M. Nielsen, A. Brückner, M. Beller, *Nat. Chem.* **2013**, *5*, 537–543.

[49]   F. Chen, A.-E. Surkus, L. He, M.-M. Pohl, J. Radnik, C. Topf, K. Junge, M. Beller, *J. Am. Chem. Soc.* **2015**, *137*, 11718–11724.

[50]   J. Long, Y. Zhou, Y. Li, *Chem. Commun.* **2015**, *51*, 2331–2334.

[51]   Z. Wei, Y. Chen, J. Wang, D. Su, M. Tang, S. Mao, Y. Wang, *ACS Catal.* **2016**, *6*, 5816–5822.

[52]   Z. Wei, J. Wang, S. Mao, D. Su, H. Jin, Y. Wang, F. Xu, H. Li, Y. Wang, *ACS Catal.* **2015**, *5*, 4783–4789.

[53]   a) T. Schwob, R. Kempe, *Angew. Chem. Int. Ed.* **2016**, *55*, 15175–15179; b) B. Chen, F. Li, Z. Huang, G. Yuan, *ChemCatChem* **2016**, *8*, 1132–1138.

[54]   F. Chen, C. Topf, J. Radnik, C. Kreyenschulte, H. Lund, M. Schneider, A.-E. Surkus, L. He, K. Junge, M. Beller, *J. Am. Chem. Soc.* **2016**, *138*, 8781–8788.

[55] Examples for hydrogenation reactions with heterogeneous catalysts, obtained from pyrolysis of cobalt precursors by Beller and co-workers: a) R. V. Jagadeesh, T. Stemmler, A.-E. Surkus, M. Bauer, M.-M. Pohl, J. Radnik, K. Junge, H. Junge, A. Brückner, M. Beller, *Nat. Protoc.* **2015**, *10*, 916–926; b) R. V. Jagadeesh, D. Banerjee, P. Beatrice Arockiam, H. Junge, K. Junge, M.-M. Pohl, J. Radnik, A. Brückner, M. Beller, *Green Chem.* **2015**, *17*, 898–902; c) F. A. Westerhaus, I. Sorribes, G. Wienhöfer, K. Junge, M. Beller, *Synlett* **2015**, *26*, 313–317; d) D. Formenti, C. Topf, K. Junge, F. Ragaini, M. Beller, *Catal. Sci. Technol.* **2016**, *6*, 4473–4477; e) F. Chen, B. Sahoo, C. Kreyenschulte, H. Lund, M. Zeng, L. He, K. Junge, M. Beller, *Chem. Sci.* **2017**, *8*, 6239–6246; f) B. Sahoo, D. Formenti, C. Topf, S. Bachmann, M. Scalone, K. Junge, M. Beller, *ChemSusChem* **2017**, *10*, 3035–3039; g) D. Formenti, F. Ferretti, C. Topf, A.-E. Surkus, M.-M. Pohl, J. Radnik, M. Schneider, K. Junge, M. Beller, F. Ragaini, *J. Catal.* **2017**, *351*, 79–89; h) F. K. Scharnagl, M. F. Hertrich, F. Ferretti, C. Kreyenschulte, H. Lund, R. Jackstell, M. Beller, *Sci. Adv.* **2018**, *4*, eaau1248; i) R. Ferraccioli, D. Borovika, A.-E. Surkus, C. Kreyenschulte, C. Topf, M. Beller, *Catal. Sci. Technol.* **2018**, *8*, 499–507.

[56] R. V. Jagadeesh, K. Murugesan, A. S. Alshammari, H. Neumann, M.-M. Pohl, J. Radnik, M. Beller, *Science* **2017**, *358*, 326–332.

[57] Selected examples about heterogeneous cobalt-catalyzed hydrogenation reactions with polar substrates: a) S. K. Mohapatra, S. U. Sonavane, R. V. Jayaram, P. Selvam, *Tetrahedron Lett.* **2002**, *43*, 8527–8529; b) Q. Liu, X. Guo, J. Chen, J. Li, W. Song, W. Shen, *Nanotechnology* **2008**, *19*, 365608; c) K. Manna, T. Zhang, M. Carboni, C. W. Abney, W. Lin, *J. Am. Chem. Soc.* **2014**, *136*, 13182–13185; d) M. Audemar, C. Ciotonea, K. De Oliveira Vigier, S. Royer, A. Ungureanu, B. Dragoi, E. Dumitriu, F. Jérôme, *ChemSusChem* **2015**, *8*, 1885–1891; e) P. Ji, K. Manna, Z. Lin, X. Feng, A. Urban, Y. Song, W. Lin, *J. Am. Chem. Soc.* **2017**, *139*, 7004–7011; f) X. Sun, A. I. Olivos-Suarez, L. Oar-Arteta, E. Rozhko, D. Osadchii, A. Bavykina, F. Kapteijn, J. Gascon, *ChemCatChem* **2017**, *9*, 1854–1862; g) Y. Duan, T. Song, X. Dong, Y. Yang, *Green Chem.* **2018**, *20*, 2821–2828; h) P. Patel, S. Nandi, M. S. Maru, R. I. Kureshy, N. H. Khan, *J. CO2 Util.* **2018**, *25*, 310–314; i) B. S. Kumar, A. J. Amali, K. Pitchumani, *Mol. Catal.* **2018**, *448*, 153–161; j) S. Song, D. Wang, L. Di, C. Wang, W. Dai, G. Wu, N. Guan, L. Li, *Chin. J. Catal.* **2018**, *39*, 250–257; k) X. Sun, A. I. Olivos-Suarez, D. Osadchii, M. J. V. Romero, F. Kapteijn, J. Gascon, *J. Catal.* **2018**, *357*, 20–28; l) J. Wang, R. Nie, L. Xu, X. Lyu, X. Lu, *Green Chem.* **2019**, *21*, 314–320; m) W. Li, J. Artz, C. Broicher, K. Junge, H. Hartmann, A. Besmehn, R. Palkovits, M. Beller, *Catal. Sci. Technol.* **2019**, *9*, 157–162.

[58] For more examples of heterogeneous cobalt-catalyzed hydrogenation of polar bonds also see references [55a-g] and [55i].

[59] F. Chen, C. Kreyenschulte, J. Radnik, H. Lund, A.-E. Surkus, K. Junge, M. Beller, *ACS Catal.* **2017**, *7*, 1526–1532.

[60] C. Chen, Y. Huang, Z. Zhang, X.-Q. Dong, X. Zhang, *Chem. Commun.* **2017**, *53*, 4612–4615.

[61] S. Sandl, F. Schwarzhuber, S. Pöllath, J. Zweck, A. Jacobi von Wangelin, *Chem. Eur. J.* **2018**, *24*, 3403–3407.

[62] a) Y.-C. Lin, G. W. Huber, *Energy Environ. Sci.* **2009**, *2*, 68–80; b) C. Copéret, M. Chabanas, R. P. Saint-Arroman, J.-M. Basset, *Angew. Chem. Int. Ed.* **2003**, *42*, 156–181.

[63] a) S. T. Oyama, G. A. Somorjai, *J. Chem. Educ.* **1988**, *65*, 765; b) J. M. Thomas, R. J. P. Williams, *Phil. Trans. R. Soc. A* **2005**, 363, 765–791; c) D. Astruc, F. Lu, J. R. Aranzaes, *Angew. Chem. Int. Ed.* **2005**, *44*, 7852–7872.

[64] *Metal-Catalysis in Industrial Organic Processes* (Ed.: G. P. Chiusoli, P. M. Maitlis), The Royal Society of Chemistry, Cambridge, **2006**.

[65] a) D. Astruc, F. Lu, J. R. Aranzaes, *Angew. Chem. Int. Ed.* **2005**, *44*, 7852–7872; b) C. A. Witham, W. Huang, C.-K. Tsung, J. N. Kuhn, G. A. Somorjai, F. D. Toste, *Nat. Chem.* **2010**, *2*, 36–41; c) A. Corma, H. Garcia, *Top. Catal.* **2008**, *48*, 8–31; d) S. Shylesh, V. Schünemann, W. R. Thiel, *Angew. Chem. Int. Ed.* **2010**, *49*, 3428–3459; e) J. G. de Vries, in *Selective Nanocatalysts and Nanoscience* (Ed.: A. Zecchina, S. Bordiga, E. Groppo), Wiley-VCH, Weinheim, **2011**, pp. 73–103.

[66] J. A. Widegren, R. G. Finke, *J. Mol. Catal. A* **2003**, *198*, 317–341.

[67] R. H. Crabtree, *Chem. Rev.* **2012**, *112*, 1536–1554.

[68] J. F. Sonnenberg, R. H. Morris, *Catal. Sci.Technol.* **2014**, *4*, 3426–3438.

[69] V. Artero, M. Fontecave, *Chem. Soc. Rev.* **2013**, *42*, 2338–2356.

[70] E. Bayram, J. C. Linehan, J. L. Fulton, J. A. S. Roberts, N. K. Szymczak, T. D. Smurthwaite, S. Özkar, M. Balasubramanian, R. G. Finke, *J. Am. Chem. Soc.* **2011**, *133*, 18889–18902.

[71] a) Ö. Metin, S. Özkar, *Int. J. Hydrog. Energy* **2007**, 32, 1707–1715; b) Ö. Metin, S. Özkar, *Int. J. Hydrog. Energy* **2011**, 36, 1424–1432.

[72] a) R. B. Bedford, M. Betham, D. W. Bruce, S. A. Davis, R. M. Frost, M. Hird, *Chem. Commun.* **2006**, *0*, 1398–1400; b) C. Rangheard, C. de J. Fernández, P.-H. Phua, J. Hoorn, L. Lefort, J. G. de Vries, *Dalton Trans.* **2010**, *39*, 8464–8471.

[73] P. Paklepa, J. Woroniecki, P. K. Wrona, *J. Electroanal. Chem.* **2001**, *498*, 181–191.

[74] a) D. R. Anton, R. H. Crabtree, *Organometallics* **1983**, *2*, 621–627; b) D. R. Anton, R. H. Crabtree, *Organometallics* **1983**, *2*, 855–859.

[75] a) S. Chaffins, M. Brettreich, F. Wudl, *Synthesis* **2002**, *2002*, 1191–1194; b) G. Franck, M. Brill, G. Helmchen, *Org. Synt.* **2014**, 55–65; c) S. Sandl, A. Jacobi von Wangelin, "Dibenzo[a,e]cyclooctatetraene" in *Encyclopedia of Organic Reagents*, John Wiley & Sons, New York, USA, **2019**.

2 ALKENE COBALTATES AS HYDROGENATION CATALYSTS

PHILIPP BÜSCHELBERGER, DOMINIK GÄRTNER,

EFRAIN REYES-RODRIGUEZ, FRIEDRICH KREYENSCHMIDT,

KONRAD KOSZINOWSKI, AXEL JACOBI VON WANGELIN, AND ROBERT WOLF
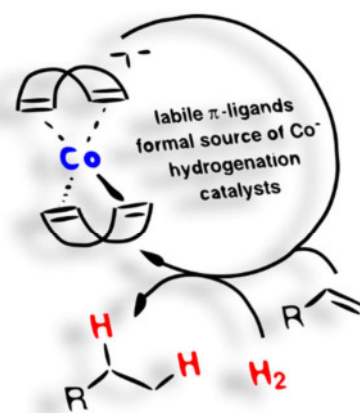
A series of six alkene and arene cobaltates were prepared and studied as pre-catalysts in hydrogenation reactions. Excellent catalytic activities in olefin hydrogenations were observed. The catalyst activation mechanism by redox-neutral π-ligand exchange was monitored by NMR and ESI-MS experiments. With carbonyl substrates, catalyst species of higher oxidation states are likely formed by SET and deprotonation reactions.

2.1   Introduction

Metal-catalyzed hydrogenations are among the largest technical processes and constitute key operations in numerous chemical syntheses.[1] Over the past decades, the use of highly active platinum group metal catalysts has grown to maturity which enabled efficient hydrogenations of unsaturated C=C and C=X bonds.[2] Apart from nickel,[3] 3d transition metal catalysts have received much less attention despite their higher abundance and often lower toxicity.[4] The emphasis on stringent economic and environmental criteria has placed the development of sustainable hydrogenation methods with base-metal catalysts into the limelight of current research activities.[5] Great progress was only recently made with the development of low-valent iron group metal catalysts (Fe, Co, Ni) for olefin hydrogenations under very mild reaction conditions. Special ligand architectures allowed the stabilization of the catalytically active species in low oxidation states. Budzelaar and coworkers reported the first application of (pyridyldiimine)cobalt catalysts to hydrogenations of mono- and disubstituted olefins (Figure 2.1, left).[6] Significantly, Chirik and coworkers introduced new catalyst derivatives and expanded the scope to include bulky alkenes; they were also able to hydrogenate geminal-disubstituted olefins enantioselectively (Figure 2.1, left).[7] Hanson and coworkers reported PNP-pincer cobalt complexes to be active in the hydrogenation of alkenes, aldehydes, ketones, and imines and to undergo transfer hydrogenations (Figure 2.1, middle left).[8] Iron and cobalt complexes bearing bis(phosphine) ligands were also used for (asymmetric) alkene hydrogenation (Figure 2.1, middle right), while a catalyst with a tridentate tris(phosphane) (= triphos) ligand was shown to reduce esters and carboxylic acids.[9, 10]

To date there are many more examples especially for PNP-pincer complexes which show impressive catalytic activities.[11] Recently, the groups of Kempe and Kirchner used PNP-pincer cobalt and iron complexes for selective hydrogenations of polar bonds with high tolerance of other unsaturated bonds.[12] Moreover, effective cobalt catalysts based on NNP-, PBP-, and CCC-pincers have been reported.[13, 14, 15]
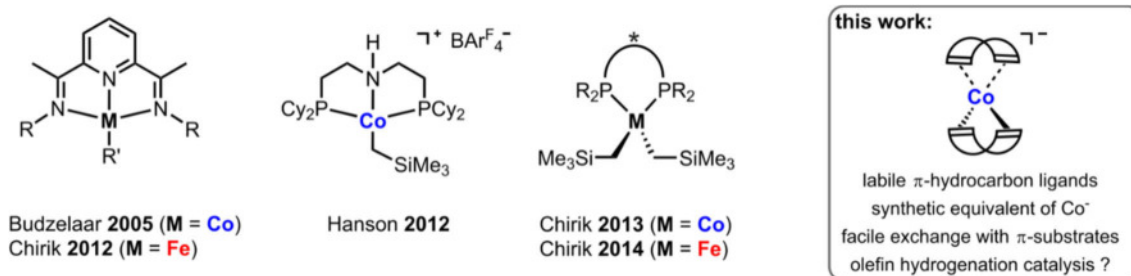

Figure 2.1   Earlier established cobalt- and iron-based hydrogenation catalysts (on the left) and the design concept of simple alkene metalate pre-catalysts (box).

Arenes are one of the most abundant and versatile classes of unsaturated organic compounds and also entertain a rich coordination chemistry with low-valent transition metals.[16, 17] Our groups recently initiated a research program aiming at the development of metalate catalysts that bear simple and cheap arenes as stabilizing ligand motifs (Figure 2.1, box).[18] Initial experiments focused on the homoleptic bis(anthracene) cobaltate **1** and -ferrate **A** originally reported by Ellis and coworkers.[18, 19] The closed-shell 18-electron complex **1** constitute an isolable representative of a homogeneous Co$^-$ source.[17]

The bis(anthracene) metalates **1** and **A** exhibited good activity in hydrogenations of various alkenes under mild conditions; cobaltate **1** was also active in catalytic hydrogenations of alkynes, ketones, and imines.[18] Based on our preliminary mechanistic investigations with this pre-catalyst, we postulated a new catalytic approach to hydrogenation reactions which involves *(i)* the facile synthetic access to a variety of modular catalyst compositions from simple starting materials (alkene/arene, metal salt, reductant), *(ii)* the presence of highly reduced, anionic cobalt species, providing sufficient reducing power for the key H$_2$ activation, *(iii)* the presence of a cheap hydrocarbon ligand that can be easily replaced with the structurally very similar substrates of olefin hydrogenations. The exchange of the labile π-ligands with the substrates is redox-neutral, requires only little structural reorganization, and can in principle be traceless, if the ligands undergo complete hydrogenation themselves under the reaction conditions (Scheme 2.1).

In an effort to explore the scope of this new mechanistic paradigm further, we prepared a series of mono-anionic alkene/arene metalates and studied their catalytic activity in alkene hydrogenations. Because of the superior catalytic activity of **1** over **A** and the better possibility of spectroscopic examination we focused on different cobaltate complexes. Here, we give a full account of these catalytic studies and describe the results of reaction monitoring and poisoning
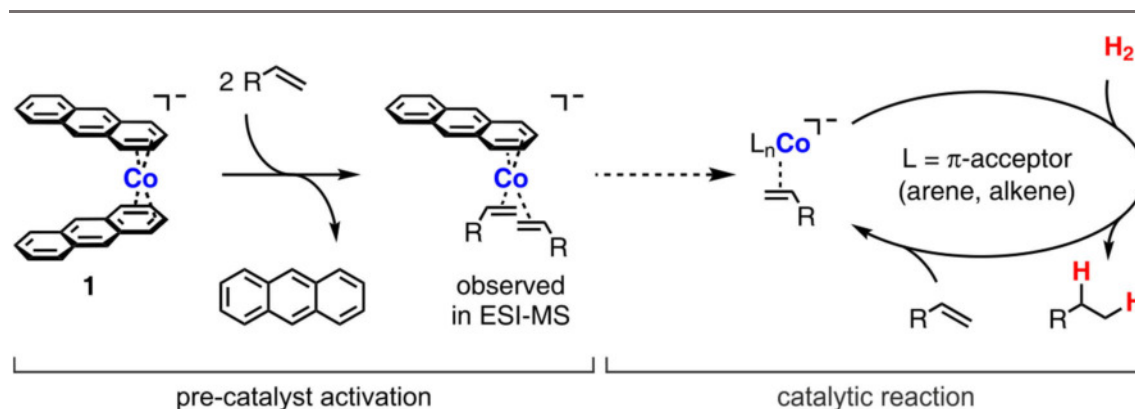
Scheme 2.1   Catalytic concept: Activation of arene cobaltate pre-catalysts by π-ligand exchange with olefinic substrates followed by hydrogenation reaction in presence of an excess of substrate and dihydrogen.

experiments designed to reveal the catalyst activation step and the homogeneous or heterogeneous nature of the catalytically active species.

2.2   Results and Discussion

2.2.1   Pre-Catalyst Syntheses

$[K(dme)_2][Co(C_{14}H_{10})_2]$ **1** ($C_{14}H_{10}$ = anthracene) was prepared in good yields according to the method by Ellis and coworkers by reduction of the cobalt dibromide with potassium in the presence of anthracene (Scheme 2.2a).[19, 20, 21] In a similar manner, treatment of the *in situ* prepared $[Co(C_{10}H_8)_2]^-$ ($C_{10}H_8$ = naphthalene) with one equivalent of 1,5-cyclooctadiene (= cod) gave the heteroleptic complex $[K([18]crown-6)][Co(C_{10}H_8)(cod)]$ (**2**) (Scheme 2.2c).[21] Following a protocol of Jonas and coworkers, we synthesized the homoleptic $[K(thf)_{0.2}][Co(cod)_2]$ (**3**) by reduction of cobaltocene with a slight excess of potassium in the presence of 3 equiv. of cod in THF (Scheme 2.2b).[22] Upon ligand exchange of **2** or **3** with styrene, we succeeded in the first preparation of the heteroleptic complex $[K([18]crown-6)][Co(cod)(styrene)_2]$ (**4**), which constitutes a potential intermediate of styrene hydrogenations with cobaltate pre-catalysts (Figure 2.2).

Reaction of $[K([18]crown-6)][Co(C_{10}H_8)(cod)]$ (**2**) with 2.2 equiv. of styrene in THF at room temperature gave the bis(styrene) complex **4** in 61% yield (Figure 2.2, top). The analogous reaction of $[K(thf)_{0.2}][Co(cod)_2]$ (**3**) with styrene in THF at room temperature required a large excess of styrene (30 equiv.) and addition of [18]crown-6 to allow the isolation of the pure bis(styrene) complex **4** in 70% crystalline yield. Isolation of a solid product was not possible in the absence of the crown ether. The formation of a putative homoleptic complex $[Co(styrene)_4]^-$
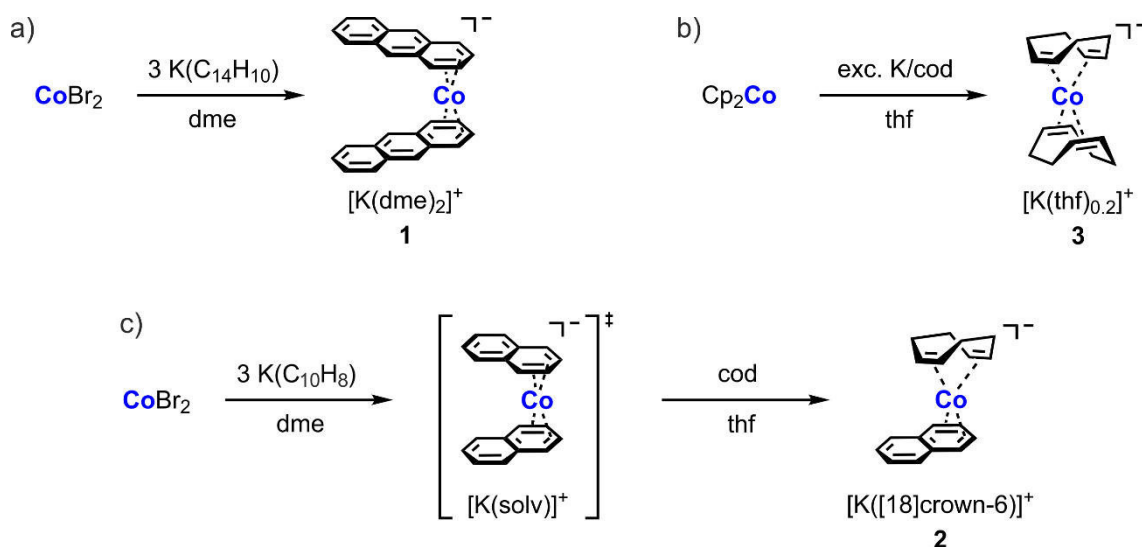
Scheme 2.2   Syntheses of cobaltate pre-catalysts according to literature procedures: a) $[K(dme)_2][Co(C_{14}H_{10})_2]$ **1**, b) $[K(thf)_{0.2}][Co(cod)_2]$ **2**, and c) $[K([18]crown-6)][Co(C_{10}H_8)(cod)]$ (**2**).[19, 20]
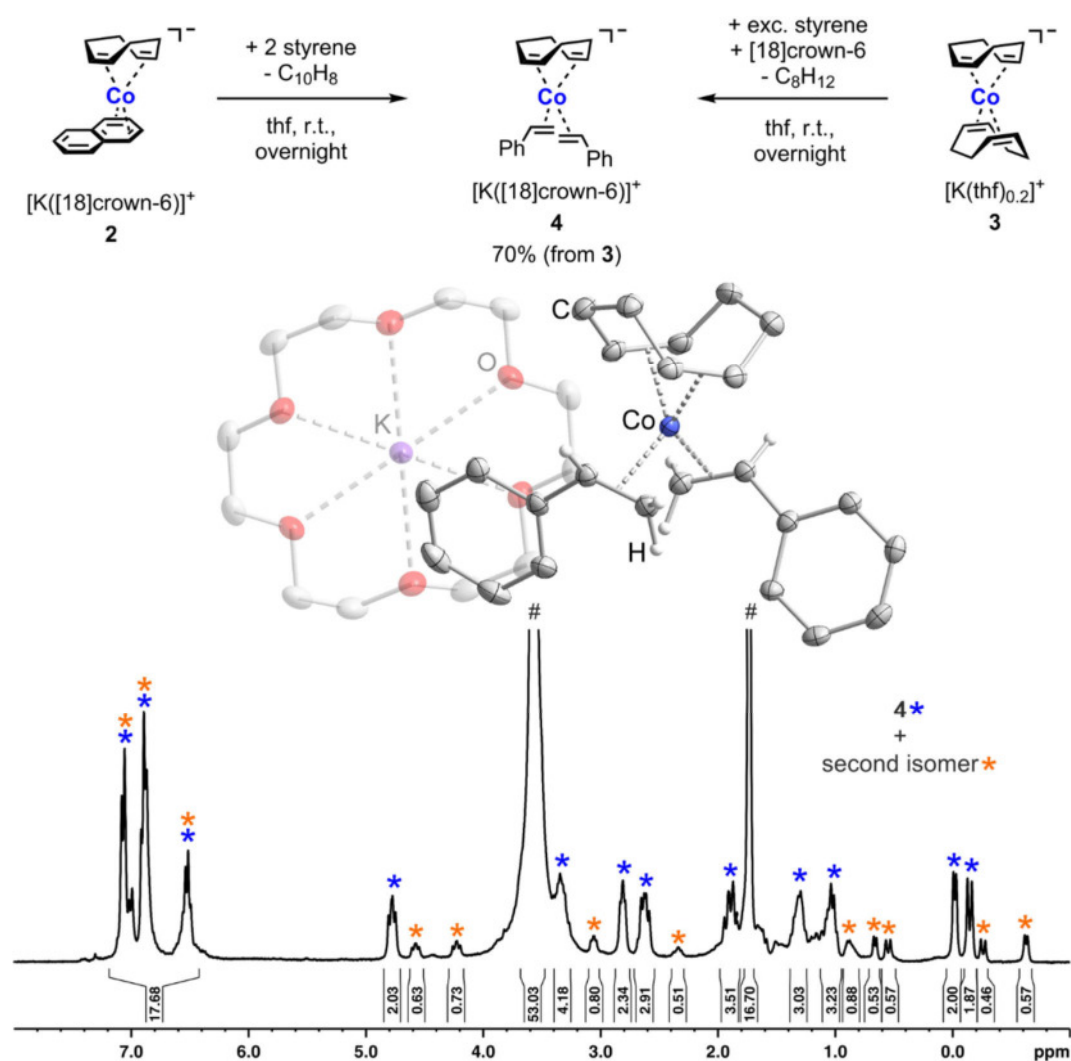
Figure 2.2   Synthesis (top), molecular structure (ellipsoids are at the 50% probability level; H atoms are omitted for clarity; middle), and ^{1}H NMR spectrum (300.13 MHz, 300 K, THF-d_8: #; bottom) of **4** and its second isomer.

was not observed. Complex **4** crystallized as bright orange blocks from a THF solution layered with *n*-hexane and was characterized by single crystal X-ray diffraction (Figure 2.2, middle), NMR spectroscopy, and elemental analysis. The compound is very air-sensitive. Exposure of solid **4** to the air is followed by immediate decomposition to a dark brown solid. A dark precipitate is formed in solution upon contact with air or moisture.

In the molecular structure of **4**, the coordination environment of the cobalt atom is distorted tetrahedral with a twist angle of 56.3°, which is somewhat smaller than the one for [K([2,2,2]cryptand)][Co(η^4-cod)$_2$] (67.3°) reported by Ellis.[19] The bite angle of the cod ligand is 90.0(3)°, and the angle between the two styrene ligands and Co is 104.3(3)°. The average C=C bond length of the styrene ligands is 1.423(1) Å, which is 0.08 Å longer than the value of free styrene.[23] The ^{1}H NMR spectrum of **4** (THF-d_8) shows two sets of signals with different intensities, which indicates the presence of a major and a minor isomer in solution (Figure 2.2,

bottom). These isomers likely arise from species with differing relative orientations of the phenyl rings, but the same overall composition.[24] According to ^{1}H NMR integration, the ratio between the main and the minor isomer is 4:1.

Similar to the preparation of **4**, [K([18]crown-6)][Co(cod)(dct)] (**5**), containing the rigid, non-planar, tub-like diene ligand dibenzo[*a,e*]cyclooctatetraene (= dct),[25, 26] was synthesized by adding 1 equiv. of dct to **2** in THF at room temperature (Figure 2.3, top). Ligand exchange is incomplete, thus, **5** could not be obtained as a pure compound. Various samples were contaminated with a minimum of 18% of [K([18]crown-6)][Co(dct)$_2$], even after several recrystallizations. X-ray quality crystals of yellow-orange **5** were obtained from a THF solution layered with diethyl ether. The crystallographically determined molecular structure (Figure 2.3, top left) is similar to that of **4** and of [K([2,2,2]cryptand)][Co(cod)$_2$].[19] Cobalt has a distorted tetrahedral coordination environment with a twist angle of 59.0°. The average C=C bond length (1.419 Å) of the coordinated dct molecules is very similar to the value found for cod in [K([2,2,2]cryptand)][Co(cod)$_2$].[19] The ^{1}H NMR spectrum of the isolated product mixture
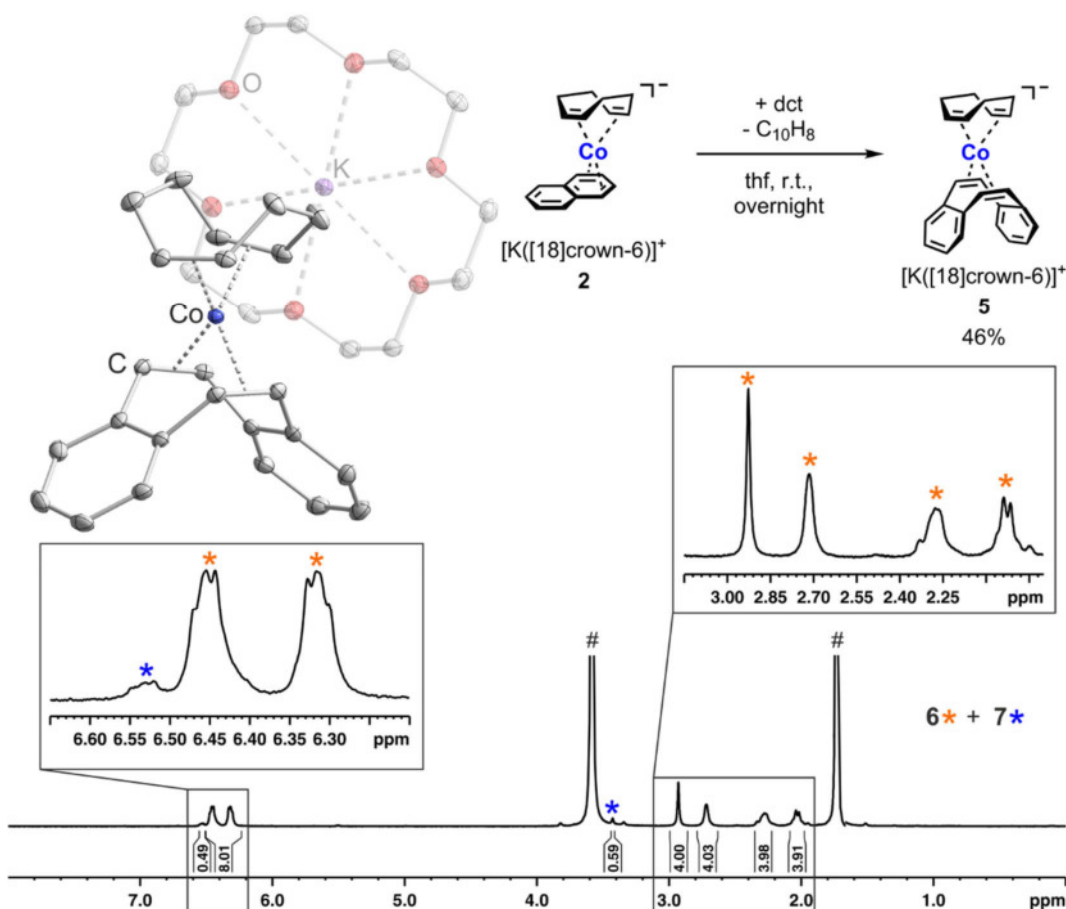

Figure 2.3   Synthesis (top right), molecular structure (ellipsoids are at the 50% probability level; H atoms are omitted for clarity; top left), and ^{1}H NMR spectrum (300.13 MHz, 300 K, THF-d_8: #; bottom) of the heteroleptic compound **5** and its homoleptic impurity.

recorded in THF-d_8 corroborates the composition of **5**. The spectrum clearly shows one set of signals assigned to **5** with the expected broad multiplets for dct and cod ligands in a 1:1 ratio, including the typical AA'BB' spin system arising from the arene protons of dct (multiplets at 6.45 and 6.32 ppm). In addition, a second set of minor signals can be assigned to [K([18]crown-6)][Co(dct)$_2$].

Treatment of [K(thf)$_{0.2}$][Co(cod)$_2$] (**3**) with dct (1.2 equiv.) resulted in a mixture of unreacted **3**, the mono-substitution product [K(solv)][Co(cod)(dct)], and homoleptic [K(thf)$_2$][Co(dct)$_2$] (**6**). The formation of such a mixture is probably due to ligand exchange equilibria, which need to be considered when using dct as a catalyst poison (*vide infra*).[26] The desired homoleptic complex **6** was cleanly produced by reacting [K(dme)$_2$][Co(anthracene)$_2$] (**1**) with two equivalents of dct in THF solution at room temperature (Figure 2.4, top) and was isolated in 19% yield by recrystallization from THF/*n*-hexane. The relatively low yield is explained by the need for several
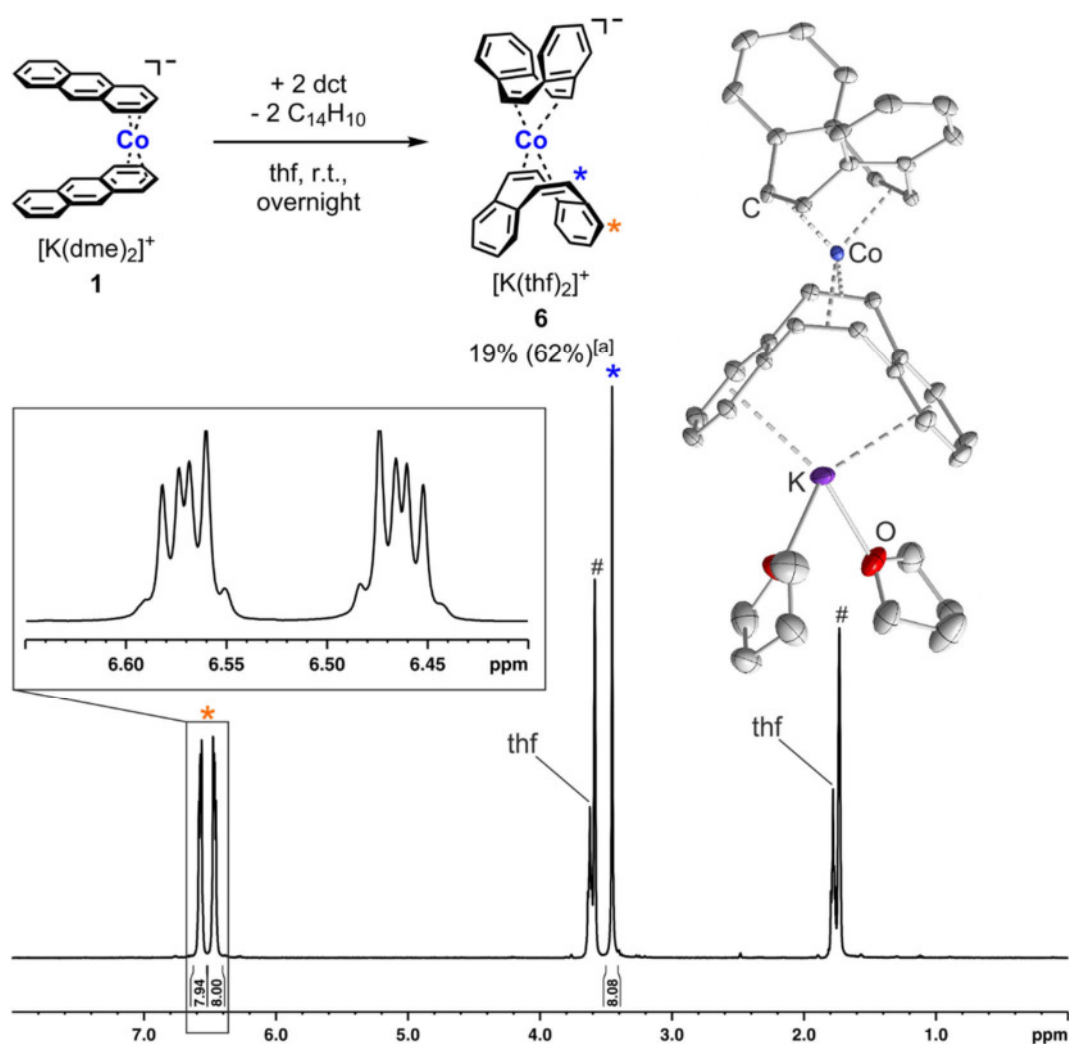

Figure 2.4   Synthesis (top left), molecular structure (ellipsoids are at the 50% probability level; H atoms are omitted for clarity, top right), and ¹H NMR spectrum (400.13 MHz, 300 K, THF-d_8: #; bottom) of **6**. [a] yield of isolated compound obtained in the presence of styrene (2 equiv.).

recrystallizations in order to remove free anthracene and dct. It seems noteworthy that the yield of **6** considerably increased when styrene (2 equiv.) was added to the reaction mixture. In this case, pure **6** was isolated in 62% yield after only one crystallization step from the clear orange reaction solution. The higher yield in this case might be due to the formation of an intermediary styrene complex such as **4**, which is subsequently converted to **6** by reaction with dct.

Orange blocks of **6** suitable for X-ray crystallography were obtained from THF/Et$_2$O. Single-crystal X-ray analysis revealed an ion-contact structure (Figure 2.4, top right) where the coordination environment of cobalt is overall similar to that in [K([2,2,2]cryptand)][Co(cod)$_2$].[19] The twist angle of 55.0(1)° is significantly smaller than for the former compound (67.3°). One set of dct signals is observed in the ^{1}H NMR spectrum of **6** in THF-d_8, consistent with the homoleptic structure of the complex (Figure 2.4 ,bottom).
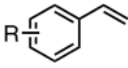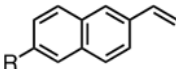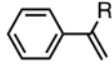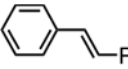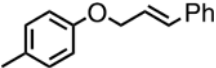
2.2.2 Catalytic Hydrogenations

Our preliminary study of catalytic hydrogenations with 1 mol% of the potassium bis(anthracene) metalates(1-) **1** and **A** revealed superior activity of the cobaltate **1** (Table 2.1).[18] Various α-, β-, and ring-substituted styrenes were hydrogenated in excellent yields in toluene solution at 2 bar dihydrogen pressure and room temperature in a stainless steel Parr™ reactor (Figure 2.5). The conversion of terminal, internal, di- and tri-substituted aliphatic alkenes and alkynes required a higher catalyst loading as well as elevated pressure and temperature (5 mol%, 10 bar H$_2$, 60 °C). The 17-valence electron pre-catalyst **A** exhibited good activi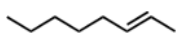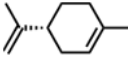ty only with unbiased styrenes and 1-alkenes but fared much poorer with deactivated olefins (EDG-substituted styrenes, internal alkenes). Rapid deactivation and unwanted side reactions were observed when the substrate contained ester and free amino groups. No significant effect of the crown ether coordinated to the potassium counterion on the catalytic activity was observed.

Figure 2.5   Parallelized hydrogenation setup in Parr™ pressure reactors.
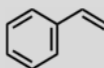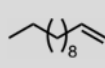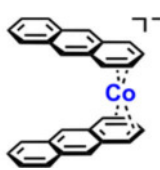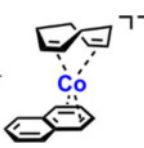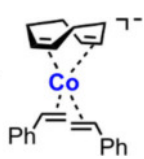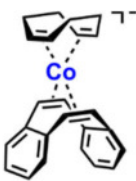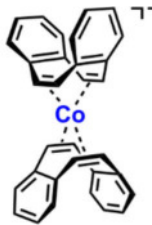
Table 2.1   Hydrogenation of alkenes with bis(anthracene) complexes **1** and **A**. Standard conditions: 0.5 mmol substrate in 2 mL toluene; yields of hydrogenation products determined by quantitative GC vs. internal reference *n*-pentadecane.

Entry	Substrate	R	1	A
1		H	95	89
2		4-F	100	100
3		4-CO$_2$Me	89	2
4		2-OMe	95	50
5		3-Me	96	27
6		4-NH$_2$	27	0
7		OMe	97[a]	58
8		OAc	69	-
9		Me	100[b]	-
10		Ph	100[c]	-
11		Me	100[b]	-
12		Ph	100[b]	-
13		CO$_2$Me	76[c]	-
14		n = 8	88[c,d]	73[c,d]
15		n = 12	92[c,d]	72[c,d]
16			92[c]	-
17			100[b]	-
18			63[c,e]	-
19			79[c]	< 5[c]
20	Ph≡Ph		99[c,f]	< 5[c,g]

[a] 2 bar. [b] 60 °C, 2 bar, 24 h. [c] 5 mol% cat., 60 °C, 10 bar, 24 h. [d] < 8% 2-alkene.
[e] 80 °C. [f] bibenzyl. [g] (*E*)-stilbene.

Table 2.2   Hydrogenation of alkenes with pre-catalysts 1-6. Standard conditions: substrate (0.5 mmol) in THF (2 mL); yields of hydrogenation products were determined by quantitative GC-FID versus internal reference *n*-pentadecane and are given in percent. In parentheses: yields of alkene isomerization products.

Entry	pre-catalyst	(styrene)	(terminal alkene)
1	1 [K(dme)$_2$]$^+$	94	58 (27)
2	2 [K([18]crown-6)]$^+$	99	93 (0)
3	3 [K(thf)$_{0.2}$]$^+$	93	62 (29)
4	4 [K([18]crown-6)]$^+$	72	85 (8)
5	5 [K([18]crown-6)]$^+$	36	71 (24)
6	6 [K(thf)$_2$]$^+$	0	0 (0)

We now set out to evaluate the series of monoanionic alkene and arene metalates **1** – **6** as pre-catalysts in parallelized olefin hydrogenations under identical conditions. Styrene and 1-dodecene were chosen as model substrates (Table 2.2). The standard conditions involved reaction with 5 mol% pre-catalyst under an atmosphere of 2 bar H_2 in THF (due to the better solubiltity of the complexes compared to toluene) at room temperature for 24 h. In general, styrene was converted in excellent yields with most pre-catalysts except **5** and **6** containing dct as a ligand. This observation is in accord with the postulate that dct is a competent catalyst poison for homogeneous low-valent monometal species.[26] The strong coordination of dct, and to a lesser extent of cod, to the formal Co^- catalytic center slows down ligand exchange with the substrate styrene. At the same time, dct is not hydrogenated, and the hydrogenation of cod is slow.

With 1-dodecene, similarly good catalytic hydrogenation activities were observed for the pre-catalysts **1** – **5** with up to 93% alkene hydrogenation and <29% alkene isomerization. The best activity and selectivity was determined in the reaction with **2**, which resulted in no observable isomerization to internal alkenes. Again, the bis(dct) cobaltate **6** was catalytically inactive due to the strong dct coordination to the cobalt center, which renders this complex inert with respect to ligand substitution and ligand hydrogenation.[26]

From both model reaction series, it became obvious that, despite only small stereoelectronic differences between the pre-catalysts **1** – **6**, the nature of the π-hydrocarbon ligands and the central metal ion has a strong influence on the overall catalytic activity. Pre-catalysts containing naphthalene or anthracene exhibited generally higher activity, presumably due to the reestablishment of aromaticity upon exchange of the polyarene ligand with the better π-accepting ligands.[16, 29]

2.2.3 Mechanistic Studies

The investigated pre-catalysts **1** and **A** did not react with dihydrogen at ambient temperature (J. Young NMR tube experiment, up to 4 bar H_2, THF-d_8). We therefore believe that the proposed mechanism of alkene hydrogenation is initiated by the substitution of the labile arene ligand by the π-substrate followed by reaction of the resulting metal catalyst with dihydrogen (Scheme 2.1). In preliminary studies with bis(anthracene) cobaltate **1**, we monitored this catalyst activation step by redox-neutral π-ligand exchange in homogeneous phase through NMR experiments. Figure 2.6 shows the ^{1}H NMR spectra of pre-catalyst **1** in THF-d_8; the reaction mixture after the addition of styrene (20 equiv.) to the complex solution at room temperature (spectrum a), and the reaction mixture after 3 h under 4 bar H_2 pressure (spectrum b). The observation of resonances of noncoordinated anthracene in the spectra a and b clearly supports
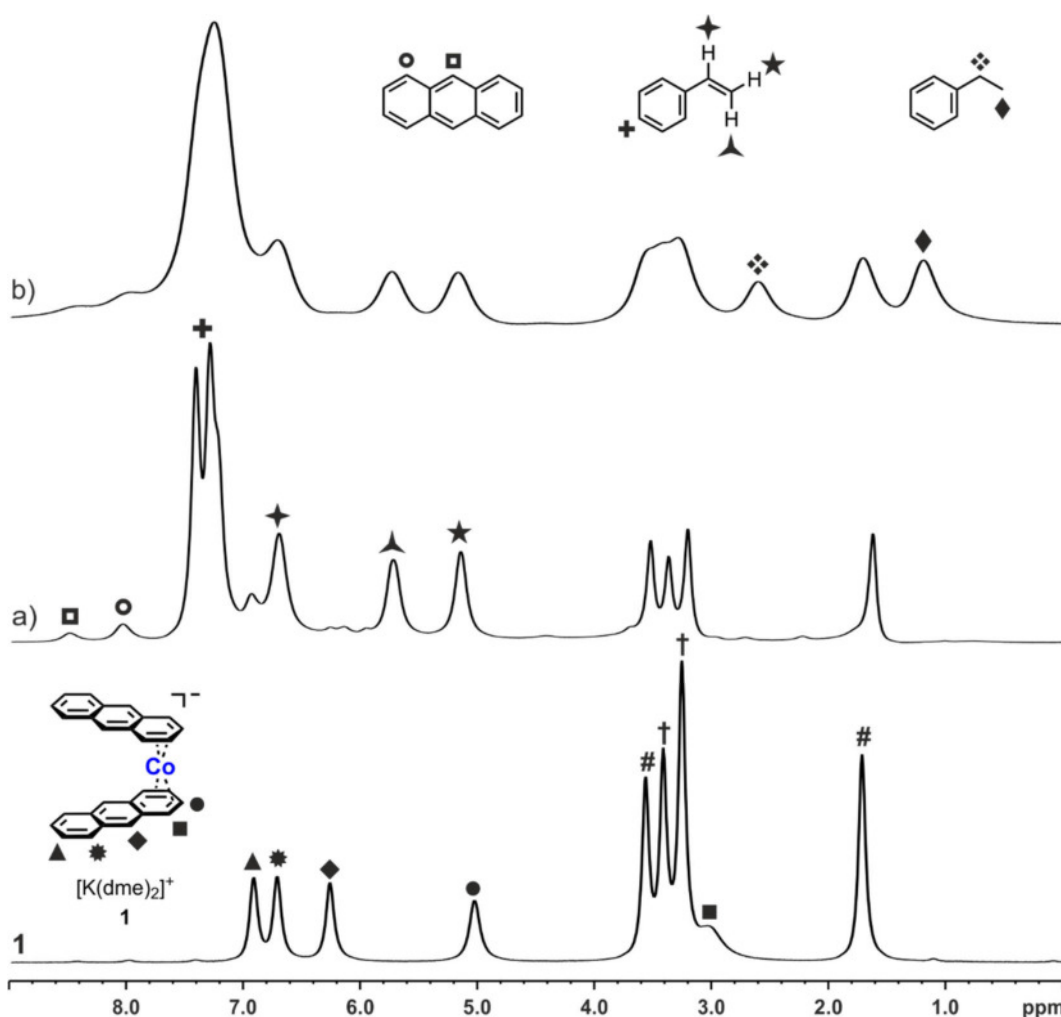
Figure 2.6 ^{1}H NMR spectroscopy monitoring (THF-d_8: #) of styrene hydrogenation with pre-catalyst **1** (dme: †). a) 3 h after the addition of styrene (20 equiv.), and b) 3 h after the addition of hydrogen.

the notion of ligand exchange prior to styrene hydrogenation. The signals of ethylbenzene are apparent in spectrum b. There were no further resonances detected in the high-field section that would indicate the formation of hydride complexes under a dihydrogen atmosphere. The observed line broadening is tentatively attributed to the slow formation of cobalt nanoparticles.

We extended the ^{1}H NMR monitoring studies to the [Co(cod)(L)]$^-$ complexes **2** (L = naphthalene) and **3** (L = cod). When assuming a pre-catalyst activation by π-ligand exchange of the weakest ligand with the substrate, both **2** and **3** should funnel through the same catalytic intermediate. We tested this mechanistic hypothesis by adding 20 equiv. of styrene to THF-d_8 solutions of **2** and **3**, respectively (Figure 2.7 & Figure 2.8). Indeed, the recorded ^{1}H NMR spectra showed the clean formation of the anticipated bis(styrene) cobaltate **4** in both cases alongside resonances of free naphthalene (from **2**) and cod (from **3**). This observation strongly supports our mechanistic proposal. Upon application of an atmosphere of H$_2$ to the NMR scale reactions, clean conversion of the substrate styrene was observed. Furthermore, the rate of substrate

conversion can be qualitatively assessed from these experiments. The loss of the π-ligand styrene upon complete hydrogenation with pre-catalyst **2** after 24 h at 2 bar H_2 and a significantly slower conversion of cod (and naphthalene) resulted in the reconstitution of the original pre-catalyst **2** by naphthalene coordination as indicated by the red color of the reaction solution. This complex is difficult to detect in the reaction mixture by ^{1}H NMR, but its formation was clearly proven by a separate experiment (Figure 2.9b). The NMR monitoring of the related **3**-catalyzed hydrogenation of styrene showed full conversion of the substrate and the ligand cod after 96 h (Figure 2.8). Likewise, as in the case of **1**, the NMR spectroscopy monitoring of complexes **2** and **3** did not show any high-field signals of hydride species.

We prepared and fully characterized the catalytically active bis(styrene) complex **4** (Figure 2.2, *vide supra*), the role of which as a key intermediate in styrene hydrogenations with alkene cobaltate precatalysts was clear from the NMR spectroscopy experiments discussed above
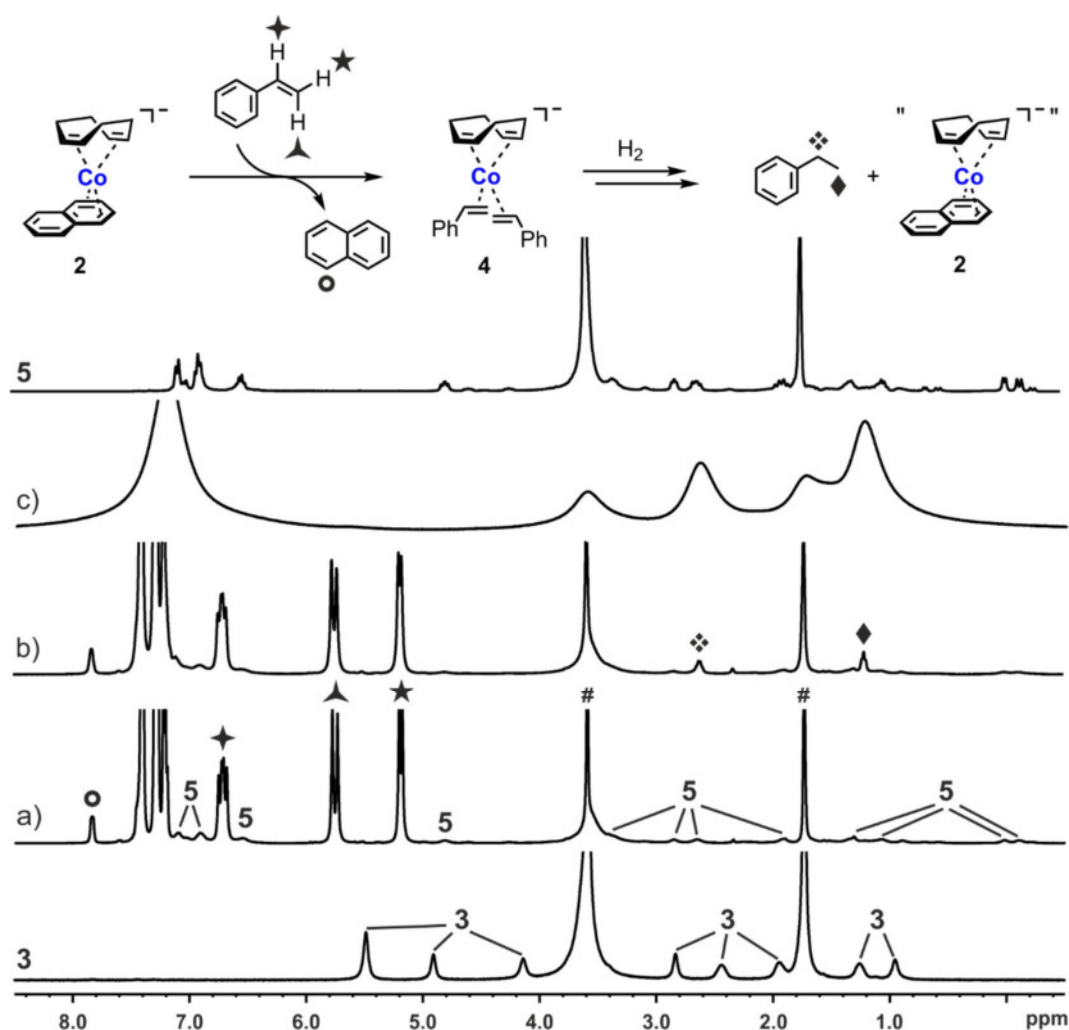
Figure 2.7   ^{1}H NMR monitoring (THF-d_8: #) of styrene hydrogenation with pre-catalyst **3**; a) 1.5 h after the addition of 20 equiv. of styrene; b) 1.5 h, and c) 24 h after addition of hydrogen; the spectrum of a clean sample of **5** is shown on top.
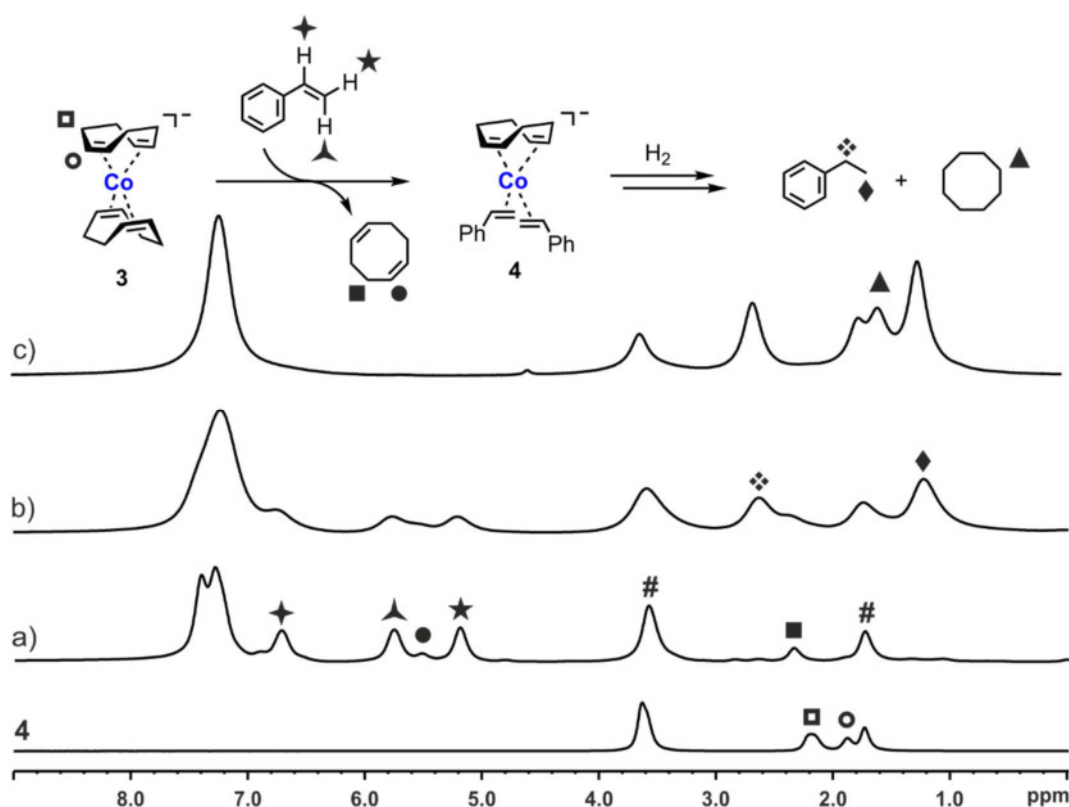
Figure 2.8 ^{1}H NMR monitoring (THF-d_8: **#**) of styrene hydrogenation with pre-catalyst **4**; a) 1.5 h after the addition of 20 equiv. of styrene; b) 1.5 h, and c) 96 h after addition of hydrogen.

(Figure 2.7 & Figure 2.8). Application of an H$_2$ atmosphere (1 bar) to a i) bright orange solution of solution of **4** in THF-d_8 effected an ii) immediate formation of a black precipitate, presumably metallic cobalt, due to the hydrogenative consumption of the π-ligands which stabilize this cobaltate species. iii) 5 minutes after H$_2$ was admitted the whole mixture has changed to a black suspension. The ^{1}H NMR spectrum at this time and GC analyses confirmed the formation of major amounts of ethylbenzene and cyclooctane and only minor amounts of cyclooctene. iv) The black precipitate was isolated by decantation of the solvent. With pre-catalyst **2**, bearing a much less reactive naphthalene ligand, sufficiently differing rates of hydrogenation, styrene > cod >> naphthalene, allowed the reconstitution of the original pre-catalyst by a release-catch mechanism after the complete hydrogenation of the reactive alkenes (Figure 2.7, top). A similar outcome was observed in reactions of bis(styrene) complex **4** in the presence of an excess of naphthalene under 1 bar H$_2$ pressure (Figure 2.9b top). The chemoselective conversion of styrene and inertness of naphthalene under the mild hydrogenation conditions also led to the formation of the (cod)(naphthalene) cobaltate **2** (Figure 2.9b bottom right), which was isolated as a dark red solid by evaporation of the volatiles.

Because the abovementioned results do not rule out the operation of a heterogeneous catalytic pathway as a background reaction,[26] we turned to reaction progress analyses by quantitative

GC analysis of all reaction components (Figure 2.10). The early reaction phase of the **1**-catalyzed hydrogenation of styrene (<20 min) showed no induction period and no sigmoidal curvature, which would indicate a nucleation step *en route* to nanoclusters and nanoparticles. An identical behavior was observed from the hydrogenation of styrene with 5 mol% of pre-catalyst **3**. Without any detectable induction period, styrene was completely hydrogenated within 45 min
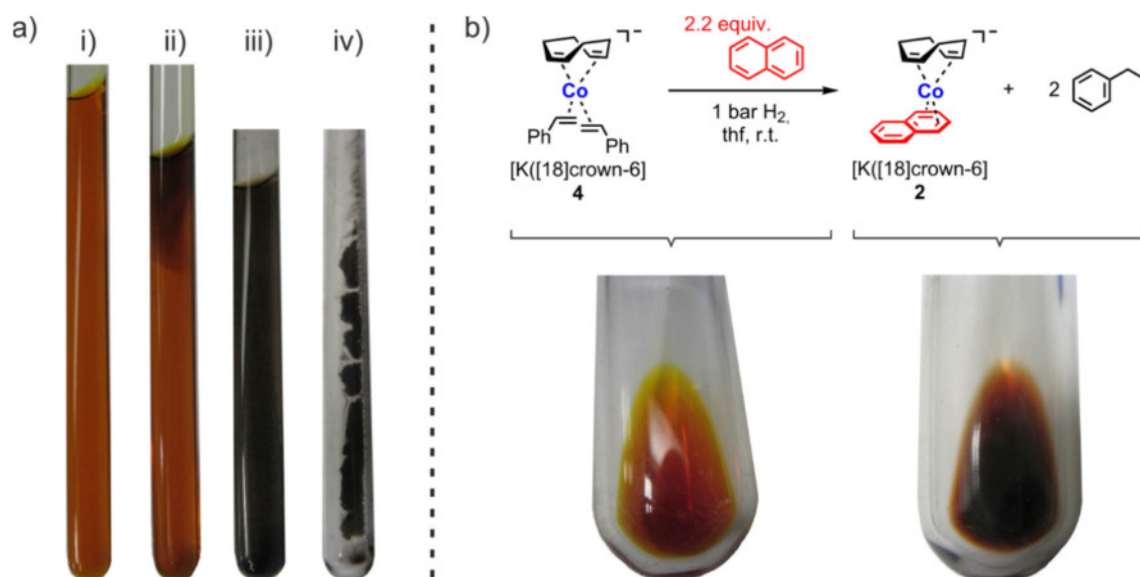
Figure 2.9   a) i) Solution of **4** in THF-d_8; ii) formation of a black precipitate is observed immediately after H$_2$ was admitted; iii) 5 minutes later more precipitate is formed and a ^{1}H NMR exclusively showed signals for ethylbenzene and cyclooctane and only minor amounts of cyclooctene; iv) the precipitate can be isolated by decantation. b) Demonstration of the ligand release-catch concept (top) by conversion of **4** (bottom left) to **2** (bottom right) upon chemoselective hydrogenation of styrene in the presence of naphthalene.
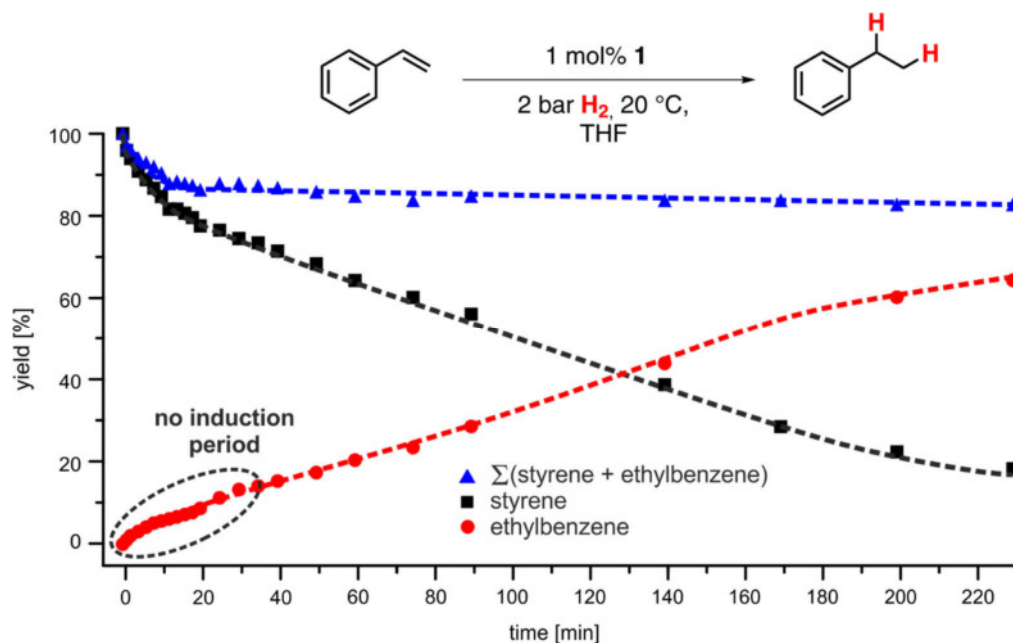
Figure 2.10   Reaction progress analysis: **1**-catalyzed hydrogenation of styrene under standard conditions without any detectable induction period. Dashed lines are only visual guides.

at 2 bar H$_2$. The conversion of the ligands cod and naphthalene largely commenced after the substrate styrene had been entirely converted to ethylbenzene (Figure 2.11).
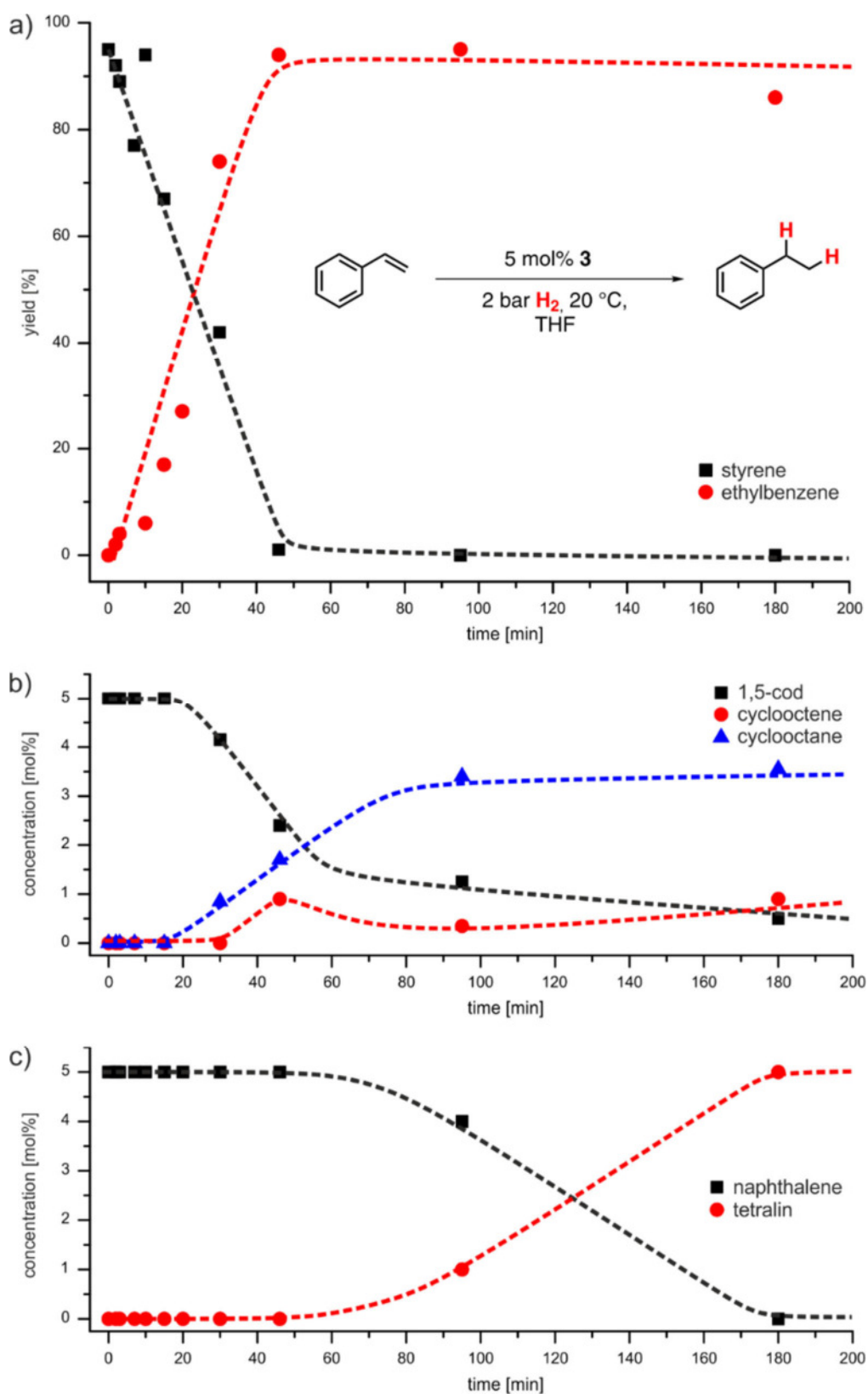
Figure 2.11   Reaction progress analysis: **3**-catalyzed hydrogenation. Conversions of styrene (a), cod (b), and naphthalene (c). Dashed lines are only visual guides.

To gain further information with respect to the homogeneous vs. heterogeneous nature of the operating catalyst, we performed kinetic poisoning studies with a scavenger reagent that is selective for mononuclear late transition metal species in low oxidation states: dibenzo[a,e]cyclooctatetraene (dct).[25, 26] Upon addition of only 2 mol% dct to a catalytic hydrogenation of styrene with 1 mol% **1** after 35 min (~17% conversion), a complete inhibition of catalyst turnover was observed, which is indicative of a homogeneous mechanism (Figure 2.12, *vide supra*). Inhibition of a potential heterogeneous pathway by amalgamation was not observed.[26]

In an extended study, we performed the two model reactions (styrene, 1-dodecene) with the two most active pre-catalysts **1** and **2** in the presence of scavengers (Hg, PMe$_3$ and dct; Table 2.3). Filtration of the freshly prepared pre-catalyst solution through a PTFE syringe filter (pore size <0.1 μm) prior to the addition of the substrate gave unaltered hydrogenation activity of pre-catalyst **1**. The addition of 300 mol% mercury did only slightly affect the catalyst activity. However, the formation of amalgams between mercury and 3d transition metals is very slow.[30] A pronounced reaction inhibition was only observed by addition of dct to the catalytic hydrogenation with the bis(anthracene) cobaltate pre-catalyst **1**. This suggests the formation of a catalytically inactive homoleptic cobaltate bearing two dct ligands, which is in perfect agreement with the observation of 0% conversion in alkene hydrogenations with the pre-catalyst [K(thf)$_2$][Co(dct)$_2$] (**6**, see Table 2.2). The rapid formation of **6** from **1** and dct was already
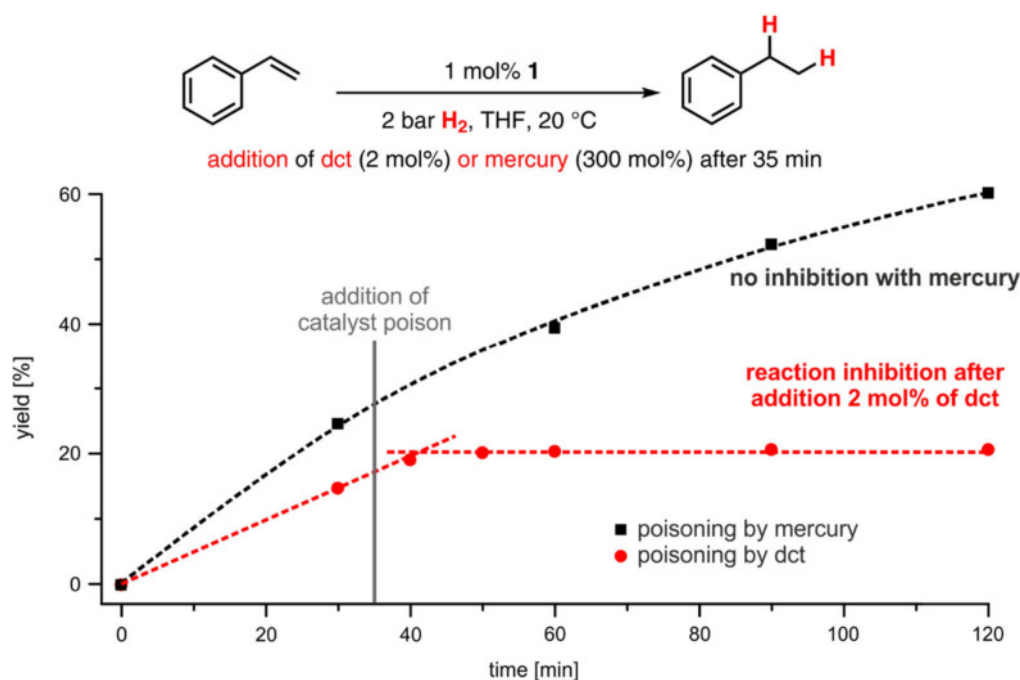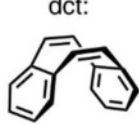
Figure 2.12   Poisoning studies with pre-catalyst **1** by addition of 300 mol% Hg and 2 mol% dct, respectively. Dashed lines are only visual guides.

demonstrated (Figure 2.4). Further support comes from ^{1}H NMR experiments of a THF solution of **7** and 20 equiv. of styrene, which showed no substitution of the dct ligands over a course of 1.5 h (Figure 2.13).

The observation of good catalytic activity of a mixture of pre-catalyst **2** and dct in Table 2.3 is a direct consequence of the presence of the strongly coordinating ligand cod in **2**, which

Table 2.3   Poisoning experiments of hydrogenations with arene cobaltate precatalysts **1** and **2**. Standard conditions: substrate (0.5 mmol) in THF (2 mL); yields of hydrogenation products were determined by quantitative GH-FID versus internal reference *n*-pentadecane and are given in percent.

Entry	Manipulation	R = Ph		R = $C_{10}H_{21}$	
		1	**2**	**1**	**2**
1	-	94	99	58[a]	93
2	< 0.1 μm filter	91	-	46[b]	-
3	300 mol% Hg	81	75	29[b]	40
4	1.12 mol% PMe$_3$	69	91	47[c]	94
5	11 mol% dct	14	81	3[d]	66

[a] 27% isomerization. [b] 34% isomerization. [c] 6% isomerization. [d] 31% isomerization
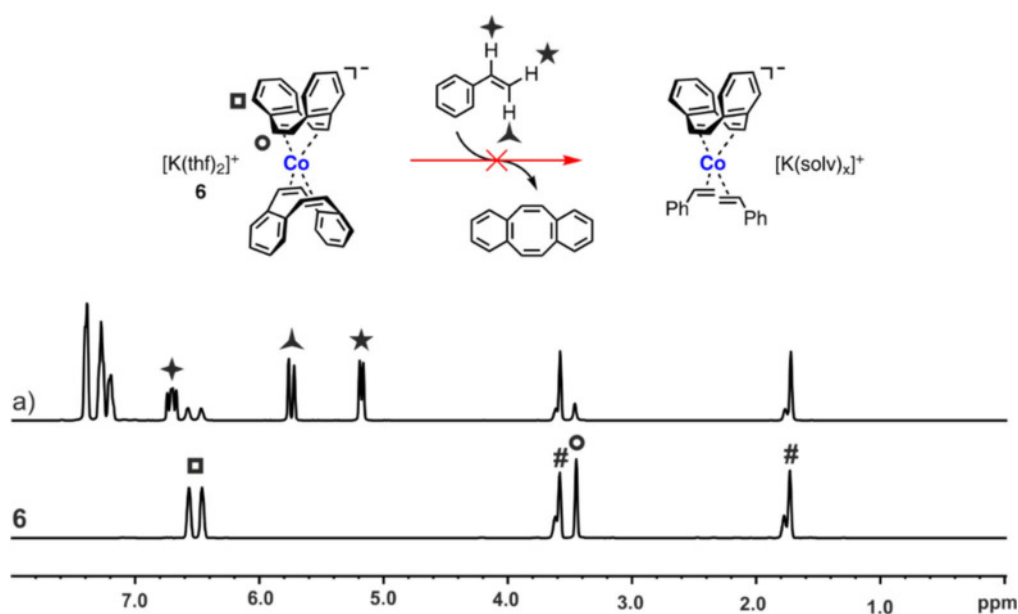
Figure 2.13 ^{1}H NMR spectrum (THF-d_8: #) of complex **7**, and a) 1.5 h after the addition of 20 equiv. of styrene.

undergoes little or no substitution with equimolar dct. This results in the exclusive substitution of the naphthalene ligand of **2** by dct and formation of the heteroleptic cobaltate **5** as the dominant catalyst species. Our catalytic experiments showed that [K([18]crown-6)][Co(cod)(dct)] (**5**) has a good activity in hydrogenations of styrene and 1-dodecene (Table 2.2, *vide supra*).

Given the anionic nature of the putative catalyst species, we also used negative-ion mode ESI mass spectrometry for their selective detection and analysis. Under carefully optimized conditions, this method is well capable of detecting even highly reactive organometallics in intact form,[31] including low-valent transition metal complexes.[32] Indeed, negative-ion mode ESI of a solution of **1** in THF afforded the free $[Co(C_{14}H_{10})_2]^-$ anion in high signal intensity (Figure S1a). In addition, the potassium-bound dimer $[K\{Co(C_{14}H_{10})_2\}_2]^-$ was also observed. Presumably, this species was not present in the diluted sample solution, but formed due to the concentration increase during the ESI process; similar behavior has been found in other cases as well.[31, 33] ESI of a solution of the heteroleptic complex **2** produced not only $[Co(cod)(C_{10}H_8)]^-$ as well as small quantities of $[K\{Co(cod)(C_{10}H_8)\}_2]^-$, but also its homoleptic counterpart $[Co(cod)_2]^-$ (Figure S1b). This observation clearly demonstrates the operation of intermolecular exchange processes in solution. ESI-mass spectrometric analysis of solutions of **3** and **4**, respectively, also resulted in the detection of the expected anionic complexes as main signals (Figure S1c and d).

After treating solutions of **2** and **1** with an excess of styrene, we observed the formation of the cobaltates **4** and **7**, respectively (Figure 2.14a & b). In both complexes, two styrene molecules had replaced one of the originally bound ligands (also compare Figure 2.7). For the heteroleptic complex **2**, only naphthalene, but not the cod ligand was released. This behavior is fully in line with the higher binding energy of the latter, which we had already derived from the NMR spectroscopic experiments. The reaction of **1** with styrene also furnished the homoleptic complex $[Co(styrene)_3]^-$ in very small abundance. The lack of any detectable $[Co(styrene)_4]^-$ suggests that this species did not form in solution or that its stability was too low to survive the ESI process. When **1** was treated with an excess of 1-dodecene, the replacement of anthracene by 1-dodecene proceeded only to a small extent (Figure 2.14c). This finding is consistent with the lower reactivity of 1-dodecene observed in the synthetic studies (*vide supra*).

Interestingly, the cobaltate complexes incorporating two molecules of styrene were accompanied by ions whose *m/z* ratios were shifted by two units to lower values, which obviously resulted from dehydrogenation reactions. According to the principle of microscopic reversibility, the catalytic activity of the cobaltate complexes with respect to hydrogenation
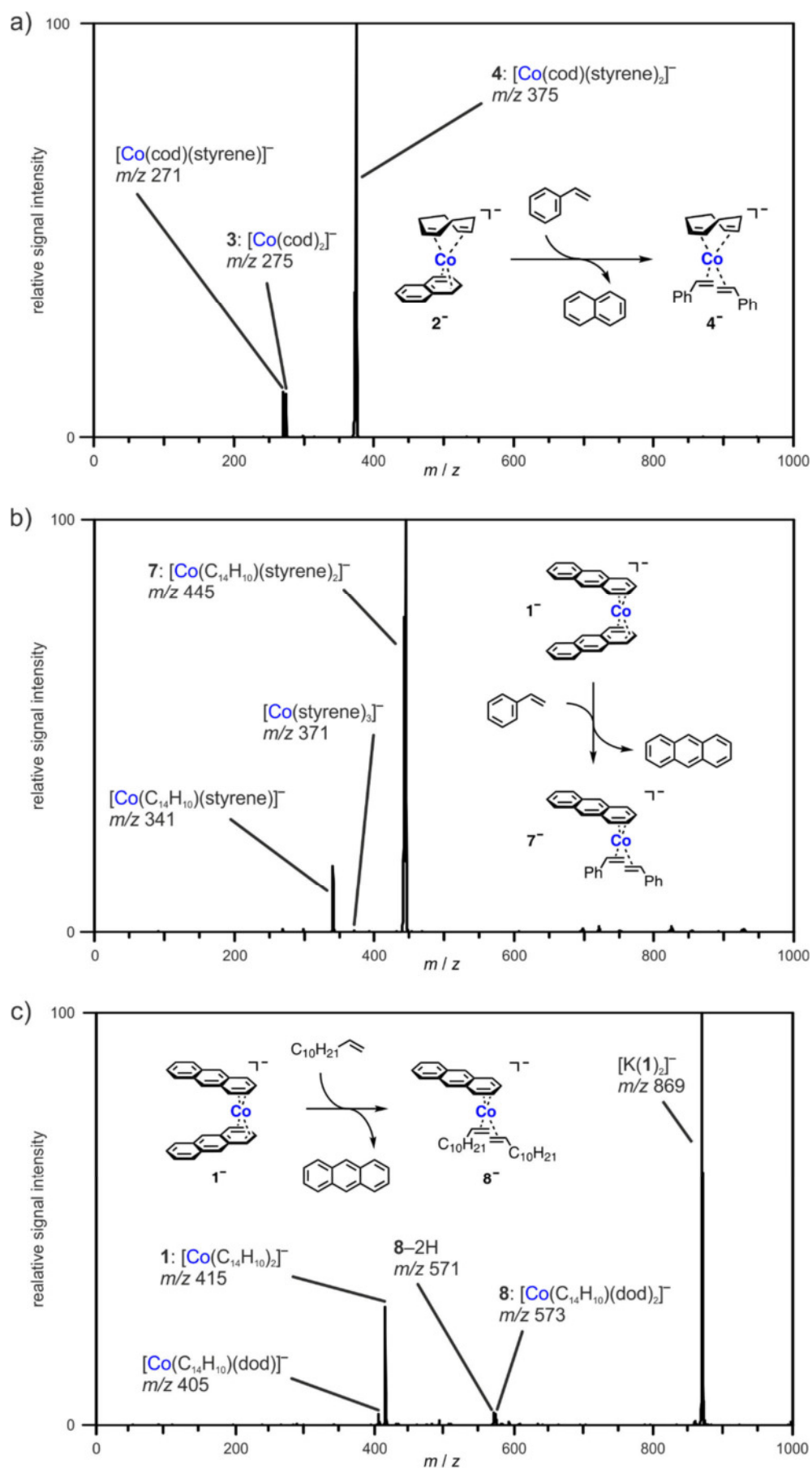
Figure 2.14   Negative-ion mode ESI mass spectra of the products formed upon reaction of: a) **2** (7.5 mM) with 10 equiv. of styrene; b) **1** (7.5 mM) with 20 equiv. of styrene; c) **1** (7.5 mM) with 20 equiv. of 1-dodecene (dod) in THF.

reactions implies that they can also catalyze dehydrogenations.[34] The absence of any ions with *m/z* ratios shifted by four units moreover indicates that the dehydrogenation reactions involved a coupling of two styryl units, which most likely gave 1,4-diphenylbuta-1,3-diene. Possibly, this diene originated from the dehydrogenation of one cobalt-bound styrene molecule and the addition of a second cobalt-bound styrene to the resulting C≡C triple bond. Low-valent cobalt complexes are known to catalyze related C–H activation reactions.[35]

Finally, we probed the unimolecular gas-phase reactivity of the mass-selected cobaltate complexes. These experiments have the advantage of excluding any interference from dynamic equilibria, counter-ion or solvent effects, which may operate in solution. Gas-phase fragmentation of the complex **2** led to the loss of cod and naphthalene, whereas **4** and **7** only released styrene (Figure S2a - d).

In conclusion, our investigations on catalytic alkene hydrogenations documented the formation of 18 valence electron (18e) bis(alkene) complexes in the reaction mixtures. These species are presumably resting states, which serve as the reservoir for the catalytically active cobalt species. One may speculate that H_2 activation is initiated by loss of an alkene ligand, forming an unsaturated and reactive 16e monoalkene complex.

2.2.4 Methodology Extensions

We also applied the pre-catalysts **1 – 6** to hydrogenations of ketones and imines. Generally, hydrogenations of such polar unsaturated compounds are accelerated by the presence of a

Table 2.4   Hydrogenation of ketone and imine with precatalysts **1-6**. Standard conditions: substrate (0.5 mmol) in THF (2 mL); yields of hydrogenation products were determined by quantitative GH-FID versus internal reference *n*-pentadecane and are given in percent. Yields from reactions at 10 bar H_2, 60 °C in parentheses.
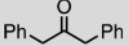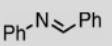
Entry		Precatalyst	Ph–C(O)–Ph	Ph–N=Ph
1	**1**	[Co(anth)₂]⁻	11 (91)	0 (99)
2	**2**	[Co(naph)(cod)]⁻	4 (65)	0 (15)
3	**3**	[Co(cod)₂]⁻	5 (60)	0 (3)
4	**4**	[Co(cod)(styrene)]⁻	5	3 (3)
5	**6**	[Co(dct)₂]⁻	0 (17)	0 (26)

Table 2.5   Hydrogenation of ketones and imines with precatalysts **1**. Standard conditions: substrate (0.5 mmol) in toluene (2 mL); yields of hydrogenation products were determined by quantitative GH-FID versus internal reference *n*-pentadecane and are given in percent.

Entry	Substrate	R	Yield
1		Me	99, 91[a]
2		Bn	96
3		-	100
4		-	88
5		-	71
6		H	96, 99[a]
7		2-Me	98
8		3-Me	100
9		4-OMe	100
10		CO$_2$Et	79[b]
11		Br	0

[a] Solvent: THF. [b] 7.5 mol% **1**, 70 °C, 10 bar H$_2$

Lewis acidic catalyst in higher oxidation states. However, the pre-catalyst complexes contain a weakly Lewis acidic K$^+$ counterion. We observed very poor catalytic activities under the standard conditions at 2 bar H$_2$ and room temperature. Elevated pressure and temperature (10 bar H$_2$, 60 °C, see Table 2.4) led to good activity of potassium bis(anthracene) cobaltate **1** in the hydrogenation of dibenzylketone and *N*-benzylideneaniline (>91% yield). The cod-containing complexes **2** and **3** exhibited moderate activity in the ketone hydrogenation (60-65%). Surprisingly, both complexes were rather inactive in the hydrogenation of the imine. The most active ketone hydrogenation catalyst **1** was subjected to a series of other carbonyl compounds (Table 2.5).[18] Good catalytic activity was only observed at elevated temperature and pressure.

SET-initiated radical reactions

$K^+ [L_nCo]^-$

1st turnover

$K^+ [L_nCo]^- + R\frown XH$ pK_a !

$[L_nCo]$

$R\frown XK + \frac{1}{2} H_2$

higher oxidation state catalysis
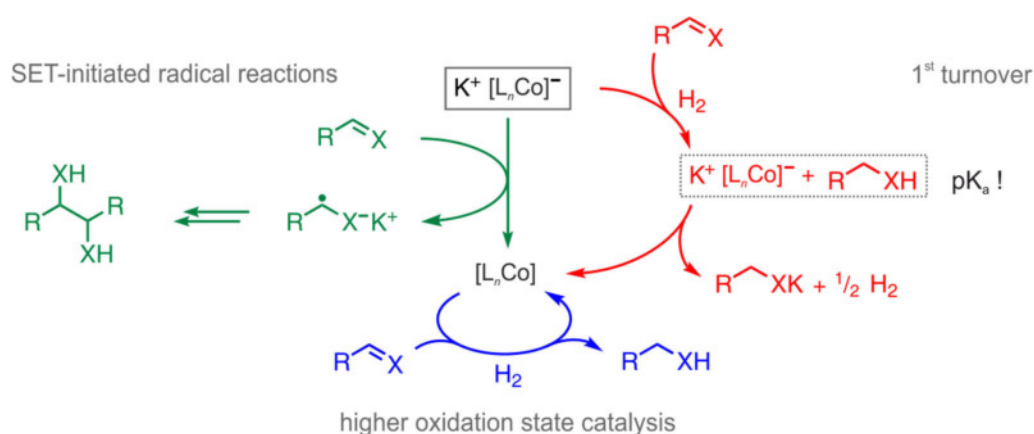
Scheme 2.3   Change of mechanism, H_2 evolution and catalyst oxidation in the hydrogenation of polar substrates.

Importantly, the employment of carbonyl compounds as hydrogenation substrates could in principle trigger three unwanted side reactions: deprotonation at the α-carbonyl position, direct reduction of the carbonyl moiety by metalate addition or single-electron transfer (SET), and deprotonation of any formed alcohol. Indeed, we have observed the operation of the latter two pathways under the present reaction conditions. The catalytic hydrogenation reaction generates an acidic proton in the resulting alcohol and amine products, both with pK_a values of ~29 (in DMSO).[36] After the first turnover, this is very likely to alter the catalytic mechanism by catalyst oxidation and H_2 evolution (Scheme 2.3).[37] Considering a catalyst oxidation after the direct electron transfer to the ketone or after the first hydrogenation catalysis turnover, we postulate the formation of a cobalt(+I) catalyst which displays lower catalytic activity and therefore requires harsher conditions. The formation of dihydrogen was observed by ^{1}H NMR in an equimolar reaction between **1** and 1,3-diphenyl-2-propanol. Furthermore, a transfer hydrogen-

a) Pinacol coupling:

0.021 mmol (64%)* with pre-catalyst **1**

* ref. to 2e transfer from $[L_nM]$

b) Ring opening:

95%	:	–	with pre-catalyst **1**
50%	:	15%	with pre-catalyst **2**
75%	:	10%	with pre-catalyst **3**
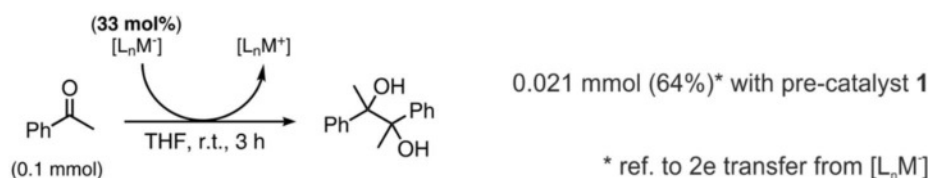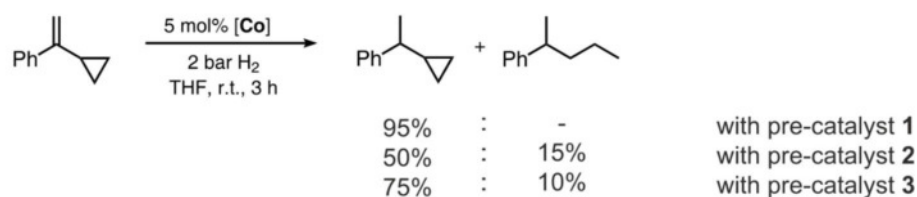
Scheme 2.4   Observation of radical side reactions.

ation experiment between 4-methylstyrene and 4 equiv. of 1,3-diphenyl-2-propanol afforded 18% yield of ethylbenzene in the presence of 5 mol% **1**.[18]

Direct SET reduction of acetophenone was observed in the presence of **1**, to give the pinacol product in good yields (Scheme 2.4a).[38] With an olefinic radical probe, such behavior was much less pronounced under standard reaction conditions (Scheme 2.4b). Catalyst **1** showed no ring-opening of α-cyclopropylstyrene but clean hydrogenation of the double bond. Significant radical character was observed in reactions with the cod-bearing catalysts **2** and **3**.

2.3 Conclusion

Bis(anthracene) cobaltate **1** is a highly active pre-catalyst for the hydrogenation of a variety of alkenes, ketones and imines at ambient H_2 pressure and temperatures.[18] In a greatly extended study, we have now compared the catalytic activity of **1** with that of $[K([18]crown-6)][Co(C_{14}H_{10})(cod)]$ (**2**) and of a series of structural related alkene metalates $[K(thf)_{0.2}][Co(cod)_2]$ (**3**), $[K([18]crown-6)][Co(cod)(styrene)_2]$ (**4**), $[K([18]crown-6)][Co(cod)(dct)]$ (**5**), $[K(thf)_2][Co(dct)_2]$ (**6**). **4** – **6** were synthesized for the first time.

1 – **5** are competent pre-catalysts for the hydrogenation of alkenes under mild conditions. Unlike **1** the bis(styrene) complex **4** rapidly reacts with H_2 (1 bar) with release of ethylbenzene. Kinetic studies and ¹H NMR monitoring experiments lead to the conclusion that the olefin hydrogenation reaction is initiated by the substitution of one labile arene ligand by a π-acceptor substrate. Further, we proved the concept of the release-catch mechanism of catalyst activation by ¹H NMR monitoring of π-ligand exchange reactions and by negative-ion mode ESI mass spectrometry investigations. The selective formation of a bis(monoalkene) cobaltate intermediate is believed to be key to a rapid dihydrogen activation because, unlike coordinated cod and naphthalene or anthracene, the monoalkene ligands of such a species are readily hydrogenated.

Poisoning experiments with dct and mercury support the hypothesis that the active species has a homogeneous nature. The validity of *Crabtree's* dct test for cobaltate complexes was confirmed by the formation of $[K(thf)_2][Co(dct)_2]$ (**6**) and $[K([18]crown-6)][Co(cod)(dct)]$ (**5**). The bis(dct) complex **6** is not a competent pre-catalyst, presumably because the dct ligands are not substituted or hydrogenated under the reaction conditions. By contrast, **5** still showed some catalytic activity because of its more labile cod ligand.

Extensions to polar substrates (ketones and imines) were also investigated, but these reactions most likely proceed via a different mechanism than alkene hydrogenations because of the operation of unwanted radical and acid-base reactions. Both pathways most likely involve

oxidation of the metalate complexes to a higher oxidation manifold which ultimately exhibits lower catalytic activity. However, the rapid onset of SET reactions with polar substrates appears to be a promising entry to future studies of radical reactions catalyzed by such alkene metalates. The general concept of redox-neutral alkene ligand substitution with metalate complexes has only recently been tapped for catalytic reaction developments. Further variations of this motif in the context of small molecule hydrogenation and hydrofunctionalization will be reported in due course.

2.4   Experimental Section

2.4.1   General Considerations

All experiments were performed under an atmosphere of dry argon by using standard Schlenk and glovebox techniques. Solvents were purified, dried, and degassed by standard techniques.

2.4.1.1   General Procedure for Hydrogenation Reactions

A dry 5 mL vial with a screw cap and PTFE septum was charged with a magnetic stir bar and a solution of the pre-catalyst (0.025 mmol) in THF (1 mL). After adding a solution of the substrate (0.5 mmol) in THF (1 mL) with a pipette, the vial was closed, and the septum was punctured with a short needle (Braun). The vial was placed into a high-pressure reactor (Parr Instr.), which was sealed, removed from the glove box, placed on a magnetic stirrer plate, and purged with hydrogen. After 24 h at room temperature under an atmosphere of hydrogen (2 bar) the pressure was released, the vial removed, and the reaction quenched with saturated aqueous NaHCO$_3$ (1 mL). For quantitative GC-FID analysis, n-pentadecane was added as an internal standard. The mixture was extracted with diethyl ether and the combined organic layers were dried over Na$_2$SO$_4$.

2.4.1.2   General Procedure for Poisoning and Filtration Experiments

The poisoning experiments were carried out according to the general procedure for hydrogenation reactions. In the case of poisoning with PMe$_3$ the pre-catalyst was dissolved in 0.5 mL THF before a THF stock solution of the phosphane (0.5 mL, $c = 1.25 \cdot 10^{-2}$ mol/L) was added. For the experiments with dct the catalyst poison was added to the solid pre-catalyst before dissolving both together in THF. When using elementary mercury as the catalyst poison, the liquid metal was added directly to the dissolved pre-catalyst with a syringe before the addition of the substrate solution. For the filtration experiments, the pre-catalyst solution was filtered through a PTFE syringe filter (Puradisc 13, Whatman, pore size < 0.1 µm) before the substrate solution was added.

2.4.1.3   General Procedure for ^{1}H NMR Monitoring

Reaction monitoring by ^{1}H NMR was carried out in a sealed J. Young NMR tube. A solution of the pre-catalyst (5 · 10^{-3} mmol, 5 mol%) in THF-d_8 (0.5 mL) was transferred into a NMR tube, and the first ^{1}H NMR spectrum was measured. In the glovebox, styrene (10 mg, 0.1 mmol, 1.0 equiv.) was added to the pre-catalyst solution. After storing the sample for 90 min, the second ^{1}H NMR spectrum was recorded. Subsequently, the atmosphere was exchanged with dihydrogen by the freeze-pump-thaw technique. Subsequent spectra were recorded after further 90 min and then

at irregular intervals until the substrate was fully consumed or until no further consumption was detected.

2.4.1.4   General Procedure for Reaction Progress Analysis

Reaction progress was monitored in a 50 mL Schlenk flask. A solution of styrene (260 mg, 2.50 mmol, 1.00 equiv.) in THF (5 mL) was added to a solution of the pre-catalyst (0.125 mmol, 5 mol%) in THF (5 mL). For quantitative GC-FID analysis, *n*-pentadecane was added as an internal standard. The reaction was started by replacing the atmosphere in the Schlenk flask by dihydrogen (2 bar). Samples of 0.1 mL were taken at regular intervals through a septum. Each sample was worked up according to the general procedure for hydrogenation reactions. Quantification of starting material and hydrogenation products was performed by GC-FID analysis.

2.4.2   Analytical Measurements

2.4.2.1   NMR Spectroscopy

^{1}H and ^{13}C NMR spectra were recorded (300 K) with a Bruker Avance 300 (300.13 MHz ^{1}H; 75.47 MHz ^{13}C) and Bruker Avance 400 (400.13 MHz ^{1}H; 100.61 MHz ^{13}C) spectrometers. Chemical shifts are reported in ppm (δ) relative to internal tetramethylsilane (TMS). NMR assignments are based on COSY, HSQC and NOESY 2D NMR experiments. Coupling constants (J) are reported in Hertz (Hz). Following abbreviations are used for spin multiplicities: s (singlet), d (doublet), t (triplet), m (multiplet), dd (doublet of dublets).

2.4.2.2   Elemental Analysis

Elemental analyses were determined by the analytical department of the University of Regensburg with a Micro Vario Cube (Elementar).

2.4.2.3   Melting Points

Determination of melting points was carried out with a SMP10 (Stuart) device. Samples were sealed in a glass ampoule under reduced pressure. The values are not corrected.

2.4.2.4   Gas Chromatography with FID

Agilent 7820A GC-Systems. Column: HP 5 19091J-413 (30 m x 0.32 mm x 0.25 μm) from *Agilent*, carrier gas: N2. GC-FID was used for catalyst screening (Calibration with internal standard *n*-pentadecane and analytically pure samples). Standard heating procedure: 50 °C (0.5 min), 25 °C/min (9.2 min) => 280 °C (3 min); 2.0 mL/min. Heating procedure for reactions with 1-dodecene: 50 °C (0 min), 5 °C/min (21 min), 30 °C/min (4.3 min) => 250 °C (1 min); 2.0 mL/min.

2.4.2.5   Gas Chromatography with Mass-Selective Detector:

Agilent 6890N Network GCSystem, mass detector 5975 MS. Column: BPX5 (30m x 0.25 mm x 0.25 µm) from *SGE*, carrier gas: H2 (1.0 mL/min). Standard heating procedure: 50 °C (2 min), 25 °C/min (10 min) => 300 °C (5 min).

2.4.2.6   ESI Mass Spectrometry

Sample solutions were transferred into a gas-tight syringe and infused into the ESI source of an HCT quadrupole-ion trap mass spectrometer (Bruker Daltonik) at a flow rate of 8 µLmin^{-1}. For the ESI process and the transfer of the ions into the helium-filled quadrupole ion trap, mild conditions similar to those reported previously were applied.[31] Mass spectra were recorded over a typical *m/z* range of 50–1000. Gas-phase fragmentation was accomplished by subjecting the mass-selected ions to excitation voltages of amplitudes V_{exc} and allowing them to collide with the helium gas.
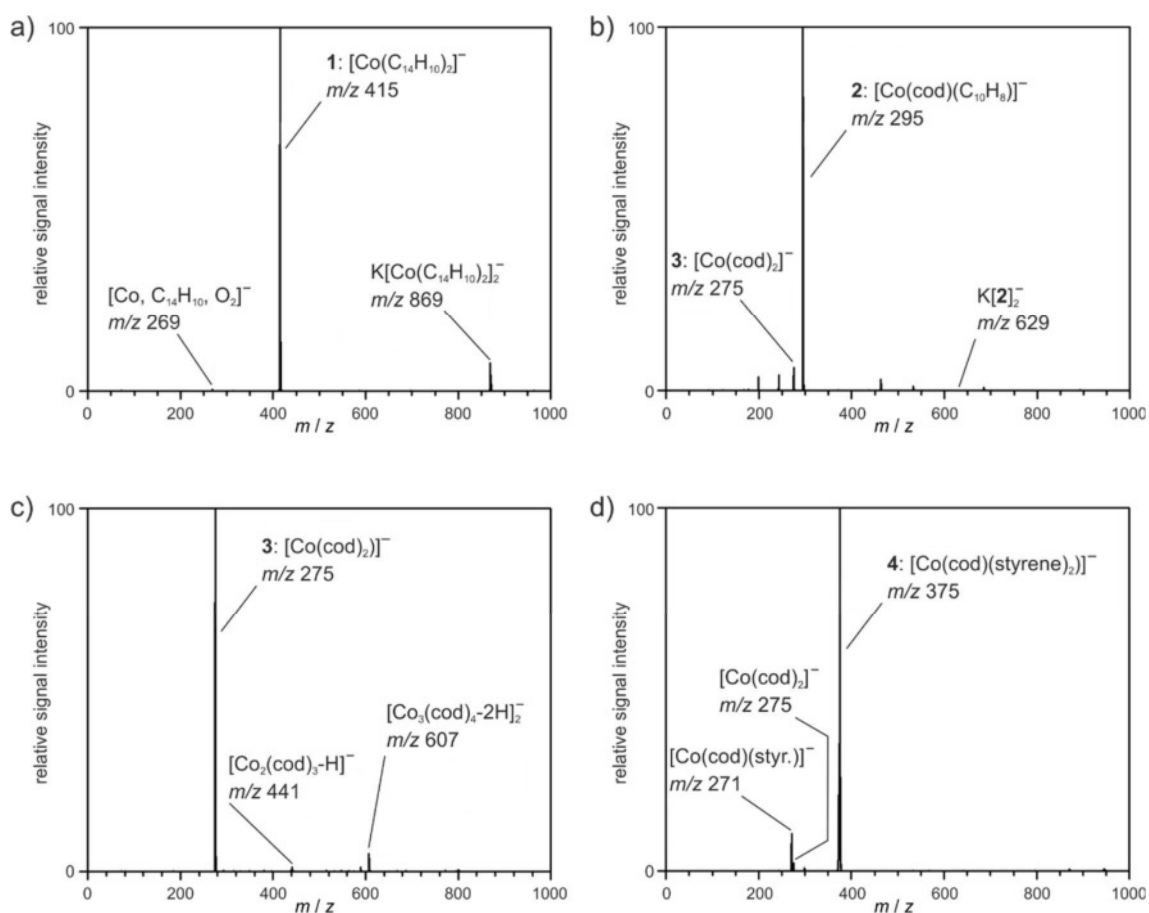

Figure S1   Negative-ion mode ESI spectra of THF solutions of selected cobaltate pre-catalysts: a) **1** (c = 10 mM); b) **3** (c = 7.5 mM); c) **3** (c = 7.5 mM); and c) **5** (c = 10 mM). styr. = styrene.
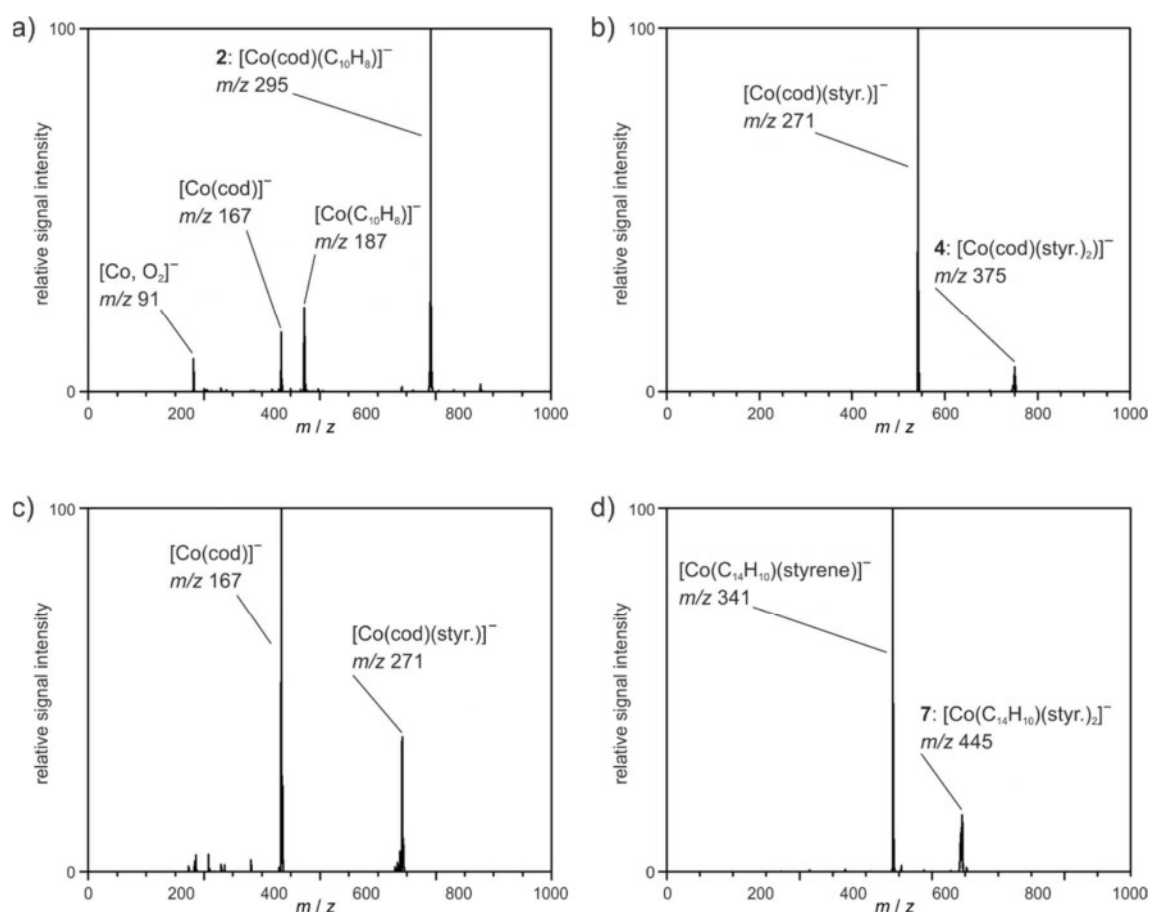
Figure S2   Mass spectra of mass selected cobaltates and its fragment ions produced upon collision-induced dissociation: a) **2** ($V_{exc} = 0.65$); b) **4** ($V_{exc} = 0.35$); c) [Co(cod)(styrene)]$^-$ ($V_{exc} = 0.55$); and c) **7** ($V_{exc} = 0.25$). styr. = styrene.

2.4.2.7   X-ray Crystallography

The single crystal X-ray diffraction data were recorded on an Agilent Technologies SuperNova diffractometer in case of compound **4** and on an Agilent Technologies Gemini Ultra diffractometer in case of **5** and **6**, using CuKα radiation for **4** and **5** and MoKα radiation for **6**. Empirical multi-scan and analytical absorption corrections were applied to the data.[39, 40] Using Olex2,[41] the structures were solved with SHELXS or SHELXT.[42, 43] Least-square refinements were carried out with SHELXL.[42] CCDC 1513657 (**4**), 1513658 (**5**), and 1513659 (**6**) contain the supplementary crystallographic data for this paper. These data can be obtained free of charge from The Cambridge Crystallographic Data Centre via www.ccdc.**cam.ac.uk/data_request/cif**.

Table S1:   Crystal data and structure refinement for compounds **4**, **5**, and **6**.

Compound	**4**	**5**	**6**
Empirical formula	$C_{36}H_{52}CoKO_6$	$C_{36}H_{48}CoKO_6$	$C_{40}H_{40}CoKO_2$
Formula weight	678.80	674.77	650.75
Temperature [K]	123.0(1)	123.0(1)	123(1)
Crystal system	triclinic	monoclinic	monoclinic
Space group	$P\text{-}1$	$P2_1/c$	$P2_1/c$
a [Å]	8.6684(3)	10.13736(6)	15.1339(4)
b [Å]	9.2481(2)	21.30324(13)	15.3434(3)
c [Å]	22.0306(8)	15.32401(9)	14.9559(4)
α [°]	79.000(3)	90	90.00
β [°]	89.777(3)	96.1754(6)	115.835(3)
γ [°]	83.456(3)	90	90.00
Volume [Å³]	1722.09(10)	3290.15(4)	3125.77(14)
Z	2	4	4
ρ_{calc} [g/cm³]	1.309	1.362	1.383
μ [mm⁻¹]	5.330	5.579	0.718
F(000)	724.0	1432.0	1368.0
Crystal size [mm³]	0.1726 × 0.1347 × 0.0951	0.5154 × 0.2368 × 0.141	0.2 × 0.15 × 0.1
Radiation	CuKα (λ = 1.54184)	CuKα (λ = 1.54184)	MoKα (λ = 0.71073)
Range for data collection [°]	8.178 < 2Θ < 146.904	7.134 < 2Θ < 133.484	6.62 < 2Θ < 60.5°
Index ranges	-9 ≤ h ≤ 10 -10 ≤ k ≤ 11 -27 ≤ l ≤ 24	-12 ≤ h ≤ 12 -24 ≤ k ≤ 25 -18 ≤ l ≤ 18	-21 ≤ h ≤ 21 -20 ≤ k ≤ 21 -21 ≤ l ≤ 21
Reflections collected	16144	42504	86933
Independent reflections	6726 R_{int} = 0.0303 R_{sigma} = 0.0369	5815 R_{int} = 0.0336 R_{sigma} = 0.0173	8906 R_{int} = 0.0423, R_{sigma} = 0.0295
Data/restraints/parameters	6726/91/427	5815/0/592	8906/36/426
Goodness-of-fit on F²	1.094	1.023	1.030
Final R indexes [I ≥ 2σ(I)]	R_1 = 0.0358 wR_2 = 0.0849	R_1 = 0.0239 wR_2 = 0.0608	R_1 = 0.0533, wR_2 = 0.1389
Final R indexes [all data]	R_1 = 0.0399 wR_2 = 0.0873	R_1 = 0.0252 wR_2 = 0.0616	R_1 = 0.0693, wR_2 = 0.1481
Largest diff. peak/hole [eÅ⁻³]	0.41/-0.33	0.21/-0.44	1.00/-0.60
CCDC	1513657	1513658	1513659

2.4.3   Complex Synthesis

Pre-catalysts [K(dme)$_2$][Co(anthracene)$_2$] (**1**),[19, 20] [K([18]crown-6)][Co(C$_{14}$H$_{10}$)(cod)] (**2**),[21] and [K(thf)$_{0.2}$][Co(cod)$_2$] (**3**),[22] were prepared according to literature procedures.

2.4.3.1   [K([18]crown-6)][Co(cod)(styrene)$_2$] (**4**)

Method 1 (from **2**):

A solution of styrene (57.4 mg, 0.551 mmol, 2.20 equiv.) in THF (2 mL) was added dropwise to a solution of [K([18]crown-6)][Co(C$_{10}$H$_8$)(cod)] (**2**) (150 mg, 0.251 mmol, 1.00 equiv.) in THF (5 mL) at room temperature. The resulting clear orange solution was stirred overnight. Afterwards the solvent was removed *in vacuo*. The solid orange residue was washed several times with diethyl ether (10 mL overall). The crude product was dissolved in THF (5 mL), the resulting solution was filtered and concentrated. Orange, Xray-quality crystals of **4** formed after layering of the THF solution with *n*-hexane (1:2). Yield: 105 mg (62%). M.p. 125 °C (decomp.). Elemental analysis calcd for C$_{36}$H$_{52}$O$_6$CoK (M = 678.84): C 63.70, H 7.72, found C 63.04, H 7.47. ^{1}H NMR (300.13 MHz, THF-d_8), major isomer: δ = –0.15 (d, J = 11.1 Hz, 2H, styrene CH$_2$), –0.02 (d, J = 7.3 Hz, 2H, styrene CH$_2$), 0.92-1.16 (m, 2H, cod CH), 1.22-1.44 (m, 2H, cod CH$_2$), 1.78-2.04 (m, 2H, cod CH$_2$), 2.62 (dd, J = 13.4, 7.9 Hz, 2H, cod CH$_2$), 2.27-2.93 (m, 2H, cod CH), 3.27-3.39 (m, 2H, cod CH$_2$), 4.77 (dd, J = 11.1, 7.3 Hz, 2H, styrene CH), 6.38-6.64 (m, 2H, styrene *p*-Ar-H), 6.89 (t, J = 7.4 Hz, 4H, styrene *m*-Ar-H) , 7.15-6.97 (m, 4H, styrene *o*-Ar-H), minor isomer: –0.63 (d, J = 6.8 Hz), –0.26 (d, J = 11.2 Hz), 0.55 (d, J = 11.2 Hz), 0.65 (d, J = 6.8 Hz), 0.87-0.89 (m), 2.29-2.39 (m), 3.02-3.10 (m), 4.17-4.27 (m), 4.50-4.62 (m). ^{13}C{^{1}H} NMR (100.61 MHz, 300 K, THF-d_8): δ = 29.4 (cod CH$_2$), 37.8 (cod CH$_2$), 47.0 (styrene CH$_2$), 60.4 (styrene CH), 71.0 ([18]crown-6 CH$_2$), 81.6 (cod CH), 89.5 (cod CH), 117.7 (styrene *p*-Ar-CH), 124.2 (styrene *m*-Ar-CH), 127.0 (styrene *o*-Ar-CH), 154.6 (styrene C$_{quart.}$-Ar); minor isomer: δ = 29.0, 29.4, 38.5, 117.6, 118.0, 124.4, 126.9, 127.5.

Method 2 (from **3**):

Styrene (2.09 mL, 18.2 mmol, 30.0 equiv.) was added to a solution of [K(thf)$_{0.2}$][Co(cod)$_2$] (**3**) (200 mg, 0.608 mmol, 1.00 equiv.) and [18]crown-6 (162.5 mg, 0.608 mmol, 1.00 equiv.) in THF (5 mL) at room temperature. The resulting clear, orange solution was stirred for 5 h. All volatile components were removed *in vacuo* afterwards. The resulting orange solid was washed with diethyl ether (5 mL), taken up in THF and layered with *n*-hexane. **4** was obtained as orange blocks by storage at room temperature. Yield: 290 mg (70%). The ^{1}H NMR spectrum of the sample prepared by method 2 was identical with those prepared by method 1.

2.4.3.2   [K([18]crown-6)][Co(cod)(dct)] (5)

A solution of dct (73.6 mg, 0.360 mmol, 1.50 equiv.) in THF (7 mL) was added dropwise to [K([18]crown-6)][Co($C_{10}H_8$)(cod)] (**2**) (143.7 mg, 0.240 mmol, 1.00 equiv.) in THF (10 mL) at room temperature. The resulting clear yellow solution was stirred overnight. Afterwards the solvent was removed *in vacuo*. The yellow-orange solid residue was washed three times with diethyl ether (15 + 10 + 5 mL). The crude product was dissolved in THF (7 mL) and filtered. Yellow-orange, X-ray-quality crystals of **5** formed after layering the filtrate with diethyl ether (1:1). Compound **5** is contaminated with a varying amount of **6**, which could not be removed by crystallization. A minimum of 18% impurity was observed. Yield: 76.3 mg (46%), referring to a mixture of **5** (82%) and **6** (18%). ^{1}H NMR (400.13 MHz, THF-d_8): δ = 1.98-2.06 (m, 4H, CH_2 of cod or dct), 2.24-2.34 (m, 4H, CH_2 of cod or dct), 2.71 (br s, 4H, alkene-CH of cod or dct), 2.93 (s, 4H, alkene-CH of cod or dct), 6.27-6.36 (m, 4H, Ar-H), 6.42-6.49 (m, 4H, dct Ar-H); in addition one set of signals assigned to the [Co(dct)$_2$]$^-$ anion of [K([18]crown-6)][Co(dct)$_2$] can be observed.

2.4.3.3   [K(thf)$_2$][Co(dct)$_2$] (6)

Method 1 (from 1): A solution of dct (733 mg, 3.59 mmol, 2.00 equiv.) in THF (60 mL) was added to a solution of **1** (1.14 g, 1.79 mmol, 1.00 equiv.) in THF (100 mL) at –80 °C, and the mixture was slowly warmed to room temperature. The resulting black suspension was concentrated, filtered and layered with *n*-hexane. A dark precipitate was isolated after 3 days. Repeated recrystallization (3x from THF/*n*-hexane 1:3) was necessary to remove remaining dct and anthracene. **6** was obtained as bright orange crystals. Yield: 220 mg (19%). M.p. 112 °C (decomp.). Elemental analysis calcd for $C_{40}H_{40}O_2CoK$ (M = 650.79): C 73.82, H 6.20, found C 73.45, H 6.04. ^{1}H NMR (400.13 MHz, THF-d_8): δ = 1.77 (m, THF), 3.45 (s, 8H, dct CH), 3.61 (m, THF), 6.45-6.48 (m, 8H, dct Ar-H), 6.56-6.58 (m, 8H, dct Ar-H). ^{13}C{^{1}H} NMR (100.61 MHz, 300 K, THF-d_8): δ = 26.3 (THF), 68.1 (THF), 87.6 (CH), 122.8 (C-Ar), 124.9 (C-Ar), 152.9 (C$_{quart}$-Ar).

Method 2 (from 1): A solution of dct (600 mg, 2.94 mmol, 2.00 equiv.) and styrene (612 mg, 5.88 mmol, 4.00 equiv.) in THF (50 mL) was added to a THF (120 mL) solution of **1** (932 mg, 1.47 mmol, 1.00 equiv.) at room temperature. The mixture was stirred overnight and filtered. Concentration of the clear orange solution to 60 mL and layering with diethyl ether (1:1) gave **6** as orange crystals. The isolated compound had the composition [K(thf)$_{0.75}$][Co(dct)$_2$] after drying in vacuo for one hour according to ^{1}H NMR and elemental analysis. Yield: 512 mg (62%). The ^{1}H NMR spectrum of samples prepared by this method was identical with those of samples prepared by method 1.

2.5   References

[1]   a) *Catalytic Hydrogenation* (Ed.: L. Cerveny), Elsevier, Amsterdam, **1986**; b) *The Handbook of Homogeneous Hydrogenation* (Eds.: J. G. de Vries, C. J. Elsevier), Wiley-VCH, Weinheim, **2007**.

[2]   a) J. A. Osborn, F. H. Jardine, J. F. Young, G. Wilkinson, *J. Chem. Soc.* **1966**, 1711-1732; b) W. S. Knowles, M. J. Sabacky, B. D. Vineyard, D. J. Weinkauff, *J. Am. Chem. Soc.* **1975**, *97*, 2567–2568; c) H. Doucet, T. Ohkuma, K. Murata, T. Yokozawa, M. Kozawa, E. Katayama, A. F. England, T. Ikariya, R. Noyori, *Angew. Chem. Int. Ed.* **1998**, *37*, 1703–1707; d) Á. Molnár, A. Sárkány, M. Varga, *J. Mol. Catal.* **2001**, *173*, 185–221.

[3]   a) M. Raney, *US patent 1628190* **1927**; b) I. M. Angulo, A. M. Kluwer, E. Bouwman, *Chem. Commun.* **1998**, 2689–2690; c) S. Kuhl, R. Schneider, Y. Fort, *Organometallics* **2003**, *22*, 4184–4186; d) T. Hibino, K. Makino, T. Sugiyama, Y. Hamada, *ChemCatChem* **2009**, *1*, 237–240.

[4]   a) W. Hess, J. Treutwein, G. Hilt, *Synthesis* **2008**, *40*, 3537-3562; b) M. S. Holzwarth, B. Plietker, *ChemCatChem* **2013**, *5*, 1650–1679; c) I. Bauer, H. J. Knölker, *Chem. Rev.* **2015**, *115*, 3170-3387; d) P. Röse, G. Hilt, *Synthesis* **2016**, *48*, 463-492.

[5]   S. Enthaler, K. Junge, M. Beller, *Angew. Chem. Int. Ed.* **2008**, *47*, 3317–3321.

[6]   Q. Knijnenburg, A. D. Horton, H. van der Heijden, T. M. Kooistra, D. G. H. Hetterscheid, J. M. M. Smits, B. de Bruin, P. H. M. Budzelaar, A. W. Gal, *J. Mol. Catal. A: Chem.* **2005**, *232*, 151–159

[7]   a) S. Monfette, Z. R. Turner, S. P. Semproni, P. J. Chirik, *J. Am. Chem. Soc.* **2012**, *134*, 4561–4564; b) R. P. Yu, J. M. Darmon, J. M. Hoyt, G. W. Margulieux, Z. R. Turner, P. J. Chirik, *ACS Catal.* **2012**, *2*, 1760–1764.

[8]   a) G. Zhang, B. L. Scott, S. K. Hanson, *Angew. Chem. Int. Ed.* **2012**, *51*, 12102–12106; b) G. Zhang, K. V. Vasudevan, B. L. Scott, S. K. Hanson, *J. Am. Chem. Soc.* **2013**, *135*, 8668–8681; c) G. Zhang, S. K. Hanson, *Chem. Commun.* **2013**, *49*, 10151-10153.

[9]   a) M. R. Friedfeld, M. Shevlin, J. M. Hoyt, S. W. Krska, M. T. Tudge, P. J. Chirik, *Science* **2013**, *342*, 1076–1080; b) M. R. Friedfeld, G. W. Margulieux, B. A. Schaefer, P. J. Chirik, *J. Am. Chem. Soc.* **2014**, *136*, 13178–13181; c) J. M. Hoyt, M. Shevlin, G. W. Margulieux, S. W. Krska, M. T. Tudge, P. J. Chirik, *Organometallics* **2014**, *33*, 5781–5790.

[10] T. J. Korstanje, J. I. van der Vlugt, C. J. Elsevier, B. de Bruin, *Science* **2015**, *350*, 298–302.

[11] Selected examples: a) X. Yang, *ACS Catal.* **2011**, *1*, 849–854; b) G. Bauer, K. A. Kirchner, *Angew. Chem. Int. Ed.* **2011**, *50*, 5798–5800; c) R. Langer, G. Leitus, Y. Ben-David, D. Milstein, *Angew. Chem. Int. Ed.* **2011**, *50*, 2120–2124; d) R. Xu, S. Chakraborty, H. Yuan, W. D. Jones, *ACS Catal.* **2015**, *5*, 6350–6354; e) A. Z. Spentzos, C. L. Barnes, W. H. Bernskoetter, *Inorg. Chem.* **2016**, *55*, 8225–8233.

[12] a) S. Rösler, J. Obenauf, R. Kempe, *J. Am. Chem. Soc.* **2015**, *137*, 7998–8001; b) N. Gorgas, B. Stöger, L. F. Veiros, K. Kirchner, *ACS Catal.* **2016**, *6*, 2664–2672.

[13] a) D. Srimani, A. Mukherjee, A. F. G. Goldberg, G. Leitus, Y. Diskin-Posner, L. J. W. Shimon, Y. Ben David, D. Milstein, *Angew. Chem. Int. Ed.* **2015**, *54*, 12357–12360; b) Z. Shao, S. Fu, M. Wei, S. Zhou, Q. Liu, *Angew. Chem. Int. Ed.* DOI: 10.1002/ange.201608345; c) S. Fu, N.-Y. Chen, X. Liu, Z. Shao, S.-P. Luo, Q. Liu, *J. Am. Chem. Soc.* **2016**, *138*, 8588–8594.

[14] a) T.-P. Lin, J. C. Peters, *J. Am. Chem. Soc.* **2013**, *135*, 15310–15313; b) T.-P. Lin, J. C. Peters, *J. Am. Chem. Soc.* **2014**, *136*, 13672–13683.

[15] K. Tokmic, C. R. Markus, L. Zhu, A. R. Fout, *J. Am. Chem. Soc.* **2016**, *138*, 11907–11913.

[16] a) S.-B. Choe, K. J. Klabunde, *J. Organomet. Chem.* **1989**, *359*, 409–418; b) S. Sun, C. A. Dullaghan, G. B. Carpenter, A. L. Rieger, P. H. Rieger, D. A. Sweigart, *Angew. Chem. Int. Ed. Engl.* **1995**, *34*, 2540–2542; c) S. Sun, L. K. Yeung, D. A. Sweigart, T.-Y. Lee, S. S. Lee, Y. K. Chung, S. R. Switzer, R. D. Pike, *Organometallics* **1995**, *14*, 2613–2615; d) J. K. Seaburg, P. J. Fischer, V. G. Young Jr., J. E. Ellis, *Angew. Chem. Int. Ed.* **1998**, *37*, 155-158.

[17] review: J. E. Ellis, *Inorg. Chem.* **2006**, *45*, 3167–3186.

[18] D. Gärtner, A. Welther, B. R. Rad, R. Wolf, A. Jacobi von Wangelin, *Angew. Chem. Int. Ed.* **2014**, *53*, 3722–3726.

[19] Preparation of [K(L)][Co(anthracene)$_2$] and related compounds: a) W. W. Brennessel, V. G. Young Jr., J. E. Ellis, *Angew. Chem. Int. Ed.* **2002**, *41*, 1211–1215; b) W. W. Brennessel, J. E. Ellis, *Inorg. Chem.* **2012**, *51*, 9076–9094.

[20] Compound **1** was prepared according to a slightly modified procedure detailed in ref. [18].

[21] W. W. Brennessel, V. G. Young, J. E. Ellis, *Angew. Chem. Int. Ed.* **2006**, *45*, 7268–7271.

[22] a) K. Jonas, R. Mynott, C. Krüger, J. C. Sekutowski, Y.-H. Tsay, *Angew. Chem.* **1976**, *88*, 808-809 b) K. Jonas, *US patent 4169845* **1979**.

[23] W. Caminati, B. Vogelsanger, A. Bauder, *J. Mol. Spectrosc.* **1988**, *128*, 384–398.

[24] In total, four isomers with differing relative orientations of the phenyl groups are conceivable for **5**, two of which have C_2 symmetry while two have C_s symmetry.

[25] a) S. Chaffins, M. Brettreich, F. Wudl, *Synthesis* **2002**, *9*, 1191–1194; b*)* G. Franck, M. Brill, G. Helmchen, *Org. Synth.* **2012**, *89*, 55-65.

[26] a) D. R. Anton, R. H. Crabtree, *Organometallics* **1983**, *2*, 855–859; b) J. A. Widegren, R. G. Finke, *J. Mol. Catal.* **2003**, *198*, 317-341; c) R. H. Crabtree, *Chem. Rev.* **2011**, *112*, 1536–1554.

[27] a) A. J. Frings, PhD dissertation, University of Bochum, Germany, **1988**; b) K. Jonas, *Pure Appl. Chem.* **1990**, *62*, 1169-1174.

[28] E.-M. Schnöckelborg, M. M. Khusniyarov, B. de Bruin, F. Hartl, T. Langer, M. Eul, S. Schulz, R. Pöttgen, R. Wolf, *Inorg. Chem.* **2012**, *51*, 6719–6730.

[29] a) S. Zhang, J. K. Shen, F. Basolo, T. D. Ju, R. F. Lang, G. Kiss, C. D. Hoff, *Organometallics* **1994**, *13*, 3692–3702; b) J. K. Seaburg, P. J. Fischer, J. Young Victor G., J. E. Ellis, *Angew. Chem. Int. Ed.* **1998**, *37*, 155–158; c) G. Zhu, K. E. Janak, J. S. Figueroa, G. Parkin, *J. Am. Chem. Soc.* **2006**, *128*, 5452–5461.

[30] P. Paklepa, J. Woroniecki, P. K. Wrona, *J. Electroanal. Chem.* **2001**, *498*, 181–191.

[31] a) B. H. Lipshutz, J. Keith, D. Buzard, *J. Organometallics* **1999**, *18*, 1571-157; b) K. Koszinowski, P. Böhrer, *Organometallics* **2009**, *28*, 100-110; c) A. Putau, K. Koszinowski, *Organometallics* **2011**, *30*, 4771-4778; d) T. K. Trefz, M. A. Henderson, M. Linnolahti, S. Collins, J. S. McIndoe, *Chem. Eur. J.* **2015**, *21*, 2980-2991; e) C. Schnegelsberg, S. Bachmann, M. Kolter, T. Auth, M. John, D. Stalke, K. Koszinowski, *Chem. Eur. J.* **2016**, *22*, 7752-7762.

[32] T. Parchomyk, K. Koszinowski, *Chem. Eur. J.* **2016**, *22*, 15609-15613.

[33] a) N. G. Tserkezos, J. Roithová, D. Schröder, M. Ončák, P. Slavíček, *Inorg. Chem.* **2009**, *48*, 6827-6296; b) A. Putau, H. Brand, K. Koszinowski, *J. Am. Chem. Soc.* **2012**, 134, 613-622.

[34] We also analyzed sample solutions prepared under a hydrogen atmosphere (1 bar), which should disfavor dehydrogenation reactions. However, we still observed the peaks of the dehydrogenated complexes. Possibly, these species formed in the ESI source, where no hydrogen atmosphere could be maintained.

[35] B. J. Fallon, E. Derat, M. Amatore, C. Aubert, F. Chemla, F. Ferreira, A. Perez-Luna, M. Petit, *J. Am. Chem. Soc.* **2015**, *137*, 2448-2451.

[36] a) http://www.chem.wisc.edu/areas/reich/pkatable/ (October 15th, 2016); b) W. N. Olmstead, Z. Margolin, F. G. Bordwell, *J. Org. Chem.* **1980**, *45*, 3295-3299; c) F. G. Bordwell, D. J. Algrim, *J. Am. Chem. Soc.* **1988**, *110*, 2964-2968.

[37] a) G. E. Dobereiner, R. H. Crabtree, *Chem. Rev.* **2010**, *110*, 681-703; b) G. Zhang, S. K. Hanson, *Org. Lett.* **2013**, *15*, 650-653.

[38] a) B. S. Terra, F. Macedo, Jr., *ARKIVOC* **2012**, 134-151; b) B. E. Kahn, R. D. Rieke, *Chem. Rev.* **1988**, *88*, 733-745.

[39] a) SCALE3ABS, CrysAlisPro, Aglient Technologies Inc., Oxford, UK, **2015**; b) G. M. Sheldrick, SADABS, Bruker AXS, Madison, USA, **2007**.

[40] a) R. C. Clark, J. S. Reid, *Acta Crystallogr. A* **1995**, *51*, 887; b) CrysAlisPro, version 171.37.35, Agilent Technologies Inc., Oxford, UK, **2015**.

[41] O.V. Dolomanov, L.J. Bourhis, R.J. Gildea, J.A.K. Howard, H. Puschmann, *J. Appl. Cryst.* **2009**, *42*, 339-341.

[42] G. M. Sheldrick, *Acta Cryst. A* **2008**, *64*, 112-122.

[43] G. M. Sheldrick, *Acta Cryst. A* **2015**, *71*, 3-8.

3 RECYCLABLE COBALT(0) NANOPARTICLE CATALYSTS FOR HYDROGENATIONS

PHILIPP BÜSCHELBERGER, EFRAIN REYES-RODRIGUEZ, CHRISTIAN SCHÖTTLE,

JENS TREPTOW, CLAUS FELDMANN, AXEL JACOBI VON WANGELIN, AND ROBERT WOLF
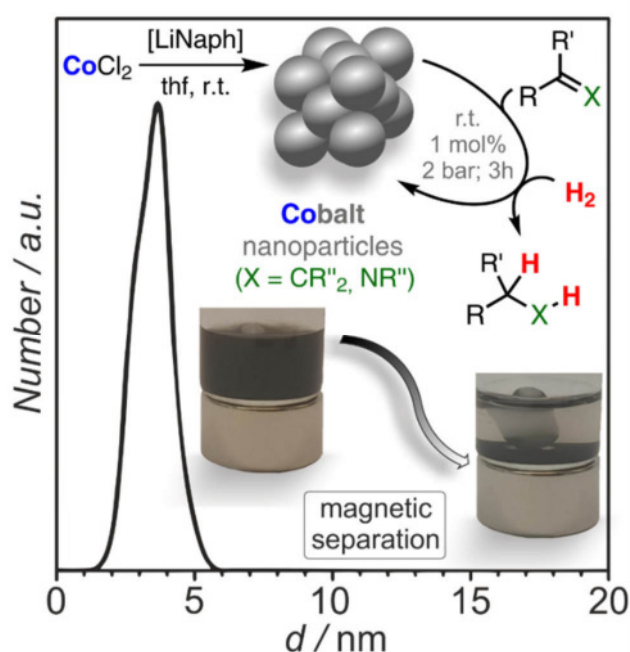
This study reports a new method for the preparation of small, monodisperse Co(0) nanoparticles (3-4 nm) from the reduction of commercial $CoCl_2$ in the absence of ligands or surfactants. High catalytic activity was observed in hydrogenations of alkenes, alkynes, imines, and heteroarenes (1-20 bar H_2). The magnetic properties enabled easy catalyst separation and multiple recycling.

3.1   Introduction

The recent advent of powerful synthetic and spectroscopic techniques for the preparation and analysis of sensitive metallic compounds has prompted a rapidly increasing interest in colloidal and nanoparticulate base metal(0) catalysts.[1] The characteristics of metallic nanoparticles as hybrids between homogeneous and heterogeneous species address the key criteria for catalytic applications: high dispersion, large surface area, good separability, rich surface coordination chemistry, and high reactivity.[2] Molecular cobalt catalysts have recently been intensively studied toward their application to hydrogenation reactions (Scheme 3.1, top left).[3, 4] The liquid-phase synthesis of base cobalt nanoparticles is often limited by their sensitivity and rapid ageing and the availability of convenient precursor molecules. Low-valent organometallic precursors (e.g. carbonyl, alkyl, aryl complexes) can be volatile and toxic or require multi-step syntheses, special conditions, and elaborate handling procedures (Scheme 3.1, bottom left).[5] Typically, tailor-made surfactants (e.g. amines, thiols, polydentate ligands, ionic liquids) are needed to control particle size and growth and prevent agglomeration.[6]
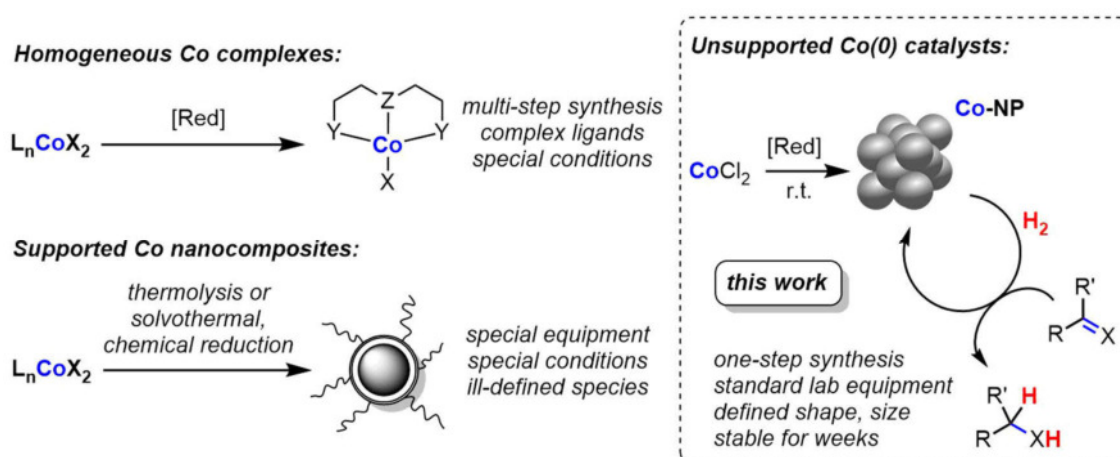
Scheme 3.1   Molecular and heterogeneous cobalt catalysts for hydrogenations.

Several heterogeneous hydrogenation catalysts were prepared by the reduction of 3d transition metal precursors with organometallic or hydride reagents and by thermal decomposition of transition metal-ligand complexes, often in the presence of stable support materials.[7] Beller and co-workers successfully applied cobalt oxide nanoparticles supported on Al_2O_3 to catalytic hydrogenations of heteroarenes, nitriles, and ketones.[8] The same group recently reported graphitic shell encapsulated Co nanoparticles for the synthesis of amines by reductive amination,[9] while Yuan reported nanocomposite Co/CoO on graphene for catalytic nitroarene hydrogenations.[10] Reusable Co nanoparticle catalysts on silicon carbon nitride were prepared

by Kempe and co-workers.[11] Zhang and co-workers developed *Z*-selective semi-hydrogenations of alkynes with an ill-defined Co/B catalyst formed from cobalt(II) acetate and $NaBH_4$.[12] Similar chemoselectivity was reported for Co@*N*-graphite nanoparticles.[13]

Here, we present a complementary synthesis of a "quasi-naked" Co nanoparticle catalyst that avoids complex ligands for controlling nucleation and agglomeration (i.e. only solvent available), high-temperature conditions for crystallization, and special support materials for deposition. Very small and monodisperse Co(0) nanoparticles are accessible by the precise control of the reducing conditions in the presence of an alkali metal/arene couple (Scheme 3.1, right).[14] The resultant Co(0) catalysts present tangible advances over the current state-of-the-art in that they are easily accessible from commercial reagents, exhibit long-term stability and activity, exhibit a wide substrate scope in hydrogenation reactions, and allow facile separation and catalyst recycling. The complementary properties of such Co nanoparticles and related molecular catalysts prepared under similar conditions demonstrate the close conceptual relationship between homogeneous and heterogeneous catalysts.[4, 15, 16]

3.2 Results and Discussion

3.2.1 Catalyst Synthesis and Characterization

Highly pure M(0) nanoparticles (M = Ti, Mo, W, Re, Fe, Zn) with diameters of ≤10 nm were prepared by the reduction of metal halides with alkaline metal naphthalenides.[17] However, the related quasi-naked Co(0) nanoparticles were still elusive due to their strong superparamagnetism and the resulting agglomeration. A modified procedure has now enabled the facile preparation of small and uniform nanoparticles in quantitative yield by reduction of $CoCl_2$ with lithium naphthalenide ([LiNaph]) at 20 °C and centrifugation (Co-NP) or magnetic separation (mCo-NP, Scheme 3.2). Alkali metal naphthalenides were also used to obtain so-called activated Rieke metals,[18] which, are barely characterized and typically represent bulk metals. Nanoparticles made *via* the Rieke approach often show significant agglomeration and oxide impurities.[18b] The here shown Co nanoparticles nevertheless may also support understanding of the mechanism of activated Rieke metals.
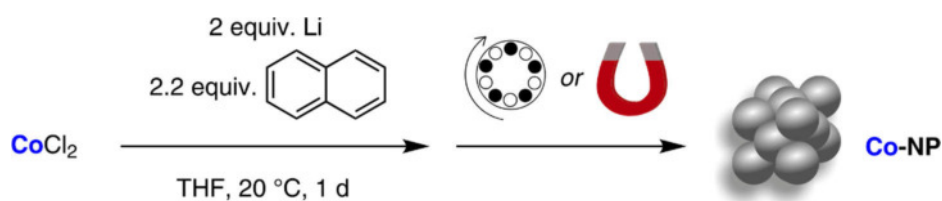
Scheme 3.2   Synthesis of defined Co(0) nanoparticles (Co-NP) by reduction of CoCl2 with LiNaph and centrifugation or magnetic separation.

Here, Co(0) formation was apparent from the immediate color change to black. Use of an excessively strong reductant (E^o([NaNaph]) = −3.1 V vs. Fc/Fc$^+$, *cf.* E^o(Co^{2+}/Co^0) = −0.28 V vs. NHE)[19, 20] ensured high oversaturation and thus enabled excellent control of nucleation and particle growth (LaMer model).[21] The precipitates were separated by centrifugation (20,000 rpm) to obtain powderous Co(0) samples with quasi-naked surfaces. The nanoparticles could be redispersed in THF or toluene.

High-resolution transmission electron microscopy (HRTEM) and high-angle annular dark-field scanning transmission electron microscopy (HAADF-STEM) displayed uniform, non-agglomerated nanoparticles of 3.4±0.4 nm diameter (Figure 3.1a and inset). HAADF-STEM images showed highly ordered lattice fringes that indicate the presence and crystallinity of the Co(0) nanoparticles. The lattice distance (2.0 Å) matches that of cubic bulk-Co^o (*d(111)* = 2.0 Å). X-ray powder diffraction (XRD) confirmed the presence of high-purity metallic Co and the absence of any oxide impurities (Figure 3.1b).

Statistical evaluation of at least 100 nanoparticles on HRTEM and HAADF-STEM images documented the size distribution of the as-prepared Co-NPs with a mean diameter of 3.6±0.9 nm (Figure 3a). Fourier transform infrared spectroscopy (FT-IR) gave very weak absorption related to surface-adhered molecules (mostly THF, Figure 3b), which documented the presence of quasi-naked nanoparticles.[17] All in all, such small size and low agglomeration in absence of specific strong binding ligands is an advancement in regard of non-blocked catalytically active surfaces and even more remarkable for nanoparticles showing attractive magnetic properties.

Glass capillaries containing the powderous Co-NPs were strongly attracted to a permanent magnet. The latter property was exploited in the development of a highly practical and
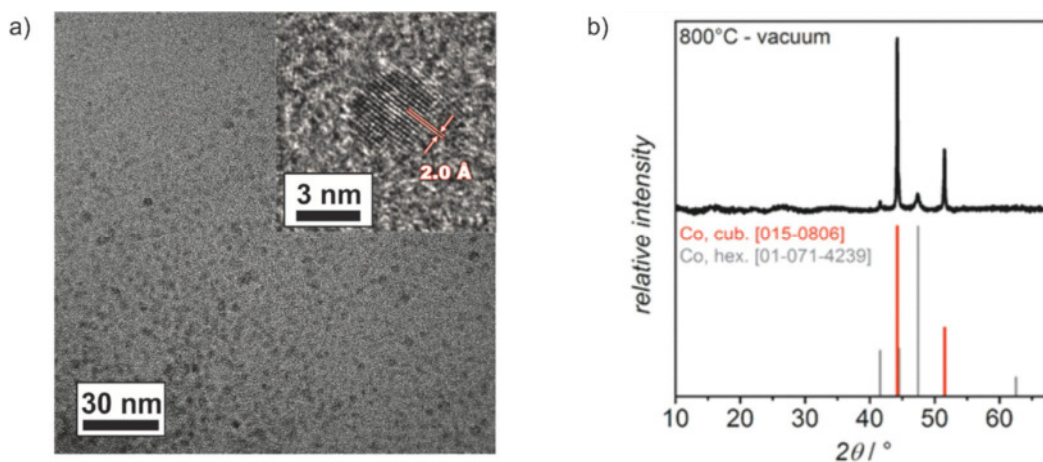

Figure 3.1   a) HRTEM overview and HAADF-STEM images (with lattice fringes and lattice distance). b) XRD Co(0) powder samples after annealing (800 °C, Ar).
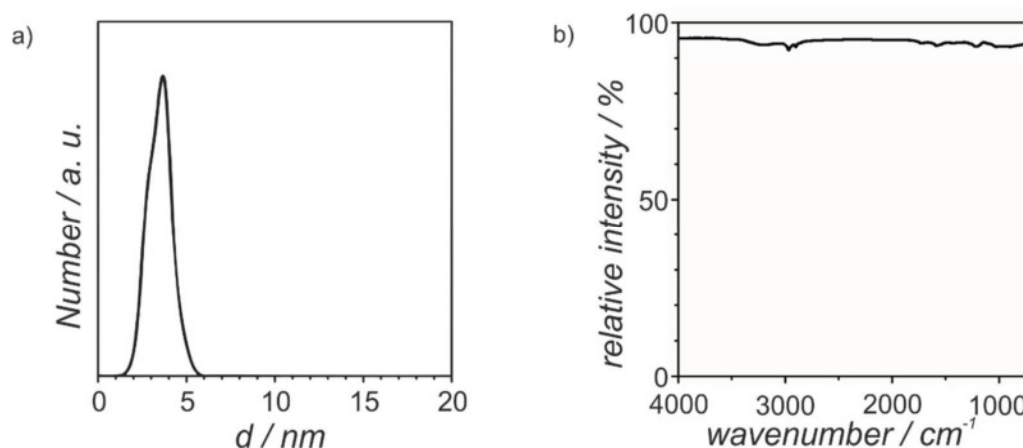
Figure 3.2   a) Particle size distribution from statistical evaluation of Co-NPs on TEM images. b) FT-IR spectrum with weak vibrations.

operationally simple procedure of preparation and work-up. The "quasi-naked" Co-NPs were successfully isolated from the suspension by magnetic immobilization (cylindrical neodymium magnet, 10x20 mm, N45, 15 min, 4 mmol Co in 20 mL THF) instead of the centrifugation.[14]

3.2.2   Catalytic Hydrogenations of C=C Bonds

We have evaluated the catalytic activity of the freshly prepared Co(0) nanoparticles in hydrogenations of unsaturated substrates that lie outside the well-explored scope of highly polar carbonyl, nitro, and cyano compounds. There are much fewer reports of Co-catalyzed hydrogenations of non-polar or less polar substrates such as alkenes, alkynes, and imines.[22] Highly reproducible catalyst activities, facile handling, and dosing were achieved by ultra-sonication of the catalyst suspension for 1 h prior to use. Mono- and di-substituted alkenes and terminal and internal alkynes were cleanly hydrogenated under very mild conditions (1 mol% Co-NP or mCo-NP, 2 bar H₂, 20°C, 3 h). Sterically demanding, functionalized, and tetra-substituted alkenes required slightly harsher conditions. Good chemoselectivities were observed for bifunctional molecules such as limonene, 2-vinylpyridine, chlorinated alkenes, enoates, alkenols, sulfones, and other N- and O-functionalities (Figure 3.3). External functional group tolerance tests (Figure S2) showed that cyano, nitro, and carbonyl functions were detrimental to the reaction, while esters, ethers, amines, fluoro and chloro groups were tolerated.[14]

The catalytic protocol was further simplified by preparing nanoparticles *in situ via* the standard protocol but without laborious work-up and isolation procedures. Control experiments showed the identical catalytic activity (Figure S3) and long-term stability of *in situ* prepared Co-NPs and the isolated Co-NPs (Table 3.1). Magnetic separation also afforded active Co(0) nanoparticles
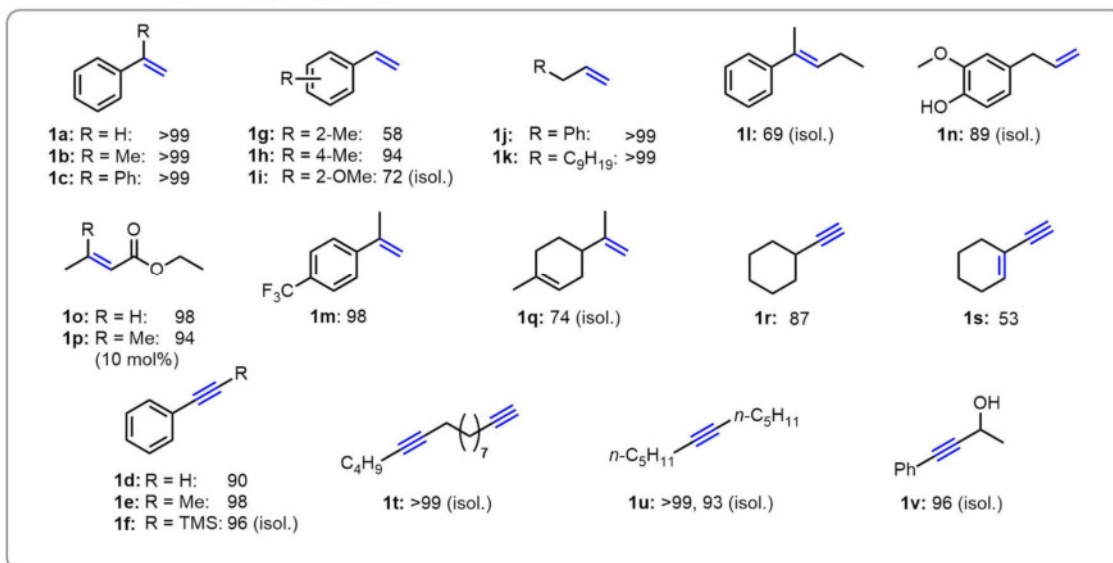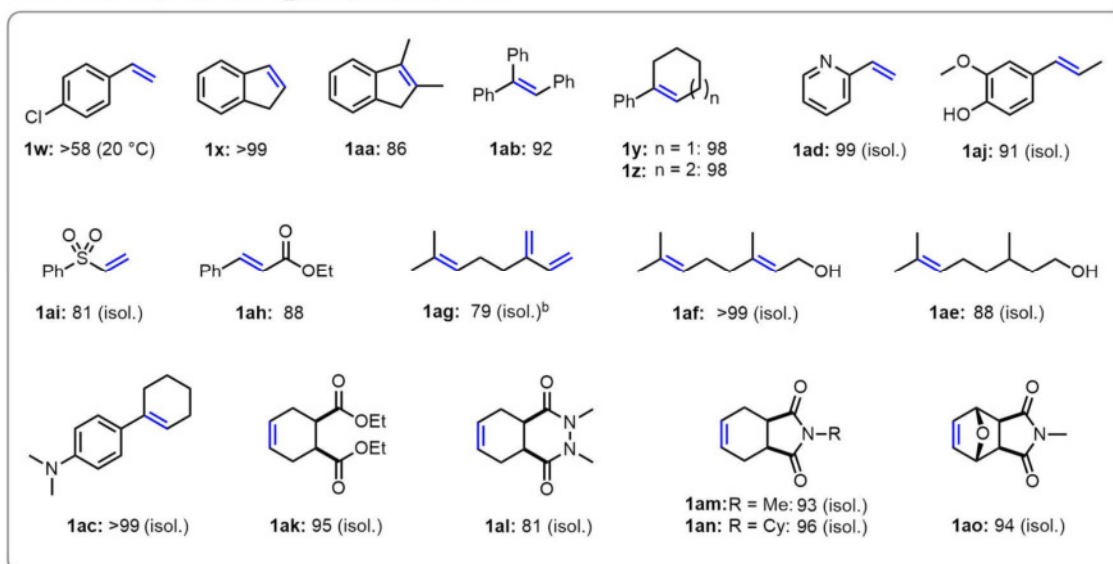
1-5 mol% Co-NP, 2 bar H$_2$, THF, 20°C, 3-24 h[14]

1a: R = H: >99
1b: R = Me: >99
1c: R = Ph: >99

1g: R = 2-Me: 58
1h: R = 4-Me: 94
1i: R = 2-OMe: 72 (isol.)

1j: R = Ph: >99
1k: R = C$_9$H$_{19}$: >99

1l: 69 (isol.)

1n: 89 (isol.)

1o: R = H: 98
1p: R = Me: 94
(10 mol%)

1m: 98

1q: 74 (isol.)

1r: 87

1s: 53

1d: R = H: 90
1e: R = Me: 98
1f: R = TMS: 96 (isol.)

1t: >99 (isol.)

1u: >99, 93 (isol.)

1v: 96 (isol.)

5 mol% Co-NP, 10-20 bar H$_2$, THF, 60-80°C, 3-48 h[14]

1w: >58 (20 °C)

1x: >99

1aa: 86

1ab: 92

1y: n = 1: 98
1z: n = 2: 98

1ad: 99 (isol.)

1aj: 91 (isol.)

1ai: 81 (isol.)

1ah: 88

1ag: 79 (isol.)[b]

1af: >99 (isol.)

1ae: 88 (isol.)

1ac: >99 (isol.)

1ak: 95 (isol.)

1al: 81 (isol.)

1am: R = Me: 93 (isol.)
1an: R = Cy: 96 (isol.)

1ao: 94 (isol.)

Figure 3.3   Co-catalyzed hydrogenation of alkenes and alkynes. Blue bonds indicate the sites of π-bond hydrogenation. Standard conditions: 0.25 mmol substrate, 1 mL in THF, 1 mol% Co-NP, 2 bar H$_2$, 20 °C, 3 h. If not otherwise noted, yields were determined by GC-FID vs. internal n-pentadecane.[14]

(mCo-NP) with identical catalytic activity (Figure S2) that could be easily recycled over multiple runs (Figure 3.4). The decoration of nanoparticles with organic surfactants is a versatile method for alteration of the surface properties and introduction of functionalities.[6, 23] The addition of oleylamine (1.5 equiv. per Co) to the freshly prepared nanoparticles resulted in the formation of a very stable, highly dispersed nanoparticle suspension (aCo-NP) that could not be magnetically separated by a standard magnet. The oleylamine-supported aCo-NP were catalytically less active and less stable than the amine-free Co-NPs so that there is no benefit of surfactant addition to Co-NP catalysis under these conditions (Table 3.1).

Table 3.1   Comparison of different Co-NP catalysts and ageing periods. Standard conditions: 0.5 mmol substrate in 2 mL THF; yields are determined by quantitative GC-FID vs. internal *n*-pentadecane. Conversion in parentheses if not >95%.

Substrate	[Co]	Yield [%] after 1 week	Yield [%] after 6-35 weeks
	Co-NP	>99	<99[a]
	mCo-NP	>99	98[b]
	In situ Co-NP	>99	97[c]
	aCo-NP	66 (69)	3 (8)
	Co-NP	96	98[a]
	mCo-NP	>99	96[b]
	In situ Co-NP	>99	96[c]
	aCo-NP	>99	91[a]

[a] 35 weeks; [b] 9 weeks; [c] 6 weeks.

The standard reaction conditions enabled effective catalyst recycling after each reaction run by an external magnet without loss of catalyst material and activity (Figure 3.4). More than 99.6% of the particles were removed from the organic phase by a commercial Nd magnet (10x20 mm, N45) and decantation (Figure 3.4b & c). ICP-OES studies documented minimal leaching (<0.4% Co, <0.02 mol%) into the liquid phase after the first run. After filtering the decanted reaction solution over silica, an insignificant amount of cobalt (0.68 ppm per Co supplied) remained in the organic phase.[14] TEM images showed only marginal differences of particle topology between the Co catalysts (Co-NPs and *in situ* Co-NPs) before and after the hydrogenations (Figure S5 & Figure S6). Multiple sequential reactions were performed with the same catalyst portion. Importantly, ultrasonication of the catalyst suspension resulted in a healing of catalytic activity after multiple recycling operations (>10) and when the catalyst aged during storage for extended periods (several days).
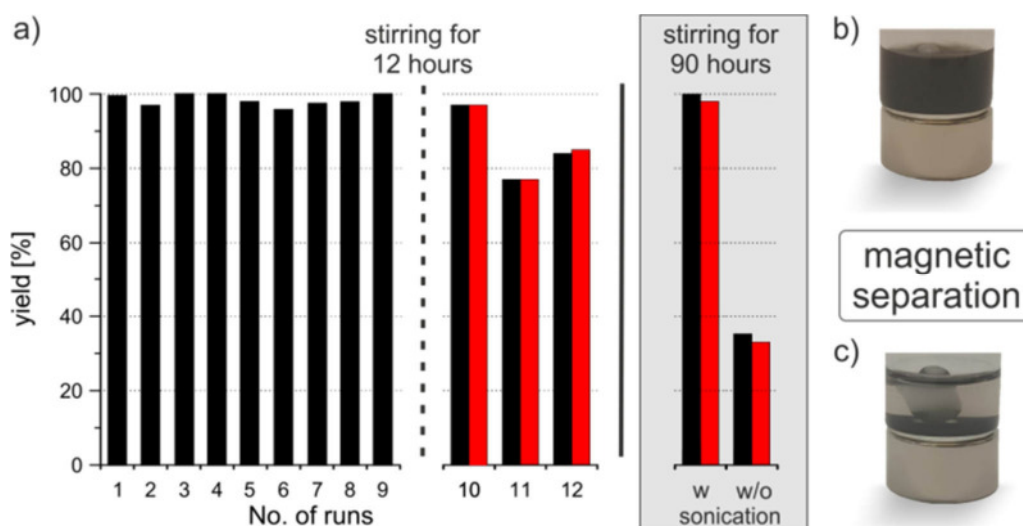
Figure 3.4   a) Consecutive hydrogenation runs of styrene (0.5 mmol) using the same catalyst particles (5 mol%) and regeneration of catalyst activity by ultrasonication (box); yields (black), conversions (red). b) Suspension of the hydrogenation reaction of styrene with 5 mol% Co-NP. c) Catalyst separation by an external magnet (after 1 min).

3.2.3   Mechanistic Studies

Proof of the heterogeneous nature of the catalyst was also derived from kinetic poisoning experiments (Figure 3.5).[16] Addition of the selective homotopic poison dibenzo[*a,e*]cyclooctatetraene (dct)[16, 24] at 40% conversion of a model hydrogenation did not change the reaction rate. Consistently, complete inhibition resulted from the addition of mercury (300 equiv. per Co). This quantitative amalgamation was accompanied by
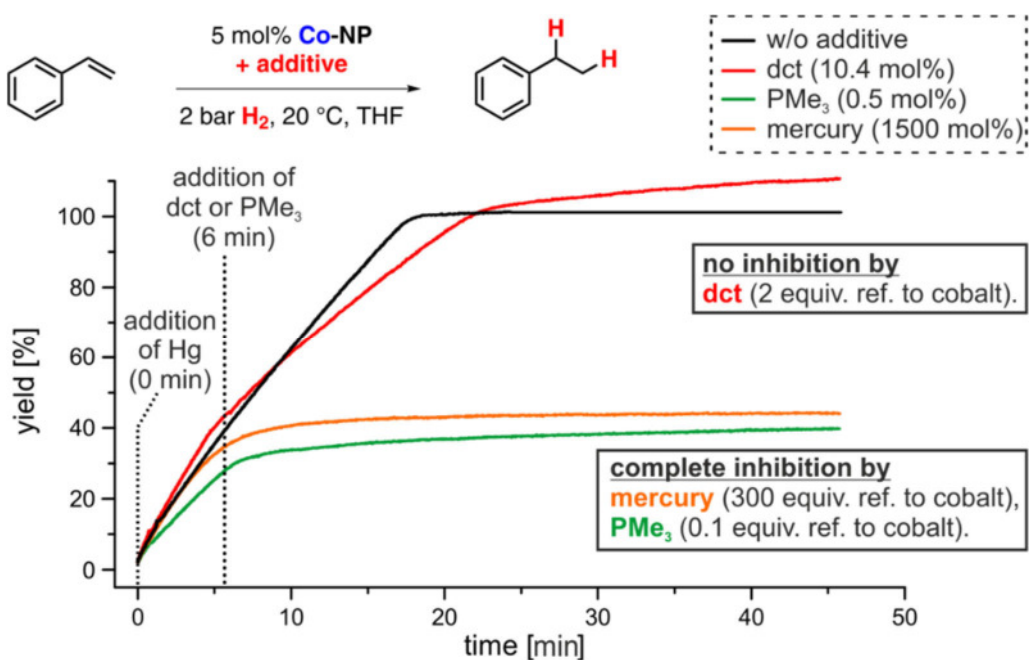
Figure 3.5   Catalyst poisoning with dct (2 equiv. per Co), PMe₃ (0.1 equiv. per Co), Hg (300 equiv. per Co). Yields were determined from the H₂ consumption.

decolorization and formation of a metallic mercury drop with silvery luster at the bottom of the reaction.[25] An identical reaction ceased immediately after addition of a 0.1 equiv. PMe$_3$ per Co. Lower amounts of PMe$_3$ (0.025 equiv.) resulted in partial catalyst poisoning. These studies provide strong indications of a heterotopic mechanism in full accord with literature reports.[16]

3.2.4 Catalytic Hydrogenation C=N Bonds

Finally, we extended the substrate scope of our nanoparticles beyond alkene hydrogenations to imines and heteroaromatic quinolines. Homogeneous and heterogeneous 3d metals that catalyze imine and quinoline hydrogenation are still relatively scarce even though such hydrogenations are an attractive, atom-economic route to amines, while compounds with a 1,2,3,4-tetrahydroquinoline scaffold are found in natural products and bioactive compounds.[26][26] Gratifyingly, our Co-NP catalysts were active in the clean hydrogenation of small and bulky aldimines, ketimines, and various quinolines (Figure 3.6). Chloro, ester, hydroxyl, benzyl, furan, and pyridine functions were tolerated. Besides the hydrogenation of the imine, the furanyl and pyridyl imines underwent partial hydrogenation of the heterocycle.[14]

3.3 Conclusion

In summary, we have established a straightforward and operationally simple synthesis of quasi-naked, colloidally and chemically stable Co(0) nanoparticles from commercial reagents. Detailed analytical studies (TEM, XRD, DLS, poisoning) documented the heterogeneous nature of the small and uniform nanoparticles of 3.6±0.9 nm. Applications to catalytic hydrogenations

5 mol% Co-NP, 10-20 bar H$_2$, THF, 60-80°C, 3-24 h[14]

2a: R = H: 91 (isol.)
2b: R = CO$_2$Me: 83 (isol.)
2c: 88 (isol.)
2d: 98 (isol.)
2e: R = Ph: 99 (isol.)
2f: R = Cy: 67 (isol.)
2g: 84 (isol.)
2h: 63 (isol.)

2i: 92 (isol.)
2j: 96 (isol.)
2k: 89 (isol.)
2l: 99 (isol.)
2m: 73 (isol.)
2n: 39 (isol.)

2o: 77 (isol.)
2p: 62 (isol.)
2q: 98 (isol.)
2r: 95 (isol.)
2s: 97% (isol.)
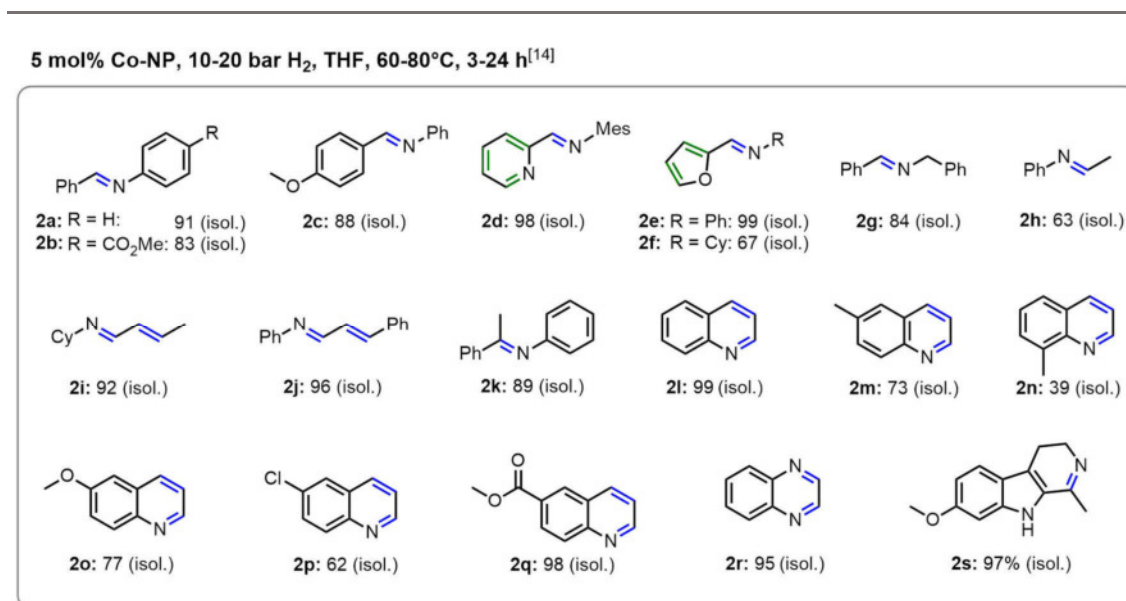
Figure 3.6   Co-catalyzed hydrogenation of imines and quinolines. Blue bonds are sites of hydrogenation. Green bonds indicate traces of overhydrogenation. Standard conditions: 0.5 mmol substrate, 2 mL THF, 5 mol% Co-NP, 10 bar H$_2$, 60 °C, 24 h. If not otherwise noted, yields were determined by GC-FID vs. *n*-pentadecane.[14]

enabled the clean conversion of alkenes, alkynes, imines, and quinolines under mild conditions (2–20 bar H_2, 20–80 °C). The catalysts could be easily mechanically separated and recycled for multiple hydrogenation runs without loss of activity. The ease of synthetic preparation in the absence of complex ligands, their wide catalytic applicability, the facile catalyst recycling and long-term stability constitute prime advantages of such cobalt catalysts that should stimulate further use in the realm of organic synthesis.

3.4 Supporting Information

3.4.1 General Considerations

All experiments were performed under an atmosphere of dry argon by using standard Schlenk and glovebox techniques. Solvents were purified, dried, and degassed by standard techniques. Commercially available olefins were distilled under reduced pressure prior to use. Oleylamine was stored over molecular sieve (4 Å) for 30 days and degassed in vacuum. Cobalt(II)chloride (99.999%, ABCR), lithium (99%, Alfa Aesar) and naphthalene (99%, Alfa Aesar) were used as received.

3.4.1.1 Analytical Thin-Layer Chromatography

Analytical thin-layer chromatography (TLC) was performed using aluminium plates with silica gel and fluorescent indicator (Merck, 60, F254). Thin layer chromatography plates were visualized by exposure to ultraviolet light (366 or 254 nm) or by immersion in a staining solution of molybdatophosphoric acid in ethanol or potassium permanganate in water.

3.4.1.2 Column Chromatography

Flash column chromatography was performed with silica gel 60 from KMF (0.040-0.063 mm). Mixtures of used solvents are noted in brackets.

3.4.1.3 High Pressure Reactor

Hydrogenation reactions were carried out in 160 and 300 mL high pressure reactors (*Parr*^{TM}) in 5 mL glass vials. The reactors were loaded under argon and purged with a continuous flow of H_2 (1 min) first, then three times with 2 bar of H_2. The reactors were sealed, and the internal pressure was adjusted. Hydrogen (99.9992%) was purchased from Linde.

3.4.2 Analytical Measurements

3.4.2.1 ^{1}H und ^{13}C NMR Spectroscopy

Nuclear magnetic resonance (NMR) spectra were recorded on *Bruker* Avance 300 (300.13 MHz ^{1}H, 75.47 MHz ^{13}C) and *Bruker* Avance 400 (400.13 MHz ^{1}H, 100.61 MHz ^{13}C) spectrometers. ^{1}H-NMR: The following abbreviations are used to indicate multiplicities: s = singlet; d = doublet; t = triplet, q = quartet; m = multiplet, dd = doublet of doublet, dt = doublet of triplet, dq = doublet of quartet, ddt = doublet of doublet of quartet. Chemical shifts δ are given in ppm relative to internal tetramethylsilane (TMS). Coupling constants are reported in Hertz (Hz).

3.4.2.2   Fourier-Transform Infrared Spectroscopy (FT-IR)

Spectra were recorded on an *Agilent* Cary 630 FTIR with ATR-device. All spectra were recorded at room temperature. Wave number is given in cm^{-1}. Bands are marked as s = strong, m = medium, w = weak and b = broad.

3.4.2.3   Gas Chromatography with FID (GC-FID)

HP6890 GC-System with injector 7683B and *Agilent* 7820A System. Column: HP-5 19091J-413 (30 m × 0.32 mm × 0.25 μm), carrier gas: N_2. GC-FID was used for reaction control and catalyst screening (Calibration with internal standard *n*-pentadecane and analytically pure samples).

3.4.2.4   Gas Chromatography with Mass-Selective Detector (GC-MS)

Agilent 6890N Network GC-System, mass detector 5975 MS. Column: HP-5MS (30 m × 0.25 mm × 0.25 μm, 5% phenylmethyl siloxane, carrier gas: H_2. Standard heating procedure: 50 °C (2 min), 25 °C/min => 300 °C (5 min)

3.4.2.5   High Resolution Mass Spectrometry (HRMS)

The spectra were recorded by the Central Analytics Lab at the Department of Chemistry, University of Regensburg, on a MAT SSQ 710 A from *Finnigan*.

3.4.2.6   Inductively Coupled Plasma Optical Emission Spectrometry (ICP-OES)

ICP-OES measurements were carried out on a *Spectro Analytical Instruments* Spectroflame (Type: FSMEA85C).

3.4.2.7   Inductively Coupled Plasma Mass Spectrometry (ICP-MS)

ICP-MS measurements were carried out on a *Perkin Elmer* Elan 9000.

3.4.2.8   Gas-Uptake Reaction Monitoring

Gas-uptake was monitored with a *Man On the Moon* X201 kinetic system to maintain a constant reaction pressure. The system was purged with hydrogen prior to use. Reservoir pressure was set to about 9 bar H_2. Calibration of the reservoir pressure drop in relation to H_2 consumption was performed by quantitative hydrogenation of various amounts of *α*-methylstyrene with a Pd/C catalyst in 1 mL of THF.

3.4.2.9   Transmission Electron Microscopy (TEM)

TEM, high-resolution (HR)TEM, and high-angle annular dark-field scanning transmission electron microscopy (HAADF-STEM) were conducted with an aberration-corrected *FEI* Titan3 80-300 microscope operating at 300 and 80 kV, a *FEI* Osiris microscope at 200 kV, and a *Philips* CM 200 FEG/ST microscope at 200 kV. TEM samples were prepared by evaporating DME, THF or

n-heptane suspensions on amorphous carbon (lacey-)film suspended on copper grids. The deposition of the samples on the carbon (lacey-)film copper grids was performed under argon atmosphere in a glovebox. The grids were thereafter transferred with a suitable vacuum/inert gas transfer module into the transmission electron microscope without any contact to air. Average particle diameters were calculated by statistical evaluation of at least 150 particles (ImageJ 1.47v software).

3.4.2.10   X-ray Powder Diffraction (XRD)

X-ray powder diffraction was carried out with a *Stoe* STADI-P diffractometer operating with Ge-monochromatized Cu-Kα radiation. Co^0 powder samples sintered at 800 °C for 7 h in vacuum for crystallization of the metal and eventual oxide impurities. The powder samples were measured on a *Stoe* IPDS II image plate diffractometer using Mo-Kα radiation (graphite monochromator). Samples were diluted with glass spheres (9-13 µm, Sigma-Aldrich) to reduce the X-ray absorption of the metal nanoparticles and prepared in glass capillaries under argon. Since the scattering power of the small-sized metal nanoparticles (diameter ≤10 nm) is low, certain non-specific background is observed for all nanoparticles. This non-specific scattering was fitted by background correction.

3.4.3   General Procedures

3.4.3.1   Synthesis of Co(0) Nanoparticles

Cobalt(II)chloride (519 mg, 4.0 mmol), lithium (56 mg, 8.0 mmol) and naphthalene (1.20 g, 9.4 mmol) were stirred in 20 mL THF for 24 h. The resultant nanoparticles were separated by centrifugation (20.000 rpm) and purified by redispersion and centrifugation (3 x 20 mL THF). Subsequently, the solids were dried in vacuum (for storage as powder) or redispersed in 40 mL THF (Co-NPs, for catalytic applications). The preparation of amine-stabilized nanoparticles (aCo-NPs) was effected by treatment of the dried solids with 38 mL THF and 2 mL oleylamine. As an alternative to the separation by centrifugation, the particles can be separated by an external commercial neodymium magnet (mCo-NPs). The preparation of related nanoparticles followed the same reduction protocol but without the washing procedures *(in situ* Co-NPs). The primary THF solutions (containing the by-products LiCl, naphthalene) were directly employed in catalytic reactions. The removal of the magnetic stir bar appeared to important to ensure long-term catalyst stability. After extended periods of storage of the catalyst suspensions, ultrasonification for 15-60 min effected complete redispersion and secured highest reproducibility.

3.4.3.2   General Procedure for Hydrogenation Reactions

Under an atmosphere of argon, a 5 mL screw cap vial with a PTFE septum and magnetic stir bar was charged with the substrate (0.25 mmol) and THF (875 µL). The catalyst suspension (125 µL; 0.0125 mmol Co) was added and the septum punctured with a short needle (*Braun*). The vial was placed into a high-pressure reactor (*Parr*^{TM}), which was sealed, removed from the glove box, placed on a magnetic stirrer plate, and purged with H_2. After 3 h at r.t. under an atmosphere of H_2 (2 bar), the pressure was released, the vial retrieved, and the reaction quenched with saturated aqueous NH_4Cl (1 mL). For quantitative GC-FID analyses, *n*-pentadecane was added as internal standard. The mixture was extracted with ethyl acetate and the combined organic layers were dried (Na_2SO_4). For isolation of the products, the reaction mixture was filtered through a Pasteur pipette filled with SiO_2. The pipette was washed with *n*-pentane (3 x 1 mL) and the solvents were evaporated. Amines were isolated as the corresponding ammonium salts after addition of HCl·Et_2O.

3.4.3.3   General Method for Kinetic Examination in Catalytic Hydrogenation

A flame-dried 10 mL two-neck flask was connected to a *Man on the Moon* X201 gas-uptake system. After purging with H_2, the system was set to a reaction pressure of 1.9 bar. The catalyst mixture in THF (2 ml) was added using a PTFE septum. Monitoring of the hydrogen uptake started with the addition of the substrate (0.5 mmol). The pressure was recorded every two seconds until the pressure in the reaction vessel remained stationary.

3.4.4 Synthesis of Starting Materials

3.4.4.1 General Procedure for the Synthesis of Imines

Silica (6 g) was weighed into a 100 ml round-bottom flask and suspended in ethanol (35 ml). After addition of the aldehyde (20 mmol) and amine (20 mmol, 1 equiv.), the flask was put into an ultrasonic bath for 20 min at room temperature.

The mixture was stirred overnight, filtered and the solvent removed. The crude product mixture was vacuum distilled (80 °C, 0.02 mbar) and the imines collected.

Modified procedure according to K. P. Guzen, A. S. Guarezemini, A. T. Órfão, R. Cella, C. M. Pereira, H. A. Stefani, *Tetrahedron Lett.* **2007**, *48*, 1845.

N-(2-Furanylmethylene)-benzenamine

$C_{11}H_9NO$

M = 171.20 g/mol

Pale yellow liquid
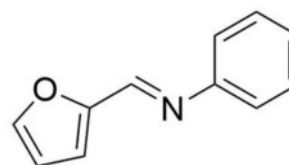
Yield	1.72 g, 10.0 mmol (50%)
^{1}H-NMR	(300.13 MHz, MeOD) δ = 8.37 (s, 1H), 7.77 (d, *J* = 1.8 Hz, 1H), 7.44-7.33 (m, 2H), 7.29-7.19 (m, 3H), 7.12 (dd, *J* = 3.5, 0.7 Hz, 1H), 6.64 (dd, *J* = 3.5, 1.8 Hz, 1H).
^{13}C{^{1}H}-NMR	(75.47 MHz, MeOD) δ = 153.08, 151.98, 150.21, 147.68, 130.38, 127.63, 122.05, 118.77, 113.52.
GC-MS	t_R = 8.044 min, (EI, 70 eV): *m/z* = 171 [M$^+$], 142, 115, 104, 93, 77, 66, 51.

Analytical data were in full agreement with H. Naka, D. Koseki, Y. Kondo, *Adv. Synth. Catal.* **2008**, *350*, 1901.

N-(2-Furanylmethylene)-cyclohexylamine

$C_{11}H_{15}NO$

M = 177.25 g/mol

Yellow liquid

Yield	2.68 g, 15.1 mmol (76%)
¹H-NMR	(300.13 MHz, MeOD) δ = 8.16 (s, 1H), 7.67 (d, *J* = 1.8 Hz, 1H), 6.91 (dd, *J* = 3.6, 0.8 Hz, 1H), 6.56 (dd, *J* = 3.5, 1.8 Hz, 1H), 3.18 (tt, *J* = 10.8, 4.1 Hz, 1H), 1.88-1.78 (m, 1H), 1.78-1.66 (m, 2H), 1.62-1.46 (m, 2H), 1.46-1.15 (m, 3H).
¹³C{¹H}-NMR	(75.47 MHz, MeOD) δ = 152.56, 150.41, 146.59, 116.23, 112.95, 70.97, 35.25, 26.56, 25.89.
GC-MS	t_R = 7.46 min, (EI, 70 eV): *m/z* = 177 [M⁺], 162, 148, 134, 122, 107, 94, 81, 67, 53.
HRMS	Calcd. for $C_{11}H_{15}NO$: 177.11482; found: 177.11437.

(rac)-N-(2-Butenylidene)-cyclohexlyamine

$C_{10}H_{17}N$

M = 151.25 g/mol
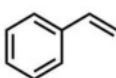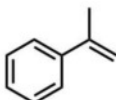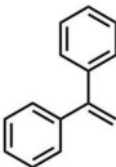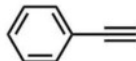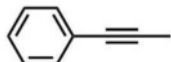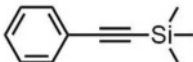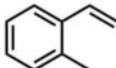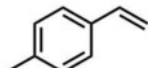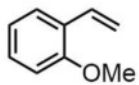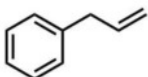
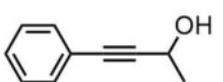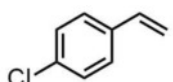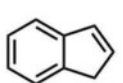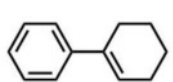|	
Yield	2.04 g, 13.5 mmol (68%)
¹H-NMR	(300.13 MHz, MeOD) δ = 7.93-7.87 (m, 1H), 7.76 (t, *J* = 2.8 Hz, 1H), 6.43-6.29 (m, 1H), 6.19 (ddq, *J* = 15.4, 8.8, 1.4 Hz, 1H), 3.67-3.56 (m, 1H), 3.08-2.95 (m, 2H), 1.89 (d, *J* = 6.7 Hz, 3H), 1.84-1.61 (m, 11H), 1.50-1.31 (m, 7H), 1.17 (d, *J* = 6.2 Hz, 3H).
¹³C{¹H}-NMR	(75.47 MHz, MeOD) δ = 164.2, 163.6, 163.6, 143.6, 143.5, 132.0, 75.8, 70.5, 70.0, 36.9, 35.4, 35.3, 35.3, 26.6, 26.3, 25.8, 25.8, 19.5, 18.6, 18.5.
GC-MS	t_R = 6.26 min, (EI, 70 eV): *m/z* = 150 [M⁺-H], 136, 122, 110, 94, 82, 68, 55.
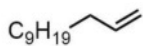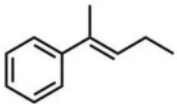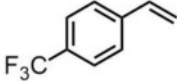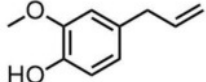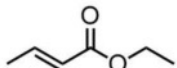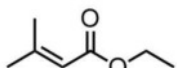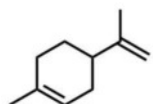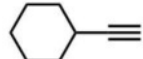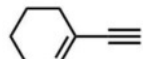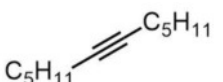
Analytical data were in full agreement with A. Saoudi, A. Benguedach, H. Benhaoua, *Synth. Commun.* **1995**, *25*, 2349.
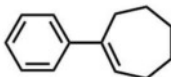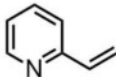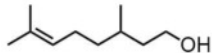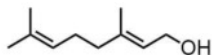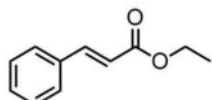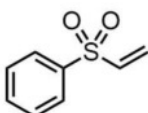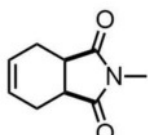
3.4.5 Hydrogenation Reactions
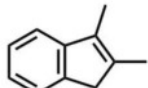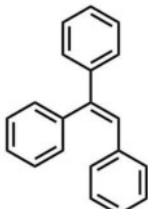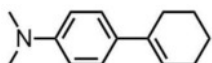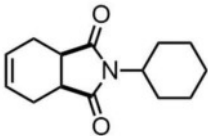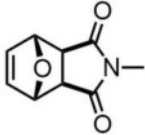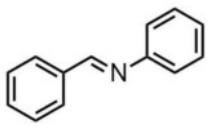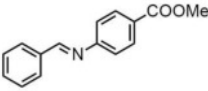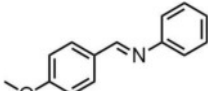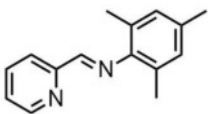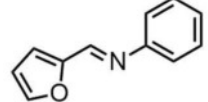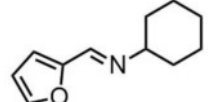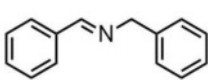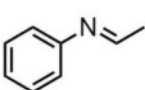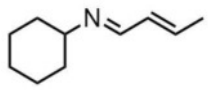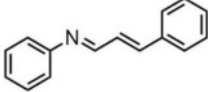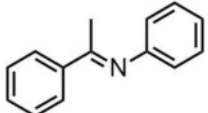
3.4.5.1 Catalyst & Substrate Screening
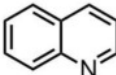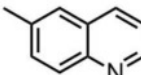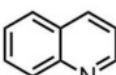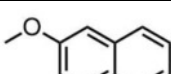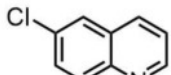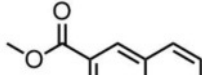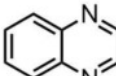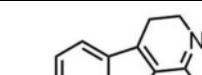
Table S 3-1   Hydrogenation of alkenes, alkynes, imines, and quinolines catalyzed by cobalt(0) nanoparticles isolated by centrifugation (Co-NP), isolated by magnetic separation (mCo-NP), prepared and used *in situ* (*in situ* Co-NP), and isolated by centrifugation and stabilized by oleyl amine (aCo-NP). Standard conditions: 0.25 mmol substrate, 1 mL THF or 0.5 mmol substrate, 2 mL THF. If not otherwise noted, yields were determined by GC-FID vs. internal n-pentadecane (isol. = isolated yield).

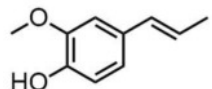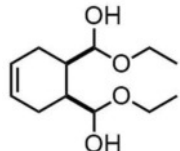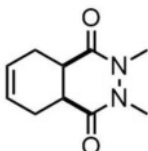| Substrate		[Co] / [mol%]	[bar]	[°C]	[h]	Yield [%]	Comment
1a		Co-NP	1			3	>99	-
		Co-NP	5			0,5	>99	-
		mCo-NP	5	2	20	0,5	98	-
		in situ Co-NP	5			0,5	97	-
		aCo-NP	1			3	16 (26)	-
1b		Co-NP	1			3	>99	-
		Co-NP	5			1	98	-
		mCo-NP	5	2	20	0,5	>99	-
		in situ Co-NP	5			0,5	>99	-
		aCo-NP	1			3	16 (26)	-
1c		Co-NP	1				>99	-
				2	20	3		
		in situ Co-NP	5				99	-
1d		Co-NP	5			8	>99	-
		mCo-NP	1	2	20	24	88	-
		mCo-NP	5			3	90	-
1e		Co-NP	5	2	20	8	98	-
1f		mCo-NP	5	2	20	3	96 (isol.)	-
1g		mCo-NP	1	2	20	3	58	-
1h		mCo-NP	1	2	20	3	94	-
1i		mCo-NP	1	2	20	3	72 (isol.)	100% according to ^{1}H-NMR of the mixture
1j		Co-NP	1				>99	-
				2	20	3		
		in situ Co-NP	5				97	-

Substrate		[Co] / [mol%]		[bar]	[°C]	[h]	Yield [%]	Comment
1k	C$_9$H$_{19}$ (allyl)	Co-NP	1	2	20	3	>96	-
		Co-NP	5			0,5	92	-
		mCo-NP	5			0,5	>99	-
		in situ Co-NP	5			0,5	>99	-
1l		mCo-NP	5	2	20	24	69 (isol.)	-
1m	F$_3$C–	mCo-NP	5	2	20	3	98	-
1n		mCo-NP	5	2	20	3	89 (isol.)	-
1o		mCo-NP	5	2	20	3	98	-
1p		mCo-NP	5	2	20	3	42	-
		mCo-NP	10				94	-
1q		mCo-NP	5	2	20	24	74 (isol.)	residual solvent (*vide infra*)
1r		mCo-NP	5	2	20	3	87	Yield refers to: ethylcyclohexane (100% conversion) Rest: M = 100
1s		mCo-NP	5	2	20	3	53	See **1q**
1t	C$_4$H$_9$ ... 7	mCo-NP	5	2	20	8	99 (isol.)	-
1u	C$_5$H$_{11}$ / C$_5$H$_{11}$	Co-NP	5	2	20	8	>99	-
		mCo-NP	5			24	93 (isol.)	-
1v	OH	mCo-NP	5	2	20	3	96 (isol.)	-
1w	Cl–	Co-NP	5	10	20	24	58	-
1x		Co-NP	5	10	60	3	>99	-
		Co-NP	5	60	20	24	>99	-
1y		Co-NP	5	10	60	24	98	-
		aCo-NP	5				80	-

Substrate	[Co] / [mol%]		[bar]	[°C]	[h]	Yield [%]	Comment
1z	Co-NP	5	10	60	24	98	-
	aCo-NP	5				79	-
1aa	Co-NP	5	10	60	24	86	-
1ab	Co-NP	5	10	20	3	71	-
	Co-NP	5		60		92	-
1ac	mCo-NP	5	10	60	24	99 (isol.)	-
1ad	mCo-NP	5	2	20	3	99 (isol.)	-
1ae	mCo-NP	5	20	80	24	88 (isol.)	-
1af	mCo-NP	5	10	60	24	99 (isol.)	-
1ag	mCo-NP	5	20	80	24	79 (isol.)	-
1ah	mCo-NP	5	2	20	3	49	-
	mCo-NP		10	60	24	88	
1ai	mCo-NP	5	10	60	24	81	Purity: *vide infra*
1aj	mCo-NP	5	10	60	24	91 (isol.)	-
1ak	mCo-NP	5	10	60	24	95 (isol.)	-
1al	mCo-NP	5	20	80	24	81 (isol.)	-
1am	mCo-NP	5	10	60	24	93 (isol.)	-

	Substrate	[Co] / [mol%]		[bar]	[°C]	[h]	Yield [%]	Comment
1an		mCo-NP	5	10	60	24	96 (isol.)	-
1ao		mCo-NP	5	10	60	24	94	-
2a		Co-NP	5			6	87	-
		Co-NP	5	10	60		>99	-
		mCo-NP	5			24	91 (isol.)	-
2b		mCo-NP	5	10	60	24	83 (isol.)	-
2c		mCo-NP	5	10	60	24	88 (isol.)	-
2d		mCo-NP	5	10	60	24	98 (isol.)	mixture (*vide infra*)
2e		mCo-NP	5	10	60	24	99 (isol.)	mixture (*vide infra*)
2f		mCo-NP	5	10	60	24	67 (isol.)	mixture (*vide infra*)
2g		mCo-NP	5	10	60	24	84 (isol.)	-
2h		mCo-NP	5	10	60	24	63 (isol.)	-
2i		mCo-NP	5	10	60	24	92 (isol.)	-
2j		mCo-NP	5	10	60	24	96 (isol.)	-
2k		mCo-NP	5	20	80	48	89 (isol.)	Purity: *vide infra*

Substrate		[Co] / [mol%]		[bar]	[°C]	[h]	Yield [%]	Comment
2l		mCo-NP	5	10	100	24	99 (isol.)	-
2m		mCo-NP	5	20	80	48	75 (isol.)	-
2n		mCo-NP	5	20	80	24	39 (isol.)	
2o		mCo-NP	5	20	80	24	77 (isol.)	
2p		mCo-NP	5	20	80	48	62 (isol.)	-
2q		mCo-NP	5	20	80	24	98 (isol.)	-
2r		mCo-NP	5	20	80	24	95 (isol.)	-
2s		mCo-NP	5	10	60	24	97 (isol)	-

3.4.5.2   Isolated Hydrogenation Reactions Products

Trimethyl(phenethyl)silane (1f)

$C_{11}H_{18}Si$

M = 178.35 g/mol
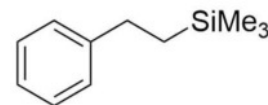
Yield	85.2 mg, 0.48 mmol (96%)
^{1}H-NMR	(300.13 MHz, CDCl$_3$) δ = 7.30-7.10 (m, 5H), 2.66-2.56 (m, 2H), 0.91-0.80 (m, 2H), 0.00 (s, 9H).
^{13}C{^{1}H}-NMR	(75.47 MHz, CDCl$_3$) δ = 145.5, 128.4, 127.9, 125.6, 30.2, 18.8, −1.6.
GC-MS	t_R = 6.16 min, (EI, 70 eV): *m/z* = 178 [M$^+$], 163, 135, 104, 91, 73, 59, 51.

Analytical data were in full agreement with E. Negishi, D. R. Swanson, C. J. Rousset, *J. Org. Chem.* **1990**, *55*, 5406.

1-Ethyl-2-methoxybenzene (1i)

$C_9H_{12}O$

136.19 g/mol
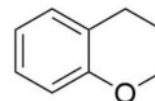
Yield	52.2 mg, 0.38 mmol (72%)
^{1}H-NMR	(400.13 MHz, CDCl$_3$) δ = 7.22-7.13 (m, 2H), 6.91 (td, *J* = 7.4, 1.1 Hz, 1H), 6.86 (dd, *J* = 8.0, 1.1 Hz, 1H), 3.84 (s, 3H), 2.66 (q, *J* = 7.5 Hz, 2H), 1.21 (t, *J* = 7.5 Hz, 3H).
^{13}C{^{1}H}-NMR	(75.47 MHz, CDCl$_3$) δ 157.5, 132.7, 129.0, 126.9, 120.6, 110.3, 55.4, 23.4, 14.3.
GC-MS	t_R = 5.30 min, (EI, 70 eV): *m/z* = 136 [M$^+$], 121, 103, 91, 77, 65, 51.

Analytical data were in full agreement with M. Mirza-Aghayan, R. Boukherroub, M. Rahimifard, *J. Organomet. Chem.* **2008**, *693*, 3567.

2-Phenylpentane (1l)

C$_{11}$H$_{16}$

148.25 g/mol
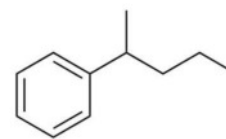
Yield   53.4 mg, 0.36 mmol (69%)

^{1}H-NMR   (300.13 MHz, CDCl$_3$) δ = 7.33-7.26 (m, 2H), 7.22-7.14 (m, 3H), 2.70 (h, J = 7.0 Hz, 1H), 1.65-1.43 (m, 2H), 1.36-1.09 (m, 5H), 0.87 (t, J = 7.3 Hz, 3H)

^{13}C{^{1}H}-NMR   (75.47 MHz, CDCl$_3$) δ = 148.1, 128.4, 127.1, 125.9, 40.9, 39.8, 22.4, 21.0, 14.3.

GC-MS t_R = 5.42 min, (EI, 70 eV): *m/z* = 148 [M$^+$], 105, 91, 77, 65, 51.

Analytical data were in full agreement with R. B. Bedford, P. B. Brenner, E. Carter, T. W. Carvell, P. M. Cogswell, T. Gallagher, J. N. Harvey, D. M. Murphy, E. C. Neeve, J. Nunn et al., *Chem. Eur. J.* **2014**, *20*, 7935.

2-Methoxy-4-propylphenol (1n/1aj)

C$_{10}$H$_{14}$O$_2$

166.22 g/mol
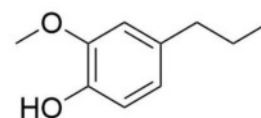
Yield   From eugenol: 75.6 mg, 0.45 mmol (89%)

from isoeugenol: 75.7 mg, 0.46 mmol (91%)

^{1}H-NMR   (300.13 MHz, CDCl$_3$) δ = 6.86-6.81 (m, 1H), 6.71-6.65 (m, 2H), 5.48 (brs, 1H), 3.88 (s, 3H), 2.52 (t, J = 7.8 Hz, 2H), 1.69-1.55 (m, 2H), 0.94 (t, J = 7.3 Hz, 3H).

^{13}C{^{1}H}-NMR   (75.47 MHz, CDCl$_3$) δ = 146.4, 143.6, 134.8, 121.1, 114.2, 111.1, 56.0, 37.9, 25.0, 14.0.

GC-MS t_R = 7.038 min, (EI, 70 eV): *m/z* = 166 [M$^+$], 137, 122, 107, 94, 77, 65, 51.

Analytical data were in full agreement with C. Smit, M. W. Fraaije, A. J. Minnaard, *J. Org. Chem.* **2008**, *73*, 9482.

4-Isopropyl-1-methylcyclohexene (1q)

C$_{10}$H$_{18}$

138.25 g/mol
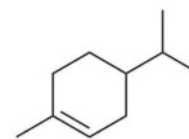
Yield   33.7 mg, 0.24 mmol (95%; 78% purity)

Due to the volatile nature of the product, the solvents could not be removed completely. NMR-analysis showed 74% hydrogenation product, 14% THF, 7% *n*-pentane

¹H-NMR   (400.13 MHz, CDCl$_3$) δ = 5.46-5.28 (m, 1H), 2.08-1.91 (m, 3H), 1.80-1.67 (m, 2H), 1.64 (s, 3H), 1.46 (dq, *J* = 13.1, 7.1, 6.5 Hz, 1H), 1.35-1.16 (m, 2H), 0.92-0.84 (m, 6H).

¹³C{¹H}-NMR   (101.61 MHz, CDCl$_3$) δ = 134.1, 121.2, 40.2, 32.4, 31.0, 29.1, 26.6, 23.6, 20.2, 19.9.

GC-MS t_R = 4.84 min, (EI, 70 eV): *m/z* = 138 [M$^+$], 123, 109, 95, 81, 67, 55.

Analytical data were in full agreement with G. Villa, G. Povie, P. Renaud, *J. Am. Chem. Soc.* 2011, *133*, 5913.

n-Hexadecane (1t)

C$_{16}$H$_{34}$

226.45 g/mol
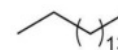
Yield   59.3 mg, 0.26 mmol (99%)

¹H-NMR   (300.13 MHz, CDCl$_3$) δ = 1.26 (s, 28H), 0.94 – 0.82 (m, 6H).

¹³C{¹H}-NMR   (75.47 MHz, CDCl$_3$) δ = 32.1, 29.9, 29.8, 29.6, 22.9, 14.3.

GC-MS t_R = 8.185 min, (EI, 70 eV): *m/z* = 226 [M$^+$], 197, 183, 169, 155, 141, 127, 113, 99, 85, 71, 57.

Analytical data were in full agreement with T. Brenstrum, D. A. Gerristma, G. M. Adjabeng, C. S. Frampton, J. Britten, A. J. Robertson, J. McNulty, A. Capretta, *J. Org. Chem.* 2004, *69*, 7635.

n-Dodecane (1u)

$C_{12}H_{26}$
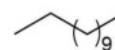
170.34 g/mol

Yield	78.6 mg, 0.46 mmol (93%)
^{1}H-NMR	(400.13 MHz, CDCl$_3$) δ = 1.26 (s, 20H), 0.94-0.84 (m, 6H).
^{13}C{^{1}H}-NMR	(101.61 MHz, CDCl$_3$) δ = 32.1, 29.9, 29.8, 29.5, 22.9, 14.3.
GC-MS	t_R = 6.01 min, (EI, 70 eV): m/z = 170 [M$^+$], 141, 127, 112, 98, 85, 71, 57.

Analytical data were in full agreement with X. Xu, D. Cheng, W. Pei, *J. Org. Chem.* **2006**, *71*, 6637.

4-Phenylbutan-2-ol (1v)

$C_{10}H_{14}O$

150.22 g/mol
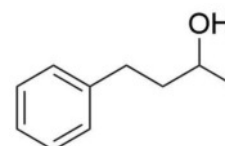
Yield	73.9 mg, 0.49 mmol (96%)
	Purity: 93%; 7% semihydrogenation product
^{1}H-NMR	(300.13 MHz, CDCl$_3$) δ = 7.26-7.31 (m, 2H), 7.17-7.24 (m, 3H), 3.84 (dq, 1H, *J* = 6.22, 12.10 Hz), 2.61-2.83 (m, 2H), 1.73-1.83 (m, 2H), 1.53 (br s, 1H), 1.24 (d, 3H, *J* = 6.17 Hz).
^{13}C{^{1}H}-NMR	(75.47 MHz, CDCl$_3$) δ = 142.2, 128.5, 125.9, 67.6, 41.0, 32.3, 23.8.
GC-MS	t_R = 6.51 min, (EI, 70 eV): m/z = 150 [M$^+$], 132, 117, 91, 77, 65, 51.
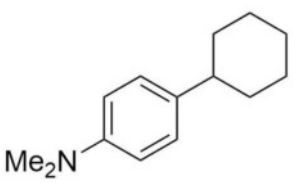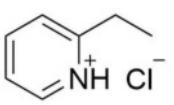
Analytical data were in full agreement with Z. E. Clarke, P. T. Maragh, T. P. Dasgupta, D. G. Gusev, A. J. Lough, K. Abdur-Rashid, *Organometallics* **2006**, *25*, 4113.

4-Cyclohexyl-N,N-dimethylaniline (1ac)

C$_{14}$H$_{21}$N

203.33 g/mol

Yield	100.7 mg, 0.50 mmol (99%)
^{1}H-NMR	(400.13 MHz, CDCl$_3$) δ = 7.15-7.08 (m, 2H), 6.77-6.70 (m, 2H), 2.93 (s, 6H), 2.43 (tq, *J* = 9.0, 3.3 Hz, 1H), 1.92-1.81 (m, 4H), 1.75 (dtt, *J* = 12.6, 3.1, 1.4 Hz, 1H), 1.47-1.33 (m, 4H), 1.27 (ddt, *J* = 14.5, 9.0, 3.3 Hz, 1H).
^{13}C{^{1}H}-NMR	(101.61 MHz, CDCl$_3$) δ = 149.1, 136.8, 127.4, 113.1, 43.6, 41.1, 34.9, 27.2, 26.4.
GC-MS	t_R = 9.15 min, (EI, 70 eV): *m/z* = 203 [M$^+$], 160, 146, 134, 115, 103, 93, 77, 51.

Analytical data were in full agreement with W. M. Czaplik, M. Mayer, A. Jacobi von Wangelin, *Angew. Chem. Int. Ed.* 2009, *48*, 607.

2-Ethylpyridine hydrochloride (1ad)

C$_7$H$_{10}$NCl

143.61 g/mol

Yield	36.1 mg, 0.25 mmol (99%)
^{1}H-NMR	(300.13 MHz, MeOD) δ = 8.75 (dt, *J* = 4.8, 2.3 Hz, 1H), 8.65 – 8.53 (m, 1H), 8.04 (d, *J* = 8.1 Hz, 1H), 8.00 – 7.90 (m, 1H), 3.21 – 3.06 (m, 2H), 2.02 (s, 1H), 1.50 – 1.41 (m, 3H).
^{13}C{^{1}H}-NMR	(75.47 MHz, MeOD) δ = 160.0, 148.3, 142.1, 128.0, 126.0, 27.8, 13.3.
GC-MS (freebase)	t_R = 3.792 min, (EI, 70 eV): *m/z* = 106 [M$^+$], 92, 79, 65, 51.

3,7-Dimethyl-1-octanol (1ae: from citronellol; 1af: from geraniol)

$C_{10}H_{22}O$

158.29 g/mol
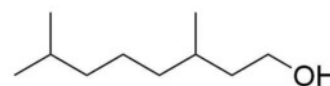
Yield	From citronellol: 68.3 mg, 0.43 mmol (88%)
	from geraniol: 40.4 mg, 0.26 mmol (99%)
^{1}H-NMR	(300.13 MHz, CDCl$_3$) δ = 3.76-3.57 (m, 2H), 1.67-1.46 (m, 3H), 1.43-1.32 (m, 2H), 1.32-1.21 (m, 3H), 1.19-1.06 (m, 3H), 0.87 (dd, *J* = 8.0, 6.5 Hz, 9H).
^{13}C{^{1}H}-NMR	(75.47 MHz, CDCl$_3$) δ = 61.4, 40.1, 39.4, 37.5, 29.6, 28.1, 24.8, 22.8, 22.7, 19.7.
GC-MS	t_R = 6.016 min, (EI, 70 eV): *m/z* = 140 [M$^+$-OH$_2$], 125, 112, 97, 83, 70, 55.
HRMS	Calcd. for $C_{10}H_{21}O$ 157.15869; found: 157.15836.
IR	3324 (b), 2955 (s), 2926 (s), 2870 (s), 1461 (m), 1379 (m), 1260 (m), 1051 (s), 805 (s) cm^{-1}.

2,6-Dimethyloctane (1ag)

$C_{10}H_{22}$

142.29 g/mol
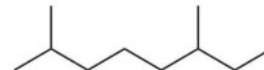
Yield	57.6 mg, 0.40 mmol (79%)
^{1}H-NMR	(300.13 MHz, CDCl$_3$) δ = 1.52 (dp, *J* = 13.1, 6.6 Hz, 1H), 1.38-1.22 (m, 5H), 1.18-1.01 (m, 4H), 0.85 (t, *J* = 6.8 Hz, 12H).
^{13}C{^{1}H}-NMR	(75.47 MHz, CDCl$_3$) δ = 39.5, 37.0, 34.6, 29.7, 28.2, 25.0, 22.9, 22.8, 19.4, 11.6.
GC-MS	t_R = 4.03 min, (EI, 70 eV): *m/z* = 142 [M$^+$], 127, 113, 97, 85, 71, 57.

Analytical data were in full agreement with R. V. Ottenbacher, D. G. Samsonenko, E. P. Talsi, K. P. Bryliakov, *Org. Lett.* 2012, *14*, 4310.

(Ethylsulfonyl)benzene (1ai)

$C_8H_{10}O_2S$

170.23 g/mol
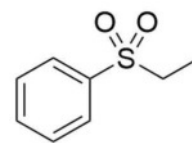
Yield	77.1 mg, 0.45 mmol (91%)
	Purity: 89%; 12% starting material
¹H-NMR	(300.13 MHz, CDCl₃) δ = 7.93-7.86 (m, 2H), 7.72-7.59 (m, 1H), 7.60-7.53 (m, 2H), 3.11 (q, *J* = 7.4 Hz, 2H), 1.26 (t, *J* = 7.4 Hz, 3H).
¹³C{¹H}-NMR	(75.47 MHz, CDCl₃) δ = 138.6, 133.8, 129.4, 128.3, 50.7, 7.6.
GC-MS	t_R = 9.00 min, (EI, 70 eV): *m/z* = 170 [M⁺], 154, 141, 125, 105, 94, 77, 65, 51.

Analytical data were in full agreement with R. V. Kupwade, S. S. Khot, U. P. Lad, U. V. Desai, P. P. Wadgaonkar, *Res. Chem. Intermed.* **2017**, *43*, 6875.

Diethyl cis-1,2-cyclohexanedicarboxylate (1ak)

$C_{12}H_{20}O_4$

228.29 g/mol
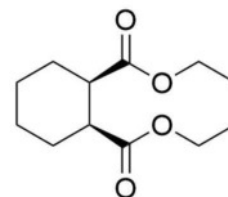
Yield	107.8 mg, 0.47 mmol (95%)
¹H-NMR	(300.13 MHz, CDCl₃) δ = 4.12 (q, *J* = 7.1 Hz, 4H), 2.85-2.74 (m, 2H), 2.10-1.89 (m, 2H), 1.83-1.66 (m, 2H), 1.58-1.30 (m, 4H), 1.23 (t, *J* = 7.2 Hz, 6H).
¹³C{¹H}-NMR	(75.47 MHz, CDCl₃) δ = 173.8, 60.4, 42.8, 26.4, 23.9, 14.3.
GC-MS	t_R = 9.33 min, (EI, 70 eV): *m/z* = 228 [M⁺], 183, 154, 140, 125, 108, 99, 81, 67, 55.

Analytical data were in full agreement with T. Volk, D. Bernicke, J. W. Bats, H.-G. Schmalz, *Eur. J. Inorg. Chem.* **1998**, *12*, 1883.

2,3-Dimethyloctahydrophthalazine-1,4-dione (1al)

$C_{10}H_{16}N_2O_2$

196.25 g/mol

Yield   79.5 mg, 0.41 mmol (81%)
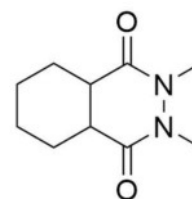
¹H-NMR   (300.13 MHz, CDCl$_3$) δ = 3.24 (s, 6H), 2.79-2.62 (m, 2H), 1.97-1.49 (m, 6H), 1.49-1.29 (m, 2H).

¹³C{¹H}-NMR   (75.47 MHz, CDCl$_3$) δ = 170.4, 32.7, 24.3.

GC-MS t_R = 8.78 min, (EI, 70 eV): *m/z* = 196 [M$^+$], 180, 166, 153, 141, 125, 109, 96, 81, 67, 59.

(3aR,7aS)-2-Methylhexahydro-1H-isoindole-1,3(2H)-dione (1am)

$C_9H_{13}NO_2$

167.21 g/mol

Yield   78.3 mg, 0.47 mmol (93%)
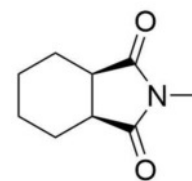
¹H-NMR   (300.13 MHz, CDCl$_3$) δ = 2.96 (s, 3H), 2.90 2.79 (m, 2H), 1.93-1.66 (m, 4H), 1.51-1.34 (m, 4H).

¹³C{¹H}-NMR   (75.47 MHz, CDCl$_3$) δ = 180.1, 39.9, 24.8, 23.8, 21.7.

GC-MS t_R = 7.46 min, (EI, 70 eV): *m/z* = 167 [M$^+$], 152. 138. 125. 113. 82. 67. 54.

Analytical data were in full agreement with T. N. Gieshoff, U. Chakraborty, M. Villa, A. Jacobi von Wangelin, *Angew. Chem. Int. Ed.* 2017, *56*, 3585.

(3aR,7aS)-2-Cyclohexylhexahydro-1H-isoindole-1,3(2H)-dione (1an)

$C_{14}H_{21}NO_2$

235.33 g/mol
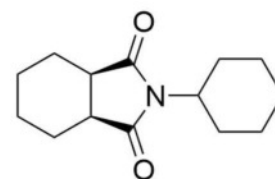
Yield 111.0 mg, 0.47 mmol (96%)

^{1}H-NMR (300.13 MHz, CDCl$_3$) δ = 3.92 (tt, J = 12.3, 3.9 Hz, 1H), 2.77 (ddd, J = 6.4, 4.4, 2.1 Hz, 2H), 2.11 (qd, J = 12.3, 3.4 Hz, 2H), 1.89-1.76 (m, 4H), 1.75-1.51 (m, 5H), 1.49-1.34 (m, 4H), 1.34-1.15 (m, 3H).

^{13}C{^{1}H}-NMR (75.47 MHz, CDCl$_3$) δ = 180.0, 51.3, 39.7, 28.9, 26.0, 25.2, 24.0, 21.8.

GC-MS t_R = 9.83 min, (EI, 70 eV): m/z = 235 [M$^+$], 207, 192, 178, 164, 154, 136, 124, 108, 98, 81, 67, 55.

Analytical data were in full agreement with M. Ostendorf, R. Romagnoli, I. C. Pereiro, E. C. Roos, M. J. Moolenaar, W. Speckamp, H. Hiemstra, *Tetrahedron: Asymmetry* **1997**, *8*, 1773.

exo-3,6-Epoxy-N-methyl-hexahydrophthalimide (1ao)

$C_9H_{11}NO_3$

181.19 g/mol
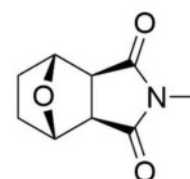
Yield 85.2 mg, 0.47 mmol (94%)

^{1}H-NMR (300.13 MHz, CDCl$_3$) δ = 4.86 (dd, J = 3.3, 2.1 Hz, 2H), 2.95 (s, 3H), 2.87 (s, 2H), 1.92 1.80 (m, 2H), 1.64 1.53 (m, 2H).

^{13}C{^{1}H}-NMR (75.47 MHz, CDCl$_3$) δ = 177.4, 79.1, 50.1, 28.7, 25.2.

GC-MS t_R = 9.65 min, (EI, 70 eV): m/z = 181 [M$^+$], 152, 140, 125, 108, 99, 81, 67, 55.

N-Benzylaniline hydrochloride (2a)

$C_{13}H_{14}ClN$
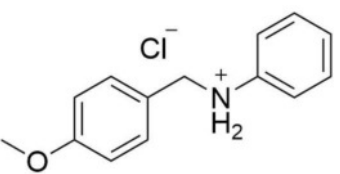
219.71 g/mol
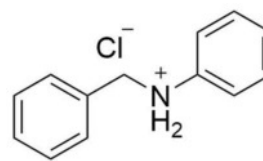
Yield	99.4 mg, 0.45 mmol (91%)
¹H-NMR	(300.13 MHz, MeOD) δ = 7.59-7.50 (m, 3H), 7.48-7.38 (m, 7H), 4.61 (s, 2H).
¹³C{¹H}-NMR	(75.47 MHz, MeOD) δ = 136.2, 131.9, 131.5, 131.4, 131.0, 130.9, 130.2, 124.3, 57.0.
GC-MS (freebase)	t_R = 8.97 min, (EI, 70 eV): *m/z* = 183 [M⁺], 154, 107, 91, 77, 65, 51.
Elemental Analysis	Calcd: 71.07% C, 6.42% H, 6.38% N; found: 70.57% C, 6.80% H, 6.27% N

Analytical data were in full agreement with T. Li, X. Cui, L. Sun, C. Li, *RSC Adv.* **2014**, *4*, 33599.

Methyl 4-(benzylamino)benzoate (2b)

$C_{15}H_{15}NO_2$
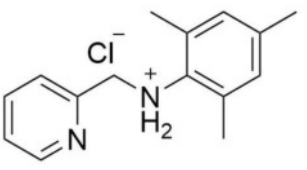
241.29 g/mol
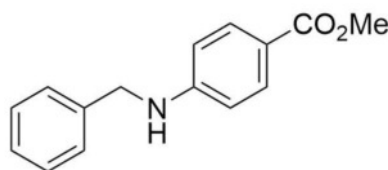
Yield	49.0 mg, 0.20 mmol (83%)
¹H-NMR	(300.13 MHz, CDCl₃) δ = 7.87 (d, *J* = 8.8 Hz, 2H), 7.41-7.27 (m, 5H), 6.61 (d, *J* = 8.8 Hz, 2H), 4.81 (br s, 1H), 4.39 (s, 2H), 3.85 (s, 3H).
¹³C{¹H}-NMR	(75.47 MHz, CDCl₃) δ = 167.4, 151.6, 138.3, 131.7, 128.9, 127.7, 127.6, 119.0, 112.0, 51.7, 48.0.
GC-MS	t_R = 11.24 min, (EI, 70 eV): *m/z* = 241 [M⁺], 210, 180, 164, 151, 135, 119, 104, 91, 78, 65, 51.
Elemental Analysis	Calcd: 74.67% C, 6.27% H, 5.81% N; found: 73.82% C, 6.37% H, 5.63% N

Analytical data were in full agreement with L. Fan, J. Jia, H. Hou, Q. Lefebvre, M. Rueping, *Chem. Eur. J.* **2016**, *22*, 16437.

N-(4-Methoxybenzyl)aniline hydrochloride (2c)

	$C_{14}H_{16}ClNO$
	249.74 g/mol
Yield	110.1 mg, 0.44 mmol (88%)
¹H-NMR	(400.13 MHz, MeOD) δ = 7.59-7.48 (m, 3H), 7.45-7.36 (m, 2H), 7.35-7.30 (m, 2H), 6.97-6.92 (m, 2H), 4.54 (s, 2H), 3.80 (s, 3H).
¹³C{¹H}-NMR	(101.61 MHz, MeOD) δ = 162.29, 136.10, 133.05, 131.34, 130.97, 124.34, 123.53, 115.41, 56.77, 55.82.
GC-MS (freebase)	t_R = 10.12 min, (EI, 70 eV): m/z = 213 [M⁺], 196, 180, 168, 152, 142, 121, 106, 91, 77, 65, 51.
HRMS	Calcd. for $C_{14}H_{16}NO$: 214,1226; found: 214.1226.
IR	3060 (w), 2896 (m), 2840 (m), 2669 (s), 2550 (s), 2423 (s), 1595 (s), 1513 (s), 1305 (m), 1249 (s), 1033 (s), 815 (s), 795 (s) cm⁻¹.

N-(2,4,6-Trimethylphenyl)-2-pyridinemethanamine hydrochloride (2d)

	$C_{15}H_{19}ClN_2$
	262.78 g/mol
Yield	128.2 mg, 0.49 mmol (98%)
	23% pyridine hydrogenation
¹H-NMR	(300 MHz, MeOD) δ 8.85 (ddd, J = 5.5, 1.6, 0.8 Hz, 1H), 8.37 (td, J = 7.9, 1.7 Hz, 1H), 7.93 (dd, J = 7.9, 1.1 Hz, 1H), 7.93 – 6.99 (m, 1H), 7.03 (s, 2H), 4.77 (s, 2H), 2.41 (s, 6H), 2.29 (s, 3H).
¹³C{¹H}-NMR	(75 MHz, MeOD) δ 151.3, 146.4, 144.4, 139.8, 132.8, 131.8, 127.5, 127.3, 52.7, 20.8, 18.0.
GC-MS (freebase)	t_R = 9.839 min, (EI, 70 eV): m/z = 226 [M⁺], 211, 196, 181, 148, 134, 120, 107, 93, 79, 65, 51.
HRMS	Calcd. for $C_{15}H_{19}N_2$ 227.1543; found: 227.1543;
	Calcd. for $C_{15}H_{25}N_2$ 223.2012; found: 223.2011.

N-(2-Furanylmethyl)aniline (2e)

$C_{11}H_{11}NO$

173.22 g/mol
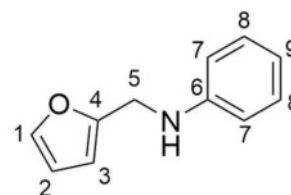
Yield	88.8 mg, 0.51 mmol (99%)
	Selectivity: 81%
	Only detectable side product:
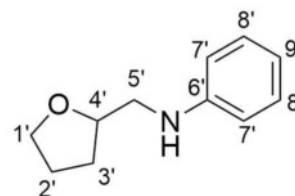
¹H-NMR (400.13 MHz, CDCl$_3$) δ = 7.38 (dd, *J* = 1.9, 0.8 Hz, 1H, 1), 7.20 (qd, *J* = 6.6, 6.1, 1.7 Hz, 3H, 8), 6.76 (t, *J* = 7.3 Hz, 1H, 9), 6.73-6.62 (m, 2H, 7), 6.34 (dd, *J* = 3.2, 1.9 Hz, 1H, 2), 6.25 (dd, *J* = 3.2, 0.9 Hz, 1H, 3), 4.33 (s, 2H, 5).

Side product (400.13 MHz, CDCl$_3$) δ = 7.18-7.15 (m, 2H, 8'), 6.67-6.63 (m, 3H, 7'/9'), 4.15 (qd, *J* = 7.2, 3.8 Hz, 1H, 4'), 3.91 (dt, *J* = 8.3, 6.7 Hz, 1H, 1'), 3.80 (dt, *J* = 8.2, 6.8 Hz, 1H, 1'), 3.28 (dd, *J* = 12.3, 3.8 Hz, 1H, 5'), 3.10 (dd, *J* = 12.3, 7.5 Hz, 1H, 5'), 2.10-2.00 (m, 1H, 3'), 1.99-1.89 (m, 2H, 2'), 1.67 (ddt, *J* = 11.6, 8.3, 7.0 Hz, 1H, 3').

¹³C{¹H}-NMR (101.61 MHz, CDCl$_3$) δ = 152.9 (6), 147.8 (4), 142.0 (1), 129.4 (8), 118.1 (9), 113.3 (7), 110.5 (2), 107.1 (3), 41.6 (5).

Side product (101.61 MHz, CDCl$_3$) δ = 148.5 (6'), 129.3 (8'), 117.6 (9'), 113.2 (7'), 77.7 (4'), 68.2 (1'), 48.3 (5'), 29.2 (3'), 25.9 (2').

GC-MS *t*$_R$ = 7.97 min, (EI, 70 eV): *m/z* = 173 [M⁺], 144, 130, 115, 104, 91, 81, 65, 53.

Analytical data were in full agreement with M. L. Kantam, G. T. Venkanna, C. Sridhar, B. Sreedhar, B. M. Choudary, *J. Org. Chem.* **2006**, *71*, 9522.

N-(2-Furanylmethyl)cyclohexylamine (2f)

$C_{11}H_{17}NO$

179.26 g/mol
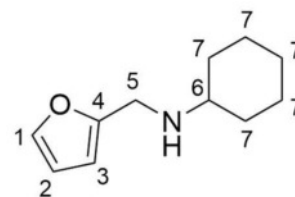
Yield	58.8 mg, 0.33 mmol (67%)

Selectivity 53%

Only detectable side product:
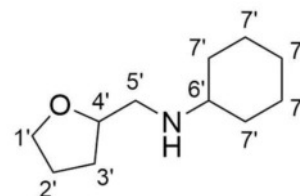
¹H-NMR	(400.13 MHz, CDCl₃) δ = 7.34 (dd, *J* = 1.9, 0.8 Hz, 1H, 1), 6.29 (dd, *J* = 3.2, 1.9 Hz, 1H, 2), 6.15 (d, *J* = 3.1 Hz, 1H, 3), 3.80 (s, 2H, 5), 2.44 (tt, *J* = 10.4, 3.8 Hz, 1H, 6), 1.91-1.83 (m, 5H, 7/7'), 1.72 (dt, *J* = 12.5, 3.6 Hz, 4H, 7/7'), 1.63-1.57 (m, 2H, 7/7'), 1.30-1.02 (m, 8H, 7/7').
	Side product (400.13 MHz, CDCl₃) δ = 3.99 (ddt, *J* = 11.1, 7.4, 3.7 Hz, 1H, 4'), 3.84 (dt, *J* = 8.4, 6.7 Hz, 1H, 1'), 3.73 (dt, *J* = 8.2, 6.8 Hz, 1H, 1'), 2.74 (dd, *J* = 11.8, 3.7 Hz, 1H, 5'), 2.63 (dd, *J* = 11.8, 8.1 Hz, 1H, 5'), 2.44 (tt, *J* = 10.4, 3.8 Hz, 1H, 6'), 2.03-1.92 (m, 1H, 3'), 1.91-1.83 (m, 2H, 2'), 1.91-1.83 (m, 5H, 7/7'), 1.72 (dt, *J* = 12.5, 3.6 Hz, 4H, 7/7'), 1.63-1.57 (m, 2H, 7/7'), 1.57-1.47 (m, 1H, 3'), 1.30-1.02 (m, 8H, 7/7').
¹³C{¹H}-NMR	(101.61 MHz, CDCl₃) δ = 154.4 (4), 141.8 (1), 110.2 (3), 106.7 (2), 55.9 (6), 43.5 (5), 33.5 (7/7'), 33.5 (7/7'), 33.4 (7/7'), 26.3 (7/7'), 25.2 (7/7'), 25.2 (7/7'), 25.1 (7/7').
	Side product (101.61 MHz, CDCl₃) δ = 78.6 (4'), 68.0 (1'), 57.1 (6'), 51.6 (5'), 33.5 (7/7'), 33.5 (7/7'), 33.4 (7/7'), 29.6 (3'), 26.3 (7/7'), 25.9 (2'), 25.2 (7/7'), 25.2 (7/7'), 25.1 (7/7').
GC-MS	t_R = 7.24 min, (EI, 70 eV): *m/z* = 179 [M⁺], 150, 136, 122, 96, 81, 67, 53.
	Side product: t_R = 7.65 min, (EI, 70 eV): *m/z* =183 [M⁺], 140, 122, 112, 105, 96, 83, 68, 55.
HRMS	Calcd. for $C_{11}H_{18}NO$ 180,1383; found: 180.1386;
	Calcd. for $C_{11}H_{22}NO$ (side product) 184,1696; found: 184.1700.

N,N-Dibenzylamine hydrochloride (2g)

$C_{14}H_{16}NCl$

233.10 g/mol
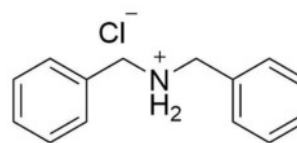
Yield	49.0 mg, 0.21 mmol (84%)
¹H-NMR	(400.13 MHz, MeOD) δ = 7.55-7.49 (m, 4H), 7.49-7.44 (m, 6H), 4.25 (s, 4H).
¹³C{¹H}-NMR	(101.61 MHz, MeOD) δ = 132.4, 131.1, 130.7, 130.3, 52.0.
GC-MS (freebase)	t_R = 10.9 min, (EI, 70 eV): *m/z* = 196 [M-H⁺], 179, 165, 152, 139, 120, 106, 91, 77, 65, 51.

Analytical data were in full agreement with L. Xing, C. Cheng, R. Zhu, B. Zhang, X. Wang, Y. Hu, *Tetrahedron* **2008**, *64*, 11783.

N-Benzylmethylamine hydrochloride (2h)

$C_8H_{12}NCl$

157.64 g/mol
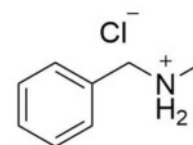
Yield	52.7 mg, 0.33 mmol (63%)
¹H-NMR	(400.13 MHz, MeOD) δ = 7.53-7.43 (m, 5H), 4.19 (s, 2H), 2.72 (s, 3H).
¹³C{¹H}-NMR	(101.61 MHz, MeOD) δ = 132.56, 130.90, 130.72, 130.31, 53.61, 33.12.
GC-MS	t_R = 5.22 min, (EI, 70 eV): *m/z* = 120 [M⁺], 104, 91, 78, 65, 51.

Analytical data were in full agreement with N. L. Lampland, M. Hovey, D. Mukherjee, A. D. Sadow, *ACS Catal.* **2015**, *5*, 4219.

N-Butyl-cyclohexylamine (2i)

$C_{10}H_{21}N$

155.29 g/mol
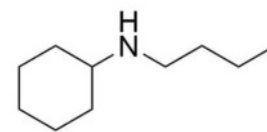
Yield	72.0 mg, 0.46 mmol (92%)
^{1}H-NMR	(400.13 MHz, MeOD) δ = 3.12-2.95 (m, 3H), 2.20-2.03 (m, 2H), 1.93-1.82 (m, 2H), 1.78-1.61 (m, 3H), 1.45 (dt, J = 15.1, 7.5 Hz, 2H), 1.42-1.31 (m, 4H), 1.31-1.15 (m, 1H), 0.99 (t, J = 7.4 Hz, 3H).
^{13}C{^{1}H}-NMR	(101.61 MHz, MeOD) δ = 58.39, 45.58, 30.35, 29.52, 26.12, 25.48, 20.90, 13.92.
GC-MS	t_R = 6.00 min, (EI, 70 eV): m/z = 155 [M$^+$], 126, 112, 98, 84, 70, 56.

Analytical data were in full agreement with R. Nacario, S. Kotakonda, D. M. D. Fouchard, L. M. V. Tillekeratne, R. A. Hudson, *Org. Lett.* **2005**, *7*, 471.

N-(3-Phenylpropyl)aniline hydrochloride (2j)

$C_{15}H_{18}ClN$

247 77 g/mol
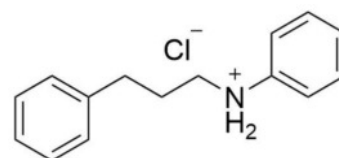
Yield	58.2 mg, 0.23 mmol (96%)
^{1}H-NMR	(300.13 MHz, MeOD) δ = 7.69-7.46 (m, 5H), 7.34-7.17 (m, 5H), 3.53-3.36 (m, 2H), 2.75 (t, J = 7.6 Hz, 2H), 2.14-1.98 (m, 2H).
^{13}C{^{1}H}-NMR	(75.47 MHz, MeOD) δ = 141.5, 136.7, 131.6, 131.1, 129.7, 129.4, 127.5, 123.8, 52.9, 33.4, 28.9.
GC-MS (freebase)	t_R = 9.88 min, (EI, 70 eV): m/z = 211 [M$^+$], 118, 106, 91, 77, 65, 51.
HRMS	Calcd. for $C_{15}H_{18}N$ 212.1434; found: 212.1436.
IR	3370 (b), 3063 (w), 3026 (m), 2870 (m), 2646 (m), 2017 (m), 1603 (m), 1491 (m), 749 (s), 690 (s) cm^{-1}.

N-(1-Phenylethyl)aniline (2k)

$C_{14}H_{15}N$

197.28 g/mol
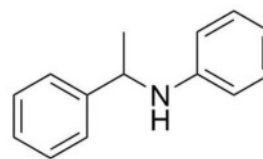
Yield   87.5 mg, 0.44 mmol (89%)

Starting material could not be separated (5%)

¹H-NMR   (400.13 MHz, CDCl₃) δ = 7.41-7.37 (m, 2H), 7.38-7.29 (m, 2H), 7.28-7.22 (m, 1H), 7.11 (dd, *J* = 8.6, 7.3 Hz, 2H), 6.68 (tt, *J* = 7.3, 1.1 Hz, 1H), 6.57-6.52 (m, 2H), 4.51 (q, *J* = 6.7 Hz, 1H), 4.20 (brs, 1H), 1.54 (d, *J* = 6.7 Hz, 3H).

¹³C{¹H}-NMR   (101.61 MHz, CDCl₃) δ = 147.2, 145.2, 129.2, 128.8, 127.0, 126.0, 117.5, 113.6, 53.7, 25.1.

GC-MS t_R = 8.83 min, (EI, 70 eV): *m/z* = 197 [M⁺], 182, 167, 152, 120, 105, 93, 77, 65, 51.

Analytical data were in full agreement with A. H. Vetter, A. Berkessel, *Synthesis* **1995**, 419.

1,2,3,4-Tetrahydroquinoline hydrochloride (2l)

$C_9H_{12}NCl$

169.65 g/mol
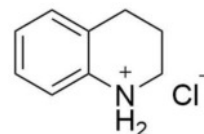
Yield   43.8 mg, 0.26 mmol (99%)

¹H-NMR   (300.13 MHz, CDCl₃) δ = 7.46-7.33 (m, 3H), 7.30 (dd, *J* = 8.2, 1.7 Hz, 1H), 3.56-3.50 (m, 2H), 2.97 (t, *J* = 6.5 Hz, 2H), 2.25-2.07 (m, 2H).

¹³C{¹H}-NMR   (75.47 MHz, CDCl₃) δ = 132.9, 132.2, 131.3, 130.4, 128.7, 124.1, 43.8, 25.8, 20.7.

GC-MS (freebase) t_R = 7.01 min, (EI, 70 eV): *m/z* = 132 [M⁺-H], 118, 104, 91, 77, 65, 51.

Analytical data were in full agreement with M. Ortiz-Marciales, L. D. Rivera, M. de Jesús, S. Espinosa, J. A. Benjamin, O. E. Casanova, I. G. Figueroa, S. Rodríguez, W. Correa, *J. Org. Chem.* **2005**, *70*, 10132.

6-Methyl-1,2,3,4-tetrahydroquinoline (2m)

C$_{10}$H$_{13}$N

147.22 g/mol
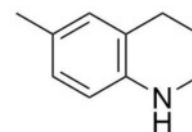
Yield	53.2 mg, 0.36 mmol (73%)
¹H-NMR	(400.13 MHz, CDCl$_3$) δ = 6.82 6.77 (m, 2H), 6.43(d, *J* = 8.6 Hz, 1H), 3.48 (brs, 1H), 3.31-3.25 (m, 2H), 2.75 (t, *J* = 6.4 Hz, 2H), 2.22 (s, 3H), 2.00-1.89 (m, 2H).
¹³C{¹H}-NMR	(101.61 MHz, CDCl$_3$) δ = 142.4, 130.2, 127.4, 126.5, 121.8, 114.7, 42.3, 27.0, 22.5, 20.5.
GC-MS	t_R = 7.53 min, (EI, 70 eV): *m/z* = 147 [M$^+$], 132, 117, 103, 91, 77, 65, 51.

Analytical data were in full agreement with R. Adam, J. R. Cabrero-Antonino, A. Spannenberg, K. Junge, R. Jackstell, M. Beller, *Angew. Chem. Int. Ed.* **2017**, *56*, 3216.

8-Methyl-1,2,3,4-tetrahydroquinoline (2n)

C$_{10}$H$_{13}$N

147.22 g/mol
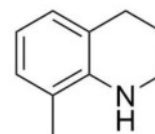
Yield	28.4 mg, 0.19 mmol (39%)
¹H-NMR	(300.13 MHz, CDCl$_3$) δ = 6.92-6.82 (m, 2H), 6.57 (t, *J* = 7.4 Hz, 1H), 3.59 (brs, 1H), 3.41-3.35 (m, 2H), 2.80 (t, *J* = 6.4 Hz, 2H), 2.09 (s, 3H), 2.00-1.90 (m, 2H).
¹³C{¹H}-NMR	(75.47 MHz, CDCl$_3$) δ = 142.6, 128.0, 127.5, 121.5, 121.2, 116.7, 42.5, 27.4, 22.3, 17.3.
GC-MS	t_R = 7.48 min, (EI, 70 eV): *m/z* = 147 [M$^+$], 132, 117, 103, 91, 77, 65, 51.

Analytical data were in full agreement with Y.-G. Ji, K. Wei, T. Liu, L. Wu, W.-H. Zhang, *Adv. Synth. Catal.* **2017**, *359*, 933..

6-Methoxy-1,2,3,4-tetrahydroquinoline (2o)

C$_{10}$H$_{13}$NO
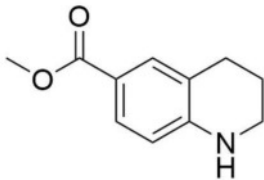
163.22 g/mol
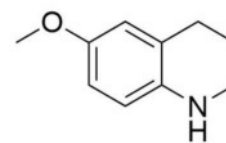
Yield	31.9 mg, 0.20 mmol (77%)
^{1}H-NMR	(400.13 MHz, CDCl$_3$) δ = 6.62-6.55 (m, 2H), 6.45 (d, *J* = 8.5 Hz, 1H), 3.73 (s, 3H), 3.44 (brs, 1H), 3.26 (t, *J* = 5.4 Hz, 2H), 2.76 (t, *J* = 6.5 Hz, 2H), 1.98-1.89 (m, 2H).
^{13}C{^{1}H}-NMR	(101.61 MHz, CDCl$_3$) δ = 151.9, 139.0, 123.0, 115.7, 115.0, 113.0, 55.9, 42.5, 27.3, 22.6.
GC-MS	t_R = 8.31 min, (EI, 70 eV): *m/z* = 163 [M$^+$], 148, 130, 118, 103, 91, 77, 65, 51.

Analytical data were in full agreement with R. Adam, J. R. Cabrero-Antonino, A. Spannenberg, K. Junge, R. Jackstell, M. Beller, *Angew. Chem. Int. Ed.* **2017**, *56*, 3216.

6-Chloro-1,2,3,4-tetrahydroquinoline (2p)

C$_9$H$_{10}$ClN

167.64 g/mol
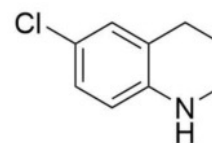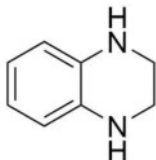
Yield	51.7 mg, 0.31 mmol (62%)
^{1}H-NMR	(400.13 MHz, CDCl$_3$) δ = 6.94-6.84 (m, 2H), 6.38 (dd, *J* = 7.9, 0.9 Hz, 1H), 3.82 (brs, 1H), 3.28 (t, *J* = 5.5 Hz, 2H), 2.72 (t, *J* = 6.4 Hz, 2H), 1.97-1.84 (m, 2H).
^{13}C{^{1}H}-NMR	(101.61 MHz, CDCl$_3$) δ = 143.4, 129.2, 126.6, 123.0, 121.3, 115.2, 42.0, 27.0, 21.9.
GC-MS	t_R = 8.35 min, (EI, 70 eV): *m/z* = 167 [M$^+$], 152, 130, 117, 103, 89 ,77, 65, 51.

Analytical data were in full agreement with R. Adam, J. R. Cabrero-Antonino, A. Spannenberg, K. Junge, R. Jackstell, M. Beller, *Angew. Chem. Int. Ed.* **2017**, *56*, 3216.

Methyl 1,2,3,4-tetrahydroquinoline-6-carboxylate (2q)

	$C_{11}H_{13}NO_2$
	191.23 g/mol
Yield	93.4 mg, 0.49 mmol (98%)
¹H-NMR	(300.13 MHz, CDCl₃) δ = 7.66-7.61 (m, 2H), 6.41-6.37 (m, 1H), 4.35 (brs, 1H), 3.83 (s, 3H), 3.35 (t, *J* = 5.7 Hz, 2H), 2.76 (t, *J* = 6.3 Hz, 2H), 2.00-1.85 (m, 2H).
¹³C{¹H}-NMR	(75.47 MHz, CDCl₃) δ = 167.6, 148.8, 131.4, 129.2, 120.0, 117.6, 112.8, 51.6, 41.8, 27.0, 21.5.
GC-MS	t_R = 9.68 min, (EI, 70 eV): *m/z* = 191 [M⁺], 176, 160, 144, 132, 117, 104, 89, 77, 64, 51.

Analytical data were in full agreement with R. Adam, J. R. Cabrero-Antonino, A. Spannenberg, K. Junge, R. Jackstell, M. Beller, *Angew. Chem. Int. Ed.* **2017**, *56*, 3216.

1,2,3,4-tetrahydroquinoxaline (2r)

	$C_8H_{10}N_2$
	134.18 g/mol
Yield	64.2 mg, 0.48 mmol (95%)
¹H-NMR	(400.13 MHz, CDCl₃) δ = 6.59 (dd, *J* = 5.8, 3.4 Hz, 2H), 6.50 (dd, *J* = 5.8, 3.4 Hz, 2H), 3.59 (brs, 2H), 3.42 (s, 4H).
¹³C{¹H}-NMR	(101.61 MHz, CDCl₃) δ = 133.8, 118.9, 114.8, 41.5.
GC-MS	t_R = 7.94 min, (EI, 70 eV): *m/z* = 134 [M⁺], 119, 104, 92, 77, 66, 51.

Analytical data were in full agreement with R. Adam, J. R. Cabrero-Antonino, A. Spannenberg, K. Junge, R. Jackstell, M. Beller, *Angew. Chem. Int. Ed.* **2017**, *56*, 3216.

Tetrahydroharmine (2s)

$C_{13}H_{16}N_2O$

216.28 g/mol
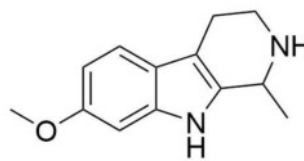
Yield	104.6 mg, 0.48 mmol (97%)

¹H-NMR (300.13 MHz, CDCl₃) δ = 8.06 (brs, 1H), 7.33 (d, *J* = 8.5 Hz, 1H), 6.83 (d, *J* = 2.2 Hz, 1H), 6.75 (dd, *J* = 8.6, 2.3 Hz, 1H), 4.14 (q, *J* = 6.6 Hz, 1H), 3.81 (s, 3H), 3.32-3.27 (m, 1H), 3.01 (ddd, *J* = 12.9, 8.6, 5.4 Hz, 1H), 2.80-2.66 (m, 2H), 2.52 (brs, 1H), 1.43 (d, *J* = 6.7 Hz, 3H).

¹³C{¹H}-NMR (75.47 MHz, CDCl₃) δ = 156.2, 136.5, 135.8, 122.0, 118.7, 108.9, 108.2, 95.2, 55.9, 48.3, 42.7, 22.7, 20.8.

GC-MS t_R = 10.76 min, (EI, 70 eV): *m/z* = 216 [M⁺], 201, 186, 172, 158, 144, 130, 115, 100, 89, 77, 63, 51.

Analytical data were in full agreement with J. Wu, D. Talwar, S. Johnston, M. Yan, J. Xiao, *Angew. Chem. Int. Ed.* **2013**, *52*, 6983.

Tetrahydroharmine (2s)

3.4.6   ICP-OES Measurements

The cobalt concentration in the organic layer after hydrogenation was determined by ICP-OES. Five stock solutions of $CoCl_2$ in 35% HNO_3 were prepared and a calibration curve was measured by integration of the emission signal of cobalt at 230.786 nm. Each data point corresponds to the mean value of three consecutive measurements correcting for the observed background signals.
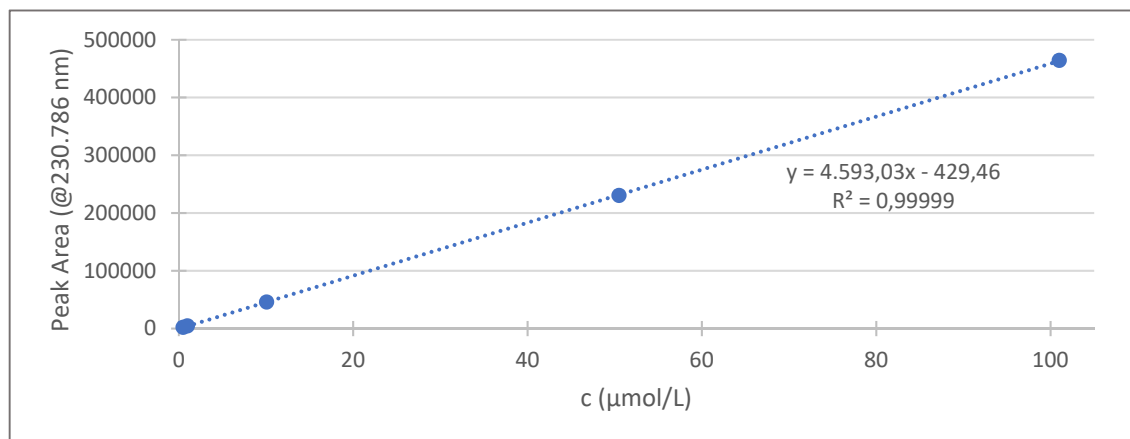
Figure S1   ICP-OES calibration curve for $CoCl_2$ in aqueous HNO_3 (35%).

For the actual measurement, styrene (0.25 mmol) was hydrogenated using 5 mol% of the cobalt nanoparticles (12.5 mmol/L Co) under standard conditions (2 bar H_2, 3 h in 1 ml THF). After reaction, two reaction vials were placed on separate neodymium magnets and allowed to settle down for 2 and 24 h respectively. The organic phase was removed with a Pasteur Pipette, the solvent removed under vacuum and the residue dissolved in 5 ml dilute HNO_3.

Table S3-2   Amounts of residual cobalt in the product phase after the catalytic reaction measured by ICP-OES.

PBcat135_2h	Peak Area	c (µmol/L)
Run 1	41231	9,07
Run 2	42226	9,29
Run 3	41338,2	9,09
Average	41598,4	9,15
StdDev	546,15	0,12

PBcat135_24h	Peak Area	c (µmol/L)
Run 1	31624,5	6,98
Run 2	31439,7	6,94
Run 3	31299,3	6,91
Average	31454,5	6,94
StdDev	163,10	0,04

This results in a cobalt concentration of 45.75±0.6 and 34.7±0.2 µmol/L in the organic phase after 2 and 24 h settle time respectively, which corresponds to 0.37 and 0.28% of the cobalt concentration in the reaction vessel.

3.4.7   ICP-MS Measurement

In preparation for the measurement, half of the vials were charged with styrene (1 mmol) and 5 mol% of the cobalt nanoparticles (12.5 mmol/L Co), the other vials omitting the cobalt catalyst (blank reaction solution). All were hydrogenated under standard conditions (2 bar H_2, 3 h in 4 ml THF). After the reaction, each vial was put on a neodymium magnet and the organic phase was transferred to a new vial, leaving behind most of the cobalt metal. The vials were washed with an additional 1 ml of ethyl acetate twice. To the first set of vials (Co-reaction and blank) 1 ml of a saturated, aqueous ammonium chloride solution was added followed by extraction with ethyl acetate (3x), the second set was eluted through a short silica plug inside a Pasteur pipette using ethyl acetate. The solvent was subsequently removed from all vials under vacuum and the residue dissolved in 50 ml dilute HNO_3.

Table S 3-3   Amounts of residual cobalt in the product phase after the catalytic reaction measured by ICP-MS.

Reactions	Peak Area	c (ng/mL)	nCo (nmol)
Extraction	838524.5	0.80	0.6780
Extraction (blank)	23595.3	0.02	0.01696
Silica	52582.7	0.05	0.0424
Silica (blank)	13541.0	0.01	0.00848

This results in a cobalt concentration of 165 nmol/L and 8.5 nmol/L in the organic phase after extraction and elution respectively, which corresponds to 13.2 and 0.68 ppm of the cobalt concentration in the reaction vessel.

3.4.8   Recycling Experiments

The reactions were set up according to the general hydrogenation procedure with styrene (0.5 mmol) as substrate in 2 ml THF. The hydrogenations were carried out for 30 min each (2 bar H_2, r.t., 5 mol% Co-NP). After reaction, the autoclave was introduced into the glovebox and the reaction vial put on top of a neodymium magnet (cylindrical, 10 x 20 mm (height x diameter), N45) for 5 min. The solvent was removed using a Pasteur pipette and the particles washed once with 2 ml THF. New substrate and solvent were added, the vial was put back into the autoclave and a new hydrogenation reaction started. The organic phase was analyzed using quantitative GC-FID. After nine consecutive reactions, the particles were dissolved in 1 mL THF and stirred inside the glovebox overnight. The next day, three more runs were carried out. After these three reactions the particles were stirred again inside the glovebox for another 72hours before a last hydrogenation reaction was started.

3.4.9 Functional Group Tolerance Tests
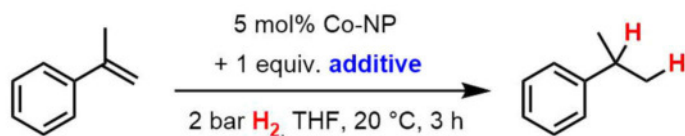
Additives and yield of cumene:

– –	Me~OH	⬡–OH	⬡–NH₂	⬡–F,F
>99 (>99)	98 (>99)	74 (>99)	>99 (>99)	97 (>99)

Figure S2   Functional group tolerance of Co-NP catalyzed hydrogenation of α-Methylstyrene in presence of 1 equiv. additive. Standard conditions: 0.25 mmol substrate in 1 mL THF; yields of hydrogenation product (cumene) determined by quantitative GC vs. internal reference *n*-pentadecane. Conversion of α-Methylstyrene shown in parentheses.

3.4.10 Comparison of Co-NPs Synthesized by Different Methods

Kinetic experiments were carried out to compare the catalytic activity of the different catalyst systems described previously. Figure S3 shows a similar catalytic activity of the various nanoparticles, yielding complete conversion after 17 to 24 minutes.
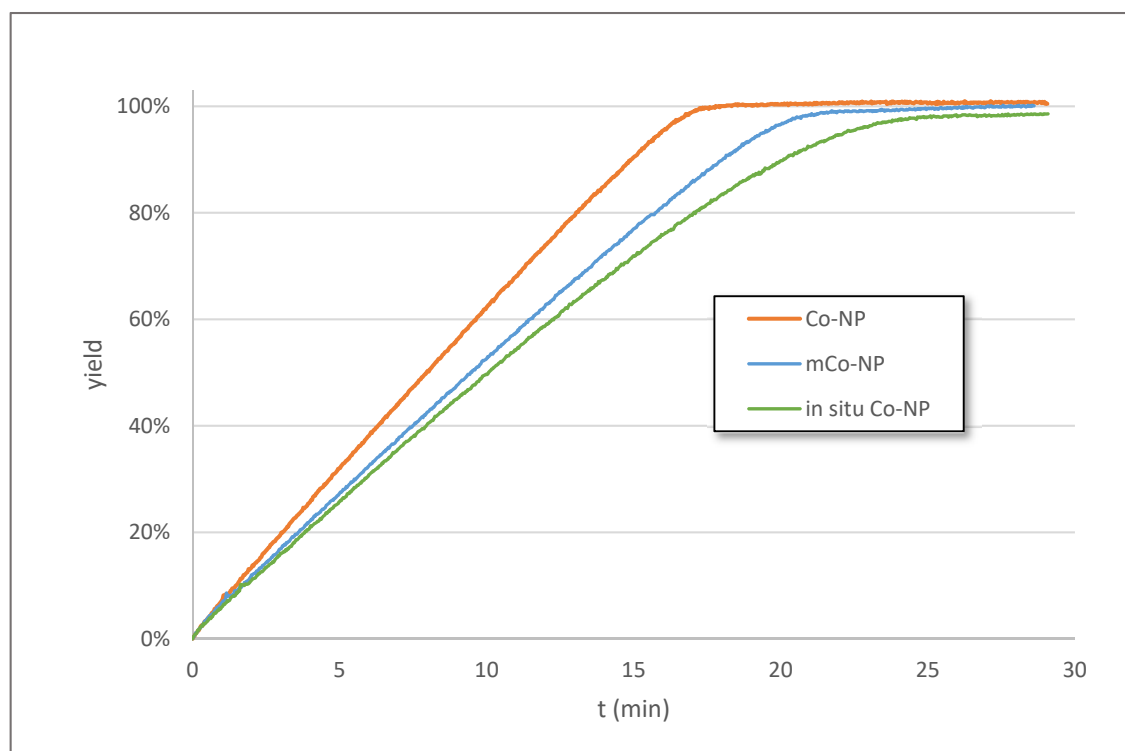
Figure S3   Hydrogenation of styrene using the nanoparticles isolated by centrifugation, separation by a magnet and using the *in situ* protocol. The conditions were 1.9 bar H_2, 5 mol% [Co], r.t., THF. The reaction yield was determined by measuring the consumption of hydrogen.

3.4.11 Particle Analyses

3.4.11.1 Purity and Crystallinity

The purity of the as-prepared Co(0) nanoparticles was proven by X-ray powder diffraction (XRD) after powder sintering (800 °C, Ar). This treatment ensured crystallization of all products including potentially amorphous residual components (e.g. oxides and hydroxides). Despite the resultant non-nanoparticulate state, the presence of pure cobalt (cubic modification as majority phase with traces of a hexagonal phase) and the absence of any cobalt oxide impurities was validated (Figure 3.1a).

3.4.11.2 Particle Size Distribution

Average particle diameters of the Co(0) nanoparticles before and after the hydrogenation reaction were calculated by statistical evaluation of >200 particles on TEM images using the *ImageJ* 1.47v software. Figure S4a shows the results for [NaNaph]-made Co(0) nanoparticles

(Co-NPs) isolated by centrifugation. Figure S4b shows the results for *in situ* generated cobalt nanoparticles (*in situ* Co-NPs). It should be noted that dynamic light scattering (DLS) as an alternative analytical tool gives less conclusive results due to the magnetic interaction of the nanoparticles.
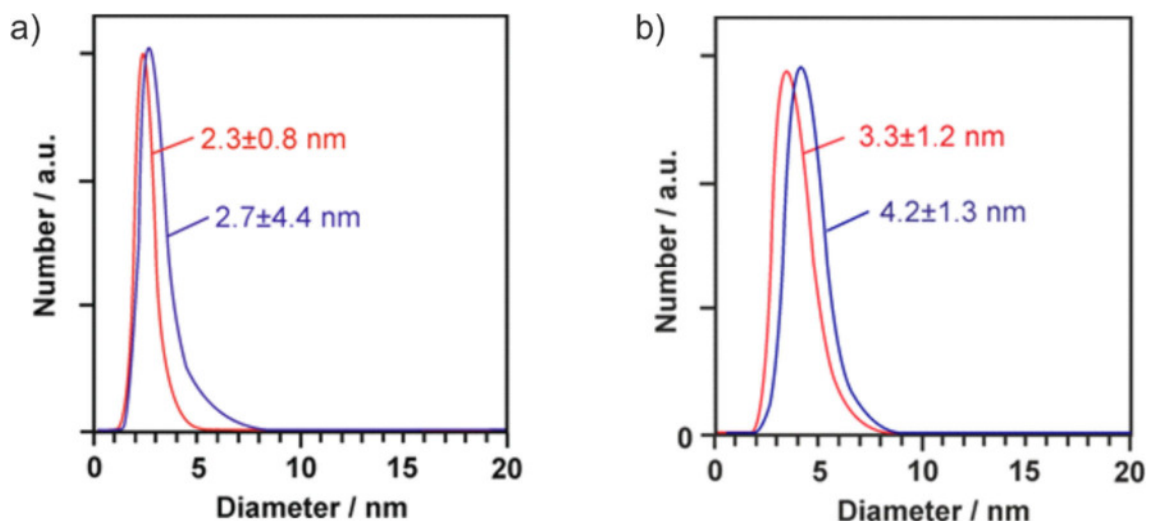
Figure S4   Particle size distribution according to statistical evaluation of TEM images (>200 particles) of a) cobalt nanoparticles (Co-NPs) and b) *in situ* generated cobalt nanoparticles (*in situ* Co-NPs) before (red) and after (blue) hydrogenation reactions.

3.4.11.3 TEM Measurements

TEM images of Co(0) nanoparticles before and after the catalytical reaction are shown in Figure S5 and Figure S6 for *ex situ* and *in situ* generated nanoparticles.
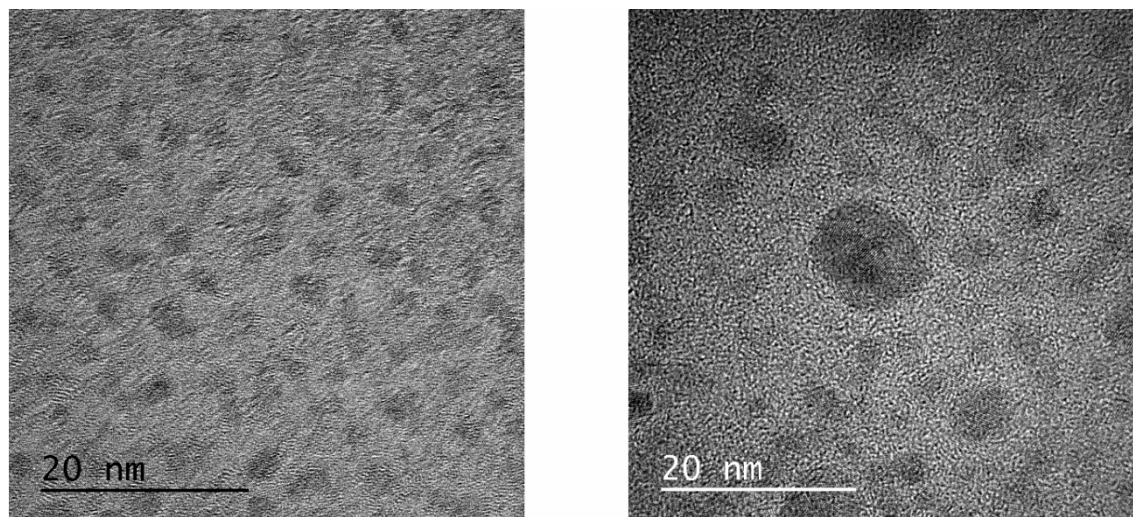
Figure S5   TEM measurement of cobalt nanoparticles (Co-NP) before (left) and after (right) hydrogenation reaction.
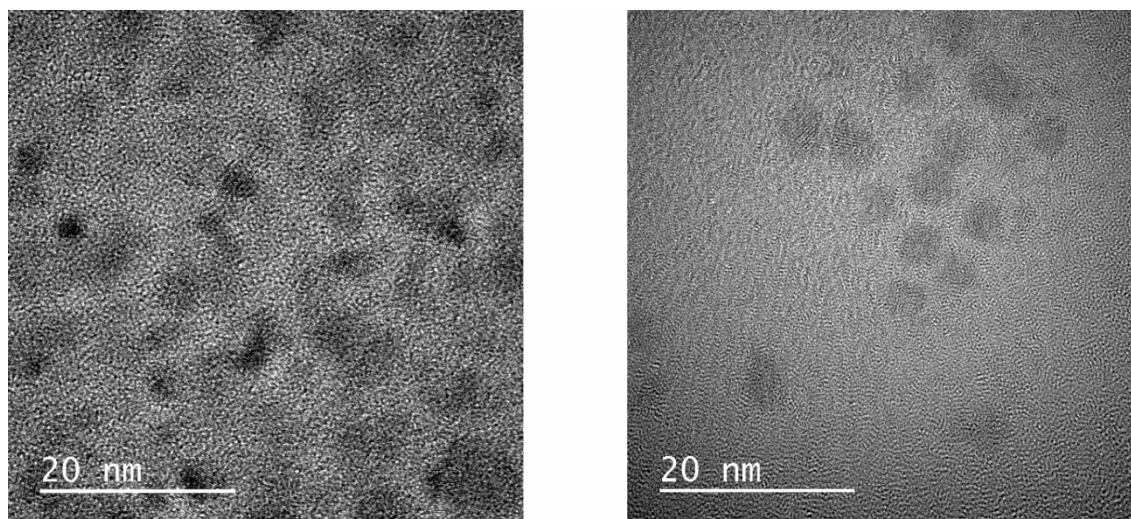
Figure S6   TEM measurement of *in situ* generated cobalt nanoparticles (*in situ* Co-NP) before (left) and after (right) hydrogenation reaction.

3.5   References

[1]   a) K. An, G. A. Somorjai, Catal. Lett. 2015, 145, 233; b) A. K. Singh, Q. Xu, ChemCatChem 2013, 5, 652; c) M. Sankar, N. Dimitratos, P. J. Miedziak, P. P. Wells, C. J. Kiely, G. J. Hutchings, Chem. Soc. Rev. 2012, 41, 8099.

[2]   a) N. Taccardi, M. Grabau, J. Debuschewitz, M. Distaso, M. Brandl, R. Hock, F. Maier, C. Papp, J. Erhard, C. Neiss, W. Peukert, A. Görling, H.-P. Steinrück, P. Wasserscheid, Nature Chem. 2017, 9, 862; b) H. Su, K. X. Zhang, B. Zhang, H. H. Wang, Q. Y. Yu, X. H. Li, M. Antonietti, J. S. Chen, J. Am. Chem. Soc. 2017, 139, 811; c) J. Jover, M. Garcia-Rates, N. Lopez, ACS Catal. 2016, 6, 4135; d) T. Yasukawa, A. Suzuki, H. Miyamura, K. Nishino, S. Kobayashi, J. Am. Chem. Soc. 2015, 137, 6616; e) Z. X. Li, W. Xue, B. T. Guan, F. B. Shi, Z. J. Shi, H. Jiang, C. H. Yan, Nanoscale 2013, 5, 1213; f) E. Gross, J. Krier, L. Heinke, G. A. Somorjai, Top. Catal. 2012, 55, 13; g) E. Bayram, J. C. Linehan, J. L. Fulton, J. A. S. Roberts, N. K. Szymczak, T. D. Smurthwaite, S. Ozkar, M. Balasubramanian, R. G. Finke, J. Am. Chem. Soc. 2011, 133, 18889.

[3]   Selected examples: a) Q. Knijnenburg, A. D. Horton, H. van der Heijden, T. M. Kooistra, D. G. H. Hetterscheid, J. M. M. Smits, B. de Bruin, P. H. M. Budzelaar, A. W. Gal, J. Mol. Catal. A 2005, 232, 151; b) G. Zhang, K. V. Vasudevan, B. L. Scott, S. K. Hanson, J. Am. Chem. Soc. 2013, 135, 8668; c) M. R. Friedfeld, M. Shevlin, J. M. Hoyt, S. W. Krska, M. T. Tudge, P. J. Chirik, Science 2013, 342, 1076; d) S. Rösler, J. Obenauf, R. Kempe, J. Am. Chem. Soc. 2015, 137, 7998; e) N. Gorgas, B. Stöger, L. F. Veiros, K. Kirchner, ACS Catal. 2016, 6, 2664; f) K. Tokmic, C. R. Markus, L. Zhu, A. R. Fout, J. Am. Chem. Soc. 2016, 138, 11907; g) J. R. Cabrero-Antonio, R. Adam, K. Junge, R. Jackstell, M. Beller, Catal. Sci. Technol. 2017, 7, 1981.

[4]   a) D. Gärtner, A. Welther, B. R. Rad, R. Wolf, A. Jacobi von Wangelin, Angew. Chem. Int. Ed. 2014, 53, 3722; b) P. Büschelberger, D. Gärtner, E. Reyes-Rodriguez, F. Kreyenschmidt, K. Koszinowski, A. Jacobi von Wangelin, R. Wolf, Chem. Eur. J. 2017, 23, 3139.

[5]   a) M. R. Buck, R. E. Schaak, Angew. Chem. Int. Ed. 2013, 52, 6154; b) Y. Lu, W. Chen, Chem. Soc. Rev. 2012, 41, 3594; c) B. Lim, Y. Xia, Angew. Chem. Int. Ed. 2011, 50, 76; d) T. K. Sau, A. L. Rogach, Adv. Mater. 2010, 22, 1781.

[6]   a) S. Mourdikoudis, L. M. Liz-Marzán, Chem. Mater. 2013, 25, 1465; b) C. Vollmer, C. Janiak, Coord. Chem. Rev. 2011, 255, 2039.

[7]   a) H. Bönnemann, W. Brijoux, R. Brinkmann, T. Joußen, B. Korall, E. Dinjus, Angew. Chem. Int. Ed. Engl. 1991, 30, 1312; b) H. Bönnemann, W. Brijoux, R. Brinkmann, N. Matoussevitch, N. Waldöfner, N. Palina, H. Modrow, Inorg. Chim. Acta 2003, 350, 617; c) R. Xu, T. Xie, Y. Zhao, Y. Li, Nanotechnology 2007, 18, 055602; d) F. Alonso, P. Riente, M. Yus, Acc. Chem. Res. 2011, 44, 379; e) M. Tejeda-Serrano, J. R. Cabrero-Antonino, V. Mainar-Ruiz, M. López-Haro, J. C. Hernández-Garrido, J. J. Calvino, A. Leyva-Pérez, A. Corma, ACS Catal. 2017, 7, 3721.

[8]   a) F. Chen, A.-E. Surkus, L. He, M.-M. Pohl, J. Radnik, C. Topf, K. Junge, M. Beller, J. Am. Chem. Soc. 2015, 137, 11718; b) F. Chen, C. Topf, J. Radnik, C. Kreyenschulte, H. Lund, M. Schneider, A.-E. Surkus, L. He, K. Junge, M. Beller, J. Am. Chem. Soc. 2016, 138, 8781.

[9]   R. V. Jagadeesh, K. Murugesan, A. S. Alshammari, H. Neumann, M.-M. Pohl, J. Radnik, M. Beller, Science 2017, 358, 326.

[10] B. Chen, F. Li, Z. Huang, G. Yuan, ChemCatChem 2016, 8, 1132.

[11] T. Schwob, R. Kempe, Angew. Chem. Int. Ed. 2016, 55, 15175.

[12] C. Chen, Y. Huang, Z. Zhang, X.-Q. Dong, X. Zhang, Chem. Commun. 2017, 53, 4612.

[13] F. Chen, C. Kreyenschulte, J. Radnik, H. Lund, A.-E. Surkus, K. Junge, M. Beller, ACS Catal. 2017, 7, 1526.

[14] For details, please see the Supporting Information.

[15] Y. Zhu, L. P. Stubbs, F. Ho, R. Liu, C. P. Ship, J. A. Maguire, N. S. Hosmane, ChemCatChem 2010, 2, 365

[16] a) D. R. Anton, R. H. Crabtree, Organometallics 1983, 2, 855; b) J. A. Widegren, R. G. Finke, J. Mol. Catal. 2003, 198, 317; c) R. H. Crabtree, Chem. Rev. 2011, 112, 1536; d) J. F. Sonnenberg, R. H. Morris, Catal. Sci. Technol. 2014, 4, 3426.

[17] a) C. Schöttle, P. Bockstaller, R. Popescu, D. Gerthsen, C. Feldmann, Angew. Chem. Int. Ed. **2015**, *54*, 9866; b) C. Schöttle, D. Doronkin, R. Popescu, D. Gerthsen, J.-D. Grunwaldt, C. Feldmann, Chem. Commun. **2016**, *52*, 6316; c) C. Schöttle, S. Rudel, R. Popescu, D. Gerthsen, F. Kraus, C. Feldmann, ACS Omega **2017**, *2*, 9144.

[18] a) R. D. Rieke, *Science* **1989**, *246*, 1260; b) L. A. Garza-Rodriguez, B. I. Kharisov, O. V. Kharisova, *Synthesis and Reactivity in Inorganic, Metal-Organic, and Non-Metal Chemistry* **2009**, *39*, 270.

[19] a) A. F. Khusnuriyalova, A. Petr, A. T. Gubaidullin, A. V. Sukhov, V. I. Morozov, B. Büchner, V. Kataev, O. G. Sinyashin, D. G. Yakhvarov, *Electrochim. Acta* **2018**, *260*, 324. b) F. Nador, Y. Moglie, C. Vitale, M. Yus, F. Alonso, G. Radivoy, *Tetrahed.* **2010**, *66*, 4318. c) F. Alonso, M. Yus, *Chem. Soc. Rev.* **2004**, *33*, 284.

[20] N. G. Connelly, W. E. Geiger, Chem. Rev. 1996, 96, 877.

[21] V. K. LaMer, R. H. Dinegar, J. Am. Chem. Soc. 1950, 72, 4847.

[22] Selected examples: a) G. Zhang, B. L. Scott, S. K. Hanson, Angew. Chem., 2012, 51, 12102; b) G. Zhang, S. K. Hanson, Chem. Commun. 2013, 49, 10151; c) M. R. Friedfeld, G. W. Margulieux, B. A. Schaefer, P. J. Chirik, J. Am. Chem. Soc. 2014, 136, 13178; d) P. J. Chirik, Acc. Chem. Res. 2015, 48, 1687; e) T.-J. Zhao, Y.-N. Zhang, K.-X. Wang, J. Su, X. Wei, X.-H. Li, RSC Adv. 2015, 5, 102736; f) G. Zhang, Z. Yin, J. Tan, RSC Adv. 2016, 6, 22419; g) V. G. Landge, J. Pitchaimani, S. P. Midya, M. Subaramanian, V. Madhu, B. Ekambaram, Catal. Sci. Technol. 2017, DOI: 10.1039/C7CY01994G.

[23] a) H. Heinz, C. Pramanik, O. Heinz, Y. Ding, R. K. Mishra, D. Marchon, R. J. Flatt, I. Estrela-Lopis, J. Llop, S. Moya, R. F. Ziolo, Surface Sci. Rep. 2017, 72, 1.

[24] a) S. Chaffins, M. Brettreich, F. Wudl, Synthesis 2002, 9, 1191; b) G. Franck, M. Brill, G. Helmchen, Org. Synth. 2012, 89, 55.

[25] Solubility Data Series – Metals in Mercury, Vol. 25 (Ed.: C. Hirayama, Z. Galus, C. Guminski), Pergamon Press: Oxford, 1986.

[26] Selected examples: a) R. H. Fish, A. D. Thormodsen, G. A. Cremer, J. Am. Chem. Soc. 1982, 104, 5234; b) A. S. Bommannavar, P. A. Montano, Appl. Surf. Sci. 1984, 19, 250; c) S. Eijsbouts, V. H. J. De Beer, R. Prins, J. Catal. 1991, 127, 619; d) K. Kaneda, Y. Mikami, T. Mitsudome, T. Mizugaki, K. Jitsukawa, Heterocycles 2010, 82, 1371; e) S. Chakraborty, W. W. Brennessel, W. D. Jones, J. Am. Chem. Soc. 2014, 136, 8564; f) R. Xu, S. Chakraborty, H. Yuan, W. D. Jones, ACS Catal. 2015, 5, 6350; g) W. Zuo,

R. H. Morris, Nature Protocols 2015, 10, 241; h) Z. Wei, Y. Chen, J. Wang, D. Su, M. Tang, S. Mao, Y. Wang, ACS Catal. 2016, 6, 5816; i) F. Chen, B. Sahoo, C. Kreyenschulte, H. Lund, M. Zeng, L. He, K. Junge, M. Beller, Chem. Sci. 2017, 8, 6239; j) D. Brenna, S. Rossi, F. Cozzi, M. Benaglia, Org. Biomol. Chem. 2017, 15, 5685.

4 CHIRAL ALKENE COBALTATES AS HYDROGENATION CATALYSTS

PHILIPP BÜSCHELBERGER, MATTEO VILLA,

AXEL JACOBI VON WANGELIN, AND ROBERT WOLF
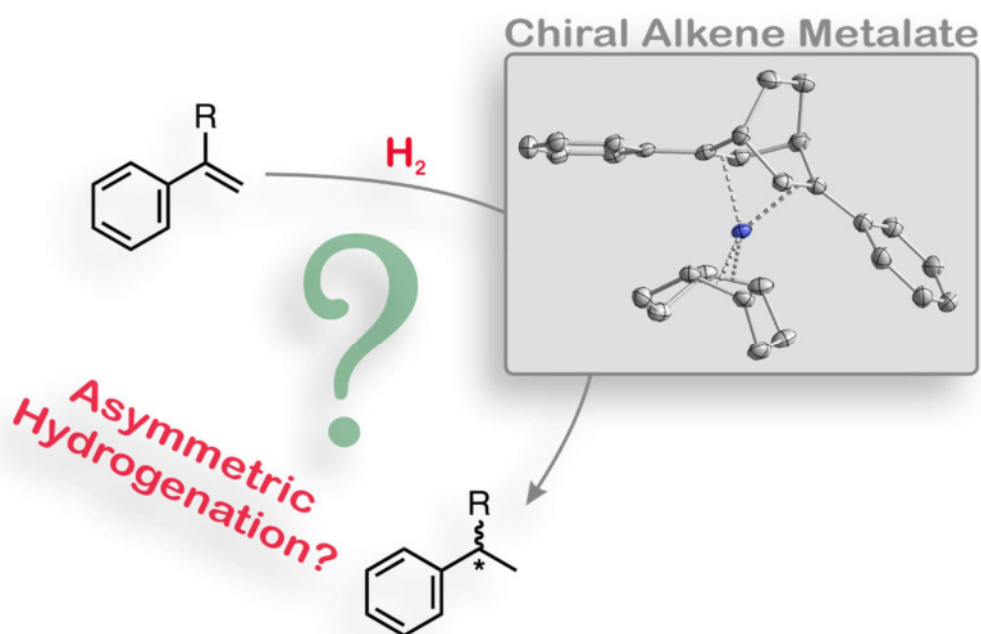
Alkene cobaltate anions with a chiral, C_2-symmetric norbornadiene ligand have been synthesized, and their catalytic activity in hydrogenation reactions has been evaluated. The complexes are active in the catalytic hydrogenation of various alkenes, but the activity towards disubstituted, prochiral substrates is low and accompanied by partial hydrogenation of the chiral norbonadiene ligand.

[I] P. Büschelberger performed the complex synthesis and characterization, prepared the catalytic experiments, analyzed several some of them, and wrote the manuscript. M. Villa synthesized and characterized the chiral ligand according to literature procedures and analyzed most of the catalytic reactions.

[II] Unpublished results.

4.1   Introduction

Asymmetric catalysis is an intensively studied academic and industrial field and, in terms of atom economy, the most attractive method for the synthesis of enantiopure chemical products.[1] Within this area, asymmetric hydrogenation constitutes a simple and efficient method to produce a multitude of chiral, chemical or biological important compounds.[2] An outstanding example for the importance of this reaction type is the rhodium-catalyzed enantioselective synthesis of L-DOPA (Figure 4.1, top), which is employed in the treatment of the Parkinson's disease.[3] Developed by William S. Knowles, this milestone reaction utilizes the rhodium complex [Rh(cod)(DiPAMP)][BF$_4$] (cod = 1,5-cyclooctadiene), bearing the chiral bisphosphine ligand DiPAMP (Figure 4.1, left).[4] Reflecting the important status of this reaction type in chemical synthesis, Knowles was honored with the Nobel Prize in 2001, together with Ryoji Noyori, for their work on enantioselective hydrogenation reactions.[5] Until today, most of the established chiral ligands in asymmetric catalysis are based on donating heteroatoms (e.g. nitrogen, phosphorus, and sulfur).[6] This tendency can also be observed for the recent examples of asymmetric cobalt-catalyzed hydrogenation reactions, driven by Chirik's complexes with C_1-symmetric bis(imino)pyridine, or chiral bisphosphine ligands (Figure 4.1, bottom right).[7]

While chiral phosphines and amines abound in the literature, chiral dienes have also attracted significant interest (albeit they have not been used for hydrogenations so far).[8] Diene ligands form significantly more stable complexes than related monoalkenes due to the chelate effect. Pioneering work in the synthesis of such chiral, chelating diene ligands and their application in asymmetric catalysis (e.g. for asymmetric conjugated additions or for the kinetic resolution of allyl carbonates) was done by Hayashi and Carreira, mainly with iridium and rhodium

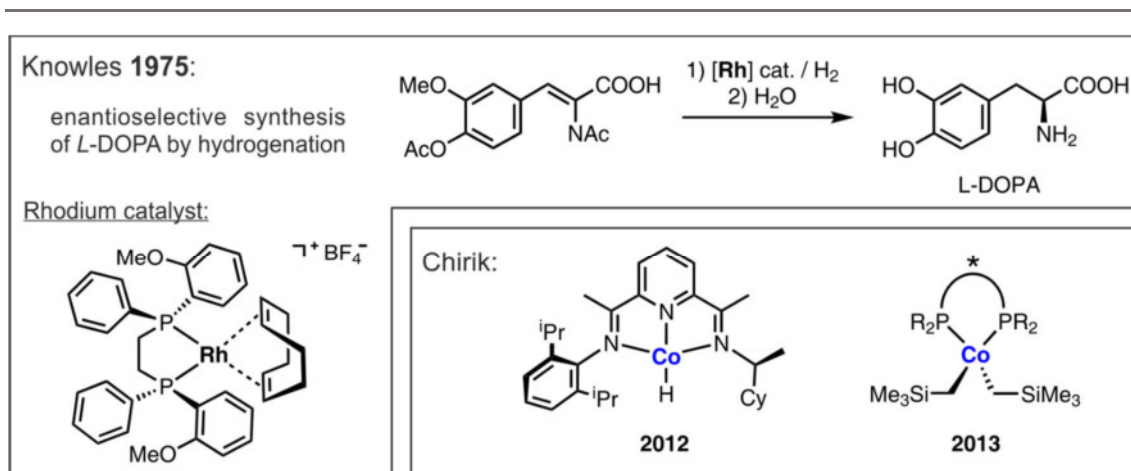Figure 4.1   Enantioselective synthesis of L-DOPA (top), according to Knowles, by asymmetric hydrogenation with the rhodium complex [Rh(cod)(DiPAMP)][BF$_4$] (left), and recent enantiopure cobalt catalysts for asymmetric hydrogenation by Chirik (bottom).

complexes.[9] Hayashi and co-workers prepared a C_2-symmetric norbornadiene derivative (Figure 4.2) and demonstrated its excellent properties as a steering ligand in the enantioselective rhodium-catalyzed 1,4-addition of organoboron and -tin reagents to enones.[10] Especially in the case of organostannanes, the catalytic activity of this new catalyst type was superior to that of classical phosphine complexes while also showing excellent stereoinduction. Independently, Carreira and co-workers applied chiral bicyclo[2.2.2]octadienes (Figure 4.2), with a convenient preparation, as ligands in the iridium-catalyzed kinetic resolution of chiral allylic carbonates.[11] For a broad range of aryl- and alkyl-substituted substrates, the products were isolated in up to 98% ee. Thereafter, a series of related chiral diene ligands were utilized in precious transition metal-catalyzed transformations displaying unique reactivities unmatched by conventional heteroatom-based chiral ligands.[9] Besides the aforementioned norbornadienes[10, 12] and bicyclo[2.2.2]octadienes,[11, 13] common ligand architectures in this field employ bicyclo[3.3.0]octadiene,[14] (bicyclic) 1,5-cyclooctadiene,[15] and acyclic diene scaffolds (Figure 4.2).[16] There are numerous applications in cyclizations and addition reactions to α,β-unsaturated compounds,[17] yet there is only one example for a chiral diene ligand in the transition metal-catalyzed asymmetric hydrogenation. Most relevant to this thesis, Grützmacher and co-workers synthesized iridium and rhodium complexes of chiral dibenzo[a,e]cyclooctatetraene (= dct) (Figure 4.2) and applied some of them successfully in hydrogenation and transfer hydrogenation reactions.[18] Unfortunately, they were not able to isolate the catalytically active compounds in an enantiomerically pure form.

Recently, we reported on the application of alkene metalates as catalysts in hydrogenation reactions.[19] Mechanistic studies showed that a diene ligand of the pre-catalyst, i.e. 1,5-cyclooctadiene or dibenzo[a,e]cyclooctatetraene, remains attached to the metal center
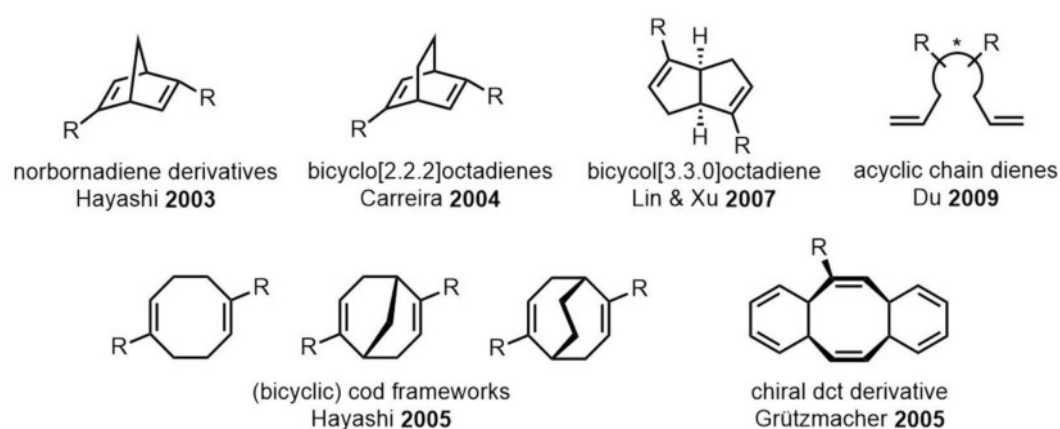

Figure 4.2   Common ligand architectures for chiral diene ligands, including norbornadiene derivatives, bicyclo[2.2.2]octadienes, bicyclo[3.3.0]octadienes, acyclic chain dienes, (bicyclic) cod frameworks and Grützmacher's chiral dct derivative.

during the whole catalytic cycle (see Chapter 2 of this thesis). Following these observations, we aimed at combining the catalytic activity of highly reduced cobaltates with the stereodirecting properties of chiral, chelating diene ligands. Here, we report on the attempts to generate a new kind of enantioselective cobalt hydrogenation catalysts with chiral diene ligands.

4.2 Results and Discussion

4.2.1 Synthesis of Chiral Diene Ligand

For our investigations, we chose Hayashi's (R,R)-2,5-diphenylbicyclo[2,2,2]octadiene (= (R,R)-Ph-bod) because of the well described synthesis and the high enantioselectivities (95-99% ee) that were obtained in other catalytic reactions using this ligand.[13a] In addition, there is no possibility of racemization of the catalyst due to the bicyclic design. Ph-bod was synthesized in five steps according to a procedure by Abele and co-workers, starting with a Michael addition-aldol reaction of the readily available phenylacetaldehyde and 2-cyclohexenone (Scheme 4.1).[20] Due to the several recrystallization steps, the enantiopure diene was only obtained in a total yield of 4%. The enantiopurity was confirmed by chiral HPLC[21] and this ligand was used for the catalytic experiments and the synthesis of the desired chiral cobaltates (vide infra).
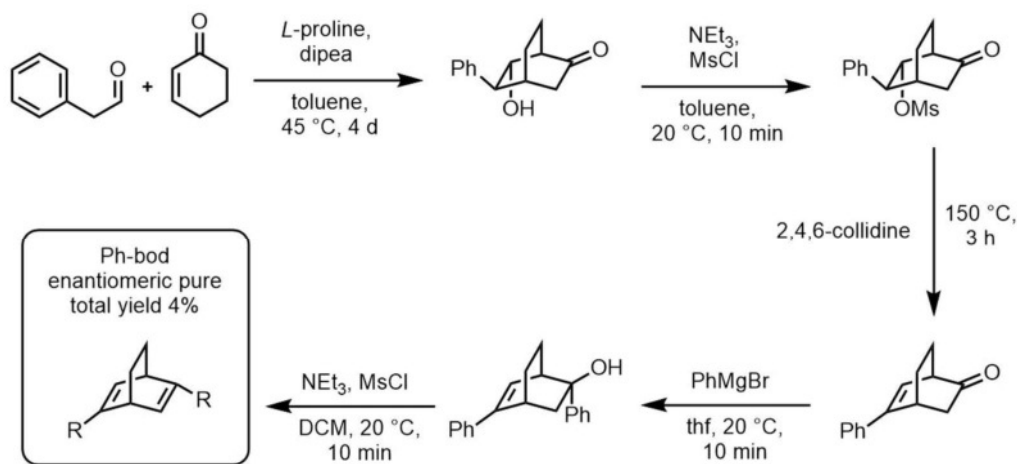
Scheme 4.1 Reaction pathway for the five step synthesis of Hayashi´s Ph-bod ligand starting from phenylacetaldehyde and 2-cyclohexenone.

4.2.2 Synthesis of Cobalt Complexes

The highly reduced compounds $[K(thf)_{0.2}][Co(cod)_2]$ (1), $[K([18]crown-6)][Co(C_{10}H_8)(cod)]$ (2) ($C_{10}H_8$ = naphthalene) and $[K(dme)_2][Co(C_{14}H_{10})_2]$ (3) ($C_{14}H_{10}$ = anthracene), originally prepared by Jonas and Ellis and co-workers,[22] respectively, served as precursors for the desired new catalysts. Reaction of 1, 2, or 3 with a slight excess (1.1 equiv.) of (R,R)-Ph-bod (Figure 4.3) led

to a replacement of one of the ligands (cod, naphthalene, or anthracene), respectively. Initial investigations resulted in crystalline complexes [K(thf)][Co(Ph-bod)(cod)] (**4**) and [K([18]crown-6)][Co(Ph-bod)(C$_{14}$H$_{10}$)] (**5**). These initial reactions were carried out with a sample of Ph-bod that was not enantiopure (e.r. = 74/26). After addition of the chiral ligand to a solution of **1** in THF at 0 °C, the clear yellow solution turned intense red. Dark red, X-ray quality crystals of [K(thf)][Co(Ph-bod)(cod)] (**4**) were obtained from a THF solution layered with *n*-hexane (1:3) in 46% yield. Single-crystal XRD revealed an enantiopure (Flack parameter = -0.024(2)) ion-contact structure (Figure 4.3a right) that crystallizes in the chiral space group $P2_12_12_1$.[21] The cobalt atom features a distorted tetrahedral coordination environment with a twist angle of 64.8°,[23] which is comparable to the one of [K([2,2,2]cryptand)][Co(cod)$_2$] (67.3°) and slightly larger than those observed for related anionic cobalt complexes, such as [K([18]crown-6)][Co(cod)(dct)] (59.0°) and [K(thf)$_2$][Co(dct)$_2$] (**6**) (55.0°).[19b, 22e] The average C=C bond lengths of cod (1.416 Å) and Ph-bod (1.420 Å) are very similar to those found for the chelating dienes in the former compounds.[19b, 22e] The potassium cation interacts with two carbon atoms of the cod ligand and with the aryl rings of two adjacent anions forming a contact ion pair structure (see Figure S 6).

For NMR characterization, the synthesis was reproduced with the enantiopure ligand. The ^{1}H NMR spectrum of **4** in [D$_8$]THF displays a set of 12 signals.[21] The phenyl groups resonate as a typical pattern of two triplets (δ = 6.37 and 6.82 ppm) and one doublet (δ = 6.94 ppm) in the aromatic region. The resonance of the bridgehead protons of Ph-bod is hidden under the signal of [D$_8$]THF at δ = 3.58 ppm but can clearly be assigned by 2D NMR experiments. One multiplet assigned to two CH protons of the cod ligand is shifted to δ = 3.4 ppm. The remaining, partly overlapping signals are located in the range between δ = 0.88 and 1.88 ppm. The crown-ether-containing salt [K([18]crown-6)][Co(Ph-bod)(cod)] (**4'**) is formed in an analogous manner as **4** by reaction of **2** with Ph-bod (Figure 4.3a bottom left) but was only identified by XRD. Again, this experiment was carried out with a sample of Ph-bod that was not enantiopure (e.r. = 74/26) resulting in a mixed crystalline product with a similar enantiomeric ratio. Due to disorders the molecular structure could not be refined. However, as **1** as a starting material features a more facile synthesis, the reaction pathway starting from **2** was not pursued.

Similar to the synthesis of **4**, [K([18]crown-6)][Co(Ph-bod)(C$_{14}$H$_{10}$)] (**5**) can be prepared by addition of 1.1. equivalents of Ph-bod to a THF solution of **3** at -20 °C (Figure 4.3b left). An intense dark green reaction solution is observed. Dark green X-ray quality crystals were obtained in 58% yield from a THF solution by layering this solution with diethyl ether. Enantiopure **5** (Flack parameter = -0.018(2)) crystallizes in the chiral hexagonal space group $P6_1$.[21] The molecular structure (Figure 4.3b right) is similar to that of [K([2,2,2]cryptand)][Co(cod)(C$_{14}$H$_{10}$)], featuring

a nonplanar anthracene ligand, coordinated as an η^4-conjugated diene, as commonly observed for such metalates.[22e] The twist angle of 72.0°[23] is marginally smaller than the one of the former compound (79.8°). The average C=C bond length of the "diene-unit" (C21=C22–C23=C24) of anthracene (1.418 Å) is almost identical with those reported for related polyarene cobaltates.[22d, e] The ^{1}H NMR spectrum of the isolated product shows one set of broad signals for Ph-bod and anthracene with an expected 1:1 ratio.
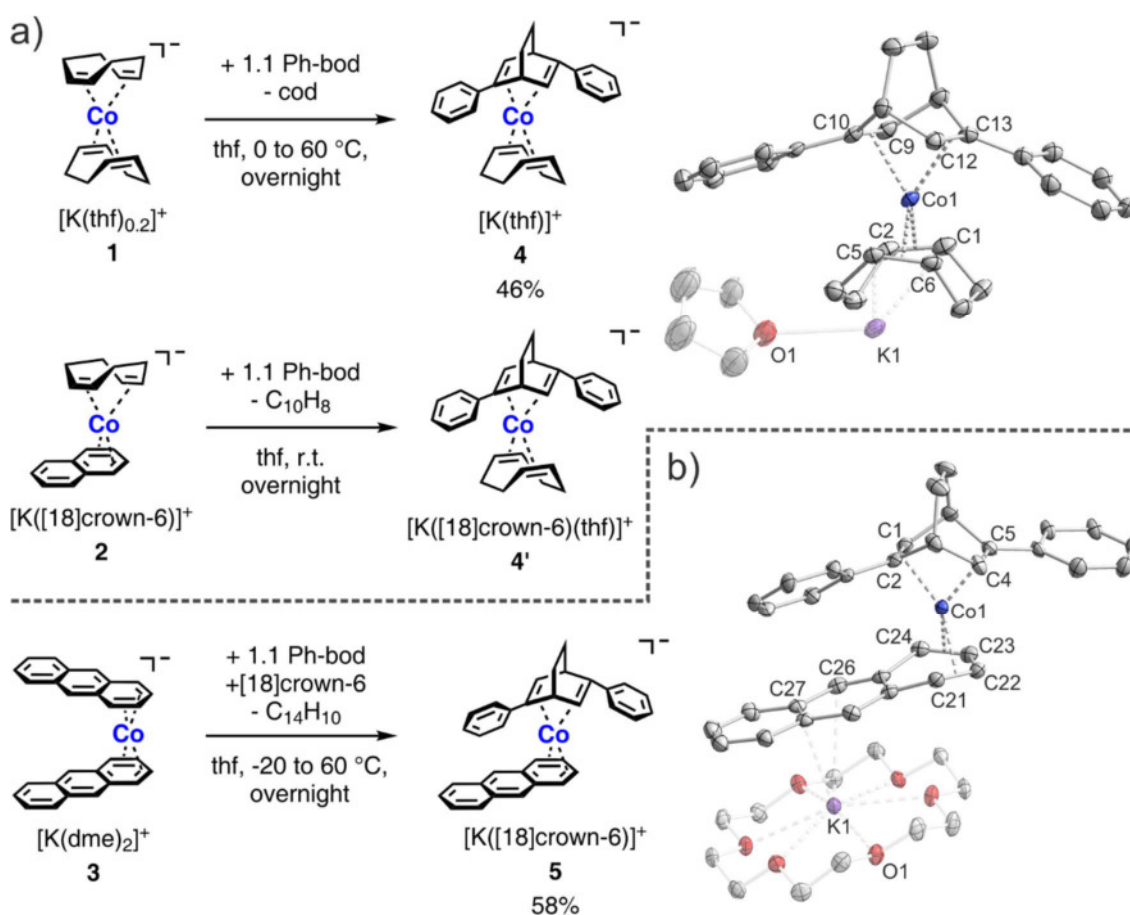

Figure 4.3   a) Synthesis of **4** (top left) and **4'** (bottom left) and molecular structure of **4** (right, ellipsoids are at the 50% probability level, H atoms and solvent molecules are omitted for clarity). Selected bond lengths [Å] and angles[°]: Co1–C1 2.039(4), Co1–C2 2.059(4), Co1–C5 2.020(4), Co1–C6 2.053(3), C1–C2 1.402(6), C5–C6 1.430(4), Co1–Centroid(C1–C2) 1.925, Co1–Centroid(C5–C5) 1.907, Co1–C9 2.052(3), Co1–C10 2.100(4), Co1–C12 2.045(4), Co1–C13 2.119(4), C9–C10 1.419(5), C12–C13 1.420(5), Co1–Centroid(C9–C10) 1.951, Co1–Centroid(C12–C13) 1.957, K1–C5 3.001(4), K1–C6 3.175(4); twist angle 64.8,[23] bite angles:[24] cod 90.6, Ph-bod 73.6. b) Synthesis (left) and molecular structure (right, ellipsoids are at the 50% probability level, H atoms are omitted for clarity) of **5**. Selected bond lengths [Å] and angles[°]: Co1–C1 2.017(4), Co1–C2 2.107(4), Co1–C4 2.045(4), Co1–C5 2.097(4), C1–C2 1.423(6), C4–C5 1.426(6), Co1–Centroid(C1–C2) 1.936, Co1–Centroid(C4–C5) 1.945, Co1–C21 2.1764), Co1–C22 2.016(4), Co1–C23 2.014(4), Co1–C24 2.169(4), C21–C22 1.423(6), C22–C23 1.410(6), C23–C24 1.412(7), Co1–Centroid(C21–C22) 1.973, Co1–Centroid(C23–C24) 1.970, K1–C26 3.137(4), K1–C27 3.329(4), twist angle 72.0,[23] bite angles:[24] C14H10 62.9, Ph-bod 74.6.

4.2.3   Catalytic Hydrogenation Reactions

For the evaluation of the catalytic activity, the enantiopure ligand (*R*,*R*)-Ph-bod was added to THF solutions of the precursors **1** - **3**. The reaction mixtures were stirred overnight inside the glovebox and used for the catalytic reactions afterwards. First, the catalytic activity of the *in situ* prepared cobaltate **5** was evaluated in the hydrogenation of styrene. Conversion to ethylbenzene was nearly quantitative under very mild conditions (2 bar H_2 at room temperature, see Table 4.1, entry 1). Unfortunately, a significant portion of the ligand (20-30% according to GC-MS analysis) was (partly) hydrogenated in this reaction. Initially, it was assumed that the ligand hydrogenation occurs *after* full consumption of the substrate as reported for other alkene metalates.[19b] However, further experiments showed that the hydrogenation of Ph-bod is competitive to that of substrate molecules. Subsequently, α-cyclopropylstyrene and α-ethylstyrene were tested as prochiral model substrates. Mild reaction conditions (2 bar H_2, r.t.) allowed only minor conversion of the 1,1-disubstituted alkene, while partial hydrogenation of the steering ligand (*R*,*R*)-Ph-bod already took place (Table 4.1, entries 2-4). Under harsher conditions (5 bar H_2, 60 °C), the substrate conversion did not improve, despite a higher degree of ligand hydrogenation (Table 4.1, entries 9-11). The highest substrate conversions of 35% and 25%, were achieved using precursors **2** and **3** but the desired hydrogenation product was formed in only 17% yield besides 10% of byproducts resulting from cyclopropane ring-opening or isomerization (Table 4.1, entries 3 & 11).

Additional experiments were motivated by the known use of styrene as a promotor of ligand exchange reactions.[19b] Styrene is well-known to be easily hydrogenated. With 0.3-0.5 equiv. of styrene as an additive, full conversion of styrene and partial hydrogenation of (*R*,*R*)-Ph-bod was observed, while almost no conversion of the prochiral substrate was detected (Table 4.1, entries 5-8). In general, the competitive hydrogenation of the ligand is a serious problem as it is also observed in hydrogenation reactions with 1,1-diphenylethylene, which delivered significant ligand hydrogenation (5-20%) and only small amounts of the desired product (Table S 4.1, entries S5-S7).

As it is known that **1** - **3** are able to hydrogenate disubstituted substrates (Table S 4.1, entries S1 & S8-S10) in the absence of Ph-bod,[19b] it seems that the Ph-bod ligand acts as a catalyst poison similar to dct.[25] In fact, one equivalent of dct with respect to pre-catalyst effectively inhibits the catalytic hydrogenation reaction in case of **3** (see Table S 4.1, enties S2 & S3). Nonetheless, dct is more stable towards hydrogenation and was not converted under the conditions applied. With dct and Ph-bod both decreasing the catalytic activity, and the fact that the latter is hydrogenated under reaction conditions it is not suitable as a steering ligand for hydrogenations in this case.

Table 4.1   Hydrogenation reactions with *in*-situ prepared chiral cobaltates. Standard reaction conditions: 0.25 mmol substrate in 1 mL THF, 1 equiv. of diene ligand per cobalt atom. Conversions and yields were estimated by GC-MS and are given as area percent of the substrates and their corresponding products. In parentheses: yield of isomerization or ring opening products.

Entry	Cobaltate	Ligand	Conditions	Additive[c]	Additive hydrogenation [%]	Hydrogenation of Ph-bod [%]	Substrate	Conv. [%]	Yield [%]
1	1	(R,R)-Ph-bod	mild[a]	-	-	20-30		95	95
2	1			-	-	5-10		1	1
3	2	(R,R)-Ph-bod	mild[a]	-	-	5-10		35	17 (18)
4	3			-	-	5-10		2	2 (traces)
5	2			styrene	>99	5-10		1	1
6	1			styrene	>99	5-10		1	1
7	2	(R,R)-Ph-bod	harsh[b]	styrene	>99	5-10		1	traces
8	3			styrene	>99	60		4	4
9	1			-	-	20		4	4 (traces)
10	2	(R,R)-Ph-bod	harsh[b]	-	-	20		8	6 (2)
11	3			-	-	50		25	16 (9)

[a] 2 bar H₂, r.t. [b] 5 bar H₂, 60 °C. [c] 0.3-0.5 equiv with respect to the substrate

4.3   Conclusion

For the first time, we have isolated and characterized chiral alkene cobaltate complexes **4** and **5** containing Hayashi's (*R*,*R*)-Ph-bod ligand. The use of these anionic complexes as pre-catalysts was tested in catalytic hydrogenation reactions. Unfortunately, the Ph-bod ligand is partly hydrogenated even under mild reaction conditions, preventing its use as a steering ligand for the asymmetric hydrogenation of prochiral substrates. Nevertheless, this study confirms the possibility of using chiral dienes as ligands in anionic cobalt(−I) complexes. For an application of this catalyst type in asymmetric hydrogenation, it is necessary to find other steering ligands that should be more robust towards hydrogenation. Possible candidates are chiral dibenzocyclooctatetraene (= dct) derivatives that are more robust against hydrogenation. Enantiopure derivatives of such ligands have been reported by Grützmacher and co-workers.[18] It should be of great interest to test their catalytic properties with anionic cobaltate precatalysts.

4.4   Experimental Section

4.4.1   General Procedures

All experiments were performed under an atmosphere of dry argon by using standard Schlenk and glovebox techniques. Solvents were purified, dried, and degassed by standard techniques. NMR spectra were recorded (300 K) with Bruker Avance 300 and Avance 400 spectrometers internally referenced to residual solvent resonances. NMR assignments are based on COSY, HMBC, HSQC and NOESY 2D NMR experiments. The chiral (*R*,*R*)-Ph-bod ligand was prepared according to a procedure by Abele.[20] Only one species was observed by chiral HPLC, confirming enantiopurity.[21] Compounds **1**,[22b] **2**,[22e] and **3**[26] as well as dct[27] were synthesized according to procedures reported in the literature.

4.4.2   Complex Syntheses

4.4.2.1   [K(thf)][Co(Ph-bod)(1,5-cod)] (**4**)

A solution of 2,5-diphenylbicyclo[2.2.2]octa-2,5-diene (85.2 mg, 0.330 mmol, 1.1 equiv.) in THF (3 mL) was added to a solution of [K(thf)$_{0.2}$][Co(1,5-cod)$_2$] (98,6 mg, 0.300 mmol, 1 equiv.) in THF (5 mL) and stirred for 90 min at 0 °C giving an intense red reaction mixture. Afterwards, the solution was warmed to 60 °C overnight before the solvent and the released cod were removed *in vacuo*. The red solid residue was washed with *n*-hexane (3 · 4 mL), redissolved in THF (6 mL), filtered and layered with *n*-hexane (18 mL; 1:3) for crystallization. After several days, dark red crystals of **4** (73.5 mg, 536.69 g/mol, 0.137 mmol, 46%) were isolated by decantation of the supernatant solution, washing with *n*-hexane (5 mL), and drying *in vacuo*. XRD quality crystals

were obtained by diffusion from *n*-hexane to a concentrated THF solution. According to ^{1}H NMR spectra, small impurities of cod, naphthalene and free Ph-bod are present in the isolated product.

^{1}H NMR (400.13 MHz, [D$_8$]THF, 300 K): δ = 0.88-1.00 (m, 2H, cod C*H$_2$*), 1.13 (br s, 4H, bridge C*H$_2$*), 1.17-1.24 (m, 2H, cod C*H$_2$*), 1.24-1.33 (m, 2H, cod C*H$_2$*), 1.44 (d, ^3J = 6.3 Hz, 2H, *H*C=CPh), 1.75-1.80 (m, 2H, cod C*H*), 1.80-1.88 (m, 2H, cod C*H$_2$*), 3.34-3.43 (m, 2H, cod C*H*), 3.60-3.64 (m, 2H, bridgehead C*H*), 6.37 (t, ^3J = 6.9 Hz, 2H, *p*-Ph-*H*), 6.82 (t, ^3J = 7.5 Hz, 4H, *m*-Ph-*H*), 6.94 (d, ^3J = 7.7 Hz, 4H, *o*-Ph-*H*);

^{13}C{^{1}H} NMR (100.61 MHz, [D$_8$]THF, 300 K): δ = 28.5 (bridge *C*H$_2$), 29.9 (cod *C*H$_2$), 35.3 (cod *C*H$_2$), 37.6 (bridgehead *C*H), 44.0 (H*C*=CPh), 47.6 (HC=*C*Ph; low intensity in ^{13}C{^{1}H} NMR but intensive coupling in HMBC), 74.3 (cod *C*H; low intensity in the 1D ^{13}C{^{1}H} NMR spectrum, but intense coupling in HSQC), 75.9 (cod *C*H; low intensity in the 1D ^{13}C{^{1}H} NMR spectrum, but intense coupling in HSQC), 115.8 (*p*-Ph-*C*), 121.4 (*o*-Ph-*C*), 127.7 (*m*-Ph-*C*), 150.3 (*ipso*-Ph-*C*);

4.4.2.2 [K([18]crown-6)][Co(Ph-bod)(C$_{14}$H$_{10}$)] (5)

A solution of 2,5-diphenylbicyclo[2.2.2]octa-2,5-diene (85.2 mg, 0.330 mmol, 1.1 equiv.) and [18]crown-6 (79.2 mg, 0.300 mmol, 1 equiv.) in THF (4 mL) was added to a solution of [K(dme)$_2$][Co(C$_{14}$H$_{10}$)$_2$] (190.4 mg, 0.300 mmol, 1 equiv.) in THF (6 mL) at −20 °C. The mixture was slowly warmed to room temperature at which time it appeared dark yellowish-brown. Upon heating to 60 °C overnight, the solution became intense dark green. The solvent was removed *in vacuo* and the released anthracene was removed by sublimation (10^{-3} mbar, 70 °C, 3 h). The dark solid residue was washed with *n*-hexane (2 · 3 mL), redissolved in THF (7.5 mL), filtered and layered with *n*-hexane (15 mL; 1:2) for crystallization. After seven days, the supernatant was decanted, and the solid was washed with *n*-hexane (5 mL) and dried *in vacuo*. Dark green crystals of **5** (138 mg, 798.95 g/mol, 0.173 mmol, 58%) were isolated. X-ray quality crystals were obtained from a concentrated THF solution layered with diethyl ether. According to ^{1}H NMR spectra, the product is contaminated with residual free chiral Ph-bod ligand. A proposed assignment of the signals of **5** is given in the following.

^{1}H NMR (400.13 MHz, [D$_8$]THF, 300 K): δ = 1.16-1.37 (br m, 4H, bridge C*H$_2$*), 2.99-3.07 (m, 1H, C$_{14}$H$_{10}$ coordinating ring), 3.53 (s, 24H, [18]crown-6), 3.60 (hidden under solvent signal, but coupling in 2D spectra, 1H, C$_{14}$H$_{10}$, coordinating ring), 3.81 (br s, 1H, C$_{14}$H$_{10}$, coordinating ring), 3.90 (br s, 2H, *H*C=CPh or bridgehead C*H*), 4.63 (br s, 1H, *H*C=CPh), 4.80 (br s, 1H, C$_{14}$H$_{10}$, coordinating ring), 5.49 (s, 1H, C$_{14}$H$_{10}$, middle ring), 6.26 (br s, Ph-*H*, 1H,), 6.35-6.41 (m, Ph-*H*, 2H), 6.45 (br s, Ph-*H*, 3H), 6.54-6.67 (m, 8H, Ph-H (4H) & C$_{14}$H$_{10}$, external ring (4H));

$^{13}C\{^1H\}$ NMR (100.61 MHz, [D$_8$]THF, 300 K): δ = 27.4 (bridge CH$_2$), 39.8, 61.8, 63.8, 71.0 ([18]crown-6, CH$_2$), 80.9, 87.9, 106.7, 108.0, 120.6, 120.7, 122.7, 123.1, 123.7, 128.1.

4.4.3   General Procedure for Hydrogenation Reactions

A dry 5 mL vial with a screw cap and PTFE septum was charged with a magnetic stir bar and a solution of the metalate **1**-**3** and the Ph-bod ligand (0.0125 mmol each, 5 mol%) in THF (0.5 ml). This solution was stirred overnight in the glovebox to guarantee a quantitative ligand exchange with the chiral alkene. After adding a solution of the substrate (0.25 mmol) in THF (0.5 mL) with a pipette, the vial was closed and the septum was punctured with a short needle (Braun). The vial was placed into a high-pressure reactor (Parr Instr.), which was sealed, removed from the glovebox, placed on a magnetic stirrer plate, and purged with hydrogen. For higher temperature reactions the autoclave was warmed with a heating mantle. The reaction was stopped by releasing the H$_2$ pressure, the vial was removed from the autoclave, and the reaction was quenched with a saturated aqueous solution of NaHCO$_3$ (1 mL). The mixture was extracted with diethyl ether and the combined organic layers were dried over Na$_2$SO$_4$. Yields were estimated by GC-MS and are given as area percent of the substrates and their corresponding products.

4.5   Supporting Information

4.5.1   General Information

High Pressure Reactor: Hydrogenation reactions were carried out in 160 and 300 mL high pressure reactors (*Parr^{TM}*) in 4 mL glass vials. The reactors were loaded under argon, purged with H$_2$ (1 min), then three times with 2 bar H$_2$, sealed and the internal pressure was adjusted. Hydrogen (99.9992%) was purchased from Linde.

^1H and ^{13}C NMR spectroscopy: Nuclear magnetic resonance spectra were recorded on *Bruker* Avance 300 (300.13 MHz ^1H, 75.47 MHz ^{13}C) and *Bruker* Avance 400 (400.13 MHz ^1H, 100.61 MHz ^{13}C). Chemical shift δ is given in ppm to tetramethylsilane. The following abbreviations are used to indicate multiplicities: s = singlet, d = doublet, t = triplet, m = multiplet.

X-ray crystallography: The single crystal X-ray diffraction data were recorded on an Agilent Technologies SuperNova diffractometer using CuKα radiation. Empirical multi-scan and analytical absorption corrections were applied to the data.[28][29] Using Olex2,[30] the structures were solved with SHELXT.[31] Least-square refinement was carried out with SHELXL.[32]

Gas chromatography with mass-selective detector (GC-MS): Agilent 6890N Network GC System, mass detector 5975 MS. Carrier gas: H$_2$ (1.0 mL/min). Column: HP-5MS (30 m x 0.25 mm x

0.25 µm, 5% phenylmethylsiloxane). *Agilent* 7820A GC system, mass detector 5977B MSD. Carrier gas: H_2 (1.2 mL/min). Column: HP-5MS (30 m x 0.25 mm x 0.25 µm).

High performance liquid chromatography with DAD detector (HPLC): Agilent 1260 Infinity, DAD detector. Column: ChiralPAK IA (4.6 mm x 250 mm, particle size 5 µm). Solents: *n*-hexane, isopropanol.

4.5.2 HPLC
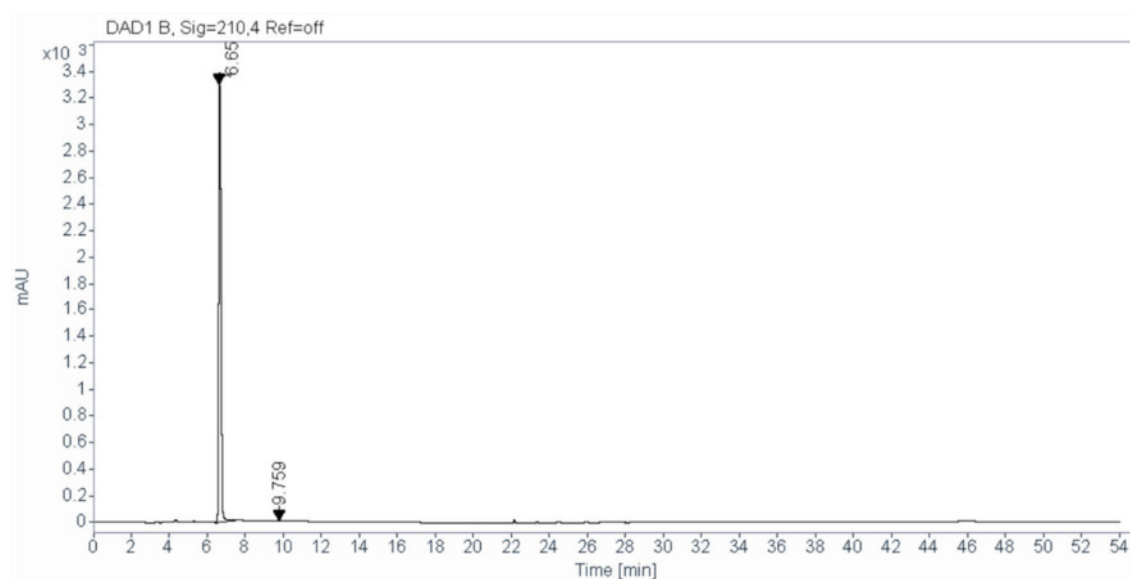
Figure S 1   HPLC chromatogram (*n*-hexane/isopropanol: 99/1, 0.7 mL/min) of the enantiopure chiral diene (*R*,*R*)-Ph-bod. Detection wavelength: 210 nm.

4.5.3 NMR Spectra
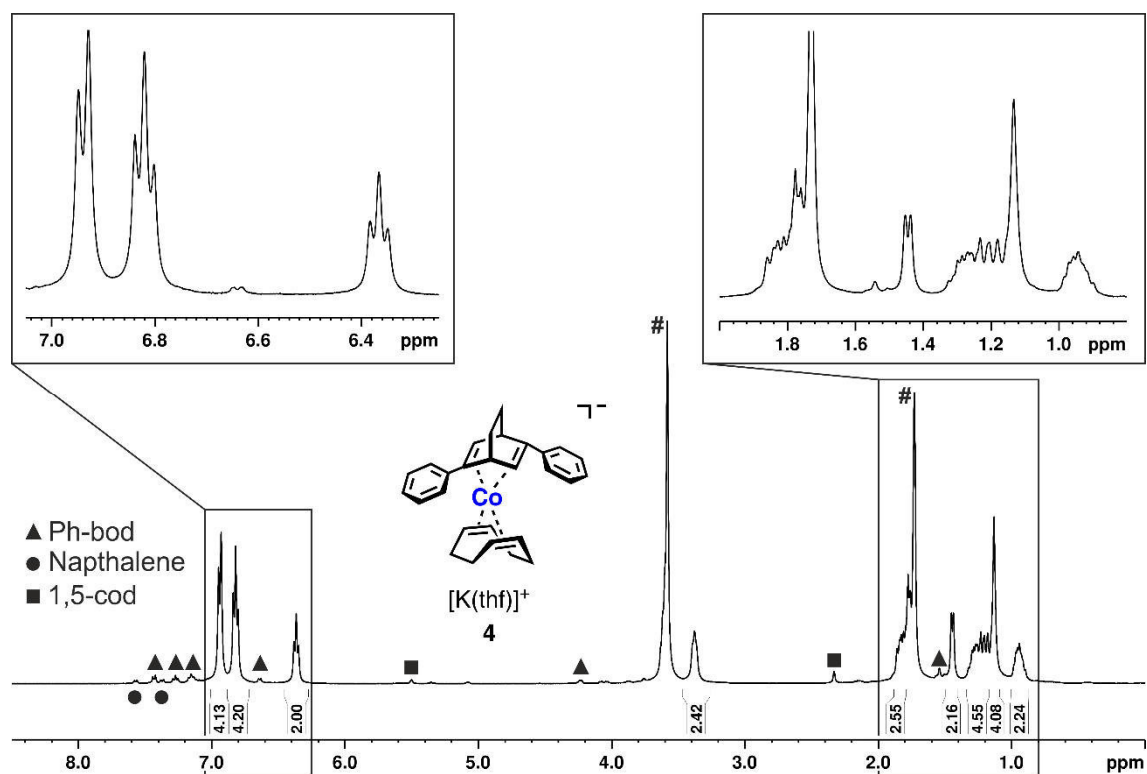
Figure S 2 ^{1}H NMR spectrum (400.13 MHz, [D$_8$]THF (#), 300 K) of [K(thf)][Co(Ph-bod)(cod)] (**4**) with impurities of Ph-bod (▲), naphthalene (●) and 1,5-cod (■).
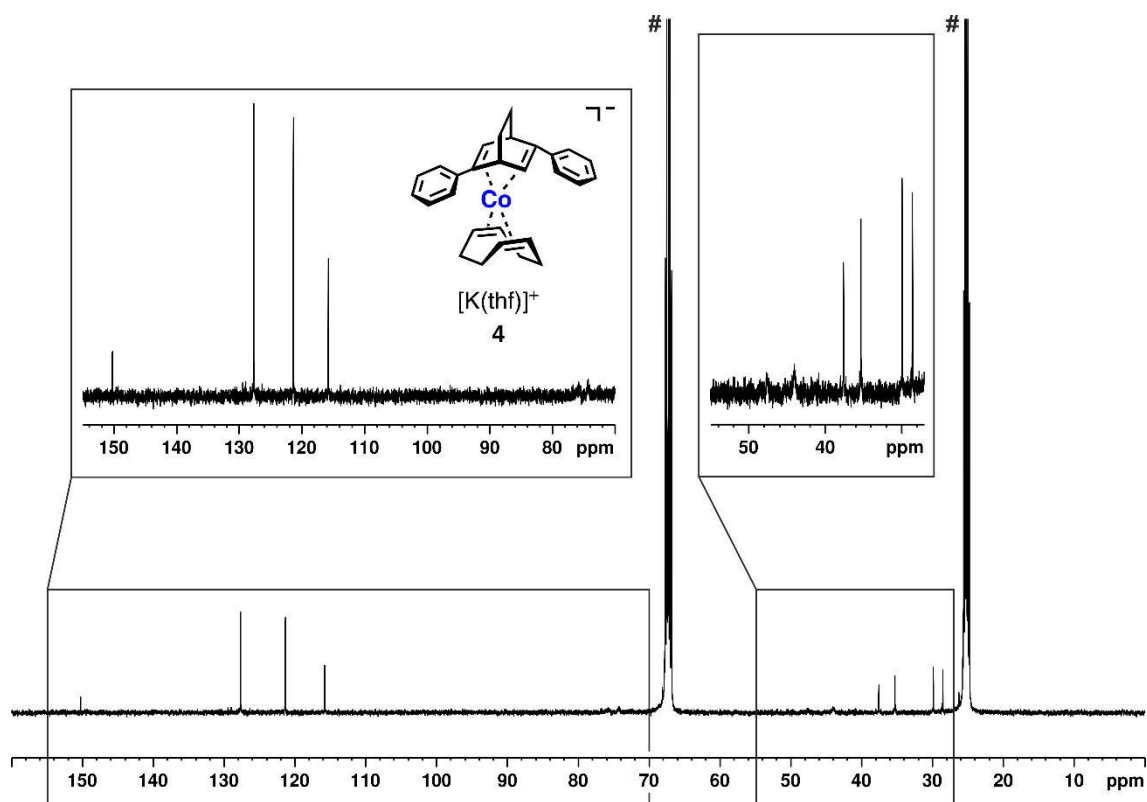
Figure S 3 ^{13}C{^{1}H} NMR spectrum (100.61 MHz, [D$_8$]THF (#), 300 K) of [K(thf)][Co(Ph-bod)(cod)] (**4**).
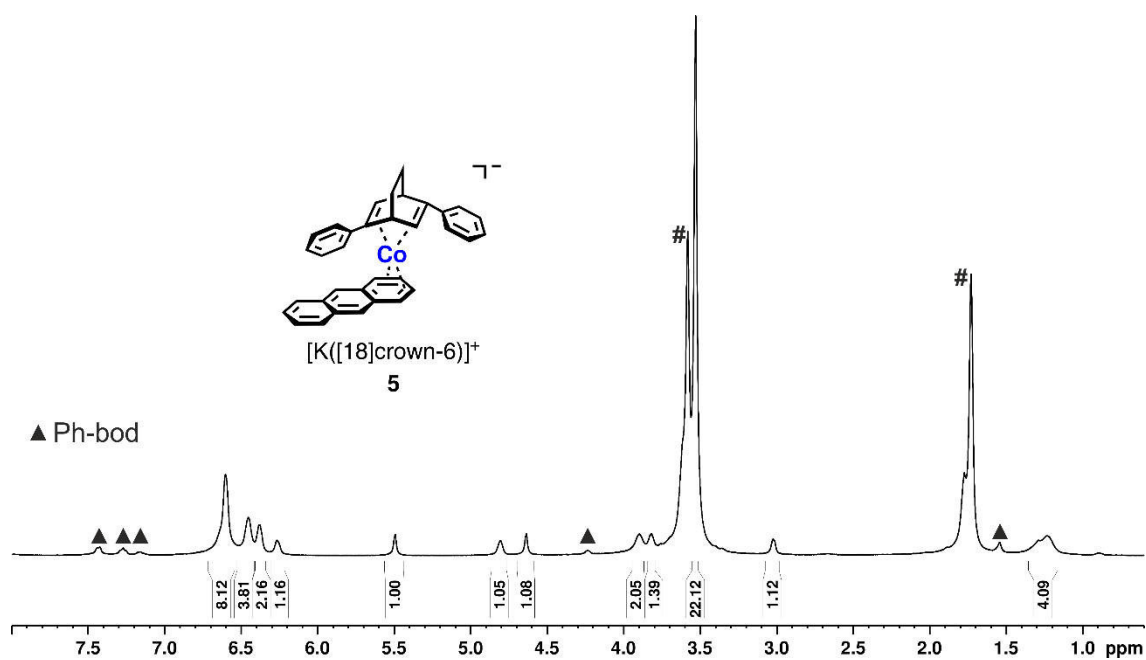
Figure S 4 ^{1}H NMR spectrum (400.13 MHz, [D$_8$]THF (#), 300 K) of [K([18]crown-6)][Co(Ph-bod)(C$_{14}$H$_{10}$)] (**5**) with impurities of Ph-bod (▲).
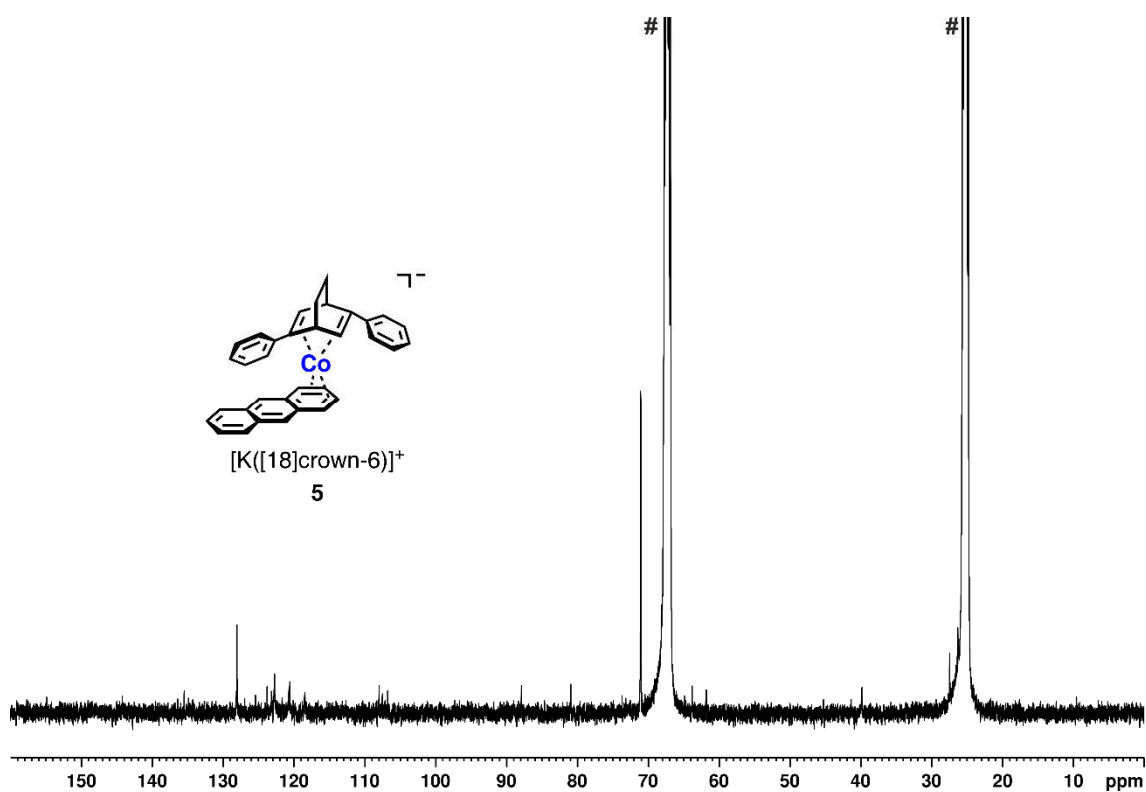
Figure S 5 ^{13}C{^{1}H} NMR spectrum (100.61 MHz, [D$_8$]THF (#), 300 K) of [K([18]crown-6)][Co(Ph-bod)(C$_{14}$H$_{10}$)] (**5**).

4.5.4 Hydrogenation Reactions

Table S 4.1   Hydrogenation reactions with (*in*-situ prepared chiral) cobaltates. Standard reaction conditions: 0.25 mmol substrate in 1 mL THF. Conversions and yields were estimated by GC-MS and are given as area percent of the substrates and their corresponding products. In parentheses: yield of isomerization or ring opening products

| Entry	Cobaltate	Ligand	Conditions	Additive	Additive hydrogenation [%]	Chiral ligand hydrogenation [%]	Substrate	Conv. [%]	Yield [%]
S1	3	-				-		90	81 (9)
S2	3	dct (5 mol%)[a]	harsh[c]	-	-	-		4	3 (1)
S3	3	dct (10 mol%)[b]				-		1	1
S4	6	-	harsh[c]	-	-	-		2	2
S5	1			-	-	10-20		2	2
S6	2	Ph-bod[a]	harsh[c]	-	-	5-10		8	8
S7	3			-	-	5-10		1	1
S8	1			-	-	-		85	75 (10)
S9	2	-	mild[d]	-	-	-		65	50 (15)
S10	3			-	-	-		95	95

[a] 1 equiv per cobalt atom. [b] 2 equiv. per cobalt atom. [c] 5 bar H_2, 60 °C. [d] 2 bar H_2, r.t.

4.5.5 X-ray Crystallography

Table S 4.2   Crystal data and structure refinement for compounds **4** and **5**.

| Compound	4	5
Empirical formula	$C_{36}H_{46}O_2KCo$	$C_{46}H_{52}O_6KCo$
Formula weight	608.76	798.90
Temperature [K]	123.0(1)	123.0(1)
Crystal system	orthorhombic	hexagonal
Space group	$P2_12_12_1$	$P6_1$
a [Å]	8.7085(1)	10.7327(2)
b [Å]	15.1436(3)	10.7327(2)
c [Å]	22.9749(4)	59.934(1)
α [°]	90	90
β [°]	90	90
γ [°]	90	120
Volume [Å³]	3029.89(9)	5978.9(2)
Z	4	6
ρ_{calc} [g/cm³]	1.335	1.331
μ [mm⁻¹]	5.898	4.696
F(000)	1296.0	2532.0
Crystal size [mm³]	0.183 × 0.133 × 0.0753	0.1103 × 0.1333 × 0.1662
Radiation	CuKα (λ = 1.54184)	CuKα (λ = 1.54184)
Range for data collection [°]	9.664 < 2Θ < 147.192	8.852 < 2Θ < 147.108
Index ranges	-10 ≤ h ≤ 10 -18 ≤ k ≤ 18 -28 ≤ l ≤ 28	-13 ≤ h ≤ 11 -12 ≤ k ≤ 13 -74 ≤ l ≤ 74
Reflections collected	37186	34481
Independent reflections	6033 R_{int} = 0.0505 R_{sigma} = 0.0302	7924 R_{int} = 0.0586 R_{sigma} = 0.0528
Data/restraints/parameters	6033/37/379	7924/1/487
Goodness-of-fit on F²	1.038	1.052
Final R indexes [I ≥ 2σ(I)]	R_1 = 0.0412 wR_2 = 0.1076	R_1 = 0.0464 wR_2 = 0.0819
Final R indexes [all data]	R_1 = 0.0454 wR_2 = 0.1111	R_1 = 0.0524 wR_2 = 0.0833
Largest diff. peak/hole [eÅ⁻³]	0.80/-0.57	0.26/-0.33
Flack parameter	-0.024(2)	-0.018(2)
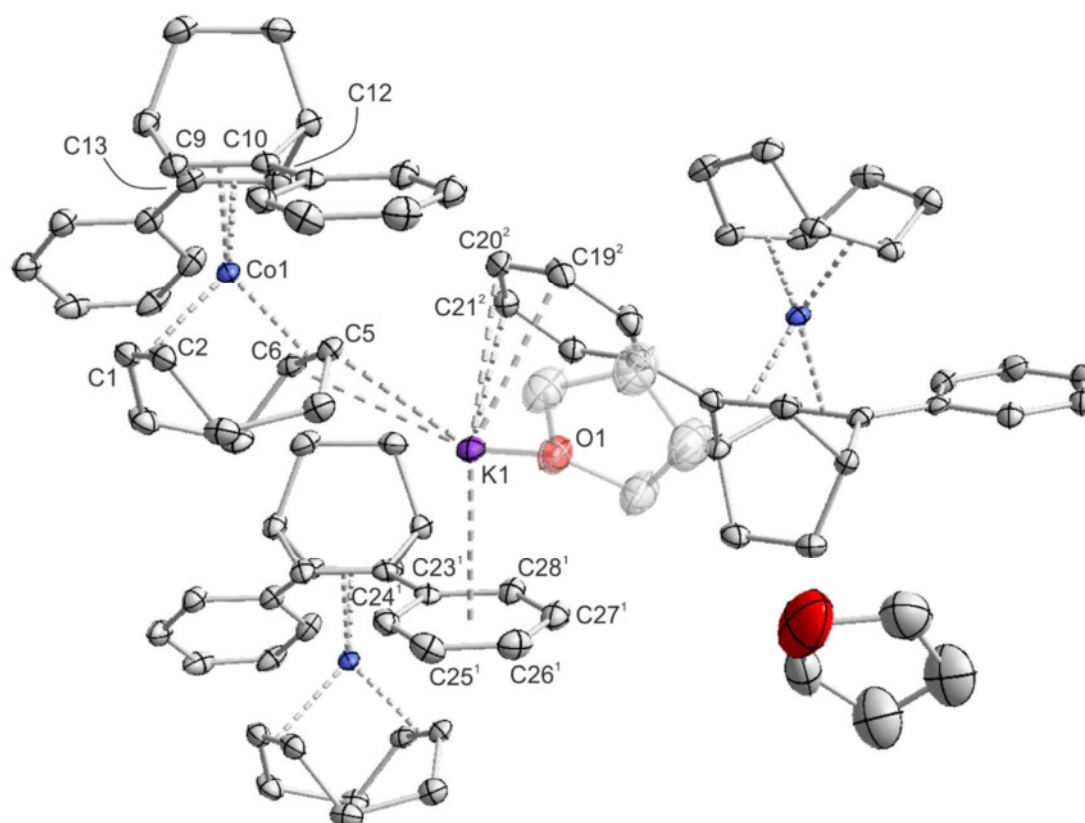
Figure S 6   Molecular structure of **4** (ellipsoids are at the 40% probability level, H atoms are omitted for clarity). Selected bond lengths [Å] and angles[°]: Co1–C1 2.039(4), Co1–C2 2.059(4), Co1–C5 2.020(4), Co1–C6 2.053(3), C1–C2 1.402(6), C5–C6 1.430(4), Co1–Centroid(C1–C2) 1.925, Co1–Centroid(C5–C5) 1.907, Co1–C9 2.052(3), Co1–C10 2.100(4), Co1–C12 2.045(4), Co1–C13 2.119(4), C9–C10 1.419(5), C12–C13 1.420(5), Co1–Centroid(C9–C10) 1.951, Co1–Centroid(C12–C13) 1.957, K1–C5 3.001(4), K1–C6 3.175(4), K1–C19² 3.167(4), K1–C20² 3.183(5), K1–C21² 3.265(5), K1–C23¹ 3.231(4), K1–C24¹ 3.254(4), K1–C25¹ 3.274(4), K1–C26¹ 3.224(4), K1–C27¹ 3.151(4), K1–C28¹ 3.140(3), K1–Centroid(C23¹-C28¹) 2.895(1); twist angle 64.8,[23] bite angles:[24] cod 90.6, Ph-bod 73.6

4.6   References

[1]   a) C. E. Song, S. Lee, *Chem. Rev.* **2002**, *102*, 3495–3524; b) R. Noyori, Angew. Chem. Int. Ed. **2002**, 41, 2008–2022.

[2]   a) M. J. Burk, *J. Am. Chem. Soc.* **1991**, *113*, 8518–8519; b) Q.-A. Chen, Z.-S. Ye, Y. Duan, Y.-G. Zhou, *Chem. Soc. Rev.* **2013**, *42*, 497–511.

[3]   W. S. Knowles, Acc. Chem. Res. 1983, 16, 106-112.

[4]   a) W. S. Knowles, M. J. Sabacky, B. D. Vineyard, D. J. Weinkauff, *J. Am. Chem. Soc.* **1975**, *97*, 2567–2568; b) B. D. Vineyard, W. S. Knowles, M. J. Sabacky, G. L. Bachman, D. J. Weinkauff, *J. Am. Chem. Soc.* **1977**, *99*, 5946–5952.

[5]   "The Nobel Prize in Chemistry 2001" NobelPrize.org. Nobel Media AB 2019. Thu. 11 Apr 2019. http://www.nobelprize.org/prizes/chemistry/2001/summary/

[6]   a) H. B. Kagan in *Asymmetric Synthesis - Vol. 5* (Ed.: J. D. Morrison), Elsevier, Amsterdam, **1985**, pp. 1–40; b) F. Fache, E. Schulz, M. L. Tommasino, M. Lemaire, *Chem. Rev.* **2000**, *100*, 2159–2232; c) *Comprehensive Asymmetric Catalysis – Supplement 1* (Eds.: E. N. Jacobsen, A. Pflatz, H.

Yamamoto), Springer-Verlag, Berlin, **2003**; d) W. Tang, X. Zhang, *Chem. Rev.* **2003**, *103*, 3029–3070; e) C. Gennari, U. Piarulli, *Chem. Rev.* **2003**, *103*, 3071–3100; f) S. Gladiali, E. Alberico, *Chem. Soc. Rev.* **2006**, *35*, 226–236; g) *Privileged Chiral Ligands and Catalysts* (Ed.: Q.-L. Zhou), John Wiley & Sons, Hoboken, **2011**.

[7]   a) S. Monfette, Z. R. Turner, S. P. Semproni, P. J. Chirik, *J. Am. Chem. Soc.* **2012**, *134*, 4561–4564; b) M. R. Friedfeld, M. Shevlin, J. M. Hoyt, S. W. Krska, M. T. Tudge, P. J. Chirik, *Science* **2013**, *342*, 1076–1080; c) R. P. Yu, J. M. Darmon, C. Milsmann, G. W. Margulieux, S. C. E. Stieber, S. DeBeer, P. J. Chirik, *J. Am. Chem. Soc.* **2013**, *135*, 13168–13184; d) K. H. Hopmann, *Organometallics* **2013**, *32*, 6388–6399; e) M. R. Friedfeld, G. W. Margulieux, B. A. Schaefer, P. J. Chirik, *J. Am. Chem. Soc.* **2014**, *136*, 13178–13181; f) M. R. Friedfeld, M. Shevlin, G. W. Margulieux, L.-C. Campeau, P. J. Chirik, *J. Am. Chem. Soc.* **2016**, *138*, 3314–3324; g) M. R. Friedfeld, H. Zhong, R. T. Ruck, M. Shevlin, P. J. Chirik, *Science* **2018**, *360*, 888–893; h) G. R. Morello, H. Zhong, P. J. Chirik, K. H. Hopmann, *Chem. Sci.* **2018**, *9*, 4977–4982.

[8]   F. Glorius, Angew. Chem. Int. Ed. **2004**, 43, 3364–3366.

[9]   X. Feng, H. Du, Asian J. Org. Chem. **2012**, 1, 204–213.

[10]   T. Hayashi, K. Ueyama, N. Tokunaga, K. Yoshida, *J. Am. Chem. Soc.* **2003**, *125*, 11508–11509.

[11]   C. Fischer, C. Defieber, T. Suzuki, E. M. Carreira, *J. Am. Chem. Soc.* **2004**, *126*, 1628–1629.

[12]   a) M. K. Brown, E. J. Corey, *Org. Lett.* **2010**, *12*, 172–175; b) W.-T. Wei, J.-Y. Yeh, T.-S. Kuo, H.-L. Wu, *Chem. Eur. J.* **2011**, *17*, 11405–11409; c) C.-C. Liu, D. Janmanchi, C.-C. Chen, H.-L. Wu, *Eur. J. Org. Chem.* **2012**, *2012*, 2503–2507; d) J.-F. Syu, H.-Y. Lin, Y.-Y. Cheng, Y.-C. Tsai, Y.-C. Ting, T.-S. Kuo, D. Janmanchi, P.-Y. Wu, J. P. Henschke, H.-L. Wu, *Chem. Eur. J.* **2017**, *23*, 14515–14522.

[13]   a) N. Tokunaga, Y. Otomaru, K. Okamoto, K. Ueyama, R. Shintani, T. Hayashi, *J. Am. Chem. Soc.* **2004**, *126*, 13584–13585; b) C. Defieber, J.-F. Paquin, S. Serna, E. M. Carreira, *Org. Lett.* **2004**, *6*, 3873–3876; c) J.-F. Paquin, C. Defieber, C. R. J. Stephenson, E. M. Carreira, *J. Am. Chem. Soc.* **2005**, *127*, 10850–10851; d) K. Okamoto, T. Hayashi, V. H. Rawal, *Org. Lett.* **2008**, *10*, 4387–4389; e) T. Shibata, T. Shizuno, *Angew. Chem. Int. Ed.* **2014**, *53*, 5410–5413; f) B. Zhou, C. M. So, Y. Lu, T. Hayashi, *Org. Chem. Front.* **2015**, *2*, 127–132; g) X. Dou, Y. Huang, T. Hayashi, *Angew. Chem. Int. Ed.* **2016**, *55*, 1133–1137.

[14]   a) Z.-Q. Wang, C.-G. Feng, M.-H. Xu, G.-Q. Lin, *J. Am. Chem. Soc.* **2007**, *129*, 5336–5337; b) S. Helbig, S. Sauer, N. Cramer, S. Laschat, A. Baro, W. Frey, *Adv. Synth. Catal.* **2007**, *349*, 2331–2337; c) Z.-Q. Wang, C.-G. Feng, S.-S. Zhang, M.-H. Xu, G.-Q. Lin, *Angew. Chem. Int. Ed.* **2010**, *49*, 5780–5783; d) S.-S. Zhang, Z.-Q. Wang, M.-H. Xu, G.-Q. Lin, *Org. Lett.* **2010**, *12*, 5546–5549; e) H.-Q. Dong, M.-H. Xu, C.-G. Feng, X.-W. Sun, G.-Q. Lin, *Org. Chem. Front.* **2015**, *2*, 73–89;

[15]   a) Y. Otomaru, N. Tokunaga, R. Shintani, T. Hayashi, *Org. Lett.* **2005**, *7*, 307–310; b) Y. Otomaru, A. Kina, R. Shintani, T. Hayashi, *Tetrahedron: Asymmetry* **2005**, *16*, 1673–1679; c) A. Kina, K. Ueyama, T. Hayashi, *Org. Lett.* **2005**, *7*, 5889–5892.

[16]   a) X. Hu, M. Zhuang, Z. Cao, H. Du, *Org. Lett.* **2009**, *11*, 4744–4747; b) X. Hu, Z. Cao, Z. Liu, Y. Wang, H. Du, *Adv. Synth. Catal.* **2010**, *352*, 651–655; c) Z. Cao, H. Du, *Org. Lett.* **2010**, *12*, 2602–2605; d) Y. Wang, X. Hu, H. Du, *Org. Lett.* **2010**, *12*, 5482–5485; e) Q. Li, Z. Dong, Z.-X. Yu, *Org. Lett.* **2011**, *13*, 1122–1125; f) B. M. Trost, A. C. Burns, T. Tautz, *Org. Lett.* **2011**, *13*, 4566–4569; g) Y. Liu, H. Du, *J. Am. Chem. Soc.* **2013**, *135*, 6810–6813.

[17] Reviews: a) C. Defieber, H. Grützmacher, E. M. Carreira, *Angew. Chem. Int. Ed.* **2008**, *47*, 4482–4502; b) J. B. Johnson, T. Rovis, *Angew. Chem. Int. Ed.* **2008**, *47*, 840–871.

[18] F. Läng, F. Breher, D. Stein, H. Grützmacher, *Organometallics* **2005**, *24*, 2997–3007.

[19] a) D. Gärtner, A. Welther, B. R. Rad, R. Wolf, A. Jacobi von Wangelin, *Angew. Chem. Int. Ed.* **2014**, *53*, 3722–3726; b) P. Büschelberger, D. Gärtner, E. Reyes-Rodriguez, F. Kreyenschmidt, K. Koszinowski, A. Jacobi von Wangelin, R. Wolf, *Chem. Eur. J.* **2017**, *23*, 3139–3151.

[20] a) S. Abele, R. Inauen, J.-A. Funel, T. Weller, *Org. Process Res. Dev.* **2012**, *16*, 129–140; b) S. Abele, R. Inauen, D. Spielvogel, C. Moessner, *J. Org. Chem.* **2012**, *77*, 4765–4773.

[21] See the supporting information for more details.

[22] a) K. Jonas, R. Mynott, C. Krüger, J. C. Sekutowski, Y.-H. Tsay, *Angew. Chem. Int. Ed. Engl.* **1976**, *15*, 767–768; b) K. Jonas, "Method of Preparing Transition Metal-Olefin Complex Compounds and Alkali Metal-Transition Metal-Olefin Complex Compounds", **1979**, Patent US4169845A; c) W. W. Brennessel, C. G. Young Jr., J. E. Ellis, *Angew. Chem. Int. Ed.* **2002**, *41*, 1211–1215; d) W. W. Brennessel, V. G. Young, J. E. Ellis, *Angew. Chem. Int. Ed.* **2006**, *45*, 7268–7271; e) W. W. Brennessel, J. E. Ellis, *Inorg. Chem.* **2012**, *51*, 9076–9094.

[23] The twist angle corresponds to the intersection of planes that are defined by the centroids of the coordinated C–C bonds of the ligand and the cobalt center and is 90° in case of an ideal tetrahedral geometry.

[24] The bite angle is the angle that is formed by the two centroids of the coordinated C–C bonds of the (diene) ligand and the cobalt atom.

[25] a) D. R. Anton, R. H. Crabtree, *Organometallics* **1983**, *2*, 621–627; b) D. R. Anton, R. H. Crabtree, *Organometallics* **1983**, *2*, 855–859; c) J. A. Widegren, R. G. Finke, *J. Mol. Catal. A* **2003**, *198*, 317–341.

[26] P. Büschelberger, C. Rödl, R. Wolf, *Inorg. Synth.* **2018**, *37*, 72-76.

[27] a) S. Chaffins, M. Brettreich, F. Wudl, *Synthesis* **2002**, *9*, 1191–1194; b) G. Franck, M. Brill, G. Helmchen, *Org. Synth.* **2012**, *89*, 55-65.

[28] a) SCALE3ABS, CrysAlisPro, Aglient Technologies Inc., Oxford, UK, **2015**; b) G. M. Sheldrick, SADABS, Bruker AXS, Madison, USA, **2007**.

[29] a) R. C. Clark, J. S. Reid, *Acta Crystallogr. A* **1995**, *51*, 887; b) CrysAlisPro, version 171.37.35, Agilent Technologies Inc., Oxford, UK, **2015**.

[30] O.V. Dolomanov, L.J. Bourhis, R.J. Gildea, J.A.K. Howard, H. Puschmann, *J. Appl. Cryst.* **2009**, *42*, 339-341.

[31] G. M. Sheldrick, *Acta Cryst. A* **2008**, *A71*, 3-8.

[32] G. M. Sheldrick, *Acta Cryst. C* **2015**, C*71*, 3-8.

5 PHENANTHROLINES AS LIGANDS FOR COBALTATE CATALYSTS

PHILIPP BÜSCHELBERGER AND ROBERT WOLF
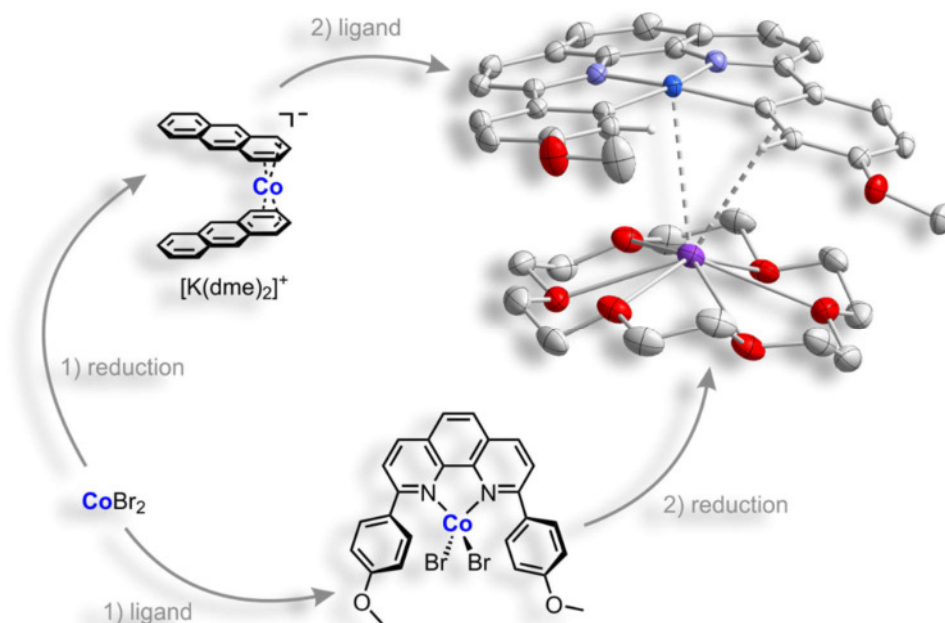
This study reports on the synthesis of new highly reduced cobalt compounds bearing 2,9-diaryl-1,10-phenanthroline ligands in an unprecedented coordination mode. New cobaltate anions are accessible *via* two different routes starting from commercially available $CoBr_2$, and the products were characterized by NMR and crystallographic techniques. Initial catalytic experiments demonstrate the activity towards the hydrogenation of alkenes and the dehydrogenation of dimethylamine-borane.

5.1   Introduction

The development of efficient, atom-economic processes which decrease the overall energy consumption and waste production is key to a sustainable future.[1] In this respect, the activation and conversion of organic molecules driven by visible light photocatalysis is a promising and intensively studied subject.[2] In photochemical processes, large amounts of energy can be delivered from sunlight, by selective absorption of photons, and used to generate reactive intermediates without considerable waste production.[3] The major drawback of this technology is the fact that, due to their high stability and excellent photoredox properties, most photocatalysts are based on (poly)pyridine or phenanthroline complexes of precious metals such as ruthenium and iridium (Figure 5.1).[2b, 4] In account of economic and environmental concerns, as well as biological compatibility, many recent research activities focus on the development of base-metal catalysts that can replace more expensive and less earth-abundant precious metal compounds.[5, 6]

Recently, Reiser and co-workers reported on carbon-carbon bond formation reactions mediated by a visible-light-driven copper catalyst.[7] They showed that [Cu(dap)$_2$]Cl (Figure 5.1, dap = 2,9-bis(*p*-anisyl)-1,10-phenanthroline) is an effective catalyst for atom-transfer radical addition (ATRA) and allylation reactions under irradiation at λ = 530 nm. Initially, [Cu(dap)$_2$]$^+$ was introduced in 1987 by Sauvage, who employed the d^{10} complex in the photo-assisted coupling of *p*-nitrobenzyl bromide.[8] Normally, copper(I) phenanthroline complexes suffer from short excited-state lifetimes compared to related Ru or Ir complexes, due to exciplex quenching by structural reorganization to a square-planar geometry of the excited-state.[9] In contrast, the homoleptic dap complex benefits from the bulky 2,9-substituents of the phenanthroline ligands,
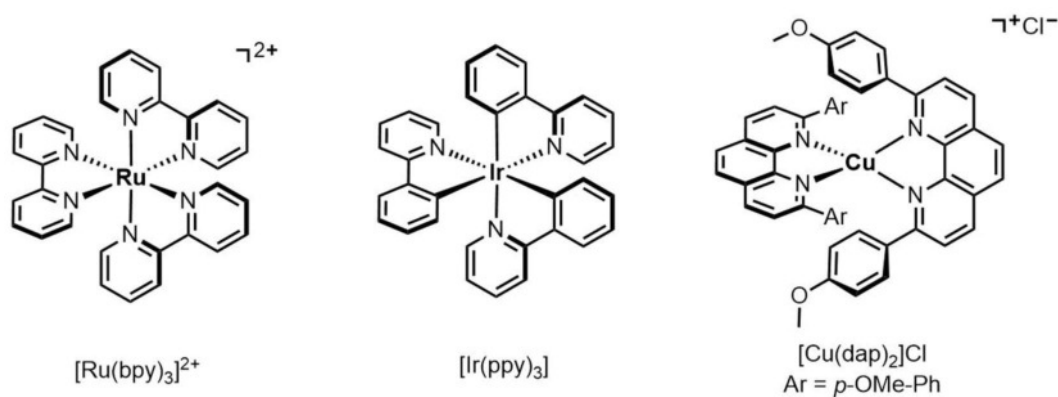

Figure 5.1   Chemical structures of the well-established photoredox catalysts [Ru(bpy)$_2$]$^{2+}$ and [Ir(ppy)$_3$] besides the structure of the base-metal alternative [Cu(dap)$_2$]Cl.

which hamper structural relaxation. Hindered exciplex quenching results in a prolonged excited-state lifetime. Thereby, $[Cu(dap)_2]Cl$ offers a real perspective as an alternative to common precious-metal-based catalysts.[10]

Following the concept of base-metal catalysis, our group has recently developed new iron and cobalt catalysts for hydrofunctionalization reactions. The catalytic properties of the alkene and arene metalates $[K(dme)_2][Co(C_{14}H_{10})_2]$ (**1**), $[K([18]crown-6)][Fe(C_{14}H_{10})_2]$ (**2**), and $[K(thf)_x][Co(cod)_2]$ (**3**) (Figure 5.2, cod = 1,5-cyclooctadiene),[11] were studied in hydrogenation reactions,[12] and a catalytic cycle was proposed after detailed investigations, which is also supported by DFT calculations reported by another group.[13]

Here, we report on our attempt to synthesize new highly reduced cobalt complexes bearing 2,9-diaryl-1,10-phenanthroline ligands. Based on earlier work by Ellis and co-workers, who reported the synthesis and molecular structures of the homo- and heteroleptic 2,2´-bipyridine (= bipy) cobaltates $[Co(bipy)_2]^-$ and $[Co(cod)(bipy)]^-$ (Figure 5.2),[14] we aimed at the isolation and characterization of salts of an analogous anion $[Co(Ar_2\text{-phen})_2]^-$ (Figure 5.2, Ar_2-phen = 2,9-diaryl-1,10-phenanthroline). Such a complex would be isoelectronic to the well-known photocatalyst $[Cu(dap)_2]^+$ and thus might give access to cobaltate-catalyzed photocatalysis and other catalytic reactions.
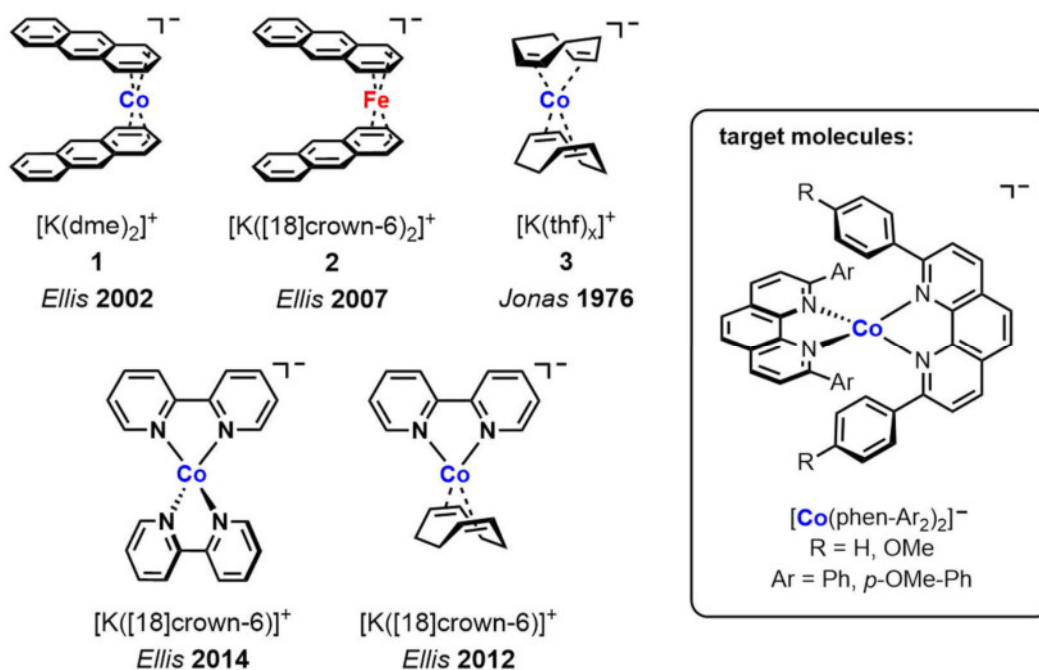

Figure 5.2   Polyarene and alkene cobaltates by Ellis (**1** and **2**) and Jonas (**3**) and the target molecule $[Co(Ar_2\text{-phen})_2]^-$.

5.2   Results and Discussion

5.2.1   Complex Synthesis

Based on Ellis's reports on the reaction of cobaltates with 2,2´-bipyridine, which led to either homo- or heteroleptic products,[14] we decided to use $[K(dme)_2][Co(C_{14}H_{10})_2]$ (**1**) as the starting compound in order to synthesize the targeted bis(phenanthroline) complexes via ligand exchange with anthracene coordinated in **1**. Aiming at an anionic (bis)phenanthroline cobalt d^{10} complex that is isoelectronic to the copper catalyst $[Cu(dap)_2]^+$, we reacted **1** with 2 equiv. of the dap ligand. The anthracene ligands were supposed to be replaced by phenanthroline via a neutral ligand exchange reaction. Surprisingly, the reaction led to a C–H activation at the *ortho*-positions of the aryl substituents of the phenanthroline ligand by formal elimination of dihydrogen. Crystals of the resulting complex [K([18]crown-6][Co(*p*-DAP-2H)] (**4**) (Figure 5.3) were isolated from THF/*n*-hexane and characterized by X-ray crystallography. The molecular structure shows a cobalt atom coordinated by two nitrogen atoms and two *ortho*-carbon atoms of the aryl rings in a slightly distorted, square planar fashion. The Co–N bond lengths (Co1–N1 1.848(2) Å, Co1–N2 1.848(2) Å) and the Co–C bond lengths (Co1–C14 1.965(2)°, Co1–C21 and 1.959(2)°) are in the range of typical coordinative bonds.[15] The aryl substituents are almost coplanar with the phenanthroline moiety. One of the substituents is slightly bent with respect to the plane formed by Co1, N1, N2, and C14 (dihedral angle between this plane and the bent aryl ring = 7.96°). *Ortho*-metalation of this ligand type was described before,[16] but to the best of our knowledge, this is the first example of a 2,9-diaryl phenanthroline acting as a tetradentate ligand. The bite angle between cobalt and the phenanthroline backbone (N1–Co1–N2 82.389(9)°) is more acute than the angle between cobalt and the two coordinated carbon atoms is (C14–Co1–C21 114.1(1)°).
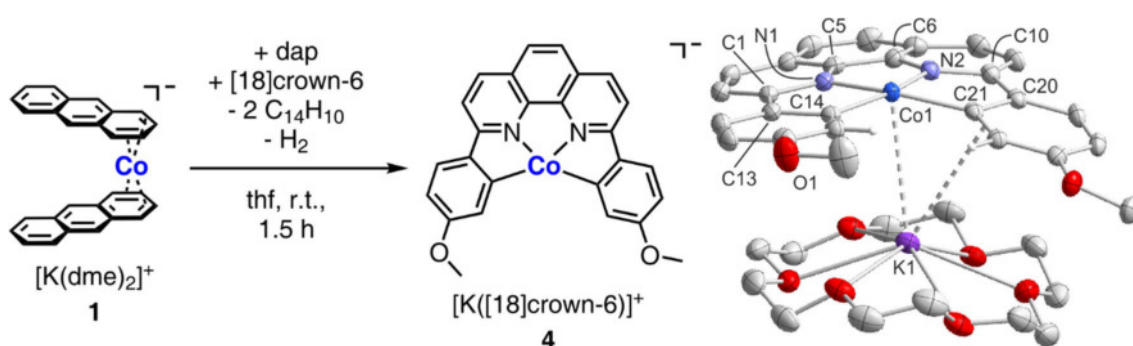

Figure 5.3   Synthesis (left) and molecular structure of **4** (right; ellipsoids are at the 50% probability level; most H atoms are omitted for clarity). Selected bond lengths and angles: Co1–N1 1.848(2) Å, Co1–N2 1.848(2) Å, Co1–C14 1.965(2) Å, Co1–C21 1.959(2) Å, N1–C5 1.360(3) Å, N2–C6 1.369(3) Å, C5–C6 1.395(4) Å; Co1–K1 3.3772(7) Å, N2–Co1–N1 82.38(9)°, N1–Co1–C14 81.5(1)°, N2–Co1–C21 81.43(9)°, C21–Co1–C14 114.1(1)°, N1–C1–C13 108.8(2)°, N2–C10–C20 108.6(2)°, torsion angles of the aryl substituents: N1–C1–C13–C14 4.2(3)° & N2–C10–C20–C21 1.2(3)°.

The anisole substituents are bent towards the metal center with N–C–C$_{Aryl}$ angles N1–C1–C13 108.8(2)° and N2–C10–C20 108.6(2)° that deviate from the expected values close to 120° for a free phenanthroline molecule. In addition, the cation [K[18]crown-6)]$^+$ is in contact with the cobalt atom (K1–Co1 3.3772(7) Å, i.e. 0.3 Å longer than the sum of the covalent radii).[15] The NMR data of **4** are discussed further below.

Unfortunately, the synthesis of **4** was difficult to reproduce. For this reason, an alternative synthesis was pursued, using a simple cobalt halide complex as the starting material. Addition of one equivalent of dap to a solution of CoBr$_2$ in THF leads to immediate precipitation of the adduct [(dap)CoBr$_2$] (**5**) (Figure 5.4, left) in quantitative yield. X-ray quality bright green crystals of **5** formed upon slow evaporation of a concentrated solution in dichloromethane (= DCM). The cobalt atom is coordinated in a distorted tetrahedral fashion (Figure 5.4, right) with a phenanthroline bite angle (N1–Co1–N2 82.96(8)°) in the expected range and a Br1–Co1–Br2 angle of 127.4(1)° that is somewhat larger than in related compounds (110° - 120°).[16] The N1–C1–C13 (118.8(2)°) and N2–C10–C20 (116.5(2)°) angles, are almost identical with the corresponding angles of the free ligand and of other Co(II) phenanthroline adducts.[16, 18] The Co–N (Co1–N1 2.053(2) Å, Co1–N2 2.053(2) Å) and Co–Br (Co1–Br1 2.3826(4) Å, Co1–Br2 2.3803(4) Å) bond lengths are in good agreement with the literature. Analogous to the structure of the free ligand, the aryl substituents are not coplanar with the phenanthroline moiety, displaying torsion angles of 43.6° (N1–C1–C13–C14) and 43.7° (N2–C10–C20–C25). The ^{1}H NMR spectrum of compound **5** in CD$_2$Cl$_2$ shows a set of six broad signals. Four singlets and one multiplet (δ = 0.81-0.89) are detected in the range δ = 0.07 and 1.53 ppm. One singlet resonates high field shifted at δ = -5.79. The unusual chemical shifts are due to the paramagnetic nature of this compound.[19]
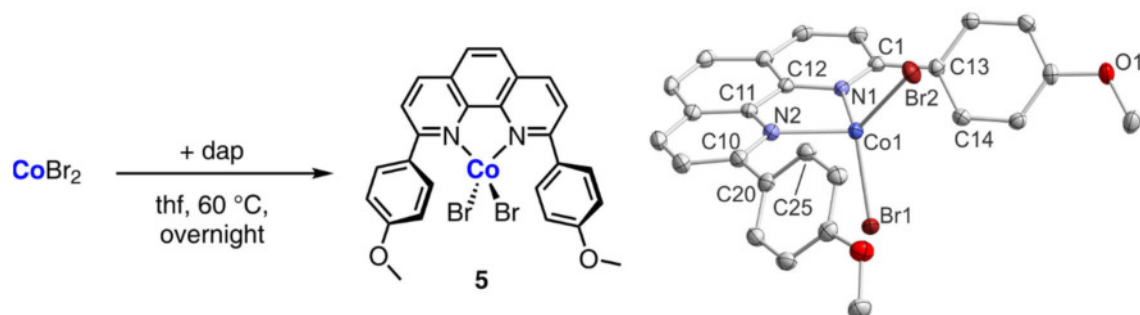

Figure 5.4   Synthesis and molecular structure of **5**. Ellipsoids are drawn at the 50% probability level; H atoms and one co-crystalline solvent molecule (DCM) are omitted for clarity. Selected bond lengths and angles: Co1–N1 2.053(2) Å, Co1–N2 2.053(2) Å, Co1–Br1 2.3826(4) Å, Co1–Br2 2.3803(4) Å, N1–C12 1.365(3) Å, N2–C11 1.367(3) Å, C11–C12 1.443(3) Å; N1–Co1–N2 82.9(1)°, Br1–Co1–Br2 127.4(1)°, N1–C1–C13 118.8(2)°, N2–C10–C20 116.5(2)°, torsion angles of the aryl substituents: N1–C1–C13–C14 43.6° & N2–C10–C20–C25 43.7°.
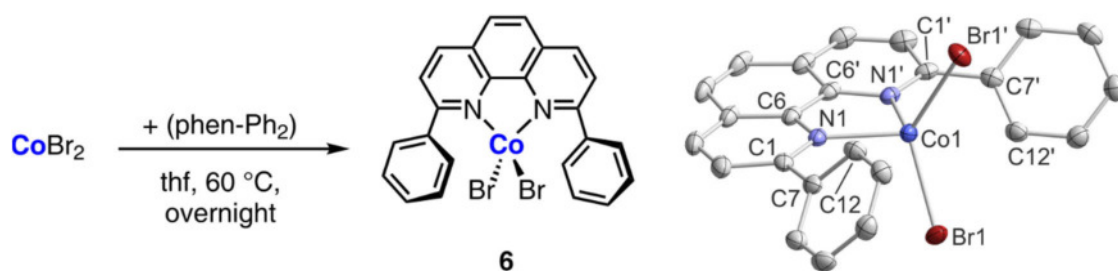
Figure 5.5   Synthesis and molecular structure of **6**. Ellipsoids are drawn at the 50% probability level; H atoms are omitted for clarity. Selected bond lengths and angles: Co1–N1 2.054(3) Å, Co1–Br1 2.3697(5) Å, N1–C6 1.370(5) Å, C6–C6' 1.442(7) Å; N1–Co1–N1' 82.9(2)°, Br1–Co1–Br1' 125.88(4)°, N1–C1–C7 118.4(3)°, torsion angle of the aryl substituents: N1–C1–C7–C12 48.704(2)°.

A similar reaction of $CoBr_2$ with dpp (= 2,9-diphenyl-1,10-phenanthroline) analogously provides [(dpp)CoBr$_2$] (**6**) (Figure 5.5), which could also be isolated by decantation of the supernatant solution in excellent yield (93%). Compound **6** shows a very similar molecular structure as **5** concerning angles and bond lengths. The ^{1}H NMR data of paramagnetic compound **6** are similar to those of **5** with signals in the range δ = -6.08 to 1.55 ppm.[19]

Reduction of **5** with 3 equiv. of $KC_{14}H_{10}$ again resulted in the formation of cobaltate **4** in 48% yield.[19] Unfortunately, it was so far not possible to remove free dap ligand and anthracene by-product completely from the isolated compound. Nevertheless, the ^{1}H NMR spectrum recorded in [D$_8$]THF confirmed the composition of **4**. A set of broad signals for the dap ligand and a singlet assigned to the [18]crown-6 molecule (δ = 3.05 ppm) are observed. The methoxy hydrogen atoms resonate at δ = 3.82 ppm. Two singlets (δ = 5.60 and 7.33 ppm) and three doublets (δ = 7.21, 9.01, and 9.50 ppm) of the phenyl ring and the phenanthroline moiety are found in the expected range. The protons in *para*-position to the nitrogen atoms resonate as a doublet with an unusual low-field shift at δ = 12.13 ppm. In addition, the ^{1}H NMR spectrum confirmed the presence of some residual free dap ligand, anthracene, and *n*-hexane. In the ^{13}C{^{1}H} NMR spectrum, the aliphatic carbon atoms of the methoxy group and the crown ether resonate at typical values of δ = 54.5 and 70.4 ppm, respectively. The aromatic signals are found between δ = 109.0 and 166.8 ppm. Notably, the metalated carbon atom (δ = 153.0 ppm) was only detected through its correlation to the *meta*-H in HMBC but is not visible in the ^{13}C{^{1}H} NMR spectrum.[19]

Reduction of [(dpp)CoBr$_2$] (**6**) with three equivalents of $KC_{14}H_{10}$ and addition of [18]crown-6 gave the desired compound [K([18]crown-6][Co(dpp-2H)] (**7**) (Figure 5.6, left), which has a very similar molecular structure as the dap complex **4**. It also features a distorted square planar cobalt atom and a weak electrostatic interaction between the anion and [K([18]crown-6]$^+$ (Figure 5.6, right). The aryl substituents are coplanar with the phenanthroline backbone in this case (torsion
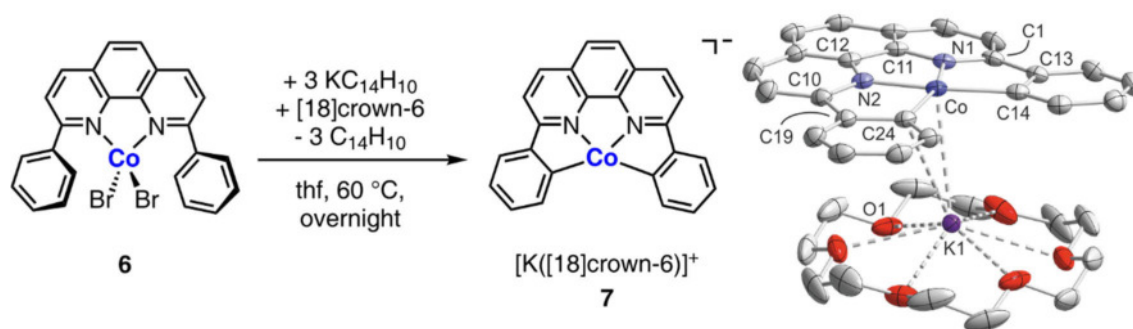
Figure 5.6   Molecular structure of **7**. Ellipsoids are at the 50% probability level; H atoms are omitted for clarity. Selected bond lengths and angles: Co1–N1 1.843(2) Å, Co1–N2 1.843(2) Å, Co1–C14 1.977(2) Å, Co1–C24 1.974(2) Å, N1–C11 1.367(3) Å, N2–C12 1.370(3) Å, C11–C12 1.394(3) Å; Co1–K1 3.3030(6) Å, N1–Co1–N2 82.79(8)°, N1–Co1–C14 80.87(9)°, N2–Co1–C24 80.60(9)°, C14–Co1–C24 115.5(1)°, N1–C1–C13 108.7(2)°, N2–C10–C19 108.7(2)°, torsion angles of the aryl substituents: N1–C1–C13–C14 3.431(2)° & N2–C10–C19–C24 2.745(2)°.
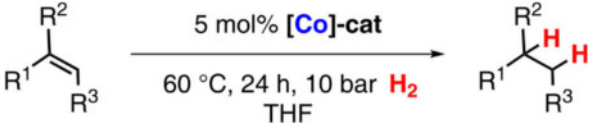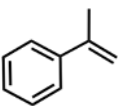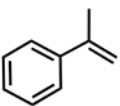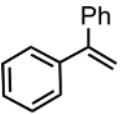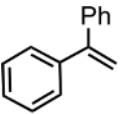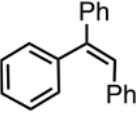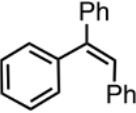
angles N1–C1–C13–C14 3.431(2)° and N2–C10–C19–C25 2.745(2)°). The ^{1}H NMR spectrum of **7** in [D$_8$]THF displays a set of six sharp signals for the dpp ligand located between δ = 5.99 and 9.70; analogous to **4,** there is also one unusually low-field shifted signal at δ = 12.46 ppm, which is assigned to the protons in *para*-position to the nitrogen atoms. The chemical shifts of the ^{13}C{^{1}H} NMR spectrum are very similar to the ones of **7**. The CH$_2$ groups of the crown ether resonate at δ = 69.9 ppm, while the aromatic protons of the anion are found in the range δ = 107.9 to 166.7 ppm.[19]

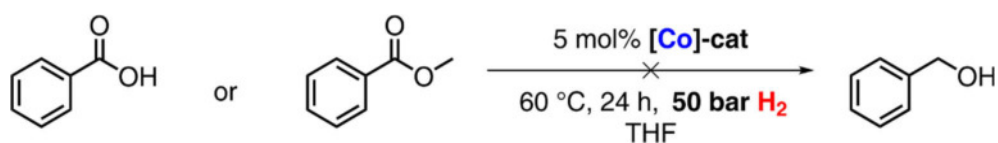## 5.2.2   Catalytic Reactivity

In preliminary catalytic studies, the new metalates **4** and **7** were employed to determine their behavior as potential catalysts of different reactions. Both compounds were found to be active in the hydrogenation of alkenes at elevated temperature and dihydrogen pressure (60 °C, 10 bar H$_2$). The disubstituted substrates α-methylstyrene and 1,1-diphenylethylene were converted in excellent yields to the corresponding alkanes (Table 5.1, entries 1-4). Reactions with the more demanding substrate triphenylethylene only gave a moderate product yield (Table 5.1, entries 5 & 6). Nevertheless, these results demonstrate the applicability of **4** and **7** for catalytic hydrogenation reactions.

An extension of the substrate scope of the hydrogenation reactions to more exotic substance classes such as carboxylic acids and esters was unsuccessful.[20] Efficient cobalt catalysts for this transformation were recently reported by the groups of de Bruin, Milstein, and Jones. Unfortunately, no evidence for the transformation of benzoic acid or its methyl ester at 50 bar H$_2$ and 60 °C, over 24 hours was found (Scheme 5.1). Notably, in the case of **4**, GC-MS analysis indicates the hydrogenation of the anthracene impurities, which are present in the catalyst precursor.[19]

Table 5.1 Hydrogenation of alkenes with **4** and **7** as pre-catalysts (5 mol%) at 10 bar H$_2$ and 60 °C for 24 hours. Standard conditions: substrate (0.25 mmol) in THF (1 mL); yields and conversions were determined by quantitative GC-FID versus internal reference *n*-pentadecane and are given in percent.

Entry	Cat.	Substrate	Conv.	Yield
1	**4**		>99	85
2	**7**		98	91
3	**4**		98	91
4	**7**		97	88
5	**4**		29	29
6	**7**		27	27

Scheme 5.1 No evidence was found for the transformation of benzoic acid or its methyl ester under 50 bar H$_2$ and 60 °C in THF, over 24 hours, with compounds **4** or **7** as potential pre-catalysts.

In an NMR scale reaction, the dehydrogenation of dimethylamine-borane, catalyzed by 5 mol% of **7**, proceeded quite selectively to the desired 1,3-diaza-2,4-diboretane (79% according to ^{11}B NMR integration, Scheme 5.2 top). In addition, the formation of two minor side-products, i.e. 13% bis(dimethylamino)borane and 8% of an unidentified BH$_3$ species, was observed. An identical behavior was already reported for related α-diimine cobaltates by our group, recently.[21] ^{11}B NMR spectroscopic reaction monitoring (Figure 5.7) suggests that the reaction pathway (Scheme 5.2 bottom) involves the two intermediates Me$_2$NH–BH$_2$–NMe$_2$–BH$_2$ (**8**) and
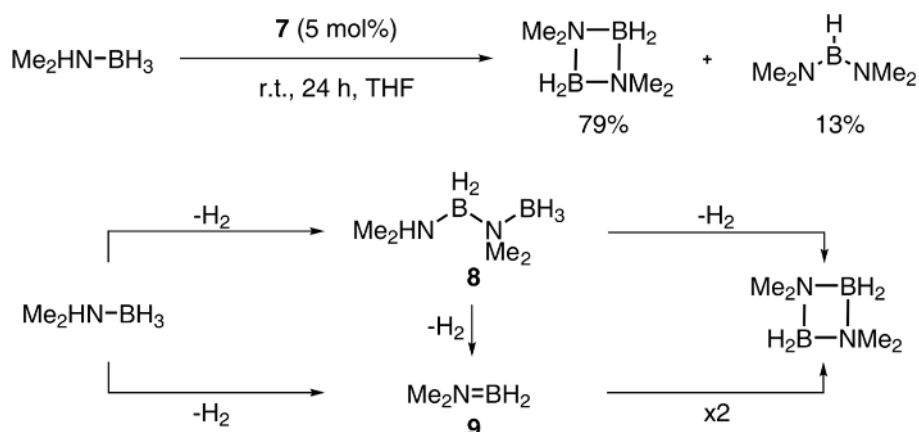
Scheme 5.2   Dehydrogenation of dimethylamine-borane catalyzed by **7** at room temperature (top); possible reaction pathway based on observed reaction intermediates (bottom).
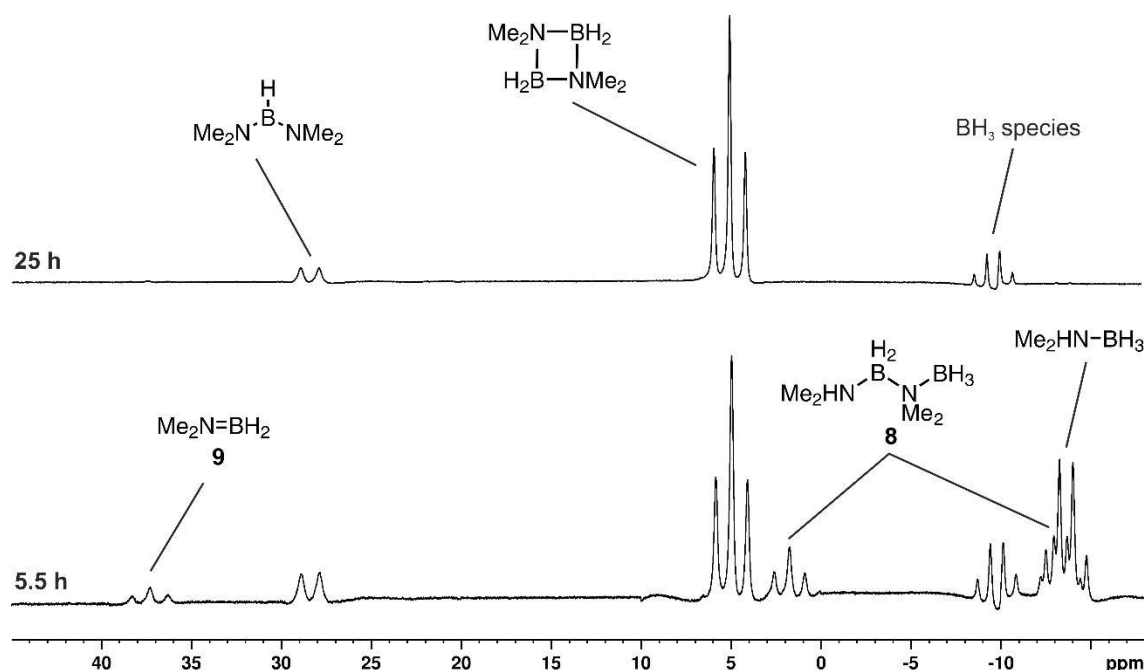

Figure 5.7 ^{11}B NMR spectroscopy monitoring (128.4 MHz, 300 K, C_6D_6-capillary) of the dehydrogenation of dimethylamine-borane, catalyzed by **7**, displays the product formation and the reaction intermediates **8** and **9**.

$Me_2N=BH_2$ (**9**). On the way to the dimeric product, the elimination of two hydrogen molecules from the starting material can include two steps, leading to formation of **8** as an intermediate. The second route, through **9**, operates by a complete loss of hydrogen in the first step, followed by cycloaddition. This mechanism, as well as the formation of bis(dimethylamino)borane as a side product were already described and well-studied for other catalysts.[21, 22] The activity of the presented catalysts towards hydrogenation as well as dehydrogenation reactions also potentially opens the possibility to carry out cobalt-catalyzed transfer hydrogenation reactions, however, these have not been investigated so far.

Due to the challenging synthesis and the unexpected composition and structure of the new complexes **4** and **7**, photochemical investigations were not conducted with these compounds, and, indeed, a utilization in photoredox chemistry does not seem promising.

5.3 Conclusion

New highly reduced cobaltates **4** and **7** bearing *ortho*-metalated diaryl-phenanthroline ligands are accessible by reduction of cobalt(II) bromide precursors or, less effectively, by the reaction of bis(anthracene) cobaltate **1** with 2 equiv. of the phenanthroline ligand. The resulting complexes **4** and **7** are active in the hydrogenation of substituted alkenes under elevated temperature and hydrogen pressure. Moreover, **7** was successfully applied to the (selective) dehydrogenation of dimethylamine-borane at room temperature, possibly qualifying this class of complexes for transfer hydrogenation reactions with amine-boranes and perhaps also other H_2 sources. Further investigation of the catalytic properties of **4** and **7** could be focused in these directions and in particular at establishing structure-activity relationships for such complexes.

5.4   Experimental Section

5.4.1   General Considerations

All experiments were performed under an atmosphere of dry argon by using standard Schlenk and glovebox techniques. Solvents were purified, dried, and degassed by standard techniques. Commercially available [18]crown-6 was purified by sublimation at 60 °C under 10^{-3} mbar and stored under argon atmosphere.

5.4.2   Analytical Measurements

5.4.2.1   NMR Spectroscopy

Nuclear magnetic resonance (NMR) spectra were recorded (300 K) on Bruker Avance 300 (300.13 MHz ^{1}H, 75.47 MHz ^{13}C) and Avance 400 (400.13 MHz ^{1}H, 100.61 MHz ^{13}C, 128.43 MHz ^{11}B) spectrometers internally referenced to residual solvent resonances. NMR assignments are based on COSY, HSQC, HMBC, and NOESY 2D NMR experiments. Chemical shifts δ are given in ppm relative to tetramethylsilane (^{1}H and ^{13}C NMR) or $BF_3 \cdot OEt_2$ (^{11}B NMR). The following abbreviations are used to indicate multiplicities (br = broad): s = singlet; d = doublet; t = triplet, m = multiplet.

5.4.2.2   Elemental Analyses

Elemental analyses were performed by the analytical department of the University of Regensburg with a Micro Vario Cube (*Elementar*).

5.4.2.3   Gas Chromatography with FID (GC-FID)

HP6890 GC-System with injector 7683B and *Agilent* 7820A System. Column: HP-5 19091J-413 (30 m × 0.32 mm × 0.25 μm), carrier gas: N_2. GC-FID was used for quantitative measurements for substrate screening (calibration with internal standard *n*-pentadecane and analytically pure samples).

5.4.2.4   Gas Chromatography with Mass-Selective Detector (GC-MS)

Agilent 6890N Network GC System, mass detector 5975 MS. Carrier gas: H_2 (1.0 mL/min). Column: HP-5MS (30 m x 0.25 mm x 0.25 μm, 5% phenylmethylsiloxane). *Agilent* 7820A GC system, mass detector 5977B MSD. Carrier gas: H_2 (1.2 mL/min). Column: HP-5MS (30 m x 0.25 mm x 0.25 μm).

5.4.2.5   X-Ray Crystallography

Single crystal X-ray diffraction data for compounds **5**, **6**, and **7** were recorded on an Agilent Technologies SuperNova diffractometer, and in case of compound **4**, on an Agilent Technologies

Gemini Ultra diffractometer. Cu$_{K\alpha}$ radiation (λ = 1.54178 Å) was used. Empirical multi-scan and analytical absorption corrections were applied to the data.[23, 24] Using Olex2,[25] the structures were solved with ShelXT,[26] and least square refinements were carried out with ShelXL.[27]

5.4.3 Procedures for Catalytic Reactions

5.4.3.1 General Procedure for Hydrogenation Reactions

A dry 5 mL vial with a screw cap and PTFE septum was charged with a magnetic stir bar and a solution of the cobaltate (0.0125 mmol) in THF (0.5 mL). After adding a solution of the substrate (0.25 mmol) in THF (0.5 mL) with a pipette, the vial was closed, and the septum was punctured with a short needle (Braun). The vial was placed into a high-pressure reactor (Parr Instr.), which was sealed, removed from the glove box, placed on a magnetic stirrer plate, and purged with hydrogen. After 24 h at 60 °C under an atmosphere of hydrogen (10 bar) the pressure was released, the vial removed, and the reaction quenched with saturated aqueous NaHCO$_3$ (1 mL). For quantitative GC-FID analysis, *n*-pentadecane was added as an internal standard. The mixture was extracted with diethyl ether (3x) and the combined organic layers were dried over Na$_2$SO$_4$.

5.4.3.2 Procedure for the Dehydrogenation of Dimethylamine-Borane

A dry 5 mL vial with a screw cap and PTFE septum was charged with a magnetic stir bar and the solid cobaltate **7** (0.005 mmol). After adding a solution of dimethylamine-borane (0.1 mmol) in THF (0.6 mL) with a pipette, the vial was closed, and the septum was punctured with a short needle (Braun). The solution was stirred inside the glovebox for 5 hours, before the reaction mixture was transferred into a J. Young NMR tube and the [11]B spectra were collected. After the measurement, the reaction mixture was introduced back into the glovebox and the solution was transferred back into the vial for further stirring. After 24 hours, another ^{11}B NMR spectrum was recorded to confirm full conversion of the starting material.

5.4.4 Complex Synthesis

5.4.4.1 [(dap)CoBr2] (**5**)

THF (10 mL) was added to a Schlenk flask containing CoBr$_2$ (167 mg, 0.764 mmol, 1 equiv.) and 2,9-bis(4 methoxyphenyl)-1,10-phenantroline (300 mg, 0.764 mmol, 1 equiv.) and the mixture was stirred at 60 °C overnight. A bright green suspension was formed. Afterwards, the solvent was carefully decanted by cannula, the solid residue was washed with THF (3 x 5 mL) and diethyl ether (2 x 5 mL) and dried *in vacuo*. Compound **5** was isolated as a green, waxy solid (426 mg, 91%). X-ray quality green crystals were obtained by slow evaporation from a concentrated solution in DCM. Complex **5** dissolves well in dichloromethane, but it is insoluble in diethyl ether, THF, acetonitrile, and toluene.

^{1}H NMR (300.13 MHz, CD$_2$Cl$_2$, 300 K): δ = −5.79 (br s), 0.07 (s), 0.59 (s), 0.81 0.90 (m), 1.25 (br s), 1.53 (s).

Elemental analysis for C$_{26}$H$_{20}$N$_2$O$_2$CoBr$_2$ (M = 611.20) (%):   calcd.: C 51.90, H 3.30, N 4.58;

found: C 52.91, H 4.13, N 3.98.

5.4.4.2   [(dpp)CoBr$_2$] (6)

THF (10 mL) was added to a Schlenk flask containing CoBr$_2$ (132 mg, 0.602 mmol, 1 equiv.) and 2,9-diphenyl-1,10-phenantroline (200 mg, 0.602 mmol, 1 equiv.) and the mixture was stirred at 60 °C overnight, giving a bright, turquoise suspension. Afterwards, the solvent was carefully decanted by cannula, and the solid residue was washed with THF (2 x 2.5 mL) and diethyl ether (5 mL) before drying *in vacuo*. The product **6** was isolated as a turquoise, waxy solid (310 mg, 93%). Bright turquoise colored, X-ray quality crystals were obtained by slow evaporation from a concentrated solution in DCM.

^{1}H NMR (300.13 MHz, CD$_2$Cl$_2$, 300 K): δ = −6.08 (br s), 0.06 (s), 0.29 (br s), 0.81-0.89 (m), 1.23-1.34 (m), 1.55 (s).

Elemental analysis for C$_{24}$H$_{16}$N$_2$CoBr$_2$ (M = 551.15) (%): calcd.: C 52.30, H 2.93, N 5.08;

found: C 54.35, H 3.92, N 4.38.

5.4.4.3   [K([18]crown-6)][Co(dap-2H)] (4)

Route 1 – from [K(dme)$_2$][Co(C$_{14}$H$_{10}$)$_2$]: A solution of dap (34.0 mg, 0.0866 mmol, 2.00 equiv.) in THF (2 mL) was added to a solution of [K(dme)$_2$][Co(C$_{14}$H$_{10}$)$_2$] (**1**) (27.5 mg, 0.0433 mmol, 1.00 equiv.) and [18]crown-6 (11.5 mg, 0.0433 mmol, 1.00 equiv.) in THF (3 mL) at room temperature giving a dark green solution. After stirring for 1.5 h, the solvent was removed *in vacuo,* and the dark solid residue was washed with diethyl ether (5 mL). The extract had a light green color. The solid was dissolved in THF (5 mL), and the resulting mixture was filtered. Dark green, X-ray quality crystals of **4** formed after diffusion of *n*-hexane into the solution.

^{1}H NMR (300.13 MHz, [D$_8$]THF, 300 K): δ = 2.68 (s, 24H, [18]crown-6], 3.65 (s, 6H, OC*H*$_3$), 7.13 (s, 2H), 7.29-7.37 (m, 2H), 9.15-9.29 (m, 2H), 9.65-9.79 (m, 2H), 12.27-12.40 (m, 2H). One expected signal with the intensity of 2H is not observed presumably due to overlap with a signal of [D$_8$]THF at δ = 1.73 ppm.

Route 2 – from [(dap)CoBr$_2$]: Potassium anthracene was prepared by stirring potassium (58.6 mg, 1.50 mmol, 3.00 equiv.) and anthracene (267.4 mg, 1.50 mmol, 3.00 equiv.) in THF (12 mL) for 12 h. A suspension of [(dap)CoBr$_2$] (**5**) (305.6 mg, 0.500 mmol, 1.00 equiv.) in THF (12 mL) was added to the solution of potassium anthracene at −80 °C. The resulting dark red-brown solution was slowly warmed to room temperature and stirred overnight giving an intense

dark green solution. After filtration, the solvent was removed *in vacuo*, and the dark green solid residue was washed with toluene (3 x 5 mL) first and subsequently with diethyl ether (3 x 5 mL). The toluene solution was light reddish first and colorless after the third addition of toluene, while the diethyl ether solutions were slightly red first and almost colorless at the end. The solid residue was dried under vacuum and subsequently dissolved in THF (8 mL). The resulting suspension was filtered, the frit was rinsed with 7 + 3 mL of THF, [18]crown-6 (132.1 mg, 0.500 mmol, 1.00 equiv.) was added, and the mixture was sonicated (10 min) to completely dissolve the residue. The reaction mixture was concentrated until solid began to form (to 5 mL) and layered with toluene (15 mL, 1:3). The next morning, **5** (180 mg, 0.239 mmol, 48%) had precipitated as a dark green solid on the bottom of the flask. The product was isolated by carefully decantation of the supernatant, washed with *n*-hexane (5 mL), and dried *in vacuo*. According to the ^{1}H NMR spectrum, the sample is contaminated with residual *n*-hexane, anthracene, and free dap ligand.

^{1}H NMR (400.13 MHz, [D$_8$]THF, 300 K): δ = 3.05 (s, 24H, [18]crown-6), 3.82 (s, 6H, H^{13}), 5.60 (s, 2H, H^2), 7.21 (d, ^3J = 7.8 Hz, 2H, H^4), 7.33 (s, 2H, H^{11}), 9.01 (d, ^3J = 7.54 Hz, 2H, H^8), 9.50 (d, ^3J = 8.0 Hz, 2H, H^5), 12.13 (d, ^3J = 7.35 Hz, 2H, H^9).

^{13}C{^{1}H} NMR (100.61 MHz, [D$_8$]THF, 300 K): δ = 54.5 (C^{13}), 70.4 ([18]crown-6), 109.0 (C^9), 113.6 (C^4), 122.1 (C^5), 123.0 (C^{11}), 124.2 (C^2 or C^8), 124.3 (C^8 or C^2), 133.4 (C^{10}), 145.1 (C^{12}), 153.0 (C^1, only detected through coupling to H^5 in HMBC), 157.4 (C^3), 160.0 (C^6), 166.8 (C^7).
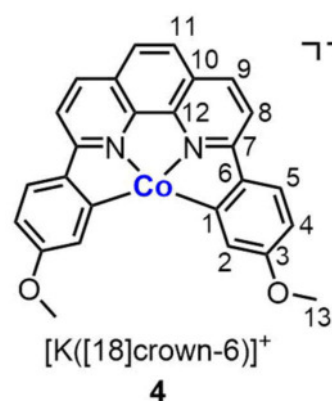
### 5.4.4.4 [K([18]crown-6)][Co(dpp-2H)] (7)

A suspension of [(dpp)CoBr$_2$] (**6**) (531.2 mg, 0.200 mmol, 1 equiv.) in THF (4 mL) was added to a solution of potassium (23.5 mg, 0.600 mmol, 3 equiv.) and anthracene (107.0 mg, 0.600 mmol, 3 equiv.) in THF (4 mL) at −80 °C. The resulting dark red-brown solution was slowly warmed to room temperature and stirred overnight giving an intense dark green solution. After filtration the solvent was removed *in vacuo* and the dark green solid residue was washed with toluene (3 x 5 mL), and then with diethyl ether (3 x 5 mL). The toluene solutions were light reddish, while the diethyl ether solutions had a light green color. The solid residue was dissolved in THF (5 mL), filtered, and [18]crown-6 (52.8 mg, 0.200 mmol, 1 equiv.) in THF (1 mL) was added. Layering with toluene (6 mL, 1:1) did give crystalline product. After layering of the resulting THF/toluene mixture with *n*-hexane (6 mL, 1:1:1) a few dark crystals formed. The crystallization of the crude product was completed by layering of the mixture with of another 6 mL of *n*-hexane. After a few

days, dark green X-ray quality crystals of **7** (47.0 mg, 34%) could be isolated. After decanting the supernatant solution, the product was washed with *n*-hexane (5 mL) and dried *in vacuo*. The product is still contaminated with minor impurities of an *n*-hexane and unidentified species showing ^{1}H NMR resonances at δ =7.59, 8.12, 8.53, 8.63, 8.82, and 10.85 ppm.

^{1}H NMR (400.13 MHz, [D$_8$]THF, 300 K): δ = 2.69 (s, 24H, [18]crown-6), 5.99 (d, ^3J = 6.8 Hz, 2H, *H^2*), 7.46 (s, 2H, *H^{11}*), 7.67 (t, ^3J = 7.2 Hz, *H^4*), 8.18 (t, ^3J = 7.0 Hz, *H^3*), 9.07 (d, ^3J = 7.8 Hz, 2H, *H^8*), 9.70 (d, ^3J = 7.5 Hz, 2H, *H^5*), 12.46 (d, ^3J = 7.7 Hz, 2H, *H^9*).

^{13}C{^{1}H} NMR (100.61 MHz, [D$_8$]THF, 300 K): δ = 69.9 ([18]crown-6), 107.9 (*C^9*), 121.6 (*C^5*), 123.3 (*C^{11}*), 124.8 (*C^3*), 126.3 (*C^8*), 127.9 (*C^4*), 134.3 (*C^{10}*), 141.6 (*C^2*), 145.6 (*C^{12}*), 148.3 (*C^1*, detected through coupling to H^2, H^3, and H^5 in HMBC), 166.5 (*C^7*), 166.7 (*C^6*).
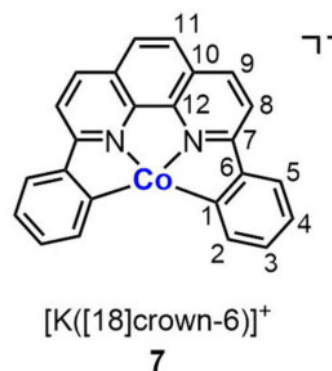
5.5 Acknowledgement

5.6 Supporting Information

5.6.1 NMR Spectra
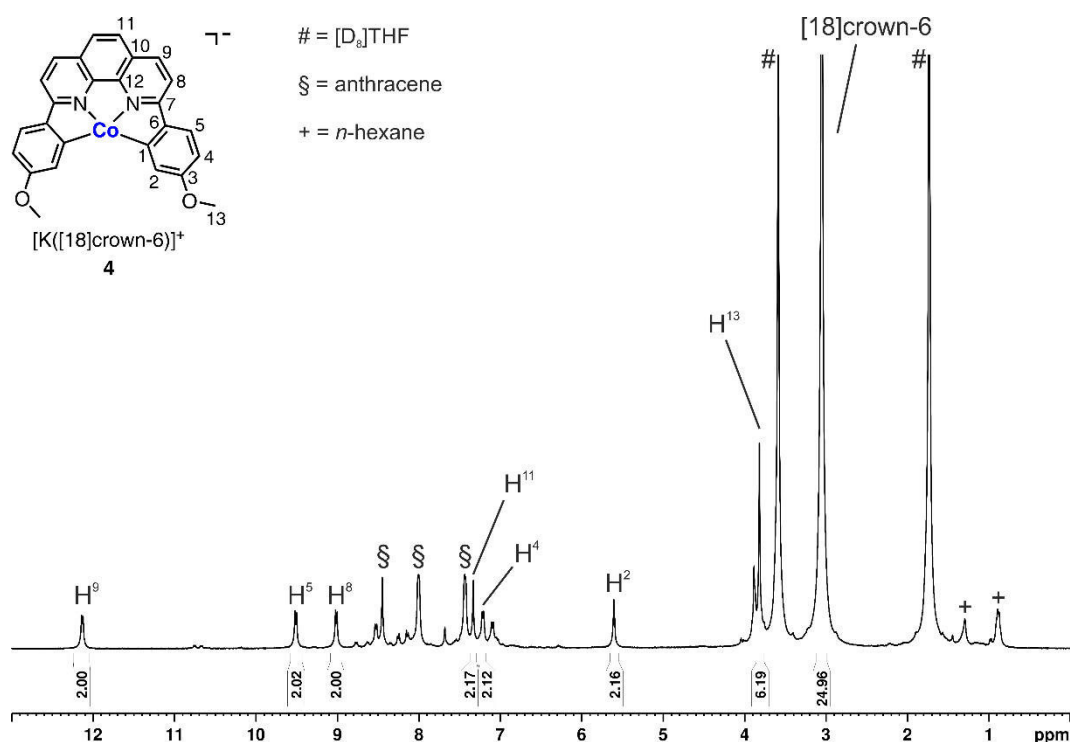

Figure S 1   ¹H NMR spectrum (400.13 MHz, [D$_8$]THF (#), 300 K) of [K([18]crown-6][Co(dap−2H)] (**4**) with residual impurities of dap, anthracene (§), and *n*-hexane (+).
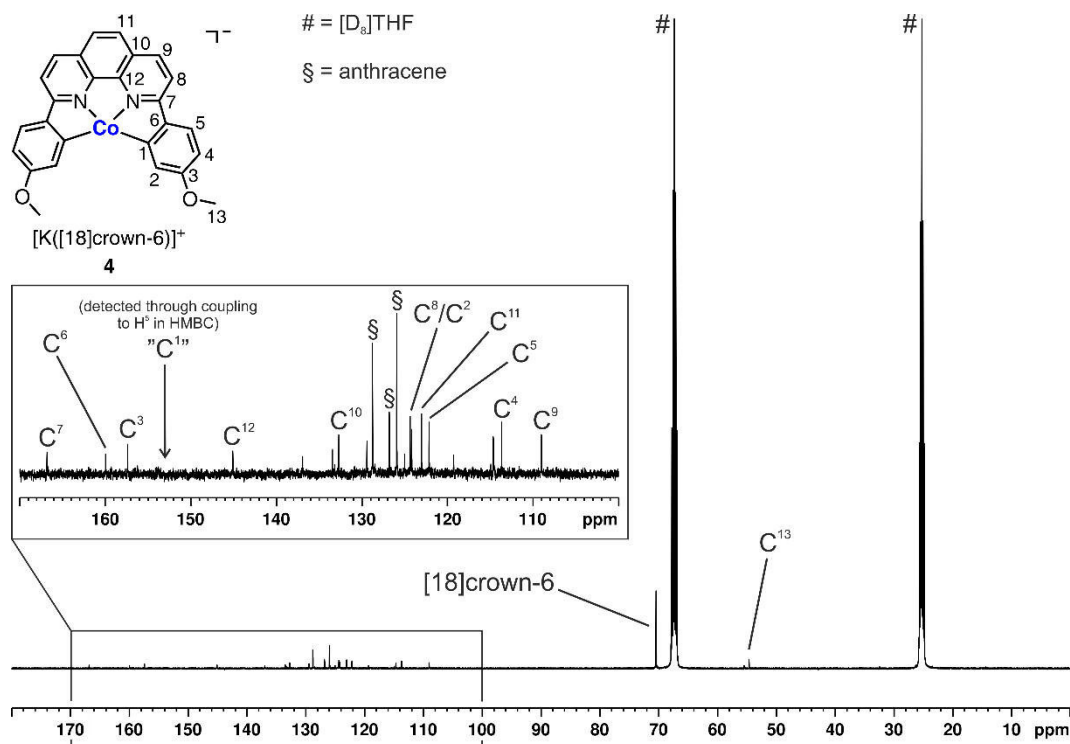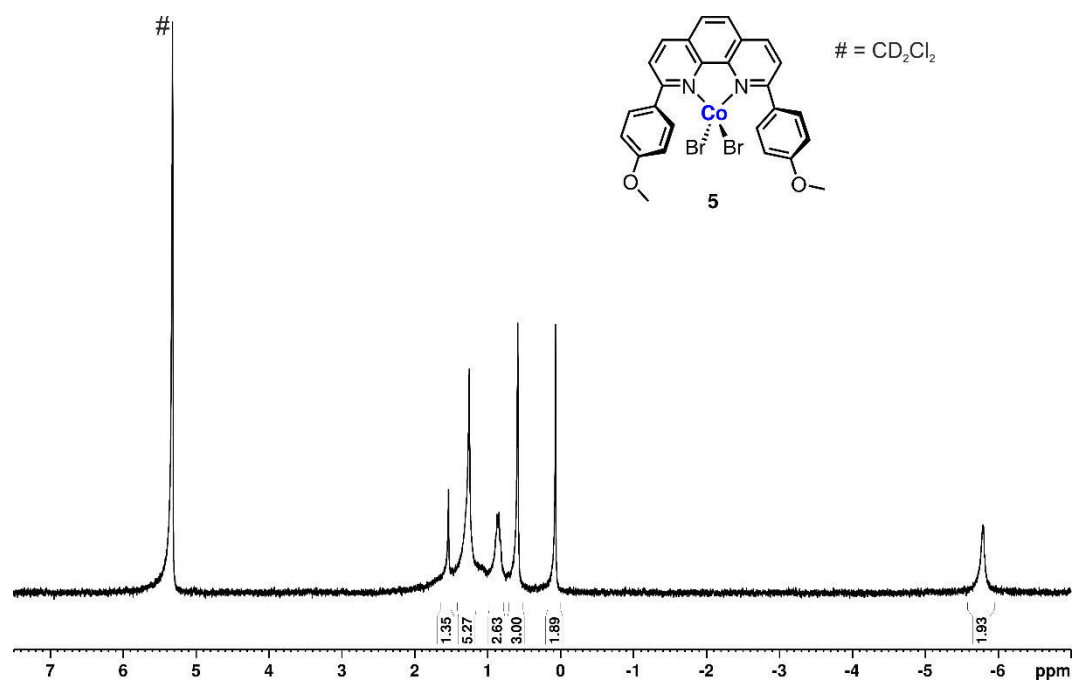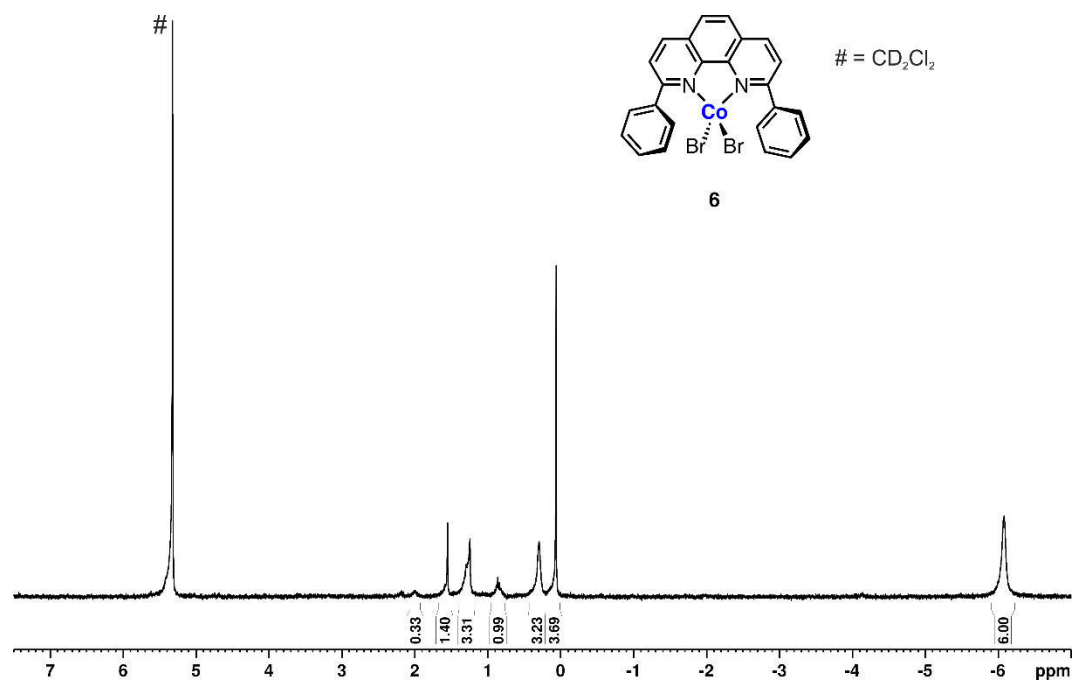

Figure S 2   ¹³C{¹H} NMR spectrum (100.61 MHz, [D$_8$]THF (#), 300 K) of [K([18]crown-6][Co(dap−2H)] (**4**) with residual impurities of dap and anthracene (§).

Figure S 3   ¹H NMR spectrum (300.13 MHz, CD₂Cl₂ (#), 300 K) of the paramagnetic compound [(dap)CoBr₂] (**5**).

Figure S 4   ¹H NMR spectrum (300,13 MHz, CD₂CL₂ (#), 300 K) of the paramagnetic compound [(dpp)CoBr₂] (**6**).

Figure S 5 ¹H NMR spectrum (400.13 MHz, [D₈]THF (#), 300 K) of [K([18]crown-6][Co(dpp−2H)] (**7**) with small impurities of an unidentified species (§) and *n*-hexane (+).
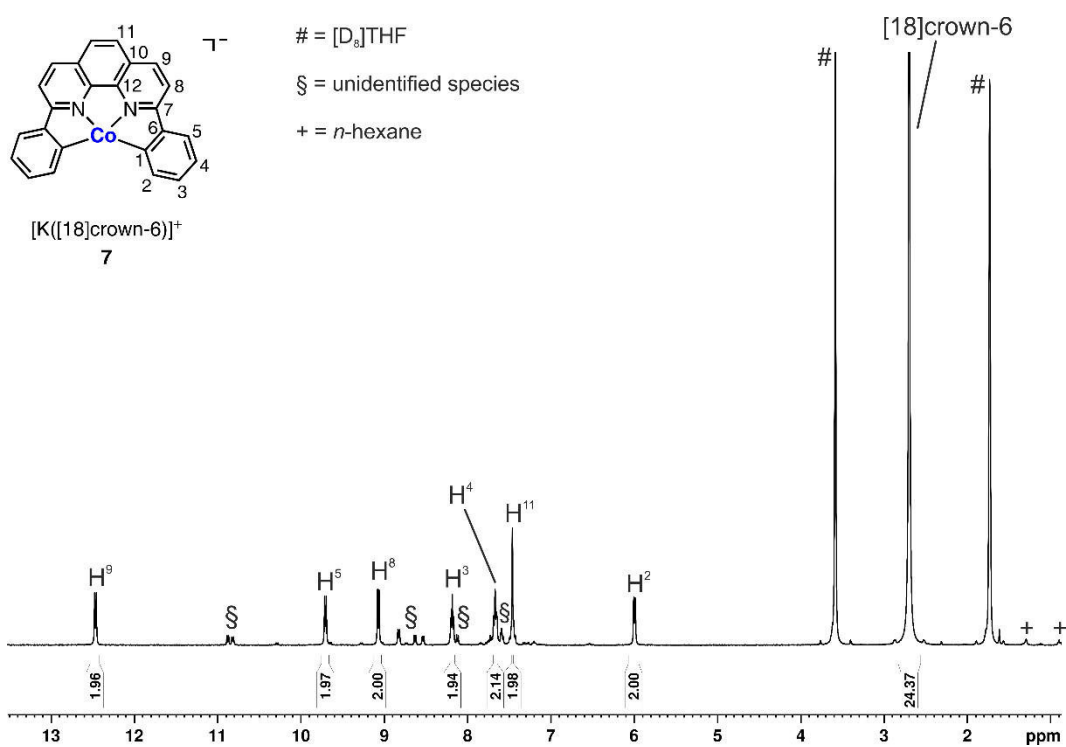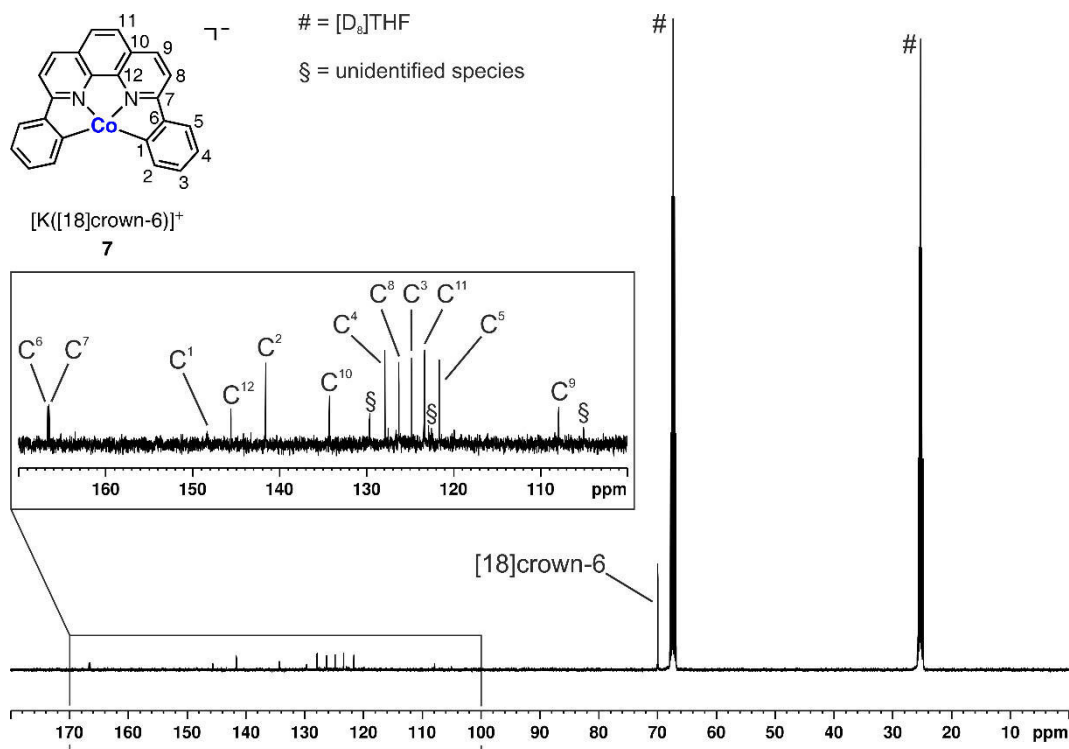

Figure S 6 ¹³C{¹H} NMR spectrum (100.61 MHz, [D₈]THF (#), 300 K) of [K([18]crown-6][Co(dpp−2H)] (**7**) with small impurities of an unidentified species (§).

5.6.2   X-Ray Crystallography

Table S 5-1   Crystal data and structure refinement for compounds **4** and **7**.

Compound	**4**	**7**
Empirical formula	$C_{38}H_{42}N_2O_8KCo$	$C_{36}H_{38}N_2O_6KCo$
Formula weight	752.76	692.72
Temperature [K]	123.0(1)	123.0(1)
Crystal system	orthorhombic	Monoclinic
Space group	$P\mathrm{ca}2_1$	$P2_1/c$
a [Å]	21.2298(2)	9.2871(2)
b [Å]	10.5081(2)	20.2006(5)
c [Å]	15.8631(2)	17.3649(4)
α [°]	90	90
β [°]	90	93.014(2)
γ [°]	90	90
Volume [Å³]	3538.82(5)	3253.2(2)
Z	4	2
ρ_{calc} [g/cm³]	1.413	1.414
μ [mm⁻¹]	5.315	5.684
F(000)	1576.0	1448.0
Crystal size [mm³]	0.1207 × 0.2028 × 0.2317	0.268 × 0.254 × 0.158
Radiation	CuKα (λ = 1.54184)	CuKα (λ = 1.54184)
Range for data collection [°]	8.414 < 2Θ < 133.454	6.718 < 2Θ < 148.39
Index ranges	-25 ≤ h ≤ 25 -12 ≤ k ≤ 12 -18 ≤ l ≤ 18	-8 ≤ h ≤ 11 -25 ≤ k ≤ 24 -21 ≤ l ≤ 21
Reflections collected	32951	18638
Independent reflections	6207 R_{int} = 0.0365 R_{sigma} = 0.0257	6420 R_{int} = 0.0336 R_{sigma} = 0.0291
Data/restraints/parameters	6207/1/453	6420/0/439
Goodness-of-fit on F²	1.046	1.033
Final R indexes [I ≥ 2σ(I)]	R_1 = 0.0228 wR_2 = 0.0539	R_1 = 0.0445 wR_2 = 0.1119
Final R indexes [all data]	R_1 = 0.0243 wR_2 = 0.0547	R_1 = 0.0475 wR_2 = 0.1143
Largest diff. peak/hole [eÅ⁻³]	0.26/-0.26	0.61/-0.62
Flack parameter	-0.028(2)	-

Table S 5-2   Chrystal data and structure refinement for comounds **5** and **6**.

Compound	5	6
Empirical formula	$C_{27}H_{22}N_2O_2CoCl_2Br_2$	$C_{24}H_{16}N_2CoBr_2$
Formula weight	696.11	551.14
Temperature [K]	123.0(1)	123.0(1)
Crystal system	Monoclinic	Monoclinic
Space group	$P2_1/c$	$P2/c$
a [Å]	7.3108(1)	14.7115(4)
b [Å]	21.5424(4)	9.5518(2)
c [Å]	16.5062(3)	15.3278(4)
α [°]	90	90
β [°]	94.041(2)	107.332(3)
γ [°]	90	90
Volume [Å³]	2593.14(8)	2056.08(9)
Z	4	4
ρ_{calc} [g/cm³]	1.783	1.780
μ [mm⁻¹]	10.933	11.189
F(000)	1380.0	1084.0
Crystal size [mm³]	0.179 × 0.134 × 0.082	0.146 × 0.06 × 0.058
Radiation	CuKα (λ = 1.54184)	CuKα (λ = 1.54184)
Range for data collection [°]	6.756 < 2Θ < 147.276	7.312 < 2Θ < 147.342
Index ranges	-8 ≤ h ≤ 9 -24 ≤ k ≤ 26 -17 ≤ l ≤ 20	-18 ≤ h ≤ 18 -11 ≤ k ≤ 9 -19 ≤ l ≤ 17
Reflections collected	14949	11363
Independent reflections	5126 R_{int} = 0.0335 R_{sigma} = 0.0337	4014 R_{int} = 0.0318 R_{sigma} = 0.0312
Data/restraints/parameters	5126/0/413	4014/0/263
Goodness-of-fit on F²	1.039	1.165
Final R indexes [I ≥ 2σ(I)]	R_1 = 0.0278 wR_2 = 0.0660	R_1 = 0.0348 wR_2 = 0.0935
Final R indexes [all data]	R_1 = 0.0318 wR_2 = 0.0682	R_1 = 0.0373 wR_2 = 0.0948
Largest diff. peak/hole [eÅ⁻³]	0.62/-0.45	0.66/-0.78
Flack parameter	-	-

5.7 References

[1] a) C.-J. Li, B. M. Trost, *Proc. Natl. Acad. Sci. USA* **2008**, *105*, 13197–13202; b) P. Anastas, N. Eghbali, *Chem. Soc. Rev.* **2009**, *39*, 301–312; c) C. M. Friend, B. Xu, *Acc. Chem. Res.* **2017**, *50*, 517–521.

[2] a) S. Losse, J. G. Vos, S. Rau, *Coord. Chem. Rev.* **2010**, *254*, 2492–2504; b) C. K. Prier, D. A. Rankic, D. W. C. MacMillan, *Chem. Rev.* **2013**, *113*, 5322–5363; c) R. S. Khnayzer, C. E. McCusker, B. S. Olaiya, F. N. Castellano, *J. Am. Chem. Soc.* **2013**, *135*, 14068–14070.

[3] a) V. Balzani, A. Credi, M. Venturi, *ChemSusChem* **2008**, *1*, 26–58; b) T. P. Yoon, M. A. Ischay, J. Du, *Nat. Chem.* **2010**, *2*, 527–532; c) D. Ravelli, S. Protti, M. Fagnoni, *Chem. Rev.* **2016**, *116*, 9850–9913.

[4] a) K. Zeitler, Angew. Chem. Int. Ed. **2009**, 48, 9785–9789; b) J. M. R. Narayanam, C. R. J. Stephenson, *Chem. Soc. Rev.* **2011**, *40*, 102–113; c) J. Xuan, W.-J. Xiao, Angew. Chem. Int. Ed. **2012**, 51, 6828–6838; d) L. Shi, W. Xia, *Chem. Soc. Rev.* **2012**, *41*, 7687–7697; e) J. W. Tucker, C. R. J. Stephenson, *J. Org. Chem.* **2012**, *77*, 1617–1622; f) M. H. Shaw, J. Twilton, D. W. C. MacMillan, *J. Org. Chem.* **2016**, *81*, 6898–6926.

[5] Examples in catalysis in general: a) S. Enthaler, K. Junge, M. Beller, *Angew. Chem. Int. Ed.* **2008**, *47*, 3317–3321; b) M. S. Holzwarth, B. Plietker, *ChemCatChem* **2013**, *5*, 1650–1679; c) P. J. Chirik, *Acc. Chem. Res.* **2015**, *48*, 1687–1695; d) W. Ai, R. Zhong, X. Liu, Q. Liu, *Chem. Rev.* **2019**, *119*, 2876–2953.

[6] Examples in photocatalysis: a) N. Armaroli, *Chem. Soc. Rev.* **2001**, *30*, 113–124; b) M. Majek, A. Jacobi von Wangelin, *Angew. Chem. Int. Ed.* **2013**, *52*, 5919–5921; c) S.-P. Luo, E. Mejía, A. Friedrich, A. Pazidis, H. Junge, A.-E. Surkus, R. Jackstell, S. Denurra, S. Gladiali, S. Lochbrunner, M. Beller, *Angew. Chem. Int. Ed.* **2013**, *52*, 419–423; d) E. Mejía, S.-P. Luo, M. Karnahl, A. Friedrich, S. Tschierlei, A.-E. Surkus, H. Junge, S. Gladiali, S. Lochbrunner, M. Beller, *Chem. Eur. J.* **2013**, 19, 15972–15978; e) B. van den Bosch, H.-C. Chen, J. I. van der Vlugt, A. M. Brouwer, J. N. H. Reek, *ChemSusChem* **2013**, *6*, 790–793.

[7] M. Pirtsch, S. Paria, T. Matsuno, H. Isobe, O. Reiser, *Chem. Eur. J.* **2012**, *18*, 7336–7340.

[8] J.-M. Kern, J.-P. Sauvage, *J. Chem. Soc., Chem. Commun.* **1987**, 546–548.

[9] a) S. Paria, O. Reiser, *ChemCatChem* **2014**, *6*, 2477–2483; b) O. Reiser, *Acc. Chem. Res.* **2016**, *49*, 1990–1996.

[10] A. Hossain, A. Bhattacharyya, O. Reiser, *Science* **2019**, *364*, eaav9713.

[11] a) K. Jonas, R. Mynott, C. Krüger, J. C. Sekutowski, Y.-H. Tsay, *Angew. Chem. Int. Ed.* **1976**, *15*, 767–768; b) K. Jonas, "Method of Preparing Transition Metal-Olefin Complex Compounds and Alkali Metal-Transition Metal-Olefin Complex Compounds", **1979**, US4169845A; c) W. W. Brennessel, Jr. Young Victor G., J. E. Ellis, *Angew. Chem. Int. Ed.* **2002**, *41*, 1211–1215; d) W. W. Brennessel, R. E. Jilek, J. E. Ellis, *Angew. Chem. Int. Ed.* **2007**, *46*, 6132–6136.

[12] a) D. Gärtner, A. Welther, B. R. Rad, R. Wolf, A. Jacobi von Wangelin, *Angew. Chem. Int. Ed.* **2014**, *53*, 3722–3726; b) P. Büschelberger, D. Gärtner, E. Reyes-Rodriguez, F. Kreyenschmidt, K. Koszinowski, A. Jacobi von Wangelin, R. Wolf, *Chem. Eur. J.* **2017**, *23*, 3139–3151.

[13] S.-B. Wu, T. Zhang, L. W. Chung, Y.-D. Wu, *Org. Lett.* **2019**, *21*, 360–364.

[14] a) W. W. Brennessel, J. E. Ellis, *Inorg. Chem.* **2012**, *51*, 9076–9094; b) W. W. Brennessel, J. E. Ellis, *Acta Cryst C* **2014**, *70*, 828–832.

[15] P. Pyykkö, *J. Phys. Chem. A* **2015**, *119*, 2326–2337.

[16] There are a few examples of Au, Pd, Pt, and Ru complexes with tridentate 2,9-diaryl-1,10-phenanthroline ligands, where one aryl ring is *ortho*-metalated: a) Pd: A. J. Blake, C. O. Dietrich-Buchecker, T. I. Hyde, J.-P. Sauvage, M. Schröder, *J. Chem. Soc., Chem. Comm.* **1989**, 1663–1665; b) Pt: C. W. Chan, T. F. Lai, C. M. Che, S. M. Peng, *J. Am. Chem. Soc.* **1993**, *115*, 11245–11253; c) Au: C.-W. Chan, W.-T. Wong, C.-M. Che, *Inorg. Chem.* **1994**, *33*, 1266–1272; d) Ru: J.-P. Collin, R. Kayhanian, J.-P. Sauvage, G. Calogero, F. Barigelletti, A. D. Cian, J. Fischer, *Chem. Commun.* **1997**, 775–776; e) Pd: M. Kuritani, S. Tashiro, M. Shionoya, *Chem. Asian J.* **2013**, *8*, 1368–1371.

[17] a) S. A. Shirvan, M. Aghajeri, S. Haydari Dezfuli, F. Khazali, A. Borsalani, Acta Cryst 2012, 68, m1407–m1407; b) L. Smolko, J. Černák, M. Dušek, J. Titiš, R. Boča, New J. Chem. 2016, 40, 6593–6598.

[18] c) M. M. Cetin, R. T. Hodson, C. R. Hart, D. B. Cordes, M. Findlater, D. J. C. Jr, A. F. Cozzolino, M. F. Mayer, Dalton Trans. 2017, 46, 6553–6569.

[19] Please see the supporting information for further details.

[20] a) T. J. Korstanje, J. I. van der Vlugt, C. J. Elsevier, B. de Bruin, *Science* **2015**, *350*, 298–302; b) D. Srimani, A. Mukherjee, A. F. G. Goldberg, G. Leitus, Y. Diskin-Posner, L. J. W. Shimon, Y. Ben David, D. Milstein, *Angew. Chem. Int. Ed.* **2015**, *54*, 12357–12360; c) J. Yuwen, S. Chakraborty, W. W. Brennessel, W. D. Jones, *ACS Catal.* **2017**, *7*, 3735–3740.

[21] T. M. Maier, S. Sandl, I. G. Shenderovich, A. Jacobi von Wangelin, J. J. Weigand, R. Wolf, *Chem. Eur. J.* **2019**, *25*, 238–245.

[22] a) A. Friedrich, M. Drees, S. Schneider, *Chem. Eur. J.* **2009**, *15*, 10339–10342; b) L. J. Sewell, G. C. Lloyd-Jones, A. S. Weller, *J. Am. Chem. Soc.* **2012**, *134*, 3598–3610; c) J. R. Vance, A. Schäfer, A. P. M. Robertson, K. Lee, J. Turner, G. R. Whittell, I. Manners, *J. Am. Chem. Soc.* **2014**, *136*, 3048–3064; d) A. Glüer, M. Förster, V. R. Celinski, J. Schmedt auf der Günne, M. C. Holthausen, S. Schneider, *ACS Catal.* **2015**, *5*, 7214–7217; e) U. Chakraborty, S. Demeshko, F. Meyer, C. Rebreyend, B. de Bruin, M. Atanasov, F. Neese, B. Mühldorf, R. Wolf, *Angeww Chem. Int. Ed.* **2017**, *56*, 7995–7999; f) J. Turner, N. F. Chilton, A. Kumar, A. L. Colebatch, G. R. Whittell, H. A. Sparkes, A. S. Weller, I. Manners, *Chem. Eur. J.* **2018**, *24*, 14127–14136.

[23] a) SCALE3ABS, CrysAlisPro, Aglient Technologies Inc., Oxford, UK, **2015**; b) G. M. Sheldrick, SADABS, Bruker AXS, Madison, USA, **2007**.

[24] a) R. C. Clark, J. S. Reid, *Acta Crystallogr. A* **1995**, *51*, 887; b) CrysAlisPro, version 171.37.35, Agilent Technologies Inc., Oxford, UK, **2015**.

[25] O.V. Dolomanov, L.J. Bourhis, R.J. Gildea, J.A.K. Howard, H. Puschmann, *J. Appl. Cryst.* **2009**, *42*, 339-341.

[26] G. M. Sheldrick, *Acta Cryst.* **2015**, *A71*, 3-8.

[27] G. M. Sheldrick, *Acta Cryst.* **2015**, C*71*, 3-8.

6 SUMMARY

Chapter 1 – Cobalt in Homogeneous and Heterogeneous Hydrogenation Catalysis

Catalytic hydrogenation is one to the most important technical processes in chemical synthesis and therefore constitutes a significant research area. Although this field was mainly dominated by precious metal catalysts, over the last decades, the focus of current research activities has more and more moved towards the development of sustainable base-metal catalysts. This chapter gives a short overview over recent innovations concerning cobalt catalyzed-hydrogenation reactions, differentiated in homogeneous and heterogeneous systems. A detailed understanding of the operational mechanism is essential for further improvements of catalytic systems and many modern catalysts are at the boundary between these two main types in classical catalysis. Therefore, various methods and techniques for the differentiation between homogeneous and heterogeneous reaction pathways are summarized and discussed.

Chapter 2 – Alkene Cobaltates as Hydrogenation Catalysts[1]

The aim of this thesis is the search for new catalysts based on cobalt in low oxidation states. This chapter reports on the synthesis and characterization of a series of cobaltates **1** - **6** (Scheme 6.1) and on their behavior as pre-catalysts in the hydrogenation of alkenes, ketones, and imines. Compounds **4** - **6** were synthesized for the first time. Complexes **1** - **5** were found to be active
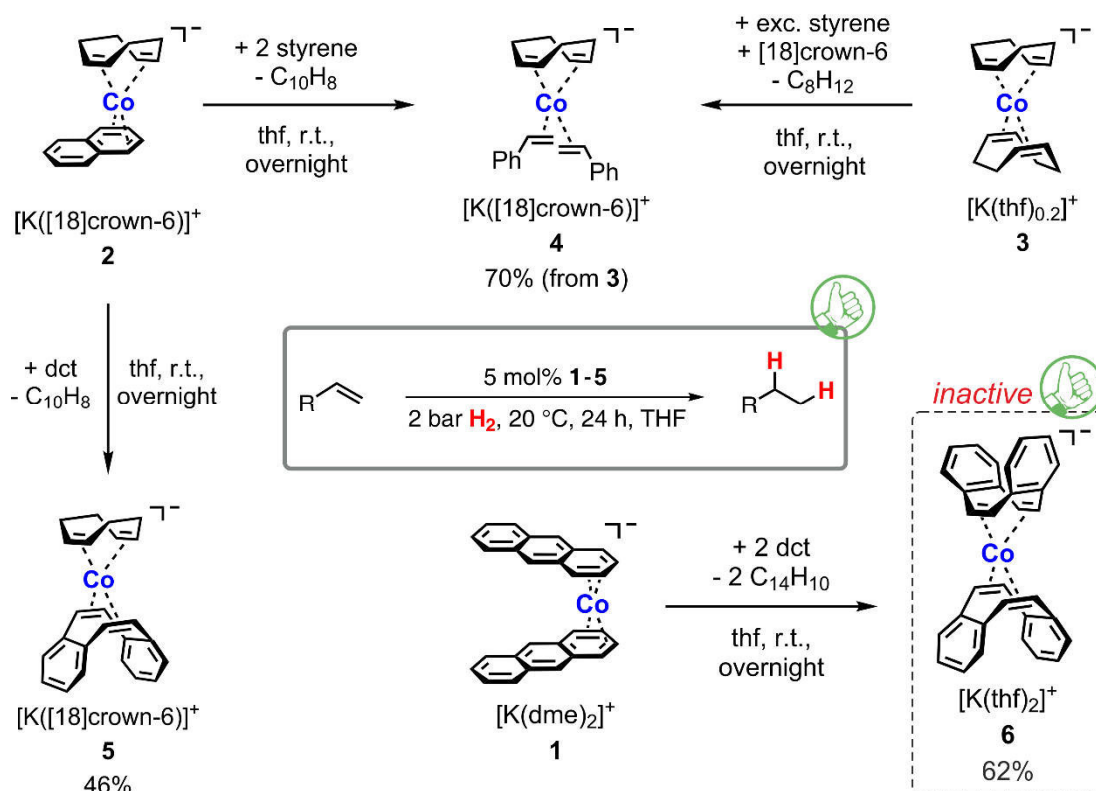
Scheme 6.1   Compounds **1** - **6** were prepared and studied as pre-catalysts in hydrogenation reactions.
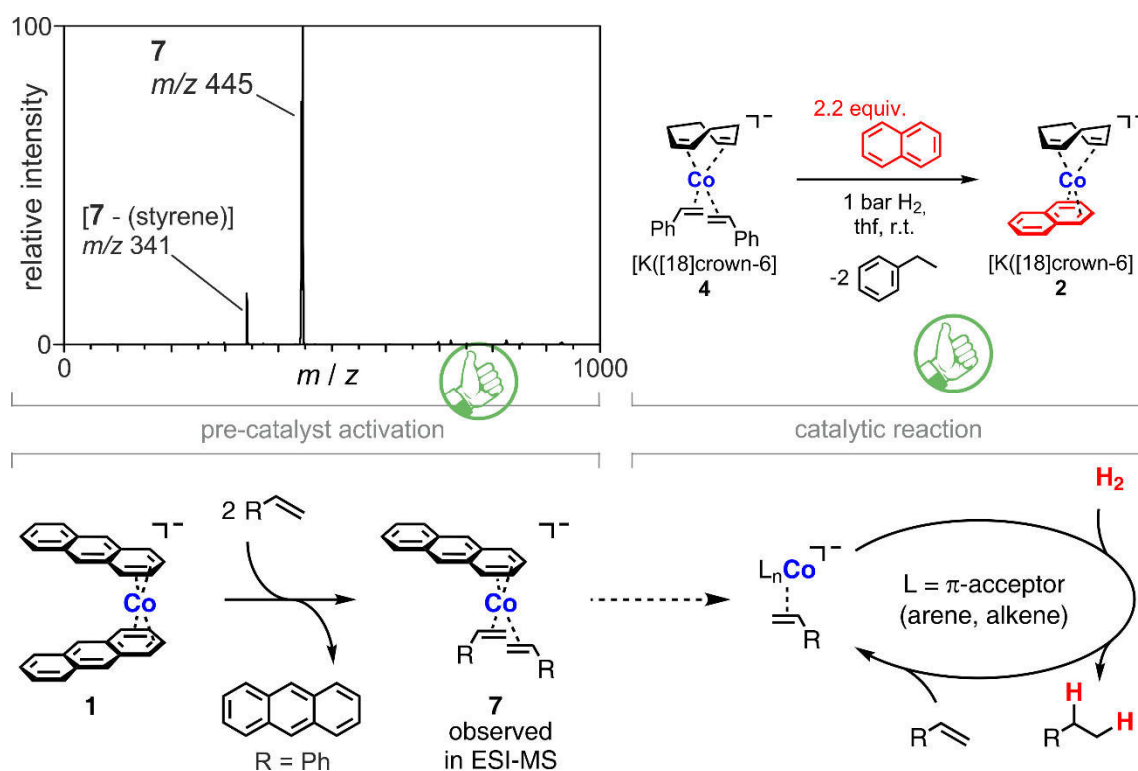
Figure 6.1   Negative-ion mode ESI mass spectrum of a reaction mixture of **1** (7.5 mM) with 20 equiv. of styrene (top left), proof of the ligand-catch concept with compound **4** (top right), and the mechanism for alkene hydrogenation (bottom).

in the hydrogenation of alkenes under mild conditions while the catalytic inactivity of **6** confirmed the validity of Crabtree's dct test for cobalt complexes. Detailed mechanistic investigations by ^{1}H NMR monitoring, ESI-MS (Figure 6.1, top left) and poisoning experiments, stoichiometric reactions (Figure 6.1, top right), and reaction progress analysis confirmed the homogeneous nature of the catalysts. All these experiments also support the proposed mechanism (Figure 6.1, bottom) for alkene hydrogenation, which is initiated by a redox-neutral ligand exchange of the labile π-accepting polyarene or alkene ligand of the pre-catalyst.

For the hydrogenation of polar substrates (ketones, imines) all other compounds showed significantly lower activities than **1**, and most likely catalyst species of higher oxidation states are formed by SET and deprotonation reactions.

Chapter 3 – Recyclable Cobalt(0) Nanoparticle Catalyst for Hydrogenations[2]

A new method for the preparation of small, monodisperse Co(0) nanoparticles from commercial starting materials is presented in Chapter 3. In the absence of any ligands or surfactants $CoCl_2$ is reduced with $LiC_{10}H_8$ in a straightforward and operationally simple synthesis, resulting in the formation of this highly active hydrogenation catalyst (Figure 6.2, top). Various alkenes, alkynes, imines and quinolines were cleanly converted to the corresponding hydrogenation products and
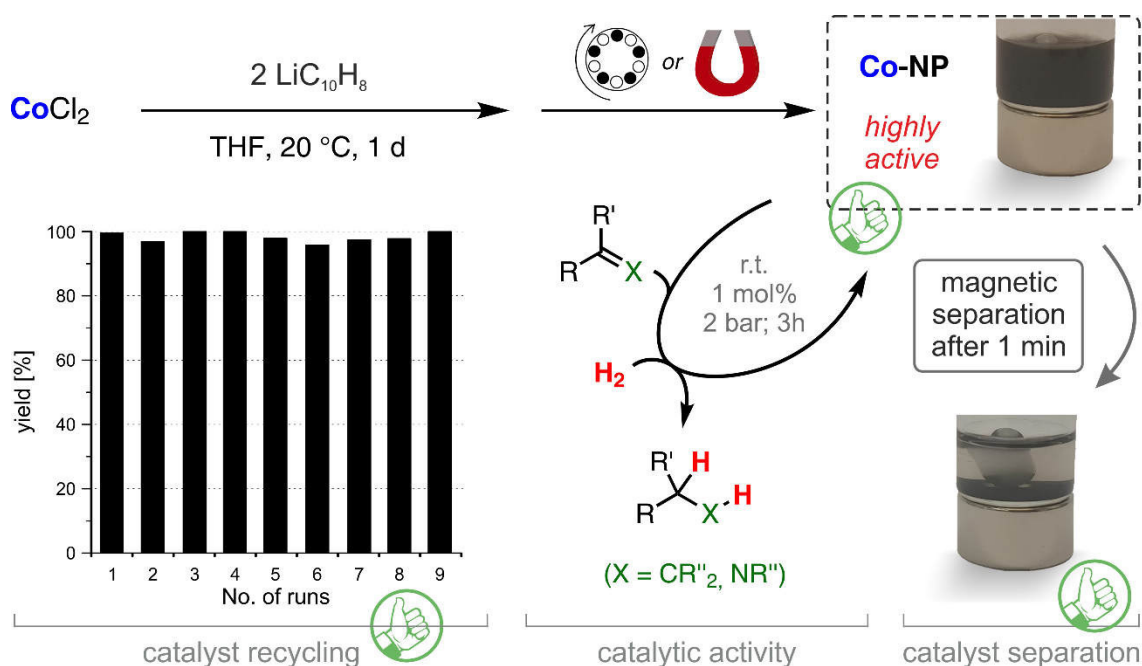
Figure 6.2   Synthesis of Co(0) nanoparticles from commercial starting materials (top), yields of consecutive hydrogenation runs with recycled particles (bottom left), hydrogenation of various substrates under mild conditions (bottom center), and catalyst separation by an external magnet after 1 min (bottom right).

under mild conditions (Figure 6.2, bottom center). Multiple recycling (Figure 6.2, bottom left) of the catalyst is enabled by an easy separation (Figure 6.2, bottom right), utilizing the magnetic properties of the long-term stable catalyst. Detailed analytical studies by TEM, XRD, DLS and poisoning reactions document the heterogeneous nature of the nanoparticulate system. Especially the results of the poisoning studies verify the applicability of these methods for cobalt systems, and thus, support the results from Chapter 2.

Chapter 4 – Chiral Alkene Cobaltates as Hydrogenation Catalysts[3]

In extension to our studies about alkene cobaltates as hydrogenation catalysts in Chapter 2, we aimed at the development of an enantioselective cobalt catalyst bearing C_2-symmetric norbornadiene derivatives as steering ligands. By reaction of **1** and **2** with 1.1 equiv. of Hayashi's (*R*,*R*)-Ph-bod ligand, we isolated and characterized the chiral complexes **4** and **5** (Figure 6.3) for the first time. Indeed, these compounds showed good catalytic activity towards the hydrogenation of styrene under mild conditions, but unfortunately, the Ph-bod ligand is also partly hydrogenated as well. In addition, only minor conversion of 1,1-disubstituted, prochiral substrates was detected under similar conditions. Harsher conditions even led to a higher degree of ligand hydrogenation without any improvement of the substrate conversion. Even though the Ph-bod ligand is not applicable as a steering ligand in asymmetric cobalt catalyzed hydrogenation, this study confirms the possibility of using chiral dienes for this purpose.
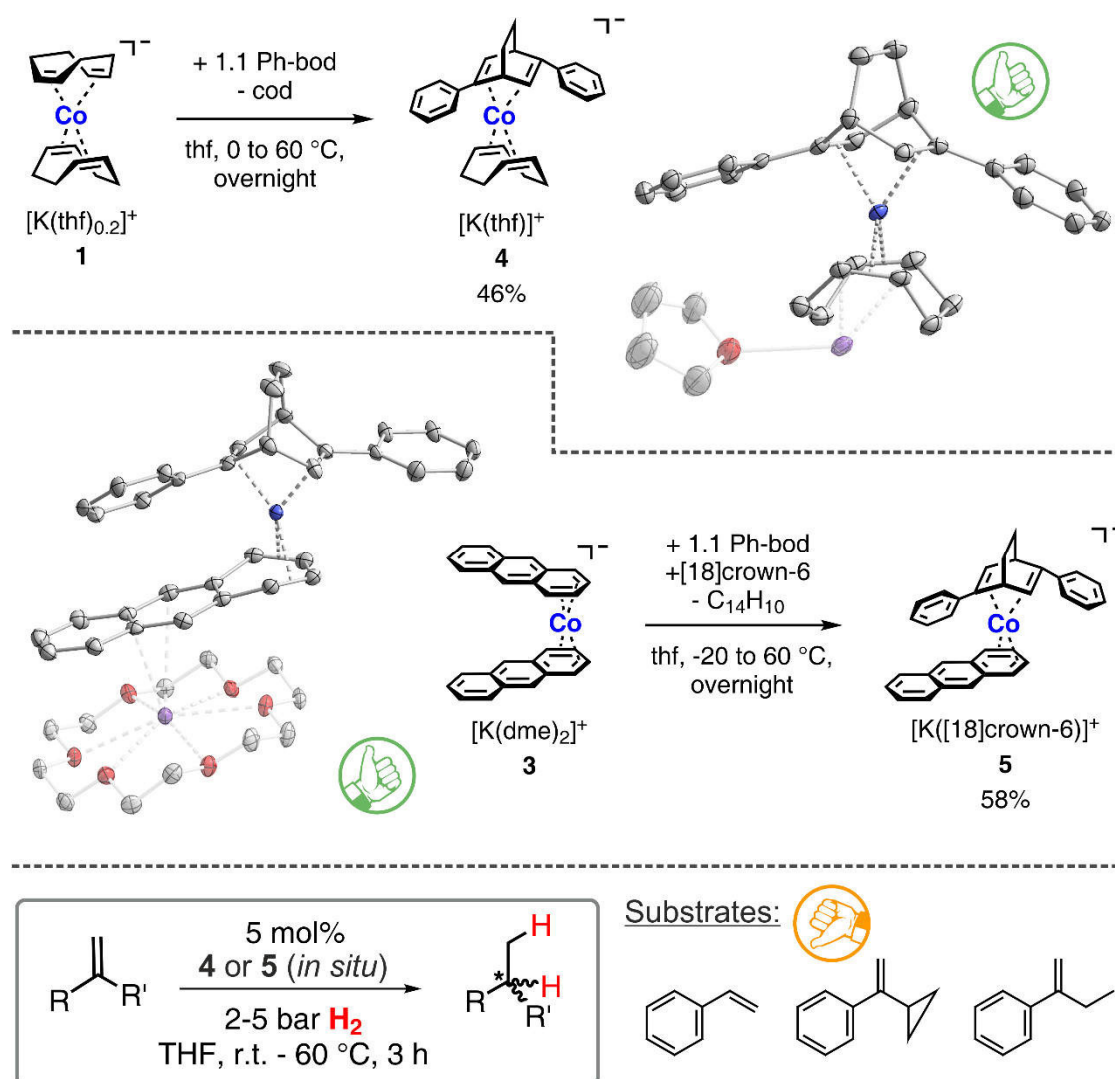
Figure 6.3   Synthesis and molecular structures of the chiral cobaltates **4** (top) and **5** (center) bearing Hayashi's (*R,R*)-Ph-bod ligand. The compounds are easily accessible by reaction of **1** and **2** with 1.1 equiv. of the ligand, respectively. In the hydrogenation of 1,1-disubstituted, prochiral substrates (bottom) only minor conversion was observed.

Chapter 5 – Phenanthrolines as Ligands for Cobaltate Catalysts[3]

This study demonstrates two different methods for the preparation of a new class of cobaltates with *2*,9-diaryl-1,10-phenanthroline (= phen) ligands in an unprecedented, *ortho*-metalated coordination mode. Complexes **4** and **7** can either be synthesized by ligand exchange *via* the established $[K(dme)_2][Co(C_{14}H_{10})_2]$ (**1**), or by reduction of the easy accessible phenanthroline adducts of the metal halide, $[(phen)CoBr_2]$ (**5** and **6**) (Figure 6.4, top). Both pathways start from commercially available $CoBr_2$ and contain one ligand association and one reduction step, apparently only in different order.

The new complexes **4** - **7** were characterized by ^1H and ^{13}C NMR spectroscopy and crystallographic techniques and were utilized for initial catalytic investigations. Both compounds

showed good activity in the hydrogenation of disubstituted alkenes (Figure 6.4, center). For an analogous, trisubstituted substrate, only moderate conversions and yields were detected. Moreover, **7** was found to be active in the selective dehydrogenation of dimethylamine-borane at room temperature, in an NMR scale reaction (Figure 6.4, bottom).
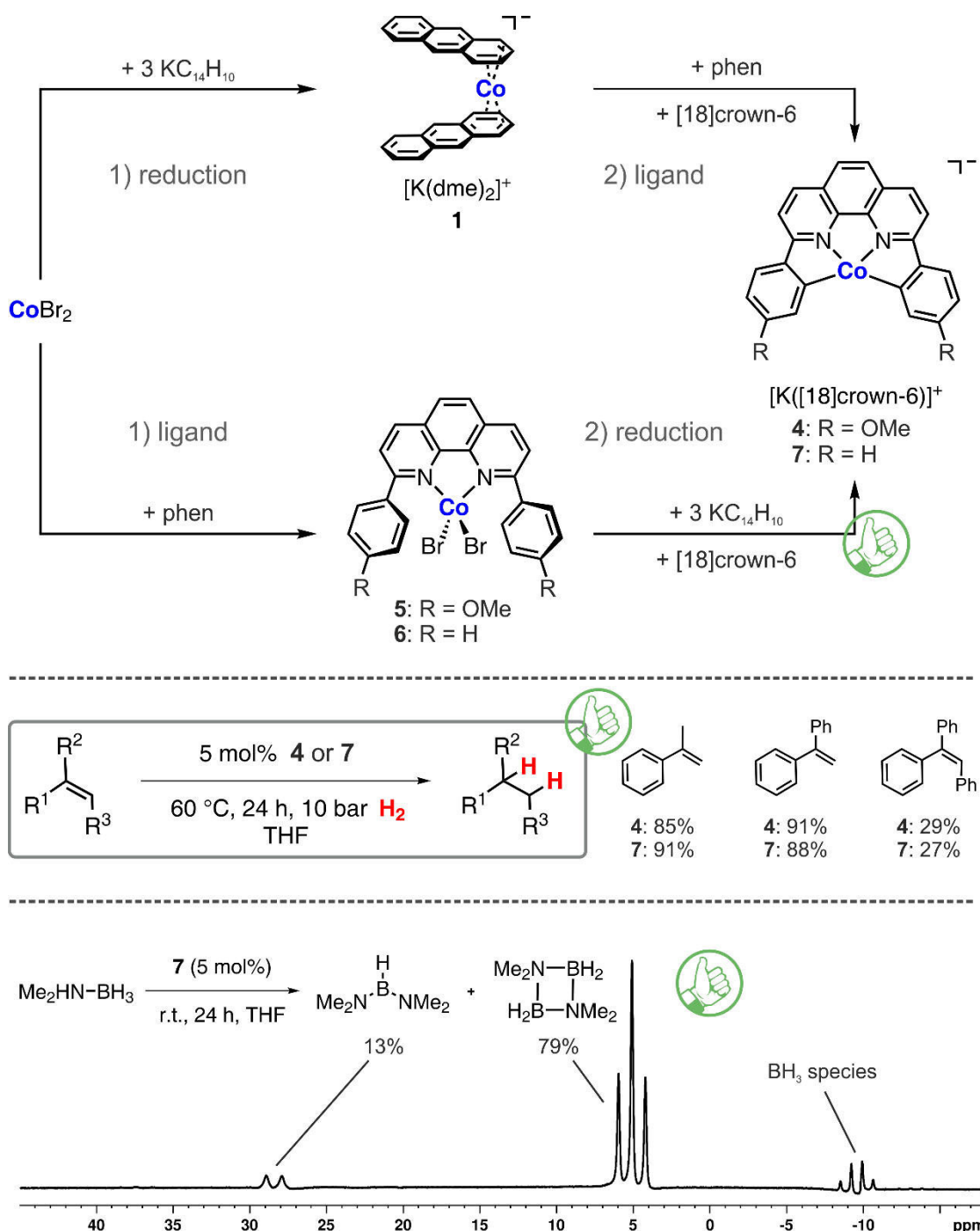

Figure 6.4   Two possible synthetic pathways for the synthesis of compounds **4** and **7**, bearing a doubly deprotonated 2,9-diaryl-1,10-phenanthrolinediyl (= phen) ligand (top), hydrogenation of di- and trisubstituted alkenes (center), and ^{11}B NMR spectrum (128.4 Hz, 300 K, C_6D_6-capillary) of the reaction mixture of the dehydrogenation of dimethylamine-borane, catalyzed by **7**, after 25 h (bottom).

References

[1] P. Büschelberger, D. Gärtner, E. Reyes-Rodriguez, F. Kreyenschmidt, K. Koszinowski, A. Jacobi von Wangelin, R. Wolf, *Chem. Eur. J.* **2017**, *23*, 3139–3151.

[2] P. Büschelberger, E. Reyes-Rodriguez, C. Schöttle, J. Treptow, C. Feldmann, A. Jacobi von Wangelin, R. Wolf, *Catal. Sci. Technol.* **2018**, *8*, 2648-2653.

[3] Unpublished results.

7 Acknowledgement

Stunden während der Mittags- & Kaffeepausen, den Grillabenden, sowie den ganzen Weihnachts- und Doktorfeiern und für die Hilfsbereitschaft in allen möglichen Situationen.

Den Mitarbeitern der analytischen Abteilungen und der Werkstätten der Universität Regensburg - vor allem der Glasbläserei - danke ich für die meist problemlose und unkomplizierte Zusammenarbeit und für die Hilfe bei so mancher Herausforderung.

All meinen Freunden möchte ich für die Ablenkungen und Unternehmungen danken, die mir immer den nötigen Ausgleich verschaffen. Die schönen Momente, die Ihr mir beschert sind unbezahlbar!

Der größte Dank geht an meine Frau Ines und meine Familie für die grenzenlose Unterstützung, nicht nur während meiner gesamten Studien- und Promotionszeit, sondern allgemein in meinem Leben!

8 CURRICULUM VITAE

PHILIPP BÜSCHELBERGER

Familienstand	verheiratet
Geburtstag	18. April 1988
Geburtsort	Mellrichstadt
Nationalität	deutsch

AUSBILDUNG

Nov. 2014 – heute	**Promotion** an der *Universität Regensburg*
	am Arbeitskreis von Prof. Dr. Robert Wolf an der Fakultät für Chemie & Pharmazie (Institut für Anorganische Chemie): *„Homogeneous vs. Heterogeneous Cobalt-Catalyzed Hydrogenations: An Evaluation of Cobaltates and Cobalt Nanoparticles as Catalysts"*
Jun. 2015	**Forschungsaufenthalt** an der Georg-August-*Universität Göttingen*
	am Arbeitskreis von Prof. Dr. Konrad Koszinowski an der Fakultät für Chemie (Institut für Organische und Biomolekulare Chemie)
Okt. 2012 – Sep. 2014	**Master of Science** in **Chemie** an der *Universität Regensburg*, mit Schwerpunkt organische und anorganische Chemie sowie Biologie im Grundmodul, **Gesamtnote 1,4**
	Masterarbeit am Arbeitskreis von Prof. Dr. Robert Wolf an der Fakultät für Chemie & Pharmazie (Institut für Anorganische Chemie): *„Cobalt katalysierte Hydrierungen: Anwendungsbreite und Mechanismus"*, **Note 1,3**
Okt. 2009 – Sep. 2012	**Bachelor of Science** in **Chemie**, *Universität Regensburg*, **Gesamtnote 2,5**
	Bachelorarbeit am Arbeitskreis von Prof. Dr. Kirsten Zeitler an der Fakultät für Chemie & Pharmazie (Institut für Organische Chemie): *„Ringöffnung von α-Diketonen katalysiert durch N-heterocyclische Carbene"*, **Note 1,3**
Jul. 2007 – Jul. 2009	**Ausbildung zum Offizier der Reserve**, *FschJgBtl 261* (Lebach), Bundeswehr
Sep. 1998 – Jun. 2007	**Abitur**, *Martin-Pollich-Gymnasium*, Mellrichstadt, **Gesamtnote 2,5**
	Leistungskurse: Chemie und Sport

WISSENSCHAFTLICHE PRÄSENTATIONEN

24. – 27.09.2018	Poster – *19. Vortragstagung der Wöhler-Vereinigung* in **Regensburg**
22. - 25.07.2018	Vortrag – *International Symposium on Relations between Homogeneous and Heterogeneous Catalysis 18* in **Sydney**, Australien
	Ermöglicht durch Reise-Stipendien des DAAD und der GDCh
20. - 25.08.2017	Vortrag – *Wissenschaftliches Kolloquium von Arbeitsgruppen für Anorganische Chemie* 2017 in **Hirschegg**, Österreich
09. – 13.07.2017	Poster – *22nd European Conference on Organometallic Chemistry* in **Amsterdam**, Niederlande
19. - 21.02.2017	Poster – *15th Ferrocene Colloquium* in **Mainz**
26. - 28.09.2016	Poster – *18. Vortragstagung der Wöhler-Vereinigung* in **Berlin**
23. - 28.08.2015	Vortrag – *Wissenschaftliches Kolloquium von Arbeitsgruppen für Anorganische Chemie* 2015 in **Hirschegg**, Österreich
27. - 31.07.2015	Poster – *14th International Symposium on Inorganic Ring Systems* in **Regensburg**
22. - 24.03.2015	Poster – *11. Koordinationschemiker Tagung* in **Paderborn**

MITGLIEDSCHAFTEN

Gesellschaft Deutscher Chemiker e.V.

ChemPharm Graduate School Regensburg

Alumniverein Chemie der Universität Regensburg e.V.

Fladunger Fasnachts-Club FFC (Vorstandschaftsmitglied)

FC Bayern Fladungen, Freier TuS Regensburg

9 LIST OF PUBLICATIONS

[1] R. J. Wilson, F. Hastreiter, K. Reiter, P. Büschelberger, R. Wolf, R. Gschwind, F. Weigend, S. Dehnen; „[Co@Sn$_6$Sb$_6$]$^{3-}$: An Off-Center Endohedral 12-Vertex Cluster"; *Angew. Chem. Int. Ed.*, **2018**, *57*, 15359-15363.

[2] P. Büschelberger, E. Reyes-Rodriguez, C. Schöttle, J. Treptow, C. Feldmann, A. Jacobi von Wangelin, R. Wolf; *„Recyclable Cobalt(0) Nanoparticle Catalysts for Hydrogenations"*; *Catal. Sci. Technol.* **2018**, *8*, 2648-2653.

[3] P. Büschelberger, C. Rödl, R. Wolf, *„Bis(1,2-dimethoxyethane)potassium bis(1,2,3,4-η^4-anthracene)-cobaltate [K(dme)$_2$][Co(C$_{14}$H$_{10}$)$_2$]"*; *Inorg. Synth.* **2018**, *37*, 72-76.

[4] F. Abels, D. Loeffler, H. Wilmer, R. Wolf, C. Roedl, P. Büschelberger, *„Process for the Generation of Thin Inorganic Films"* **2017**, Int. Patent WO2017/129440.

[5] P. Büschelberger, D. Gärtner, E. Reyes-Rodriguez, F. Kreyenschmidt, K. Koszinowski, A. Jacobi von Wangelin, R. Wolf, *„Alkene Metalates as Hydrogenation Catalysts"*; *Chem. Eur. J.* **2017**, *23*, 3139-3151

10 EIDESSTATTLICHE ERKLÄRUNG

167

Ich erkläre hiermit an Eides statt, dass ich die vorliegende Arbeit ohne unzulässige Hilfe Dritter und ohne Benutzung anderer als der angegebenen Hilfsmittel angefertigt hab; die aus anderen Quellen direkt oder indirekt übernommenen Daten und Konzepte sind unter Angabe des Literaturzitats gekennzeichnet. Die Arbeit wurde bisher weder im In- noch im Ausland in gleicher oder ähnlicher Form einer anderen Prüfungsbehörde vorgelegt.

Philipp Büschelberger